universität wien

DISSERTATION / DOCTORAL THESIS

Titel der Dissertation /Title of the Doctoral Thesis

Epithelial morphogenesis, mechanotransduction and the role of cadherins during early development of the sea anemone *Nematostella vectensis*

verfasst von / submitted by

Ekaterina Pukhlyakova

angestrebter akademischer Grad / in partial fulfilment of the requirements for the degree of

Doctor of Philosophy (PhD)

Wien, 2020 / Vienna 2020

Studienkennzahl lt. Studienblatt / degree programme code as it appears on the student record sheet:	UA 794 685 437
Dissertationsgebiet lt. Studienblatt / field of study as it appears on the student record sheet:	Biologie / Biology
Betreut von / Supervisor:	Univ.-Prof. Dipl.-Biol. Dr. Ulrich Technau

Table of Contents

ACKNOWLEDGEMENTS

I would like to thank my supervisor Prof. Uli Technau for giving me the opportunity to perform my PhD studies in his laboratory, one of the best in the field. I am very grateful for his all-around support, whether in terms of scientific guidance and advice on better management strategies or providing the necessary funding for research. I would like to thank Uli, on the one hand, for giving a lot of the scientific freedom, and on the other hand, for focusing my attention on the most important points of the research. I could always rely on his experience and get competent advice whenever needed.

My PhD studies would never have been so much fun without the people in the laboratory. I would especially like to thank the very talented former postdocs in Uli's lab: Andy Aman, Grisha Genikhovich and Yehu Moran, who spent hours and days with me, teaching the finer points of scientific work and sharing their invaluable professionalism with me. I am very thankful to my master students David Aminger and Michi Jovic for being so great and helping me to discover my mentoring potential. I want to thank Rohit Dnyasagar for teaching me how to cook delicious Indian food, and sharing all the difficulties of the PhD life and laughing through tears together. I thank Edi for the excellent laboratory coordination, organizing super-fun trips for the entire group and for always being there for everything what was needed. I thank all the former and current members of the Technau group for their kind words in difficult moments and for being very supportive and creating a friendly and positive atmosphere in the lab.

Last, but not least, I want to thank my parents who have always been cherishing education and fundamental knowledge. They always gave me all the best they could and even more. I thank my friend Server who taught me how to make illustrations for the presentations and papers, and was always ready to help with the posters and talks design. I would like to thank my dear friend Dominik, for being there for me in the very last stage of my doctoral thesis, for supporting me in the restless moments of writing, for careful listening, for cooking for me and taking me on the amazing travels together.

ZUSAMMENFASSUNG

Das Auftreten von Vielzellern während der Evolution korreliert mit der Entstehung des Epithels. Während der epithelialen Morphogenese verwandeln sich zweidimensionale Epithelschichten in komplexe dreidimensionale Strukturen. Sie bilden Gewebe, Organe und definieren die Form eines Organismus. Um den evolutionären Ursprung der Epithelbildung und Keimblattbildung besser zu verstehen, ist das Studium der nicht-bilateralen, frühen Eumetazoa von wesentlicher Bedeutung. Die Seeanemone *Nematostella vectensis* ist eines der beliebtesten Nesseltier-Modellorganismen für Forschung der Entwicklungs- und Evolutionsbiologie.

Um die Epithelstruktur und die Funktion der Zelladhäsion während der Morphogenese von *Nematostella* zu erklären, habe ich Antikörper gegen Cadherin1 und Cadherin3 generiert und erstmals die subzelluläre Lokalisation, die Proteindynamik und die Funktion der Cadherine während der Embryonalentwicklung bei Cnidaria detailliert beschrieben. Die Ergebnisse zeigen, dass Verbindungen zwischen Zellen sowohl an der apikalen als auch an der basalen Zellseite lokalisiert sind, was das Nesseltier-Epithel unter den Metazoen einzigartig macht. Es ist hervorzuheben, das die Keimschichtbildung bei *Nematostella* mit einem Cadherin-Switching einhergeht, ähnlich wie bei einigen Bilateria. Die Ergebnisse lassen darauf schließen, dass ein Cadherin-Switching im Laufe der Evolution mehrere Male unabhängig voneinander auftrat.

Meine Studien zeigen, dass das Epithel von *Nematostella* während der Gastrulation von MyosinII abhängige mechanische Kräfte ausübt. Diese erhöhte mechanische Spannung auf die Zellen der Urmundlippe erleichtert die β-catenin-abhängige *Brachyury*-Expression. Eine ähnliche von β-catenin abhängige mechanosensitive Expression von Transkriptionsfaktoren wurde zuvor für Zebrafische und *Drosophila* beschrieben. Meine Ergebnisse zeigen erstmals die mechanosensitive Genexpression in Cnidaria. Dies deutet darauf hin, dass die mechanoabhängige Genexpression ein uralter Genregulationsmechanismus ist, welcher der Spaltung von Cnidaria und Bilateria vorausging.

ABSTRACT

The appearance of multicellular animals during evolution is tightly correlated with the emergence of epithelium. During epithelial morphogenesis two-dimensional epithelial layers convert into complex three-dimensional structures, forming tissues, organs and defining a shape of an organism. To better understand the evolutionary origin of epithelia formation and germ layer establishment, studying of non-bilaterian early-branching Eumetazoa is essential. The starlet sea anemone *Nematostella vectensis,* became one of the favorite cnidarian model organisms for developmental and evolutionary studies.

To reveal the epithelia structure and function of cell adhesion during *Nematostella* morphogenesis, I have generated antibodies against Cadherin1 and Cadherin3 and for the first time described in detail the subcellular localization, protein dynamics and function of cadherins during embryo development in Cnidaria. The results show that cell-cell junctions are located at both apical and basal cellular sides, making the cnidarian epithelium unique among Metazoa. Interestingly, germ layer formation in *Nematostella* is accompanied by a cadherin switching, similar to some Bilateria. The results suggest a cadherin switching appeared independently several times during the evolution.

I have shown that the epithelium exerts myosinII-dependent mechanical forces during *Nematostella* gastrulation. This increased mechanical tension on the blastopore lip cells facilitates β-catenin-dependent *brachyury* expression. Similar β-catenin-dependent mechanosensitive expression of transcription factors was previously shown for zebrafish and *Drosophila*. My results demonstrate the mechanosensitive gene expression in Cnidaria for the first time, suggesting that mechanodependent gene expression is an ancient gene regulatory mechanism predating the split of Cnidaria and Bilateria.

INTRODUCTION

EPITHELIA

Structure and functions of the epithelium

In complex multicellular organisms like animals, cells are organized into either mesenchymal or epithelial tissues. Epithelial cells can reversibly transform into mesenchymal and vice versa as a result of epithelial-mesenchymal (EMT) and mesenchymal-epithelial transitions (MET) during embryonic development, regeneration or in pathological states. Therefore epithelia define to a great degree morphogenetic pathways of an embryo and determine a body shape of the animals.

Epithelium, together with muscle, nervous and connective tissues is one of the four major tissue types and one of the defining characteristics of Metazoa. Epithelium is a continuous cell layer, which covers all outside surfaces; lines inner organs, blood vessels and body cavities and separates different physiological environments within the organism. Skin, digestive, respiratory, reproductive and urinary tracts and other parts, which come in contact with an exterior, are covered with epithelia (Spassky and Meunier, 2017; Turksen, 2017; Yuksel and Turkeli, 2017). Being positioned at the interface between ‘’self ‘’and ‘’non-self’’ territories, epithelial cells are the first ones, which contact with external stimuli.

Epithelium prevents pathogen invasion and forms a protective barrier between an internal milieu of an organism and its outside (Powell, 1981; Wertz and Squier, 1991). Epithelial cells act as the gatekeepers of the body. All substances, entering an organism must cross the epithelium. It permits nutrient and metabolite exchange, controls permeability and selective absorption and transport of the substances (Palmer, 2017). In addition to the ability to absorb substances, epithelia are responsible for the exocrine and endocrine secretion. Epithelia form most of the glands and ducts of the body, releasing hormones, sweat, sebum, saliva, breast milk, etc. (Rehfeld et al., 2017). Epithelial cells secret digestive enzymes in the digestive tract, release mucus, which traps dust and microorganisms in the respiratory tract. Many epithelia are covered with cilia. Beating of cilia directs fluid flow inside the body tracts. Various epithelia participate in sensory reception. Specialized epithelial structures in sensory organs perceive sounds, odors, sights and mechanical pressure and transform these stimuli into electrical signals of the nervous system (Alberts, 2007).

To provide those vital functions for the organism, epithelial tissues require a certain unique and structural cellular organization (Figure 1). All epithelia types share some important structural features.

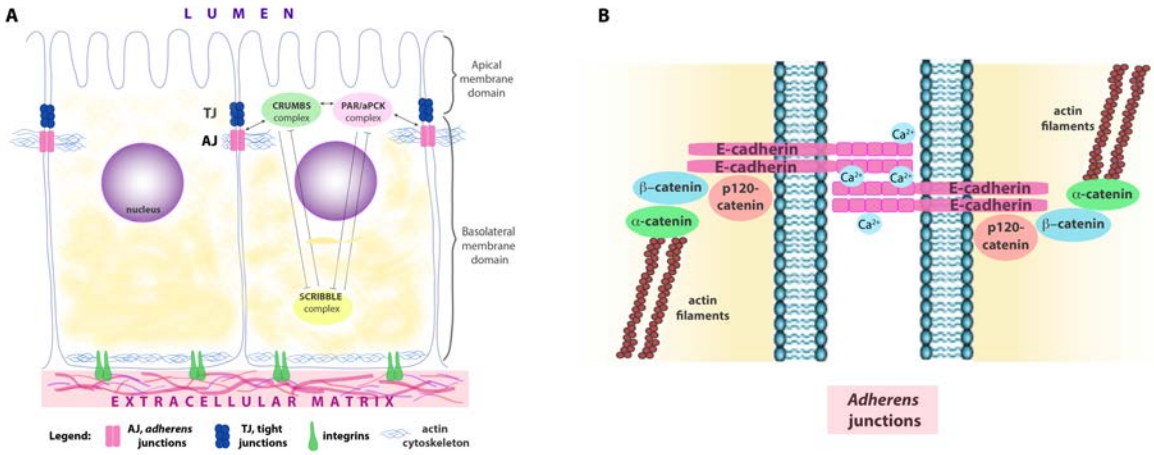

Figure 1. Schematic view of an epithelium. A. Structure of an epithelium. Establishment of epithelial polarity. **B.** *Adherens* junctions. After (Canel et al., 2013).

Epithelia are organized in mono or multilayered sheets, where cells are tightly interconnected via cellular junctions with no or very little space between cells. Epithelial cell junctions provide a barrier function and close intracellular communication. Epithelial cells have a defined apical-basal cell polarity: an apical side of the cell facing the external environment or lumen and a basal side attached to the extracellular matrix (ECM). Failure to generate and preserve epithelial cell polarity leads to the multiple pathologies and diseases (Apodaca et al., 2012; Mellman and Nelson, 2008).

Apical-basal cell polarity is presumably an ancestral trait. Interestingly, cell polarity is already present in colonial choanoflagellates, the closest unicellular relatives of metazoans (Brunet and King, 2017; King et al., 2008; Laundon et al., 2019). Proteins and molecular networks, which regulate epithelia polarization and cellular junctions establishment are highly conserved (Knust and Bossinger, 2002; Rodriguez-Boulan and Macara, 2014; Salinas-Saavedra et al., 2015; St Johnston and Ahringer, 2010; Tepass et al., 2001).

There are two levels of epithelial cell polarity organization. First, epithelial cell polarity is clearly visible at the morphological level and characterized by the asymmetrical organelle distribution (Sekiguchi and Yamada, 2018; Tanos and Rodriguez-Boulan, 2008). Asymmetrically distributed cellular organelles, such as nucleus, endoplasmic reticulum, Golgi apparatus, secretory vesicles, cytoskeleton, cilia and microvilli, direct molecular trafficking, governing sorting and delivery of substances to the apical and basolateral membrane domains (Tanos and Rodriguez-Boulan, 2008). Second, epithelial cell polarity is also characterized by the asymmetrical localization of receptors, ion channels, molecule transporters and signaling proteins which are

organized into structurally and functionally distinct domains on the cellular membrane. Specialized adhesion complexes ensure polarity of epithelial cells: apical adhesion complexes in between cells, and basal adhesion complexes between cells and ECM. Adhesion complexes not only maintain cell-cell connections and attach cells to the ECM, preserving epithelial architecture and integrity. They also provide important cues for the polarization and asymmetry of epithelial cells (Eaton and Simons, 1995; Yeaman et al., 1999). Membrane receptors located on the basal side of the epithelium and interacting with ECM proteins are called integrins. They act as bidirectional signal transmitters between ECM and cells. ECM proteins act as a depot of the multiple growth factors. Interaction of cell receptors with ECM activates cell signaling and supports establishment and maintenance of the basal membrane epithelial domain (Roignot et al., 2013; Tanentzapf et al., 2000).

Apical adhesion complex: structure and role in cell signaling

The presence of the apical adhesion complex is a hallmark of any polarized epithelium. Apical adhesion complexes are belt-like junctions, which tightly interconnect epithelial cells around their apical cell margins. The apical adhesion complex sets up a border between apical and basolateral membrane domains, maintaining their distinct protein and lipid composition (Figure 1) (Apodaca et al., 2012). The adhesion belt is comprised of two cell junction types: tight junctions and *adherens* junctions. Despite the fact that *adherens* and tight junctions have always been historically considered as two discrete complexes, there is a high level of codependency between them (Campbell et al., 2017; Ikenouchi et al., 2007). *Adherens* and tight junctions are physically coupled and form a large protein complex, which recruits signaling molecules, polarity proteins and cytoskeletal modifiers. Close association of the adhesion complexes with cytoskeleton creates huge signaling clusters, providing biochemical and mechanical integrity of the tissue and of the entire organism.

Tight junctions function as a seal between adjacent epithelial cells. They restrict free molecule diffusion and control transport of substances through the intracellular space. Tight junctions also regulate lateral movement of lipids and proteins, and prevent mixing between apical and basolateral membrane compartments and maintain their unique molecular composition. *Adherens* junctions bridge cellular membranes of the neighboring cells and provide strong and flexible connections between cells stabilizing the epithelium.

Adherens junctions are tightly associated with polarity proteins. Polarity proteins are very conserved among Metazoa and play a fundamental role in maintaining and regulation of the apical-basal epithelial cell polarity. There are three major polarity complexes. The Crumbs complex and the Par complex (Par3,Par6, aPKC) localize at

the apical cell membrane; the Scribble complex (Scribble, Lgl, Dgl) is at the basolateral side of the cell (Figure 1). They antagonize each other as result of complex interactions of the apical and basolateral polarity regulators. Since Par-1 and aPKC have kinase activity, one of the mechanisms of the polarity regulation is phosphorylation-dependent inhibition. Basolateral polarity proteins Lgl, Numb, Mir have high affinity to bind a negatively charged cortical side of the plasma membrane due to the abundance of the positively charged domains. Phosphorylation of these sites by aPKC neutralizes the charges and directly prevents binding of the proteins to the apical cortex, maintaining them in the basolateral membrane. Phosphorylation can also change conformation of the targets, their activity and affinity to the other proteins (Hong, 2018). Conversely, Lgl inhibits aPKC kinase activity. These and many other regulatory mechanisms establish a unique apical and basolateral membrane identity (Riga et al., 2020; Royer and Lu, 2011).

Establishment and maintenance of epithelial polarity is a complex biological process, which remains an unsolved question in cell biology. A current model suggests that the formation of the primordial spot-like *adherens* junctions recruits actin bundle polymerization and MyosinII-driven contractions. This sequentially engages *adherens* and tight junctions components and triggers the assembly of polarity complexes, which in turn reinforce the maturation of adhesion junctions and strengthen the polarity (Baum and Georgiou, 2011; Roignot et al., 2013; Vaezi et al., 2002; Vasioukhin et al., 2000).

Although the exact hierarchy between apical adhesion complex and polarity complexes in establishing cell polarity is poorly understood, they have been shown to have reciprocal importance. It has been shown that the polarity proteins contain several domains, which are interacting with the proteins of the apical adhesion complex. Polarity proteins likely recruit multiple proteins, necessary for the cell adhesion complex maturation. Interference with any member of the polarity complexes leads to the defects in the apical junction formation (Roignot et al., 2013; Yamanaka et al., 2001). Therefore polarity proteins maintain cell adhesion junctions and thus are required for the formation and maintenance of the epithelium.

The core component of *adherens* junctions is the cell adhesion molecule cadherin. Cadherins cluster at the cell surface and their extracellular parts form homophilic interactions with other cadherin molecules of the neighboring cells, physically linking cells together. Although *adherens* junctions were originally appreciated as simple mediators holding cells together and maintaining tissue integrity, discoveries of dozens of different cadherin types, showed that cadherins are involved in numerous physiological processes and participate in multiple signaling pathways (Stepniak et al., 2009; Takeichi, 1988). At least 100 different cadherins are expressed within a single mammalian species. They include classical cadherins, Fats, protocadherins, Fat-like, Dachsous, Flamingo/CELSR, cadherin-related and desmosomal cadherin subfamilies (Hulpiau and van Roy, 2010; Peinado et al., 2004; van Roy, 2014; Yagi

and Takeichi, 2000). The best-studied cadherins are classical cadherins, which are expressed in almost all tissues, including epithelia.

Classical cadherins are transmembrane cell adhesion proteins. Extracellular cadherin domains of the adjacent cells interact with each other. The extracellular cadherin region consists of a varying number of so-called cadherin repeats, approximately 110 amino acids long, which are interacting in a calcium-dependent manner (Ivanov et al., 2001; Takeichi, 1995). The number of the extracellular cadherin repeats and the extracellular domain composition can vary drastically between species. On the contrary, the intracellular cadherin region has a very conserved structure among various animal phyla (Hulpiau and van Roy, 2010). The intracellular domain always includes binding sites for β-catenin and p120-catenin, which through α-catenin and other actin-binding proteins link adhesion complex to actin filaments (Figure 1) (Ozawa et al., 1990).

Catenins regulate strength and dynamics of cell adhesion through modulation of cadherin clustering and cytoskeletal binding (Reynolds and Roczniak-Ferguson, 2004; Yap et al., 1998). Besides connecting *adherens* junctions to the cytoskeleton, the cadherin-catenin complex plays an important role in activation of key signaling pathways (Nelson, 2004). Catenins have a dual function inside the cell: they are components of cell junctions and act as factors, which may regulate gene transcription. (Behrens, 1999; Daniel, 2007; Daniel and Reynolds, 1999; Daugherty et al., 2014). β-catenin is a major component of a canonical Wnt signaling pathway. Cadherins sequester β-catenin from the cytoplasmic pool to the membrane bound state and modulates its activity (Gottardi et al., 2001; Stockinger et al., 2001). Dissociation of *adherens* junctions can lead to increase of β-catenin in the cytoplasm. Cytoplasmic β-catenin translocates to the nucleus, where it acts as a transcription factor and together with its co-factors TCF and LEF activates transcription of the downstream genes, which control cell proliferation, differentiation, cell adhesion, cell migration and tissue morphogenesis (Clevers, 2006; Tian et al., 2011).

Furthermore, multiple studies showed that there are complex interactions between *adherens* junctions and EGFR/EGF, Notch/Delta, Eph/Ephrin, FGFR/FGF, Hippo/YAP signaling pathways (Bryant et al., 2005; Hatakeyama et al., 2014; Kim et al., 2011; Orsulic and Kemler, 2000; Qian et al., 2004; Sasaki et al., 2007; Schlegelmilch et al., 2011; Suyama et al., 2002; Williams et al., 1994; Williams et al., 2001). Receptors and their ligands predominantly localize to the apical cell junctions and form complexes with cadherins and other components of the *adherens* junctions. Cadherin homophilic binding recruits cadherin associated cytoplasmic partners to the cell-cell contacts, modulating signaling cascades, cortical tension and coordinating cell behavior (Aladin et al., 2020). Interaction of cadherins with signaling receptors and signaling pathways (Basilicata et al., 2016) makes cadherins important for morphogenesis independent of their differential adhesion and cell sorting properties (Basilicata et al., 2016). In addition to the classical biochemical signaling pathways,

adhesion molecules participate in sensing and transmitting the physical signals from the environment. Epithelial cells are subjected to the myriad of mechanical forces, including fluid shear stress in the blood vessels, hydrostatic pressure and compressive and tensile forces of the surrounding cells. Since *adherens* junctions are physically attached to actin filaments, cadherins join acto-myosin cytoskeleton networks and signaling machineries of individual cells into a coherent net and transmit mechanical forces and tensions of acto-myosin cell contractions across the epithelium in a coordinated manner, maintaining epithelial integrity. Mechanical forces applied to the cadherin junctions and intracellular signaling cascades can reciprocally largely regulate *adherens* junctions stability, dynamics of and their interaction with cytoskeleton (Gumbiner, 2000; Gumbiner, 2005; Maitre and Heisenberg, 2013). *Adherens* junctions and cadherin molecules in particular, act as sensors of various biochemical and physical stimuli, coming from the cell itself, from the environment and the neighboring cells. *Adherens* junctions transmit the signals in the outside-inside and inside-outside modes across the epithelium activating numerous signaling cascades. This allows cells to communicate to their close and remote neighbors and creates multiple feedback loops, which coordinate cell behavior, drives tissue remodeling and harmonize complex morphogenetic movements (Cavey and Lecuit, 2009; Perez-Moreno and Fuchs, 2006; Tian et al., 2011; Yap et al., 1998).

Epithelial tissue and its role in morphogenesis

Epithelium is a hallmark for all Eumetazoa. The emergence of multicellularity is closely associated with the appearance of *adherens* junctions and formation of epithelia. It was likely an important evolutionary event for the radiation of metazoans. The emergence of epithelium during evolution made cell communication and tissue integrity possible, which is important for diverse morphogenetic movements and it provided essential conditions to generate the large variety of shapes and morphological complexity among animals (Tyler, 2003; Yang and Weinberg, 2008).

Morphogenesis of all multicellular animals starts with the formation of a single epithelial layer. The epithelium forms immediately after the first successive zygote divisions, uniting blastomeres into a continuous layer and creating the first tissue of the embryo. The blastula stage of many metazoans has a simple spherical morphology usually with no obvious symmetry axes. The layer of blastomeres, called blastoderm surrounds a fluid-filled or a yolk-filled cavity. Blastoderm can be multilayered or monolayered. However, an outer layer remains an epithelium, which covers inner ‘mesenchymal’ layers of cells. Epithelial layer establishes an impermeable barrier, which separates an embryo from the environment, provides its physiological continuity and protects its stability. Cadherin junctions mechanically stabilize an embryo and enable its integrity. Integration and coupling of cells is an

important step for the next crucial morphogenetic event - gastrulation. During gastrulation the symmetry breaks and new complex shapes emerge within the initially simple and symmetrical embryo. The complex organization of the organism arises progressively. Throughout gastrulation cells separate into distinct groups and undergo multiple highly coordinated rearrangements, which lead to internalization of the surface cells and segregation of several embryonic germ layers. Successful gastrulation results in a proper position of the germ layers within an embryo. In the triploblastic Bilateria, the outer germ layer is called ectoderm; the inner germ layer is called endoderm; and middle germ layer is termed mesoderm.
Gastrulation can occur by different modes: by invagination of the epithelial sheet from one pole, by cell ingression from one or from multiple sites, or by delamination of the cell layer as a result of the oriented cell division. Morphogenetic movements of gastrulation are remarkably similar in a wide variety of organisms, in spite of the diverse body plans among the various animals (Wolpert, 1992).
The mode and the mechanics of gastrulation may differ depending on the egg size, amount of yolk and number of cell cleavages prior to gastrulation. Nevertheless, all gastrulation modes require cell migration, cell shape changes and cell rearrangements.

During gastrulation a large number of cells (in some cases a few cells) drastically change their shape, neighbors and position within the embryo. To successfully complete gastrulation, cells in different embryo regions must operate in a spatially and temporary highly coordinated manner. In all these processes, modulation of cell adhesion and rearrangement of cell-cell junctions plays a major role. Coupling via *adherens* junctions ensures communication between cells and coordinates apical constriction, elongation and shortening of the cells, leading to the deformation of the whole epithelial sheet. Stretching, bending and invaginations of the epithelial sheets arise new structures and dramatically change the dimensions and the shape of an embryo. Cell junction communication also synchronizes cell proliferation, cell differentiation and cell migration, which lead to the balanced tissue growth, tissue transformations and organ morphogenesis (da Silva and Vincent, 2007; Dumstrei et al., 2002; Fritz et al., 2013; Irvine and Wieschaus, 1994; Keller, 1980; Klezovitch and Vasioukhin, 2015; Perrais et al., 2007; Wei and Mikawa, 2000).

CELL ADHESION AND ITS REGULATION

Epithelial to mesenchymal transition – EMT

One of the central events during gastrulation and germ layer formation is epithelial to mesenchymal transition (EMT). Throughout EMT, immobilized epithelial cells undergo drastic morphological changes and convert into highly motile mesenchymal cells. EMT often starts with an apical constriction of epithelial cells. Apical

constriction plays a central role in gastrulation of many invertebrate and vertebrate animals (Keller et al., 2003; Kimberly and Hardin, 1998; Lee, 2003; Lee et al., 2007; Young et al., 1991). Fast phase of apical constriction occurs over cells across the epithelium, in a coordinated fashion, simultaneously with apical-basal elongation. In the final phase, cells shorten their apical-basal axes, broaden their basal ends, and become bottle–shaped. (Shook and Keller, 2003). Apical constriction initiates bending of the epithelium and shapes the primary invagination into the blastopore (Lee, 2011). It is followed by epithelial cell delamination: cells leave the epithelium and migrate through the ECM. After cell rearrangements and cell differentiation cells establish the germ layers re-forming the epithelia de novo (Cano et al., 2000; Nieto, 2002; Shook and Keller, 2003).

EMT is a widespread event in embryogenesis. Besides gastrulation EMT is involved in numerous tissue transformations and organ morphogenesis such as neural crest formation, cardiogenesis, decondensation of somites and parietal endoderm development in embryos, as well as in tissue growth, regeneration and pathological processes in the adults, such as cancer formation (Gumbiner, 2005; Halbleib and Nelson, 2006; Kim et al., 2017; Nieto, 2002; Romano and Runyan, 2000; Sefton et al., 1998; Thiery et al., 2009; Tian et al., 2011; Veltmaat et al., 2000).

In all tissue contexts EMT is characterized by change in cell adhesion, down-regulation of the key epithelial genes and activation of cell migratory and invasive genetic program. During EMT epithelial layer undergoes de-epithelialization, meaning disassembly of epithelial cell junctions, transcriptional repression of junction proteins, disruption of cell polarity complexes and loss of apico-basal cell polarity, reorganization of cytoskeleton and multiple protrusion formation on their basal side (Halbleib and Nelson, 2006; Nieto, 2002; Nieto et al., 2016; Thiery et al., 2009).

Cadherin switching

Cadherin switching is a process, in which cells change the expression of various cadherin isoforms at the *adherens* junctions. Cadherin switching can strongly influence the phenotype and behavior of the cells. Epithelial cells typically express E-cadherin, whereas more motile and less polarized mesenchymal cells normally express mesenchymal cadherins, in particular N-cadherin. Cadherin switching usually means that E-cadherin is down regulated and replaced by N-cadherin, but it can also refer to a situation, when two cadherins are co-expressed without a significant change in E-cadherin expression (Derycke and Bracke, 2004; Wheelock et al., 2008).

Down-regulation of the epithelial marker E-cadherin is a key event during EMT. E-cadherin repression reinforces the destabilization of existing *adherens* junctions and

prevents the formation of epithelial cell junctions *de novo* (Alves et al., 2009; Cano et al., 2000; Comijn et al., 2001; Nieto, 2002; Shook and Keller, 2003). Adhesion junction disassembly leads to the release of bound β-catenin and p120 catenin, which become available to activate Wnt/β-catenin and P13K pathways and function as transcriptional activators for cell proliferation. On the contrary, overexpression of cadherins can modulate Wnt/β-catenin signaling pathway possibly by beta-catenin sequestering (Ciruna and Rossant, 2001). As EMT progresses, Wnt/β-catenin and P13K pathways increase the expression of small GTPases Rac, Cdc42 and RhoA, which are central for to the cytoskeleton rearrangement, consequently leading to the transformation of cells from the adhesive into the motile state (Loh et al., 2019). N-cadherin establishes new, relatively weak cell junctions, which allow cell motility. Additionally, N-cadherin enables the stabilization of FGF receptor, which activates MAPK/ERK and PI3K pathways, subsequently enhancing cell survival and cell migration (Wheelock et al., 2008). E-cadherin can also interact with receptor tyrosine kinases FGFR and EGFR, inhibiting their activity (Bryant et al., 2005; Perrais et al., 2007; Qian et al., 2004).

Cadherin switching is often seen during normal embryonic development as well as in tumor progression. Cadherin switching plays a crucial role during ingression of the epiblast cells a in primitive streak during chick development (Hatta and Takeichi, 1986); during primordial germ cell migration and early gonad formation in mouse (Bendel-Stenzel et al., 2000); neural crest development (Niessen et al., 2011; Sauka-Spengler and Bronner-Fraser, 2008). N-cadherin expression activates endodermal cell migration (Ninomiya et al., 2012), promotes the commitment and differentiation of skeletal muscle precursor cells (George-Weinstein et al., 1997) and is required for the proper mesoderm differentiation (Schäfer et al., 2014). Interestingly, down-regulation of E-cadherin appears to be essential for the early stage of the EMT and up-regulation of N-cadherin is important for the later stages of development (Niessen et al., 2011; Sauka-Spengler and Bronner-Fraser, 2008). Loss of E-cadherin is also often involved in the formation of epithelial cancers, as it is a key event in metastasis. Up-regulated and imprecise N-cadherin expression in the cancer cells has been shown to induce cell migration and cell motility (Hazan et al., 2000; Loh et al., 2019; Nieman et al., 1999; Wheelock et al., 2008).

Cadherin role in cell movements and tissue morphogenesis

Along with qualitative differences in cadherin expression, quantitative differences in the cadherin levels can cause the segregation cell behavior (Duguay et al., 2003; Steinberg and Takeichi, 1994). Re-distribution and re-localization of cadherins in the cell can change cell morphology, behavior and an ability of the cell to move. The level of cadherin expression has been shown to be critical for the proper oocyte positioning in the egg chamber during *Drosophila* oogenesis (Godt and Tepass,

1998). Redistribution of cadherin molecules guides germ cell migration and plays a critical role in the initiation of cell motility (Kunwar et al., 2008). Differences in cadherin expression play an important role in the classical gastrulation movements such as epiboly, radial intercalation and convergent-extension. Down-regulation of C-cadherin during *Xenopus* gastrulation allows proper mesoderm intercalation movements (Brieher and Gumbiner, 1994; Zhong et al., 1999 in Schook ,2003). Overexpression or loss of cadherins lead to the severe gastrulation defects in terms of the cell movements, despite the normal embryo patterning and gastrulation completion (Babb and Marrs, 2004; Kane et al., 2005; Tepass et al., 2000; Zhong et al., 1999). Impaired cadherin function leads to defects in germ layer separation in *Xenopus* and elongation of the zebrafish embryo (Montero, 2005; Wacker et al., 2000).

One role of the cadherin switching is to allow a distinct cell population to separate from their neighbors. It has been shown in in vitro aggregation assays, that cells expressing different cadherins segregate from each other (Nose et al., 1988; Steinberg and Gilbert, 2004; Steinberg and Takeichi, 1994). Differential cadherin expression in adjacent cell population plays a crucial role in cell sorting, when cell physically segregate from each other forming distinct tissue compartments. Cadherins establish sharp boundaries between cell groups; demarcate the embryo and maintain tissue organization. There are several mechanisms which maintain and establish tissue border development: differential cell adhesion (Steinberg, 1970; Steinberg and Takeichi, 1994); differential cortical tension between different cell populations (Krieg et al., 2008) and cell repulsion, when cells actively migrate away from the site of heterotypic contact. Border establishment requires a close interplay of all these mechanisms, where cell adhesion plays a crucial role.

Snail as a conserved EMT and cadherin switching regulator

Cadherin expression and cadherin switching during EMT is modulated by a number of transcriptional factors, comprising members of Snail, ZEB and Twist families (Gheldof and Berx, 2013). The transcription factor Snail is one of the main regulators of EMT in bilaterian animals. Multiple studies indicate that Snail could be one of the ancestral EMT regulators (Nieto, 2002). Activation of Snail via major signaling pathways such as TGF-beta (Nodal)/BMP, Wnt, FGF, NANOS and MEK/ERK/ERG, induces apical constriction, *adherens* junctions disassembly and loss of epithelial cell polarity during EMT in morphogenesis of many vertebrate and invertebrate species (Barrallo-Gimeno and Nieto, 2005; Lim and Thiery, 2012; Nieto et al., 2016; Salinas-Saavedra et al., 2018; Shook and Keller, 2003).
Together with its relative transcription factors Slug and SIP1, in vertebrates Snail can directly bind to the promoter of E-cadherin and repress its transcription (Batlle et al., 2000; Comijn et al., 2001; Hajra et al., 2002; Yang and Weinberg, 2008). It has been

shown that cadherins are mainly redistributed through a combination of endocytosis and exocytosis which suggests a complex mechanism of cadherin density regulation (Delva and Kowalczyk, 2009; Ninomiya et al., 2012). Besides direct transcriptional cadherin repression, Snail positively regulates cadherin endocytosis, facilitating fast removal of cadherin molecules from the cell surface. Thereby Snail activates a second cellular mechanism, eliminating cadherin molecules during EMT (Wu and McClay, 2007). Down-regulation of E-cadherin leads to the expression of mesenchymal proteins such as non-epithelial cadherins (N-cadherin), ECM proteins and matrix metallopeptidases (MMP) (Alves et al., 2009; Cano et al., 2000; Comijn et al., 2001; Nieto, 2002).

Drosophila *snail* mutants show abnormalities in mesoderm formation; mesodermal cells retain epithelial features, overexpressing *E-cadherin*. *snail* mutants fail to undergo mesoderm invagination and have severe gastrulation defects (Carver et al., 2001; Leptin et al., 1992; Nieto, 2002; Oda et al., 1998). Contrary, ectopic Snail expression in mammalian epithelial cells activates an invasive behavior and a mesenchyme phenotype (Cano et al., 2000). *Snail* overexpression is sufficient to induce ectopic EMT (Fan et al., 2012). *Snail* overexpression in *Drosophila* leads to disassembly of *adherens* junctions in the ectoderm (Weng and Wieschaus, 2016).

MECHANICAL FORCES DURING MORPHOGENESIS

Morphogenesis is an extremely complex process, coordinated in time and three-dimensional space (Beloussov, 2016). It is a well-synchronized mechanism, where all embryo parts are connected and depend on each other. How morphogenesis is coordinated and how individual cells decide to activate a specific gene program and a curtain cell behavior, remaining a part of the whole, stays one of the most interesting questions in developmental biology.

Morphogenetic cell movements lead to the generation of multiple forces and tensions within the embryo as gastrulation proceeds (Heisenberg and Bellaïche, 2013). Most forces on a cellular level are generated by acto-myosin contractions. (Aguilar-Cuenca et al., 2014). The forces of acto-myosin cellular contractions control cell polarity, flow of regulatory molecules (David et al., 2010), distribution of PAR proteins (Aigouy et al., 2010; Munro et al., 2004), and stabilize cell-cell contacts (Shewan et al., 2005; Webb et al., 2004; Yamada and Nelson, 2007). Mechanical forces facilitate actin and ECM polymerization, unfolding the proteins and revealing cryptic binding sites for polymerization and signaling (Hirata et al., 2008; Kubow et al., 2015); cause cell division, elongation and cell shape change (Aguilar-Cuenca et al., 2014; Aigouy et al., 2010; Howard et al., 2011).

Cells undergoing EMT generate forces actively participating in the morphogenetic folding of the epithelium. First, these are the forces of the apical constrictions. Localization and activation of a highly contractile acto-myosin meshwork on the apical sides of cells is a common mechanism driving apical constriction in a wide variety of tissues and organisms (Keller et al., 2003; Kimberly and Hardin, 1998; Lee, 2011; Sawyer et al., 2010; Young et al., 1991). Mechanical forces affect the stability and position of the *adherens* junctions, therefore actively participating in EMT regulation. For example, acto-myosin tensions influence the E-cadherin endocytosis (Levayer et al., 2011), and pulsed actomyosin contractions temporary maintain *adherens* junctions in the mesoderm during gastrulation. Myosin contractions in *Drosophila* antagonize Snail activity, recruiting polarity proteins and stabilize the *adherens* junctions, preventing their early disassembly (Lecuit and Yap, 2015; Weng and Wieschaus, 2016; Weng and Wieschaus, 2017). In addition to the apical constriction, during gastrulation cells generate inward forces, orthogonal to the epithelia surface, through formation of the apico-basal myosin II cables. Prior delamination cells maintain strong cell-cell adhesion and create a pulling orthogonal force while constricting their apices, which constitutes a main driving force for epithelia folding and mesoderm invagination both in developmental conditions and in the context of ectopic Snail expression (Gracia et al., 2019).

Apical constriction is capable of bending the tissue and initiate gastrulation, however, additional morphogenetic movements are required to complete gastrulation. These morphogenetic movements include various coordinated cell deformations and collective cell rearrangements. Some morphogenetic movements differ among species (e.g., vegetal rotation and marginal zone involution in *Xenopus* or spreading of the enveloping cell layer over the yolk cell during zebrafish gastrulation) (Behrndt et al., 2012; Lee, 2011). Conserved cell rearrangements include cell ingression, cell intercalation and convergent extension (Cowan and Hyman, 2007; Jacinto et al., 2002; Lecuit and Lenne, 2007; Simske and Hardin, 2001; Skoglund et al., 2008; Zallen, 2007). All these processes subsequently result in morphogenesis – the process of emergence of the new shapes in the initially simple and symmetrical embryo.

Morphogenetic cell movements of gastrulation are not only establishing a shape of an embryo, they also provide information to the cells. Mechanical signals are necessary to induce a correct molecular cell identity during development when the symmetry of the blastula breaks and the embryo starts forming complex shapes. Morphogenetic movements are largely based on a biophysical feedback of the mechanical forces generated within different parts of the embryo, meaning that morphogenetic cell movements in one part of the embryo trigger and facilitate cell movements in the other embryo part (Beloussov, 2016). Cells perceive physical stimuli of mechanical pressure and pulling forces emerging by cytoskeleton contractions, changing osmotic pressure, fluid flow and ECM (Paluch and Heisenberg, 2009). The ability of cells to transduce mechanical stimuli into

biochemical signals is called mechanotransduction (Figure 2) (Chen, 2008; Lecuit et al., 2011; Wozniak and Chen, 2009). Thus, cell mechanics is originated in the cytoskeletal tensions and the tension propagates within the embryo depending on the resistance of the surrounding cells and ECM (Piccolo, 2013; Wozniak and Chen, 2009). Cadherin molecules together with other adhesion proteins and some ion channels comprise mechanosensors of the cell. Due to the adhesion junctions cells can better coordinate, drive cell sorting and transmit the signals across the epithelium (Krieg et al., 2008; Maitre et al., 2012). Depending on current state of the cell and its position within an embryo, each cell constantly receives and processes different biochemical and biophysical signals. At each specific time and space a cell makes a decision which differential path to take. If constraints defining cell development change, the fate of the cell differentiation in the new conditions can change as well (Kirillova et al., 2018; Waddington, 2014).

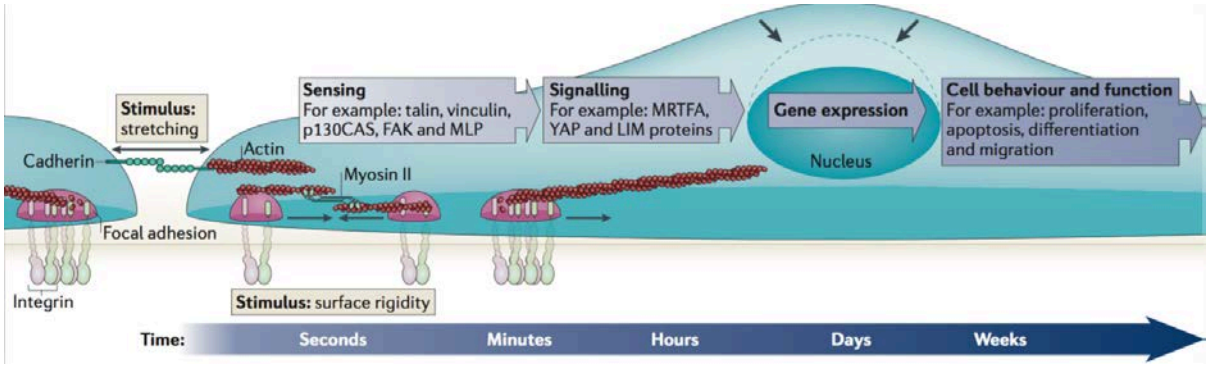

Figure 2. Mechanotransduction pathways. Mechanical stimuli of substrate rigidity, acto-myosin contractility or shear stress are converted into biochemical signals, regulating cell behavior and cell differentiation. Mechanotransduction pathways involve receptors at focal adhesions and cell–cell junctions (integrins and cadherins), mechanosensors (e.g. talin and p130CAS) and nuclear signalling factors, changing gene expression profiles. The timescale of mechanotransduction ranges from milliseconds to seconds for mechanosensor stretching, hours for change of gene expression, days for altered cell behavior, and weeks for tissue development. YAP, Yes-associated protein; MLP, muscle LIM protein; MRTFA, myocardin-related transcription factor A; FAK, focal adhesion kinase. After (Iskratsch et al., 2014).

Mechanical forces act extremely quickly – million times faster than the diffusion of signaling molecules or motor-driven vesicular transport, therefore biophysical forces play a crucial role in driving and coordinating morphogenesis (Howard et al., 2011).

EPITHELIA OF BASAL BRANCHING METAZOA

Cnidaria

Biochemical and mechanical signals transmit continuously through the cell-cell junctions. Epithelial tissue organization links cytoskeleton and signaling complexes of individual cells into a well-integrated net. The emergence of an epithelial tissue was proposed to be a primary building element for the evolution of metazoan complexity (Leys and Riesgo, 2012; Tyler, 2003). In a few model bilaterian organisms, whose epithelium has been studied, the structure of the epithelium and the molecular mechanisms of its establishment show significant similarity and seem to be conserved. Genomic analysis of different species proposes a typical epithelium organization for all Eumetazoa including Cnidaria and Ctenophores (Belahbib et al., 2018; Ringrose et al., 2013). It has been shown that the apical-basal epithelial cell polarity and cell adhesion complexes are present throughout different Metazoa (Cereijido et al., 2004; Fidler et al., 2017; Oda and Takeichi, 2011). However, more extensive comparative molecular and structural studies of basal Metazoa are needed to confirm this theory. Understanding of epithelia of the early branching non-bilaterian Metazoa can provide insight to the evolution of multicellularity, morphogenetic processes and germ layer establishment.

Cnidaria together with Ctenophora, Porifera and Placozoa belong to the group of basal Metazoa (Collins et al., 2005). Phylum Cnidaria includes five classes: Anthozoa (sea anemones, corals and sea pens), Hydrozoa (manine hydroids, hydra), Staurozoa (stalked jellyfishes), Scyphozoa (true jellyfishes) and Cubozoa (box-shaped jellyfishes) (Marques and Collins, 2004) (Kraus and Markov, 2016). Cnidarians are diploblastic animals meaning that during embryo development they form two germ layers, which later give rise to all organs and tissues: the outer ectoderm and the inner endoderm (also referred as endomesoderm). Bilateria are triploblastic animals: embryo forms three primary germ layers during the earliest stages of development. Evolution of germ layers and emergence of the third germ layer – mesoderm remain an unsolved question in developmental and evolutionary biology. Therefore, being the most closely related group to bilaterians, cnidarians became a widely studied group of model organisms for developmental and evolutionary biologists.

It has been shown that the cnidarian epithelium has a specific organization, which differs from the organization of the bilaterian epithelium. The cnidarian epithelium is characterized by a strong F-actin accumulation not only at the apical side of a cell but also at its basal side (Holz et al., 2017; Jahnel et al., 2014; Seybold et al., 2016). However, the structure of the epithelium in Cnidaria and its role in morphogenesis has been never studied in detail. Most of the knowledge on cell-cell adhesion in Cnidaria has been limited to genome analysis or biochemical studies (Clarke et al.,

2016; Hulpiau and van Roy, 2010). Despite numerous studies in Bilateria, which show that cadherins are the core components of *adherens* junctions and are associated with the regulation of morphogenesis, the role of cadherins in non-bilaterians was unknown. Understanding of the cellular mechanisms of epithelia formation, control of epithelial cell polarity, germ layer segregation and the role of cadherins at the base of metazoan tree can shed light on the evolution of these intriguing processes.

Nematostella vectensis – a cnidarian model organism

Historically, cnidarians were described as radially-symmetrical, diploblastic animals. However, recent studies in the sea anemone *Nematostella vectensis* have revealed a second body axis in *Nematostella* embryo suggesting that an ancestor of Bilateria and Cnidaria had a "bilaterian" symmetry (Rentzsch et al., 2006; Saina et al., 2009). These findings make *Nematostella* a very plausible model organism for the evolutionary and developmental studies.

The sea starlet anemone *Nematostella vectensis* has become the most extensively studied cnidarian in the last two decades (Figure 3).

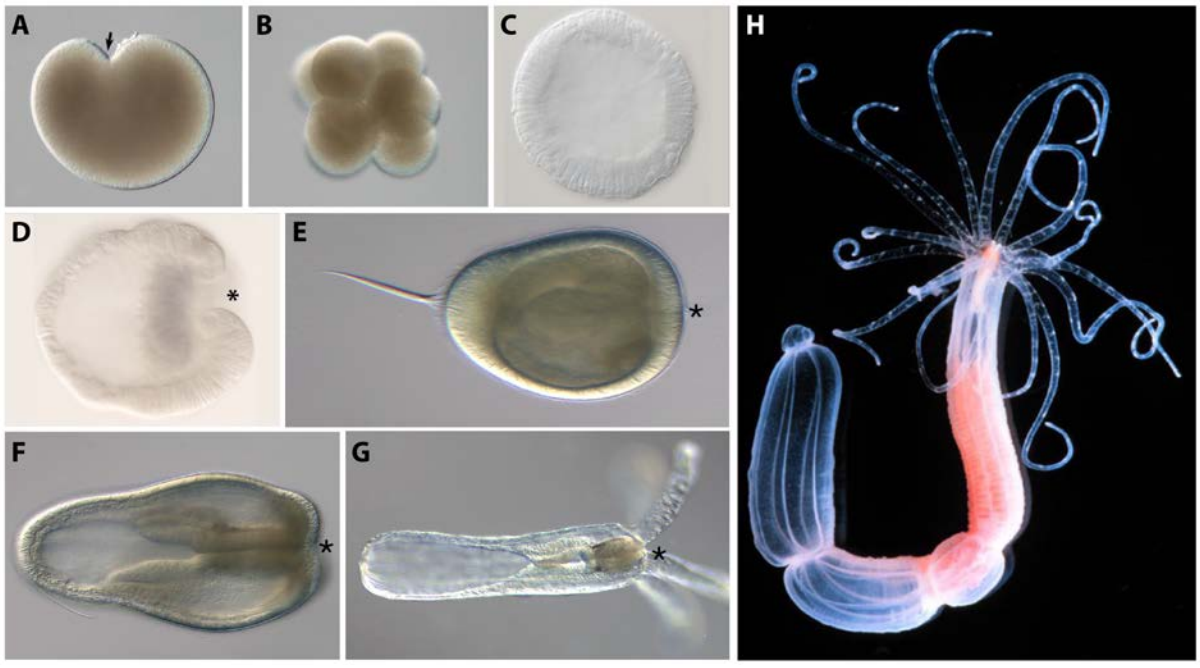

Figure 3. Life cycle of the starlet sea anemone *Nematostella vectensis.*
A. First zygote cleavage (arrow). **B.** Cleavage stage. **C.** Blastula. **D.** Gastrula. **E.** Planula. **F.** Metamorphosing planula. **G.** Primary polyp. **H.** Adult polyp. A star indicates an oral pole. After (Genikhovich and Technau, 2009).

It has gained rising research interest due to its key phylogenetic position, simple morphology, availability of the laboratory culture, and the vast amount of research tools, including mutant and transgenic lines, mutagenesis, gene knock-down, sequenced and annotated genome and transcriptome. Thus *Nematostella vectensis* is a new tractable model organism.

Nematostella vectensis is a small burrowing sea anemone living in estuarine habitats: coastal lagoons and salt marshes alone the cost of North America and the UK. *Nematostella* belongs to the Anthozoa, which represents the earliest branching class of Cnidaria (Collins et al., 2005) (Finnerty and Martindale, 1997). The morphology and development of *Nematostella* is relatively simple in comparison with the vertebrate animals. However, sequencing of *Nematostella* genome revealed its enormous complexity. *Nematostella* genome contains similar to mammals amount of protein coding genes, most major transcription factors and main signaling pathways components (Wnt, TGF-beta, FGF, Notch, Hedge hog) and a complex gene regulatory systems (Finnerty, 2004; Kusserow et al., 2005; Matus et al., 2007; Putnam et al., 2007; Rentzsch et al., 2006; Moran et al., 2014; Schwaiger et al., 2014). These studies have shown that there is no simple correlation between morphological and genomic complexity.

Ultrastructural analyses of *Nematostella* revealed the presence of cell-cell adhesion junctions, which resemble the *adherens* junctions in Bilateria, however, their molecular composition has never been investigated (Fritzenwanker et al., 2007). Bioinformatic analysis of the *Nematostella* genome revealed 16 different cadherin types, including two classical cadherins (and one putative pseudogene termed cadherin2) (Hulpiau and van Roy, 2010; Pukhlyakova et al., 2019). However the expression of cadherins in *Nematostella* and their role in adhesion, epithelia formation and morphogenesis has never been studied before.

AIMS OF THE STUDY

Epithelia in Bilateria and its role in morphogenetic processes are well studied. However, the organization of epithelia and a role of adhesion junctions in Cnidaria are largely unknown. The study of the epithelium structure and role of the cadherins - the key proteins for the epithelia polarity - during morphogenesis in Cnidaria, a sister group to Bilateria can provide a better understanding of the organization and function of the first true animal epithelium; its role during morphogenesis and the evolution of the cell adhesion molecules. In my doctoral thesis I addressed the questions: How is the epithelium of *Nematostella vectensis* organized? What is the role of cadherin molecules in epithelia formation, germ layer establishment and morphogenesis of *Nematostella*? I describe the role of the cadherin cell adhesion molecules in the partial EMT during gastrulation and further embryo development.

Paper I: A cadherin switching marks germ layer formation in the diploblastic sea anemone *Nematostella vectensis* (published in *Development*)

To understand a structure of the cnidarian epithelium and a composition of its adhesion junctions, I have generated specific antibodies against classical cadherins of *Nematostella*: Cadherin1 and Cadherin3. For the first time I have shown the subcellular localization of cadherin proteins and their role during development of a cnidarian embryo. In particular, I was able to show the organization and a role of *adherens* junctions in embryo morphogenesis, partial EMT and germ layer formation. I conclude, that despite of an unconventional protein structure of cadherins and a non-typical epithelia organization in Cnidaria, cadherins are the main components of *adherens* junctions in *Nematostella*. My results imply, that sea anemones and bilaterians independently duplicated cadherins during evolution and combinatorially use them for germ layer formation and tissue morphogenesis.

Paper II: β-catenin-dependent mechanotransduction dates back to the common ancestor of Cnidaria and Bilateria (published in *PNAS, Proceedings of the National Academy of Sciences of the United States of America*)

Epithelial morphogenesis and cell movements generate mechanical forces and tensions, which largely affect embryo development. The role of mechanical forces in morphogenesis has been extensively studied in bilaterian systems (Beloussov et al., 2006; Chen, 2008; Cram, 2014; Farge, 2003; Heisenberg and Bellaïche, 2013; Lecuit et al., 2011). However, the role of mechanotransduction in non-bilaterians is poorly understood. To gain knowledge about mechanotransduction in early branching non-bilaterian animals, I investigated mechanosensitive gene expression during *Nematostella* embryo development. I could show that epithelial morphogenesis and mechanical forces of gastrulation can affect gene expression, suggesting that mechanotransduction is an ancient gene regulatory mechanism, which was present in the ancestor of Cnidaria and Bilateria more than 600 *Mya*.

Paper III: Germ layer commitment and axis formation in sea anemone embryonic cell aggregates (published in *PNAS, Proceedings of the National Academy of Sciences of the United States of America*)

In this project we show that the aggregates of the dissociated *Nematostella* embryonic cells self-organize and re-establish germ layers *de novo* recruiting morphogenetic movements typical for the other far related cnidarians. We describe epithelialization and germ layer formation during cell aggregate development. Our results show that in the new developmental constrains, *Nematostella* embryo can take new developmental trajectories, showing the enormous plasticity of the embryonic cells and morphogenetic pathways.

RESULTS

PAPER I: “A CADHERIN SWITCH MARKS GERM LAYER FORMATION IN THE DIPLOBLASTIC SEA ANEMONE NEMATOSTELLA VECTENSIS”

Authors:
Ekaterina A. Pukhlyakova, Anastasia O. Kirillova, Yulia A. Kraus, Bob Zimmermann and Ulrich Technau

Status:

Published in *Development*, 2019, vol.146 (20), p. dev174623, doi:10.1242/dev.174623

Contributions:

E.A.P. and U.T. conceptualized the study and designed the experiments. E.A.P. performed the experimental work and analyzed the data. A.O.K. and Y.A.K. performed TEM imaging. B.Z. contributed to the phylogenetic analysis. E.A.P. and U.T. wrote the paper.

© 2019. Published by The Company of Biologists Ltd | Development (2019) 146, dev174623. doi:10.1242/dev.174623

RESEARCH ARTICLE

A cadherin switch marks germ layer formation in the diploblastic sea anemone *Nematostella vectensis*

Ekaterina A. Pukhlyakova[1], Anastasia O. Kirillova[1,2,*], Yulia A. Kraus[2], Bob Zimmermann[1] and Ulrich Technau[1,‡]

ABSTRACT

Morphogenesis is a shape-building process during development of multicellular organisms. During this process, the establishment and modulation of cell-cell contacts play an important role. Cadherins, the major cell adhesion molecules, form adherens junctions connecting epithelial cells. Numerous studies of Bilateria have shown that cadherins are associated with the regulation of cell differentiation, cell shape changes, cell migration and tissue morphogenesis. To date, the role of cadherins in non-bilaterians is unknown. Here, we study the expression and function of two paralogous classical cadherins, Cadherin 1 and Cadherin 3, in a diploblastic animal, the sea anemone *Nematostella vectensis*. We show that a cadherin switch accompanies the formation of germ layers. Using specific antibodies, we show that both cadherins are localized to adherens junctions at apical and basal positions in ectoderm and endoderm. During gastrulation, partial epithelial-to-mesenchymal transition of endodermal cells is marked by stepwise downregulation of Cadherin 3 and upregulation of Cadherin 1. Knockdown experiments show that both cadherins are required for maintenance of tissue integrity and tissue morphogenesis. Thus, both sea anemones and bilaterians use independently duplicated cadherins combinatorially for tissue morphogenesis and germ layer differentiation.

KEY WORDS: Cadherin, Cell adhesion, Morphogenesis, Germ layers, *Nematostella*, Cnidaria

INTRODUCTION

Morphogenesis is a process of tissue and organ formation during organism development (Gilbert, 2013) that is driven by coordinated cell shape changes, cell migration, cell proliferation, cell death and cell adhesion. The key morphogenetic events during early development are gastrulation, germ layer formation, folding of the neural tube and body axis elongation. Cadherins are transmembrane cell adhesion molecules that play an important role in these processes. They not only provide the mechanical connection between cells, but also control cell-cell recognition, cell sorting, tissue boundary formation, signal transduction, formation of cell and tissue polarity, cell migration, cell proliferation and cell death (Gumbiner, 2005; Halbleib and Nelson, 2006). In adult tissues, cadherins preserve stable and ordered tissue integrity (Angst et al., 2001; Halbleib and Nelson, 2006).

Classical cadherins are conserved molecules present in all animals whose genomes have been analyzed (Alberts, 2007). They are major components of the adherens junctions between cells, which are conserved structures of epithelial cells in most animals (Meng and Takeichi, 2009). In adherens junctions, cadherins form homophilic (more rarely heterophilic) calcium-dependent interactions with other cadherin molecules from neighboring cells. The cytoplasmic domain of cadherins is highly conserved among metazoans, distinguishing classical cadherins from other cadherin subfamilies (Hulpiau and van Roy, 2011; Oda and Takeichi, 2011). The cytoplasmic domain contains β-catenin and p120 binding sites. Catenins connect cadherins with the actin cytoskeleton in a dynamic manner (Meng and Takeichi, 2009). In comparison with other cadherin subfamilies, classical cadherins are unique in that they show the most noticeable variation in their extracellular region among different species (Hulpiau and van Roy, 2011). Indeed, the extracellular domain consists of a variable number of cadherin repeats of about 110 amino acids each and, depending on the species, laminin G and epidermal growth factor (EGF)-like domains.

During development, the regulation of specific cadherin expression correlates with the formation of new tissues. For instance, folding of the neural tube in vertebrates occurs in parallel with downregulation of epithelial cadherin (E-cadherin) and upregulation of neuronal cadherin (N-cadherin) (Nandadasa et al., 2009). Such cadherin switches are characteristic of several different morphogenetic processes, such as gastrulation and neural crest development (Basilicata et al., 2016; Dady et al., 2012; Detrick et al., 1990; Giger and David, 2017; Hatta and Takeichi, 1986; Pla et al., 2001; Rogers et al., 2013; Scarpa et al., 2015; Schäfer et al., 2014; Shoval et al., 2007). During mesoderm formation of *Drosophila melanogaster*, *Dme*_E-cadherin becomes replaced by *Dme*_N-cadherin (Oda et al., 1998), similar to the switch from E- to N-cadherin during mesoderm formation in chicken (Hatta and Takeichi, 1986). It has also been shown that N-cadherin expression triggers active endodermal cell migration, which leads to cell segregation and germ layer formation (Ninomiya et al., 2012). Moreover, a cadherin switch allows efficient Wnt, bone morphogenetic protein (BMP) and fibroblast growth factor (FGF) signaling, which are required for proper mesoderm differentiation in both the fruit fly and mouse (Basilicata et al., 2016; Giger and David, 2017; Ninomiya et al., 2012; Schäfer et al., 2014). For example, N-cadherin can interact with the FGF receptor and modulate the signaling pathway (Francavilla et al., 2009; Williams et al., 1994). Therefore, accurate control of the expression of cadherins is important for proper cell movements during

[1]Department for Molecular Evolution and Development, Centre of Organismal Systems Biology, University of Vienna, Althanstrasse 14, A-1090 Vienna, Austria. [2]Department of Evolutionary Biology, Biological Faculty, Moscow State University, Leninskie Gory 1/12, 119991 Moscow, Russia.
*Present address: Federal State Budget Institution 'National Medical Research Center for Obstetrics, Gynecology and Perinatology named after Academician V.I. Kulakov of the Ministry of Healthcare of Russian Federation', st. Academician Oparin 4, 117513 Moscow, Russia.

‡Author for correspondence (ulrich.technau@univie.ac.at)

E.A.P., 0000-0001-9498-3084; A.O.K., 0000-0003-4014-4618; Y.A.K., 0000-0003-1916-4200; U.T., 0000-0003-4472-8258

Received 12 December 2018; Accepted 12 September 2019

Development (2019) 146, dev174623. doi:10.1242/dev.174623

gastrulation (e.g. epiboly) and for convergence and extension of the tissue during axis elongation (Babb and Marrs, 2004; Basilicata et al., 2016; Shimizu et al., 2005; Winklbauer, 2012).

Although the role of cadherins has been studied in model bilaterian species, very little is known about their role in diploblastic organisms such as cnidarians. Most of our knowledge on cell adhesion molecules in cnidarians is restricted to genome analyses (Hulpiau and van Roy, 2009, 2011; Tucker and Adams, 2014) or biochemical studies (Clarke et al., 2016). During the last two decades, the sea anemone *Nematostella vectensis* has become one of the prime model organisms for studying embryonic development (Genikhovich and Technau, 2009a; Layden et al., 2016; Technau and Steele, 2011). Bioinformatic analysis of the available genome sequence of *Nematostella vectensis* (Putnam et al., 2007) revealed 16 different cadherins from all main groups of the cadherin superfamily (classical, flamingo, FAT, dachsous, FAT-like, protocadherins and cadherin-related proteins) (Hulpiau and van Roy, 2011). It has been shown that adherens junctions in *Nematostella* ultrastucturally resemble those in bilaterians (Fritzenwanker et al., 2007). However, the molecular composition of these junctions has not yet been described, and a recent report questioned the presence of adherens junctions in the inner layer of *Nematostella* (Salinas-Saavedra et al., 2018).

Germ layers are formed in *Nematostella* by invagination of the endoderm at the animal pole (Kraus and Technau, 2006; Magie et al., 2007). However, whether classical cadherins play a role in germ layer formation in non-bilaterians is not known. Here, we show that the classical cadherins of *Nematostella*, Cadherin 1 (Cdh1) and Cadherin 3 (Cdh3), form the adherens junctions of the epithelium of both germ layers. Germ layer differentiation in *Nematostella* is marked by a cadherin switch, whereby Cdh3 is downregulated in the inner endodermal layer and Cdh1 is upregulated and remains the only cadherin expressed in the endoderm. Unexpectedly, we found that, in addition to apical adherens junctions, both Cdh1 and Cdh3 are involved in cell junctions between cells on the basal-lateral side. Knockdown of *cdh1* and *cdh3* indicated important roles of cadherins in cell adhesion and tissue morphogenesis of this diploblastic metazoan.

RESULTS

Structure of classical cadherins of *Nematostella vectensis*

Three genes encoding classical cadherins have been predicted in the genome of *Nematostella vectensis*, *cadherin1*, *cadherin2* and *cadherin3* (*cdh1*, *cdh2* and *cdh3*) (Hulpiau and van Roy, 2011). However, our analysis of the *cdh2* gene model showed that it is a fusion of two separate gene models for which we have no evidence of its complete transcription; *cdh2* was not detectable by *in situ* hybridization. Furthermore, the hallmarks of the cadherin intracellular domain were absent. Therefore, *cdh2* could either be a pseudogene or the result of incorrect assembly. Hence, this gene model was not investigated further in this study.

Hulpiau and van Roy predicted 25-32 extracellular cadherin (EC) repeats for *Nematostella* cadherins (Hulpiau and van Roy, 2011). However, a more recent publication reported two cadherins with 14 and 30 EC repeats, respectively (Clarke et al., 2016). We cloned both Cdh1 and Cdh2 in overlapping fragments of 2-3 kb length, resulting in full-length cDNA clones of >13 kb, predicting a protein size of about 480 kDa for both cadherins. The protein model suggests a structure similar to classical cadherins, composed of a typical intracellular domain with binding sites for β-catenin and p120, and a large extracellular domain consisting of three EGF-like and two interspaced laminin G (LamG) domains, followed by 30 (Cdh1) or 31 (Cdh3) EC repeats (Fig. 1). This is similar to the original model of Hulpiau and van Roy and we therefore followed their gene terminology. By comparison, fruit fly cadherin has 17 EC repeats, chick cadherin 13 EC repeats and mouse cadherin only 5 EC repeats (Hulpiau and van Roy, 2011).

We also interrogated the genomes and transcriptomes of several other cnidarians and found that all investigated cnidarian cadherins have 30-32 EC domains and the EGF/LamG domains in the extracellular part. Notably, corals and hydrozoans had only a single classical cadherin, whereas the sea anemones underwent a lineage-specific gene duplication (Fig. 1; Fig. S1). Mammals have lost the extracellular EGF and LamG domains and have retained only a few EC domains (Hulpiau and van Roy, 2011). Interestingly, platypus has several paralogs of the short version with no EGF/LamG domains, typical for mammals, but also one classical cadherin with EGF/LamG domains and many EC domains, like other non-mammals. This suggests that an ancestral "long" cadherin gene duplicated in the ancestor of placental mammals and platypus and one of the duplicates underwent a drastic loss of EC and EGF/LamG domains. Platypus has kept both versions, whereas other mammals have retained only duplicates of the short classical cadherin version.

Expression of classical cadherins is highly dynamic during early development of *Nematostella*

To characterize the pattern of classical cadherin expression during normal development, *in situ* hybridization was performed on developmental stages from early cleavage through adult polyp. *cdh3* was maternally expressed at significant levels, detectable at the earliest cleavage stages. *cdh3* was then strongly expressed in all cells from the egg until the gastrula stage (Fig. 2A-D,M). During early gastrulation, *cdh3* expression decreased in the presumptive endoderm (Fig. 2B,C) and was completely downregulated in the endoderm by the planula stage (Fig. 2B-E).

By comparison, *cdh1* expression could not be detected by *in situ* hybridization until the early gastrula stage (Fig. 2G-I), although RNAseq data suggest that it is maternally expressed at lower levels (Casper et al., 2018). During gastrulation, *cdh1* expression first appeared and intensified in the pre-endodermal plate (Fig. 2H,I). At the late gastrula stage, *cdh1* started to be expressed in the aboral ectoderm and then expanded orally during planula development (Fig. 2J,K). Interestingly, at the late planula stage, the strongest *cdh1* expression was detected in the endoderm and in a subpopulation of ectodermal cells, which gave rise to a sensory apical organ (Fig. 2K).

In primary polyps, *cdh3* expression remained strongly expressed in the tentacles and pharynx but weakly in the body-wall ectoderm (Fig. 2F). Interestingly, *cdh3* in juveniles and adults was detectable only in the ectoderm of the pharynx and tentacles, ciliated tract, septal filaments and developing eggs, with hardly any expression in the body-wall ectoderm (Fig. S2A,B). Almost complementary to that, *cdh1* was expressed both in the ectoderm and endoderm, but was completely excluded from the ectoderm of the pharynx and tentacles (Fig. 2L). In juveniles, *cdh1* was expressed in the endoderm and body-wall ectoderm, but not in the ectoderm of most of the pharynx. Interestingly, the part of the pharynx carrying siphonoglyph and the ciliary tract below the pharynx specifically expressed low levels of *cdh1* (Fig. S2C-H). In adults, *cdh1* was expressed in the body-wall endoderm and in small oogonia (Fig. 2N; Fig. S2I).

Development (2019) 146, dev174623. doi:10.1242/dev.174623

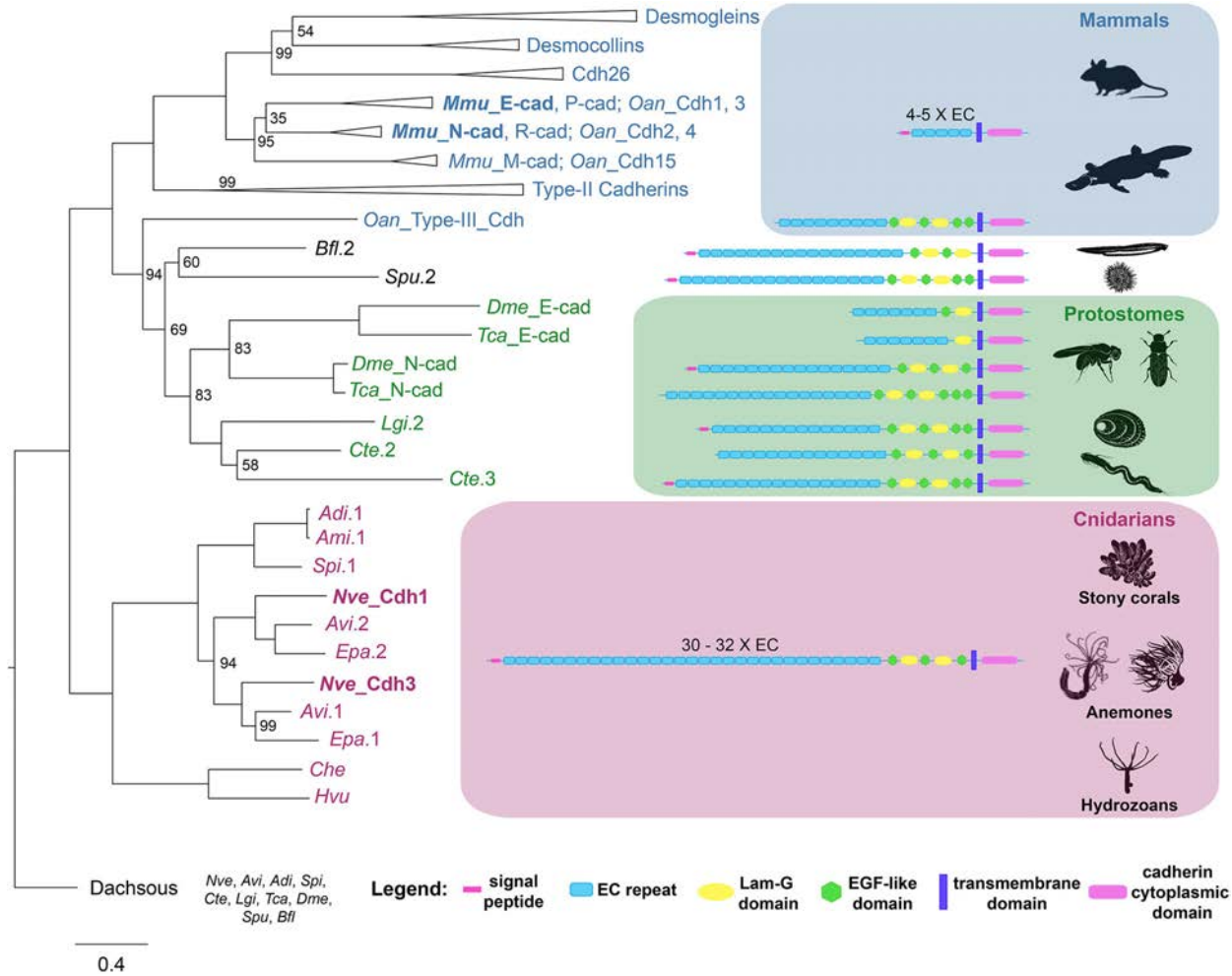

Fig. 1. Maximum likelihood phylogenetic tree of classical and other cadherins. Sequences of all proteins containing a cytoplasmic cadherin domain were extracted from the genomes and transcriptomes of *Mus musculus* (*Mmu*), *Ornithorhynchus anatinus* (*Oan*), *Branchiostoma floridae* (*Bfl*), *Drosophila melanogaster* (*Dme*), *Tribolium castaneum* (*Tca*), *Capitella teleta* (*Cte*), *Lottia gigantea* (*Lgi*), *Nematostella vectensis* (*Nve*), *Anemone viridis* (*Avi*), *Exaiptasia pallida (Epa), Acropora millepora* (*Ami*), *Acropora digitifera* (*Adi*), *Stylophora pistillata* (*Spi*) *Clytia hemisphaerica* (*Che*) and *Hydra vulgaris* (*Hvu*). Proteins with no annotation in their respective databases were assigned an arbitrary number. All gene names are based on the annotations of the respective database, except for *Oan* type-III Cdh, *Nve* Cdh1 and *Nve* Cdh3, which were annotated based on the findings of Hulpiau and van Roy (2011). Dachsous cadherin proteins, which also contain a cytoplasmic cadherin domain, were used as an outgroup. The number at the nodes indicates the bootstrap support; nodes with no label have 100% support. Domain organization is shown on the right. Some proteins lack a signal peptide. This is either an indication of a truncated protein (e.g. *Che*, *Avi*) or a result of assembly mistakes in a gene model.

Cdh3 is the main component of adherens junctions during cleavage and gastrulation

We wished to visualize the subcellular localization of Cdh3 protein during development. We generated specific polyclonal and monoclonal antibodies against two recombinant fragments of Cdh1 and three peptides of Cdh3, respectively (Fig. S3). All antibodies against the different fragments and peptides consistently showed the same pattern for Cdh1 and Cdh3, respectively (Fig. S4) (Madeira et al., 2019). Immunocytochemistry experiments were carried out at all stages of development. Cdh3 protein had already accumulated at the apical cell junctions at the first cell divisions, suggesting a role in establishing early cell polarity. It was also detectable in less confined areas at the lateral contacts between cells (Fig. 3A-C). Interestingly, cells maintained their polarity during cell divisions. In contrast to the Par system proteins (Ragkousi et al., 2017; Salinas-Saavedra et al., 2018), Cdh3 stayed localized at the apical cell junctions at different cell cycle stages (Fig. 4). It is possible that the polarized Cdh3 at the junctions guides the Par system proteins during their transient loss of polarity during cell division. Later, during blastoderm formation, apical cell junctions became more pronounced (Fig. 3D-F). Strikingly, we found that Cdh3 also localized on the basal-lateral side of the cells (Fig. 3D-L), in addition to the apical localization. Ultrastructural analysis by transmission electron microscopy (TEM) revealed that the cell-cell junctions at the basal side resembled the adherens junctions at the apical side (Fig. 3M,N). However, during the blastula stage, asynchronously dividing cells transiently lost the basal-lateral localization of Cdh3 (Fig. 3E, yellow star), similar to the early cleavage stage, when cells divided synchronously (Fig. 3B,C, Fig. 4). Thus, *Nematostella* has a unique epithelium, where cells form cell-cell contacts on both apical and basal sides. These Cdh3-positive junctions developed before any contact to an endodermal

Development (2019) 146, dev174623. doi:10.1242/dev.174623

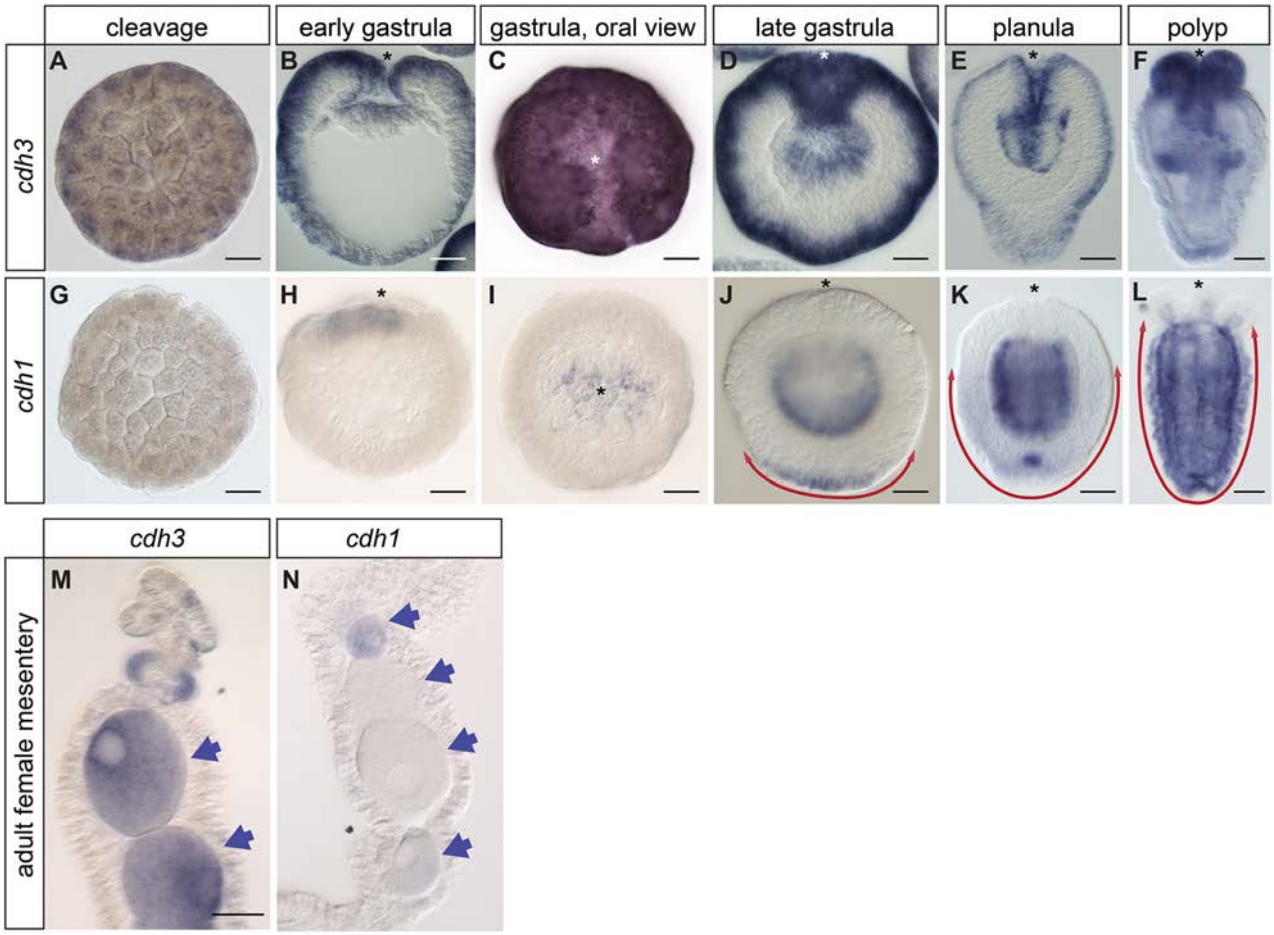

Fig. 2. Expression of *cdh3* and *cdh1* is highly dynamic during early development and polyp growth. (A,G) Cleavage. (B,H) Early gastrula, lateral section. (C,I) Early gastrula, oral view. (D,J) Late gastrula, lateral section. (E,K) Planula, lateral section. (F,L) Primary polyp. (M,N) Adult mesentery section. Double-headed red arrows show expansion of *cdh1* expression on the aboral pole. Arrows indicate the eggs. Asterisk indicates an oral pole. Scale bars: 50 µm in A-L; 100 µm in M,N.

layer or presence of the mesoglea, the extracellular matrix of Cnidaria. This is remarkable and, to our knowledge, has not been described in any other animal. Interestingly, as the pre-endodermal plate began to invaginate and the cells adopted a partial epithelial-to-mesenchymal transition (EMT) phenotype, Cdh3 disappeared from the basal junctions of the invaginating cells (Fig. 3G-I). Meanwhile, ectodermal cells of the blastoderm retained both apical and basal cell contacts. As the pre-endodermal cells lost basal junctions, its epithelium became less rigid and columnar. Pre-endodermal cells formed filopodia and became more motile on the basal side (Fig. 3O). This event is possibly one of the crucial steps of the incomplete EMT, which pre-endodermal cells undergo during gastrulation (Kraus and Technau, 2006; Salinas-Saavedra et al., 2018). Notably, apical cell junctions expressing Cdh3 were preserved in the pre-endodermal cells during the course of gastrulation (Fig. 3J-L).

After the invagination process was complete, Cdh3 fully disappeared from the cell junctions of the endoderm, concordant with the decrease in mRNA expression in the whole endoderm (Fig. 2C-F). Cdh3 remained expressed exclusively in the ectoderm, forming apical and basal cell junctions (Fig. 5A-E). Notably, although the boundary between ectoderm and endoderm is very difficult to discern by morphological criteria, Cdh3 localization at the cell junctions in the pharynx precisely marked the boundary between the last ectodermal cell and the first endodermal cell (Fig. 5B,E). At the polyp stage, Cdh3 remained exclusively expressed in the ectoderm, with especially strong expression in the pharynx and tentacles (Fig. 5F,G).

Cdh1 protein expression marks a cadherin switch during endoderm formation

After completion of gastrulation, Cdh1 protein formed pronounced cellular junctions. In early planula larvae, Cdh1 localized to the apical and basal junctions of the endoderm (Fig. 6A-D). Hence, formation of the endoderm was marked by a cadherin switch from Cdh3 to Cdh1.

It should be noted that the transcriptome data suggested some maternal deposition of *cdh1* in the embryo, even though *in situ* hybridization did not detect *cdh1* until the gastrula stage. Indeed, the anti-Cdh1 antibody detected a fuzzy signal beneath the apical cell membrane in all cells at the early gastrula stage, which might be maternal Cdh1 protein that had not yet localized to the cell junctions.

In addition to endodermal expression, Cdh1 was strongly expressed in the apical organ ectoderm and then expanded into a wider domain in the aboral ectoderm, where Cdh1 and Cdh3 were

Development (2019) 146, dev174623. doi:10.1242/dev.174623

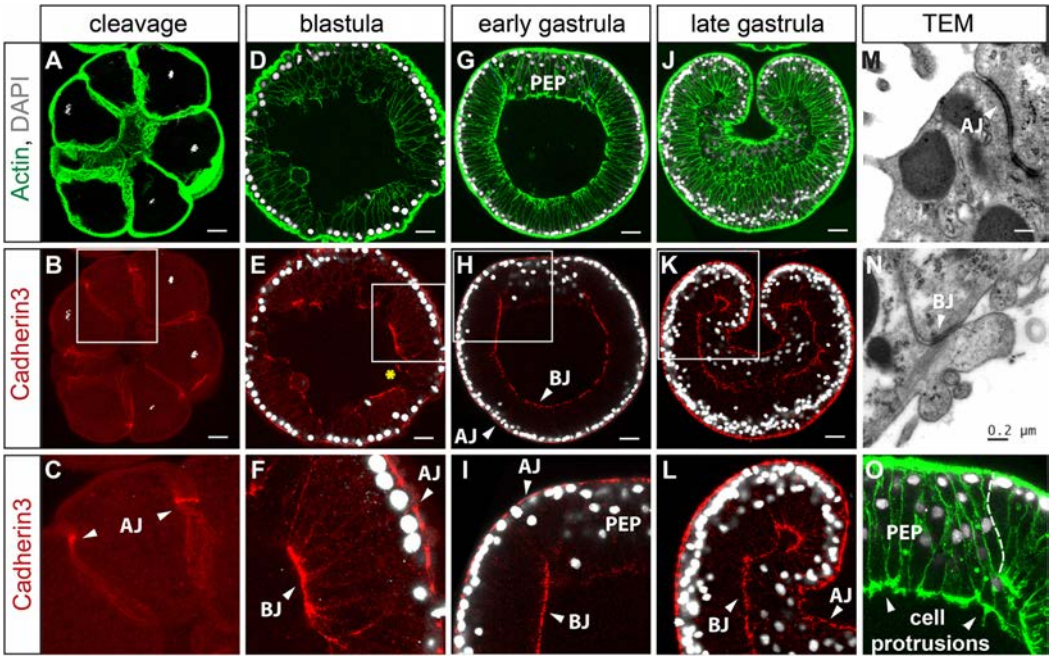

Fig. 3. Cdh3 is a major component of adhesion complexes during cleavage and gastrulation. (A-F) Besides apical junctions (AJ), strong basal epithelial contacts (BJ) form in the blastula during epithelialization. Yellow asterisk is located next to the dividing blastula cell. (G-I) As the pre-endodermal plate (PEP) starts to invaginate, Cdh3 disappears from the BJs and decreases in the AJs in the PEP. Ectodermal cells preserve both apical and basal cell contacts. (J-L) Late gastrula. AJs are present in the ectoderm and in the endoderm. C,F,I,L,O are enlargements of the boxed areas shown in B,E,H,K,G, respectively. (M,N) TEM images of the *Nematostella* epithelium. (O) Cell protrusions on the basal side of the PEP. Scale bars: 20 µm in A,B,D,E,G,H,J,K,O; 0.2 µm in M,N.

co-expressed (Fig. 6). At the ectodermal surface, expression of Cdh1 decreased along a gradient toward the oral pole (Fig. 6L). Interestingly, the ectodermal cell population that gave rise to the apical tuft was also different from the rest of the ectoderm in terms of cadherin expression. These cells lost Cdh3 basal junctions, but kept the apical junctions (Fig. 5C). This specific arrangement might be connected with the special function of these cells (Fig. S5). Indeed, the loss of Cdh3 expression in the ectodermal apical tuft cells went hand-in-hand with upregulation of Cdh1 in these cells (Fig. 2K, Fig. 6A,C).

We have demonstrated that Cdh3 is the major component of adhesion complexes during cleavage and gastrulation and is present in all cells until the late gastrula stage. Cdh3 formed apical and basal cell junctions in the blastodermal epithelium, which during invagination of the pre-endodermal plate disappeared from basal cell junctions of the future endoderm. Further endoderm differentiation led to complete Cdh3 to Cdh1 replacement. Therefore, there is a distinct boundary between ectoderm and endoderm, which is defined by the localization of Cdh1 and Cdh3.

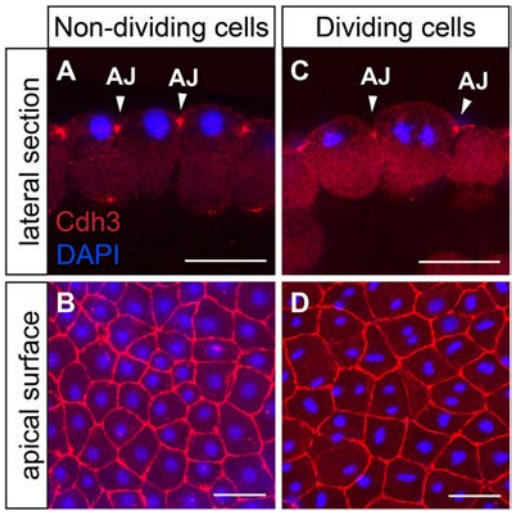

Fig. 4. Cdh3 apical junction localization and cell polarity are preserved during cell division. (A,B) Non-dividing blastula cells. (C,D) Dividing blastula cells at different mitotic phases. AJ, apical junction. Scale bars: 25 µm.

Cdh3 in apical ectodermal junctions co-localize with β-catenin

A recent biochemical study showed that the intracellular domain of classical cadherins can form a ternary complex with α-catenin and β-catenin (Clarke et al., 2016). To explore further the molecular composition of the cadherin cell junctions, we co-stained *Nematostella* embryos with the antibody against Cdh3 and with the previously described *Nematostella* antibody against β-catenin (Leclère et al., 2016; Salinas-Saavedra et al., 2018). At blastula stage, Cdh3 was co-localized with β-catenin at the apical junctions, whereas basal junctions did not show such pronounced co-localization (Fig. 7A-C,G-I). Interestingly, at the planula stage, β-catenin was detected only in the body wall ectoderm but not in the ectodermal pharynx nor the endoderm (Fig. 7D-F; Fig. S6). These results could mean that not all the cell contacts of *Nematostella* epithelium contain β-catenin, in line with other recent findings (Salinas-Saavedra et al., 2018). This is surprising, as no ultrastructural differences in the junctions of endoderm and ectoderm could be detected (Fig. S7).

Development (2019) 146, dev174623. doi:10.1242/dev.174623

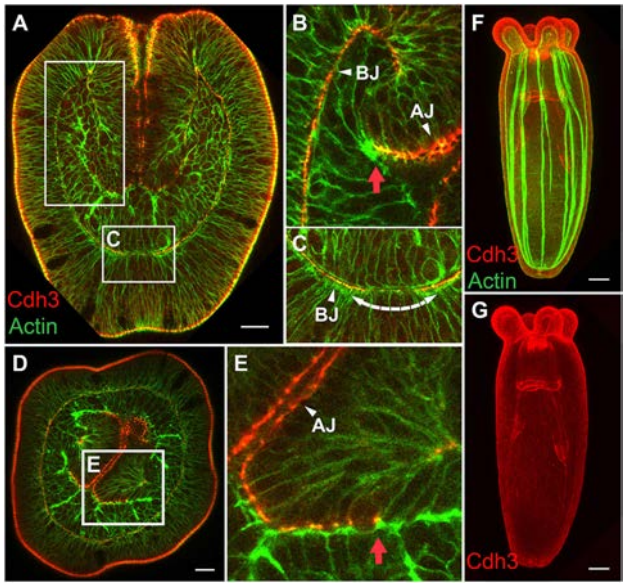

Fig. 5. Cdh3 marks the boundary between ectoderm and endoderm. (A-C) Lateral section of planula. B,C are enlargements of the boxed areas shown in A. (D,E) Cross-section of planula. Ectodermal-endodermal boundary in the pharynx is distinctly labeled by Cdh3 localization in the cell junctions. E is an enlargement of the boxed area shown in D. (F,G) Primary polyp. Cdh3 is expressed exclusively in the ectoderm, forming apical and basal adherens junctions. Red arrow indicates the boundary between the last ectodermal cell and the first endodermal cell. AJ, apical junction; BJ basal junction. Scale bars: 20 µm.

Function of classical cadherins in early development

To examine the function of cadherins, we performed knockdown experiments using morpholinos (MOs) and short hairpin RNA (shRNA). First, we injected independently two non-overlapping translation-blocking *cdh3* MOs. However, we could still detect Cdh3 in apical and basal cell junctions in the whole mount MO-injected embryos (Fig. 8). Indeed, on the ultrastructural level, the adherens cell junctions looked similar in morphants and in control embryos (Fig. 7D,H; Fig. 8C,G). These results can be explained by the significant maternal deposition of mRNA and protein (Figs 2M, 3B). However, development of Cdh3 morphants was arrested after the gastrula stage, presumably due to the block of translation of zygotically expressed *cdh3*. As a result, when Cdh3 protein became limited, post-gastrula embryos were unable to develop further (Fig. 8A,B).

The mild knockdown effect on the presence of Cdh3 in the junctions also suggests that there is relatively little turnover in established junctions. Therefore, to assess the function of Cdh3 in establishing new cell junctions we used an aggregate assay. *Nematostella* gastrulae can be dissociated into single cells and small clusters and can be re-aggregated by centrifugation into cell aggregates (Kirillova et al., 2018). We followed the establishment of cell contacts and the formation of the epithelium in developing cell aggregates (Fig. 9). Dissociated cells did not show any signs of polarization: Cdh3 was not localized to any side (Fig. 9C). Cdh3 became localized to the apical side of the outer cells of the aggregate only 30 min after re-aggregation, and the first signs of epithelialization became apparent (Fig. 9E,F,M). At 12 h after re-aggregation, the outer epithelial layer was completely formed and Cdh3 was localized at the apical and basal cell junctions (Fig. 9H,I). We have previously reported that the two epithelial layers (ectoderm and endoderm) are formed 24 h after re-aggregation (Kirillova et al., 2018). Both cell layers possessed basal and apical cadherin cell junctions (Fig. 9K,L,S). Cdh1 began to be expressed in both ectoderm and endoderm at 24 h of aggregate development (Fig. 9N,Q,T,W). Similar to the normal embryo, the ectoderm expressed both Cdh1 and Cdh3, whereas the endoderm expressed exclusively Cdh1 (Fig. 9U,X).

To address the question of how Cdh3 downregulation influences the establishment of new cell contacts in the aggregate, we dissociated equal amounts of *cdh3* MO-injected gastrulae and standard MO-injected gastrulae (as a control). The first difference we observed was that the size of the aggregates from *cdh3* morphant cells was significantly smaller than control aggregates ($P<0.0001$) (Fig. 10M-O). Moreover, aggregates from *cdh3* MO-injected embryos started to fall apart into cells immediately after re-aggregation (Fig. 10; Movies 1 and 2). Cdh3 knockdown in the aggregate at the protein level was shown by immunostaining (Fig. 10I,J). Ultrastructural imaging with TEM confirmed that cells in Cdh3 MO aggregates did not form well-defined subapical adherens junctions, whereas cell contacts were well developed in the control aggregate (Fig. 10K,L). Interestingly, cells in the Cdh3 MO aggregates made lamella-like protrusions extending to the neighboring cell on the apical surface (Fig. 10K). These results show that *cdh3* knockdown impairs the *de novo* formation of cell contacts, although it does not affect the earlier established contacts built from the maternal protein.

To further explore the role of Cdh1 protein, we downregulated *cdh1* using an independent approach, shRNA-mediated knockdown (He et al., 2018). As in MO knockdown, shRNA knockdown led to a significant decrease in Cdh1 protein, as assayed by immunohistochemistry (Fig. 11; Fig. S8). Although early development (including gastrulation) appeared largely unaffected, mesenteries did not form upon *cdh1* knockdown in the subsequent planula stage. In all MO- and shRNA-injected embryos, mesenteries were absent or impaired, whereas eight mesenteries developed in all control embryos at this stage (Fig. 11, Fig. 12D,H).

In addition to the predominant expression in the endoderm, *cdh1* was also expressed in the apical tuft region of the ectoderm (Fig. 2K). Interestingly, *cdh1* knockdown abolishes expression of FGFa1, which is responsible for apical organ development (Rentzsch et al., 2008). In most *cdh1* MO-injected embryos, the apical organ did not form and there was lack of *FGFa1* expression (Fig. 12). These results suggest that Cdh1 is crucial for morphogenesis and differentiation of the endoderm as well as for development of the apical organ.

DISCUSSION

Evolution and structure of cadherins

Although proteins with cadherin domains are present in choanoflagellates, cadherins with intracellular catenin binding domains are an important class of cell adhesion molecules that arose only in metazoans (Nichols et al., 2012). Cadherins mediate not only cell adhesion between epithelial cells, but are strongly involved in the differentiation of specific cell types. Recently, cadherins have also been shown to convey mechanotransduction (i.e. activation of gene expression in the nucleus in response to mechanical stress), which is mediated by β-catenin in *Drosophila* and *Nematostella* (Iyer et al., 2019; Pukhlyakova et al., 2018; Röper et al., 2018). However, most studies on the role of cadherins have been carried out in bilaterian model organisms such as mouse or *Drosophila*. Here, we show the localization and function of both classical cadherins in a representative of the Cnidaria, the sea anemone *Nematostella vectensis*. Phylogenetic analysis suggests

Development (2019) 146, dev174623. doi:10.1242/dev.174623

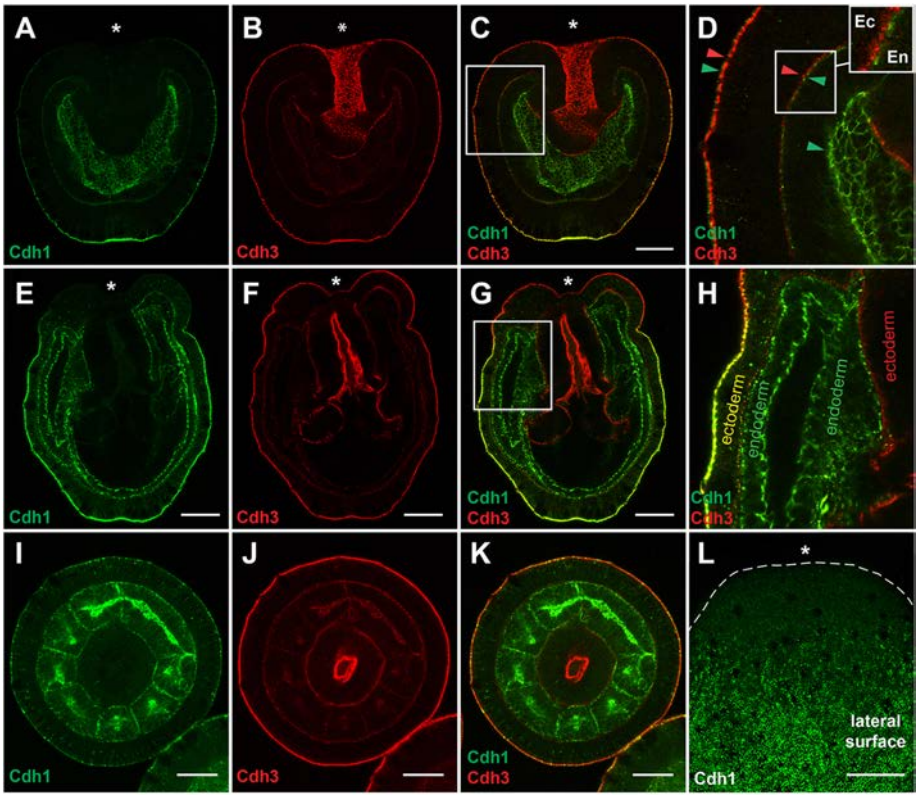

Fig. 6. Cdh1 and Cdh3 localization during germ layer differentiation. (A-D) Planula lateral section. D is an enlargement of the boxed area shown in C. (E-H) Lateral section of the primary polyp. H is an enlargement of the boxed area shown in G. (I-K) Planula cross-section. (L) Surface of the planula; the oral part of the ectoderm is free of Cdh1. Cdh1 is localized in the apical and basal junctions of the endoderm, as well as in the apical junctions and basal junctions of the aboral ectoderm, especially in the area of the apical organ. Cdh1 is gradually disappearing from the ectoderm toward the oral pole and completely excluded from the ectoderm of the tentacles and the pharynx. Cdh3 is localized to the apical and basal junctions of the body wall ectoderm, the ectoderm of the pharynx and is completely excluded from the endoderm. Asterisk marks an oral pole. Scale bars: 50 µm.

that sea anemones have duplicated an ancestral classical cadherin, whereas corals and hydrozoans have retained a single copy. The two investigated cadherin genes code for large proteins with 31-32 EC domains each, largely confirming previous predictions from the genome (Hulpiau and van Roy, 2011) and gene models based on our transcriptome assembly (Fredman et al., 2013). This significantly extends the structure of the recently published gene model for Cdh3 (termed Cad1 in Clarke et al., 2016). Thus, the classical cadherins of cnidarians and other non-bilaterians are substantially larger than those of most bilaterians and their extracellular domain structure is

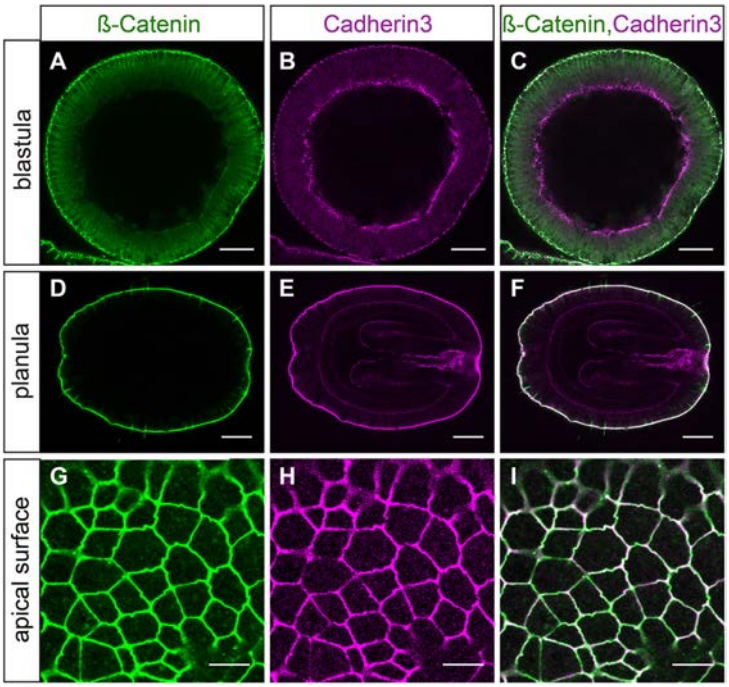

Fig. 7. Cdh3 and β-catenin are co-localized at the apical cell junctions of the ectoderm. (A-C) blastula stage. (D-F) planula stage. (G-I) Apical surface of the ectoderm. Note that only weak β-catenin staining can be detected at the basal ectodermal junction and none in the endoderm. Scale bars: 50 µm in A-F; 10 µm in G-I.

Development (2019) 146, dev174623. doi:10.1242/dev.174623

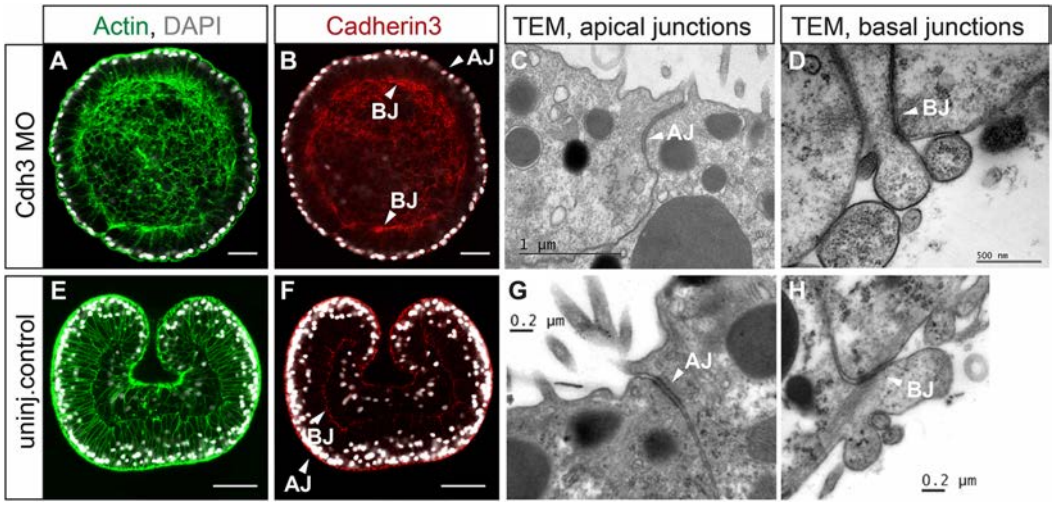

Fig. 8. Cdh3 knockdown blocks gastrulation movements. (A-D) Cdh3 MO-injected embryos at 28 h post-fertilization (hpf). (E-H) Control embryos at 28 hpf. Apical (AJ) and basal (BJ) cell junctions of Cdh3 morphants look very similar to the cell junctions of the control gastrulae. Scale bars: 40 µm in A,B,E.F.

reminiscent of the FAT-like proteins (Hulpiau and van Roy, 2009, 2011). It will be interesting to determine which extracellular domains are engaged in homophilic or heterophilic interactions.

Cadherins are localized to apical and basal junction in both germ layers

Interestingly, both cadherins localized to apical junctions as well as to basal cell-cell junctions in the epithelial cells of both ectoderm and endoderm (Fig. 13A). Electron and confocal microscopy analyses showed actin filaments attached to the junction, suggesting that these are adherens junctions (Fig. 3G,N, Fig. 8D,H). This is in contrast to a recent study claiming that the endodermal epithelium does not contain adherens junctions, since neither Par complex components nor β-catenin could be detected (Salinas-Saavedra et al., 2018). Yet, in line with this study (Salinas-Saavedra et al., 2018), we could detect β-catenin in the apical adherens junctions and weakly in the basal junction of the ectoderm, but not in the pharyngeal ectoderm and the endoderm (Fig. 7; Fig. S6). This could indicate that the basal junctions in the ectoderm and all endodermal junctions are qualitatively different. However, apical adherens junctions in the ectoderm and endoderm have a very similar structure at the ultrastuctural level (Fig. S7). As we observed co-localized actin fibers at these junctions, we assume that another protein replaced β-catenin or that β-catenin was not detected at these junctions. Indeed, we note that the antibody also failed to stain nuclear β-catenin after early cleavage stages. Therefore, as a cautionary note, we cannot fully rule out that the failure to stain β-catenin in the pharynx and the endoderm was due to technical reasons.

To our knowledge, the basal-lateral junctions involving specific cadherins have not yet been described in other animals, but fuzzy basal-lateral localization of cadherins has been observed in other systems. For instance, the midgut epithelium of *Drosophila* shows a basal-lateral localization of a cadherin (Chen et al., 2018), albeit much less defined than described here for *Nematostella*.

Basal junctions might be an innovation of Cnidaria and play a crucial role in morphogenesis of the epithelium. Formation of the basal junctions might be connected to the special properties and functions of the cnidarian epithelium. For example, Hydra epithelia are composed of multifunctional epithelio-muscular cells. These cells form basal myonemes, connected between neighboring cells by desmosomal-like junctions (Seybold et al., 2016). These basal connections could be associated with the contractile actin bundles and used for the increased synchronized contractile activity within large epithelia sheets. Basal cellular contractions also have a major contribution in the process of bud formation in Hydra (Holz et al., 2017). Such basal contacts are absent from bilaterian embryos, which are mainly connected by apical junction belts.

Cadherin and formation of epithelia

Establishment of the adherens junctions is crucial for normal development of the embryo. Knockdown of *cdh3* in normal embryos does not lead to dissociation of embryonic tissue, suggesting that maternally expressed cadherin protein localized in cell junctions might have a slow turnover and be sufficient for the early stages of development. This is consistent with the results of knockdown of E-cadherin in mouse embryos (Capaldo and Macara, 2007). However, proper formation of epithelial layers is disrupted in embryonic aggregates in response to knockdown of *cdh3*. Notably, although knockdown of endodermal *cdh1* does not disrupt gastrulation, the endoderm does not develop endodermal structures such as mesenteries. Thus, proper development of the inner germ layer is dependent on the expression of Cdh1.

The role of cadherins in germ layer formation

The role of cadherins in the formation of germ layers in a diploblast animal is of particular interest, as we might learn about the evolution and potential homology of germ layers. We found that the formation of the inner layer is accompanied by a stepwise cadherin switch. At the blastula stage, Cdh3 forms apical and basal adherens junctions. The onset of gastrulation is characterized by a change in shape of endodermal cells, which adopt a partial EMT phenotype: apical constriction of cells, loss of Cdh3-positive basal junctions, migration of nuclei basally, development of filopodia and an increase in cellular motility (Fig. 13B). We propose that the changes in the adhesion properties of the endodermal cells are crucial for the morphogenetic behavior and further differentiation. In a second step, after completion of invagination, Cdh3 also disappears from the apical junctions in the endoderm and is replaced by Cdh1, both

Development (2019) 146, dev174623. doi:10.1242/dev.174623

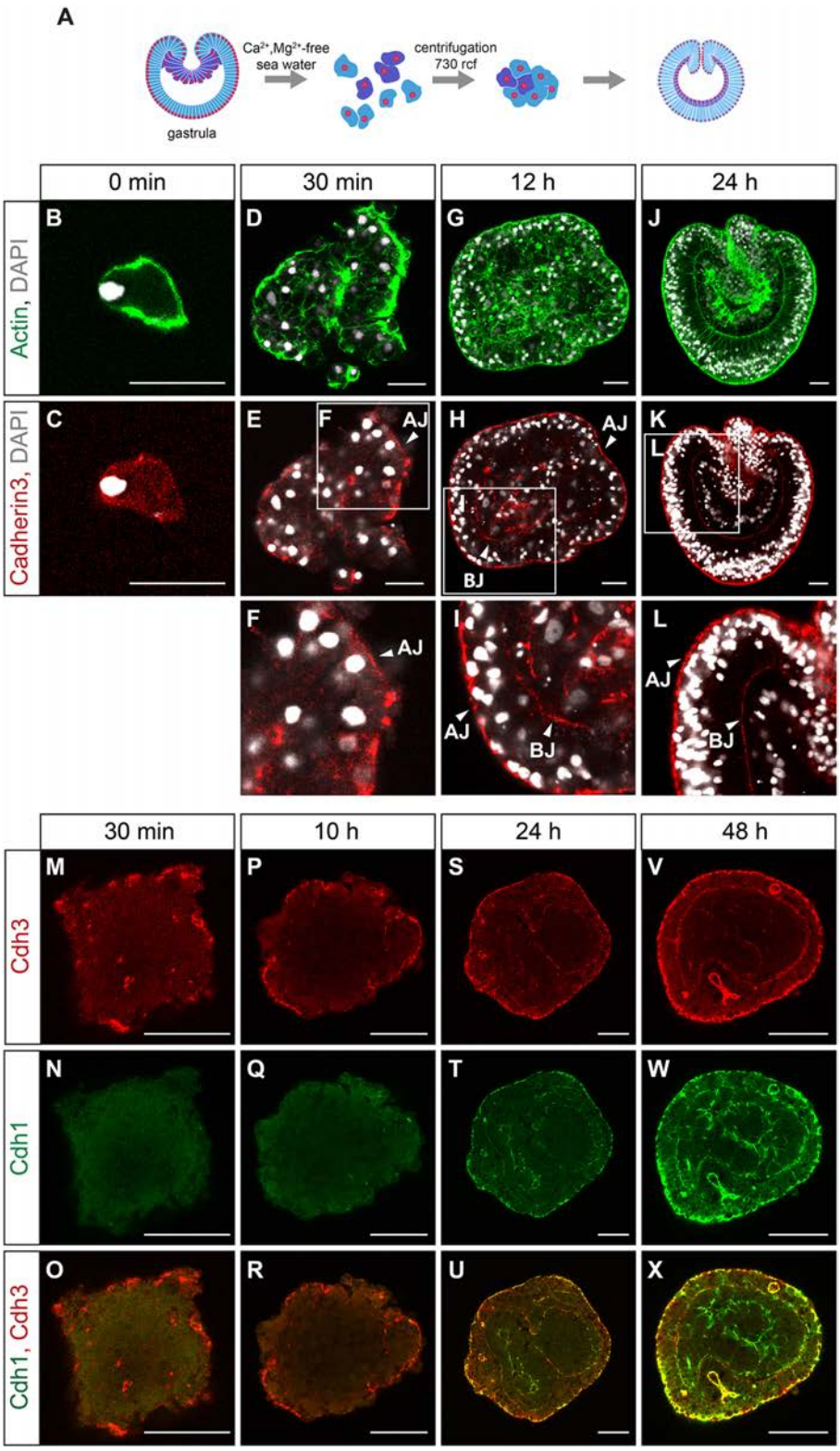

Fig. 9. Reestablishment of polarity and *de novo* formation of the germ layer in the cell aggregate. (A) Scheme of the experiment. (B,C) Dissociated cells do not show polarized Cdh3 localization. (D-F) Epithelialization of the cell aggregate starts ~30 min after re-aggregation in small groups of cells. (G-I) The ectoderm of the aggregate is fully epithelialized 12 h after dissociation. (J-L) Aggregate has formed two germ layers after 24 h. F,I,L are enlargements of the boxed areas shown in E,H,K, respectively. (M-X) Cdh1 protein appears at the junctions after 24 h of aggregate development. At 48 h after re-aggregation, Cdh1 is broadly expressed in both germ layers. AJ, apical junction; BJ basal junction. Scale bars: 20 µm in B-K; 50 µm in M-X.

at apical and basal junctions of the endoderm. Thus, we observed a cadherin switch in *Nematostella* that is analogous to the cadherin switch in vertebrates and insects. As *cdh1* and *cdh3*, like E- and N-cadherins in mammals and insects, are lineage-specific duplications (Fig. 1), we conclude that the cadherin switch evolved convergently in these animals.

Development (2019) 146, dev174623. doi:10.1242/dev.174623

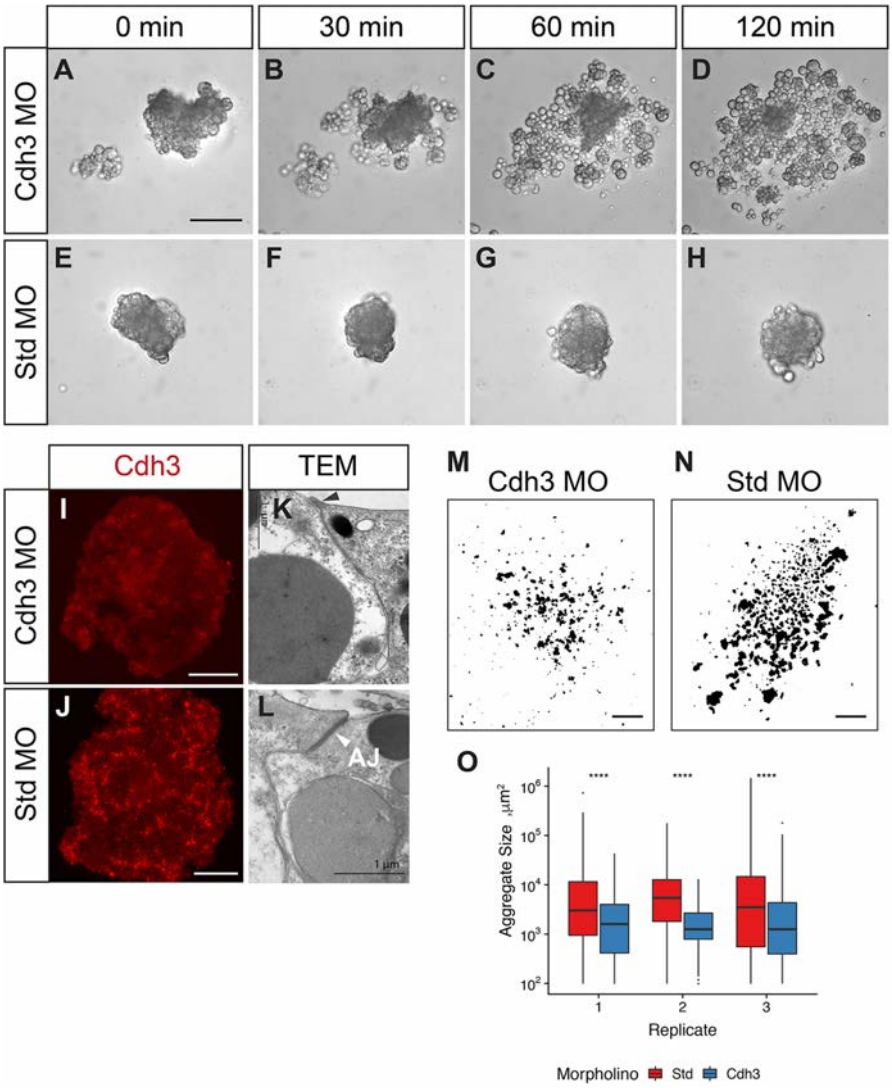

Fig. 10. Cdh3 MO aggregates fail to form adherens junctions *de novo*. (A-D) Cdh3 MO aggregates do not form new cell contacts, fail to develop and fall apart into cells. (E-H) Standard (Std) MO control aggregates stay compact. (I,J) Confocal microscopy images showing downregulation of Cdh3 protein in Cdh3 MO aggregates; Cdh3 antibody staining. (K,L) TEM images of the apical adherens junctions. Apical cell junctions (AJ) of the Cdh3 MO aggregates are much less pronounced than AJs in the control aggregates. (M-O) Cdh3 MO aggregates are significantly smaller than Std MO aggregates. Distribution means within each replicate were tested for significance using a two-sided unpaired Wilcoxon rank-sum test (****P<0.0001). Scale bars: 50 µm in A-J; 1 µm in K,L; 1 mm in M,N.

However, although Cdh3 is not expressed in the endoderm after the gastrula stage, Cdh1 shows partially overlapping expression with Cdh3 in the ectoderm. Cdh1 seems to form a decreasing gradient from aboral to oral, but the significance of this gradient is unclear at this point. Notably, the oral region and tentacles are completely devoid of Cdh1 expression. Interestingly, *cdh1* knockdown does not disrupt oral patterning. For example, expression of the blastopore marker *brachyury* was normal. However, expression of the aboral patterning gene *FGFa1* was abolished (Fig. 12). Because the aboral part is an area of strong Cdh1 expression, we assume that normal Cdh1 expression is necessary for FGF signaling and apical organ development. Our results show that *Nematostella* cadherins are important for germ layer morphogenesis and the maintenance of tissue integrity. However, so far we have no evidence that cadherins play a role in initial germ layer differentiation, as shown similarly for the knockdown of α-catenin, another component of the adhesion junction complex (Clarke et al., 2019). We conclude that, as for bilaterians (Basilicata et al., 2016; Giger and David, 2017; Huang et al., 2016; Nakagawa and Takeichi, 1998; Pla et al., 2001; Schäfer et al., 2014; Shoval et al., 2007), different combinations and concentrations of Cdh1 and Cdh3 convey different tissue properties and identities in different regions of the developing embryo. Thus, the combinatorial and differential use of cadherins is a recurring feature of metazoans (Fig. 1, Fig. 13C; Fig. S1), although the paralogous molecules have evolved independently.

Interestingly, our phylogenetic analysis of the classical cadherins showed that hydrozoans and stony corals have only cadherin protein, which groups basally with two classical cadherins of sea anemones, suggesting that *cdh1* and *cdh3* arose by a lineage-specific gene duplication within the sea anemones (Fig. 1). The expression and function of the single cadherin in other cnidarians is unknown. However, they do have a *dachsous* gene, which also encodes a cytoplasmic cadherin domain and has a similar structure to classical cadherins, except that they lack the EGF/LamG domains found in most invertebrate cadherins. It remains to be shown whether Dachsous and classical cadherin could interact during early germ layer formation in other cnidarians.

Development (2019) 146, dev174623. doi:10.1242/dev.174623

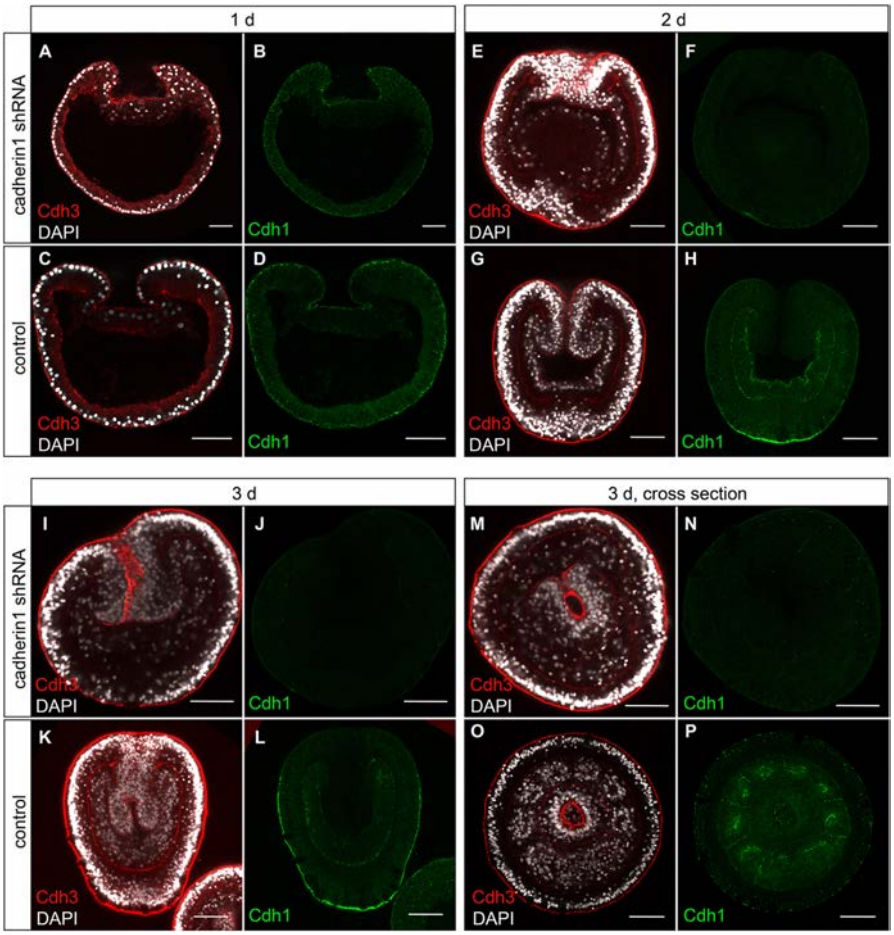

Fig. 11. Mesenteries do not develop after Cdh1 knockdown by shRNA injection. Cdh1 protein expression is strongly downregulated. (A-D) Gastrula stage at 1 day post-fertilization (dpf), lateral section. (E-H) Planula at 2 dpf, lateral section. (I-L) Planula at 3 dpf, lateral section. (M-P) Planula at 3 dpf, cross-section. Scale bars: 50 µm.

Homology of germ layers

Our study has established that cadherins play an important role in the formation and differentiation of the germ layers in a diploblastic animal. This revives the question of which germ layers in Bilateria these two cell layers are homologous with. Traditionally, they have been homologized with the endoderm and ectoderm, with the mesoderm missing. The identification of a number of mesodermal transcription factors in cnidarians and their expression in the endoderm led to the notion of an inner "mesendoderm" (Fritzenwanker et al., 2004; Kumburegama et al., 2011; Martindale, 2004; Salinas-Saavedra et al., 2018; Scholz and Technau, 2003). However, recent analysis of many endodermal and mesodermal marker genes suggests that segregation has already taken place in the *Nematostella* polyp. In fact, the inner layer corresponds to mesoderm, whereas all endodermal functions reside in the ectodermally derived extensions of the pharynx, the septal filaments (Hashimshony, 2017; Steinmetz et al., 2017). In the light of those findings, it is interesting to note that Cdh1 is specific to the inner cell layer, which corresponds to the mesoderm of bilaterians. Notably, this cell layer also expresses the zinc finger transcription factor *snailA* (Fritzenwanker et al., 2004; Martindale, 2004). Snail proteins regulate the downregulation of *E-cadherin* in vertebrates and insects in the ingressing mesoderm (Nieto, 2002). In line with this, *snail* genes appear to play a role in regulating invagination and partial EMT in *Nematostella* (Salinas-Saavedra et al., 2018). It will be of interest to investigate how cadherins are regulated by Snail in *Nematostella*.

Conclusion

This first analysis of the expression and function of classical cadherins in a diploblast shows that these molecules play a conserved role in cell adhesion, tissue morphogenesis and germ layer specification during embryogenesis. Invaginating cells show partial EMT, accompanied by a cadherin switch. The evolutionarily recurring mechanism of a cadherin switch suggests that the evolution of germ layer formation and tissue morphogenesis is facilitated by the differential expression of cadherins.

MATERIALS AND METHODS

Animals and embryo culturing

Animals were kept in artificial seawater at 18°C the dark. Spawning was induced by temperature shift to 24°C and light exposure over 10 h (Fritzenwanker and Technau, 2002). *In vitro* fertilized embryos were collected and kept at 21°C as described (Fritzenwanker and Technau, 2002; Genikhovich and Technau, 2009c).

Identification of Cdh1 and Cdh3 protein sequences

To retrieve the coding sequences of *cdh1* and *cdh3* genes the 1-3 kb overlapping coding fragments of *cdh1* and *cdh3* were amplified from cDNA of mixed embryonic stages, cloned using pJet1.2/blunt vector system (Thermo Fisher Scientific) and sequenced. The full-length sequences of

Development (2019) 146, dev174623. doi:10.1242/dev.174623

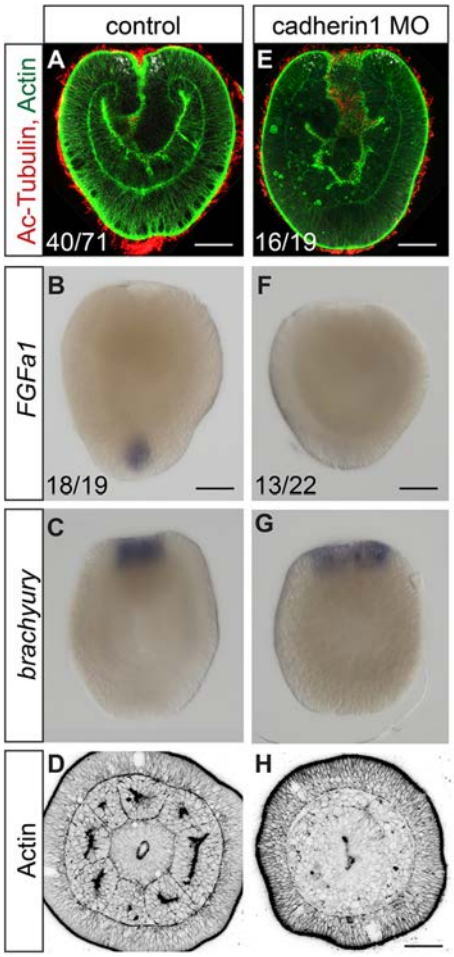

Fig. 12. Cdh1 knockdown impairs apical organ development. (A-D) Control embryo. (E-H) Cdh1 MO knockdown. Apical organs fail to develop (acetylated tubulin antibody staining). *FGFa1* is not expressed. Mesenteries do not form (phalloidin staining). *Brachyury* expression is normal. Scale bars: 50 µm.

Cdh1 and Cdh3 have been deposited in GenBank (accession numbers MK253651 and MK253652).

Assembled *cdh1* and *cdh3* protein coding sequences were derived *in silico* using Expasy translation tool (Artimo et al., 2012). Cadherin protein domain annotation was performed using SMART protein domain annotation resource (Letunic and Bork, 2018).

Morpholino injection

Knockdowns of *cdh1* and *cdh3* were performed by independent zygote injections of two non-overlapping translation blocking morpholinos (Gene Tools): cdh1MO1 5′-CCGGCCAGCACTCATTTTGTGGCTA-3′, cdh1MO2 5′-ACCCGTGAGTTTAAAAACCCATAGC-3′; cdh3MO1 5′-ACGAGTTG-CGGTGAACGAAAATAAC-3′, cdh3MO2 5′-TAGCAGAACCGTCCAGT-CCCATATC-3′ at concentrations of 500 µM. Standard morpholino injection at 500 µM was used as a control; SdtMO 5′-CCTCTTACCTCAGTTACAATT-TATA-3′.

Non-overlapping morpholinos for *cdh1* and *cdh3* knockdown had similar phenotypes.

Injection equipment used: FemtoJet (Eppendorf), CellTram Vario (Eppendorf), micromanipulator (Narishige). Needles were pulled from the glass capillaries type GB 100TF-10 (Science Products) with a micropipette puller (Sutter Instrument, Model P-97). We used holding capillaries from Eppendorf for the injection (Renfer et al., 2010).

Short hairpin RNA knockdown

cdh1 shRNA design and synthesis were performed as described (He et al., 2018). The following primers were used for *cdh1* shRNA synthesis: *cdh1* shRNA forward, 5′-TAATACGACTCACTATAGAAGCGCGCTCAGGT-AAATGTTTCAAGAGA-3′; *cdh1* shRNA reverse, 5′-AAGAAGCACG-TTCGGGTAAATGTTCTCTTGAAACATTTACCTGAGCGC-3′.

Purified shRNA was injected into zygotes at a concentration of 500 ng/µl. As a negative control, shRNA against mOrange was injected at 500 ng/µl. Uninjected embryos from the same batch were used as a control for injection. After injection, embryos were raised at 21°C.

Generation of Cdh1 and Cdh3 antibodies

To generate antibodies against Cdh1, we expressed the protein domains cdh1:domain1 (extracellular) and cdh1:domain3 (intracellular) in *E.coli.* The fragment sequences were as follows: Cdh1 domain1 (extracellular), NAPKDGSLLIIVNAYDGNFTGGVIGKPYYQDDDFDGDENTYELNS-QSPGSYFRVNEGNGDITAAPMIPMGEYNLKIRVTEKKDSPSTVTSS-VRVLVRRIDKEAVDNGVAVEFTDMRKVGYFVGDYYKGFEDVLA-STLGVPTGDIKIFSVQKAHDNGLAVVVFFTVAAKDSYMPHWDVVS-KLVDAKKPLESLGLKVSRLGMD; and Cdh1 domain3 (intracellular), RRPEPVVVYADSTDTGHVHDNVRLYHDDGGGEEDNLGYDITKLM-KYTYIETTIAPPSVAPSKASEDKISTSSDQPLLQGRPPDAVFGLTGK-EPGPKMPKYMEGDDVGDFITTRVKITDREVFLAVDELHIYRYEGDD-TDVD.

The recombinant protein fragments were purified by column-based affinity chromatography and used for immunization. Specifically, the extracellular fragment was used for immunization of two rats (polyclonal Cdh1 antibodies 1 and 2) and the intracellular fragment used for immunization of a rabbit (polyclonal Cdh1 antibody 3). All Cdh1

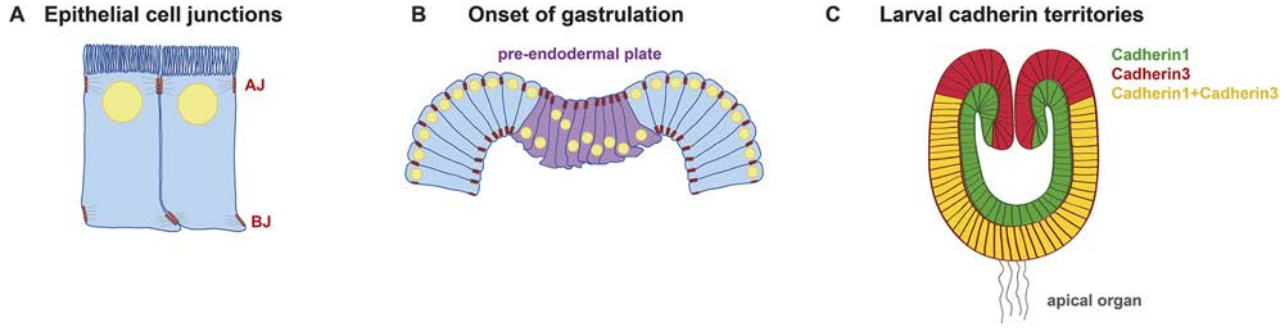

Fig. 13. Cadherin localization during early development of *Nematostella*. (A) Scheme of the apical and basal adherens junctions in both epithelial cell layers. (B) The onset of gastrulation is characterized by downregulation of Cdh3 in the basal junctions, which is accompanied by apical constriction, migration of nuclei to basal positions and formation of filopodia. (C) Overlapping and specific expression domains of Cdh1 and Cdh3 in a planula larva.

antibodies resulted in the same staining pattern (see Fig. S4). Cdh1 antibody2 was used for most experiments in this paper.

For visualization of Cdh3, monoclonal antibodies were produced in mice. The following peptides were used for immunization: SSSDRNRPPV (for Cdh3 antibody1) and DEKDPPQFSQ (for Cdh3 antibody2). Both epitopes are located in the extracellular part of Cdh3 in the third and seventh cadherin repeats, respectively. Both antibody clones (Cdh3 antibody1 and Cdh3 antibody2) resulted in the same staining patterns (see Fig. S4). Cdh3 antibody2 was used for antibody staining in this paper.

Antibody and phalloidin staining

For Cdh1 antibody staining, embryos were fixed for 1 h at 4°C with Lavdovsky's fixative (3.7% formaldehyde (FA), 50% ethanol, 4% acetic acid). For staining of Cdh3 antibody, β-catenin antibody and phalloidin, embryos were fixed for 1 h with 3.7% FA in PBS at 4°C. Primary polyps were relaxed prior the fixation in 0.1 M $MgCl_2$ in *Nematostella* medium for 10 min. After fixation, embryos were incubated on ice in ice-cold acetone (chilled at −20°C) for 7 min followed by five washes with PBSTx 0.2% (PBS with 0.2% of TritonX-100).

Then embryos were incubated in blocking solution [20% sheep serum, 1% bovine serum albumin (BSA) in PBSTx (0.2%)] for 2 h at room temperature (RT). Primary mouse anti-Cdh3 antibody (1:1000), rabbit β-catenin antibody (1:500; Sigma-Aldrich C2206) (Leclère et al., 2016; Salinas-Saavedra et al., 2018) and/or rat/rabbit anti-Cdh1 antibodies (1:500) were diluted in blocking solution and incubated with the embryos overnight at 4°C, followed by washing in PBSTx 0.2% at RT (10×10 min each). After incubation in blocking solution for 2 h at RT, embryos were placed in a secondary antibody solution of goat anti-mouse Alexa Fluor 568 antibodies (1:1000, Thermo Fischer Scientific A11019), goat anti-rat antibody DyLight 488-conjugated (1:1000, Rockland, 612-141-120) and DAPI overnight at 4°C. When fixed with FA, phalloidin Alexa Fluor 488 (1:30, Thermo Fisher Scientific) was added to the secondary antibody solution, because phalloidin staining is not compatible with the Lavdovsky's fixation. Embryos were washed in PBSTx 0.2% at RT (10×10 min each) and infiltrated with Vectashield antifade mounting medium (Vector laboratories) at 4°C overnight. For β-catenin staining of the embryo sections, fixed embryos were embedded in 10% gelatin in PBS. Gelatin blocks were postfixed in 3.7% FA in PBS overnight at 4°C and sectioned on a vibratome Leica VT 1200S. Embryo sections (50 µm) were stained with β-catenin antibody, phalloidin and DAPI as described for the whole-mount embryos. Imaging was performed with a Leica TCS SP5 DM-6000 confocal microscope.

In situ hybridization

In situ hybridizations of embryos were conducted as previously described (Genikhovich and Technau, 2009b; Kraus et al., 2016). The following regions of the coding sequence of cadherins were used to produce the *in situ* hybridization probes: 7054-9126 bp for *cdh1* and 2728-5091 bp for *cdh3*. Adult animals and juveniles were relaxed for 20 min in 0.1 M $MgCl_2$ solution in *Nematostella* medium followed by fixation and *in situ* hybridization as described (Steinmetz et al., 2017). After *in situ* hybridization embryos, adult and juvenile pieces were embedded in 10% gelatin in PBS. Gelatin blocks were postfixed in 3.7% FA in PBS overnight at 4°C and sectioned on a vibratome Leica VT 1200S. Embryos and adult and juvenile 50 µm sections were embedded in 80% glycerol and imaged with a Nikon Eclipse 80i compound microscope equipped with DIC optics and Zeiss AxioCam camera.

Time-lapse microscopy

Time-lapse imaging was carried out using a Nikon Eclipse 80i compound microscope. Pictures were taken with a Zeiss AxioCam camera. Time-lapse movies were made using FIJI software (Schindelin et al., 2012).

Transmission electron microscopy

Transmission electron microscopy was performed as previously described (Fritzenwanker et al., 2007).

Phylogenetic analysis

The protein complements of *Mus musculus* (GRCm38) (Schneider et al., 2017) and *Drosophila melanogaster* (FB2018_03) (Thurmond et al., 2019) were downloaded from Ensembl (Zerbino et al., 2018); *Strongylocentrotus purpuratus*, *Capitella teleta*, *Lottia gigantica* and *Tribolium castaneum* from Ensembl metazoan (Kersey et al., 2018); *Hydra vulgaris* and *Ornithorhynchus anatinus* from RefSeq at NCBI (O'Leary et al., 2016); *Acropora millepora* (PRJNA74409) (Moya et al., 2012), *Anemonia viridis* (PRJNA260824) (Rachamim et al., 2015), *Exaptasia pallida* (PRJNA386175) (Baumgarten et al., 2015) and *Stylophora pistilata* (PRJNA281535) (Voolstra et al., 2017) from the Sequence Read Archive at NCBI (Leinonen et al., 2011); and *Acropora digitifera* from marine genomics at OIST (Shinzato et al., 2011). Sequences were selected that had a significant domain hit (domE<1×10^{-5}) to the cadherin cytoplasmic Pfam family (PF01049) according to HMMER 3.2.1 (Finn et al., 2011). When multiple isoforms were present, the longest one was used. The genes were filtered against truncated and misassembled gene models manually. Sequences were aligned using MAFFT v7.307 in E-INS-i mode and a maximum of 1000 iterations of refinement (Katoh and Standley, 2013). The WAG+F+R6 model was determined as optimal by the Bayesian Information Criterion using ModelFinder (Kalyaanamoorthy et al., 2017). This was used to infer a maximum likelihood tree using IQTREE (Nguyen et al., 2015). Support values were determined with 1000 standard bootstrap replicates. Domain architectures were determined using standalone interproscan (Mitchell et al., 2019).

Analysis of the size of the cell aggregates

Cdh3 morpholino (MO) embryos and standard MO control embryos (50 of each) were dissociated into cells at the gastrula stage. Cell aggregates were generated by slow centrifugation as described (Kirillova et al., 2018) and photographed immediately after centrifugation. The size of the aggregates was analyzed with FIJI software. (FIJI/Image/Adjust/Threshold tool and FIJI/Analyze/Analyze particles). The threshold was set to 50. The experiment was repeated three times.

Image processing

Images were processed and adjusted for brightness and contrast using FIJI software (Schindelin et al., 2012). Focus stacking of ISH images was done using Helicon Focus software (Helicon Soft, Kharkov, Ukraine). Images were cropped and assembled into the figures; schemes were made using Adobe Illustrator CS6 software (Adobe, San Jose, USA).

Acknowledgements

We thank Eduard Renfer and Sarah Streinzer for cloning the cDNAs for the *in situ* probes of *cdh1* and *cdh3*, and for performing initial *in situ* hybridizations of these genes. We are very grateful to Prof. Bert Hobmayer for the fruitful discussions and to Dr Alison Cole for critical reading of the manuscript. We thank Rohit Dnyansagar for help with generating the phylogenetic tree and Boris Osadchenko for imaging some of the transmission electron microscopy samples. We thank Vienna Biocenter Facilities (VBCF) for support with recombinant cadherin protein generation and purification, and the Core Facility for Cell Imaging and Ultrastructure Research of the University of Vienna (CIUS) for assistance.

Competing interests

The authors declare no competing or financial interests.

Author contributions

Conceptualization: E.A.P., U.T.; Methodology: E.A.P., A.O.K., Y.A.K., B.Z.; Investigation: E.A.P.; Data curation: B.Z.; Writing - original draft: E.A.P., U.T.; Writing - review & editing: E.A.P., U.T.; Supervision: U.T.; Project administration: U.T.; Funding acquisition: U.T.

Funding

This work was funded by an Austrian Science Fund (FWF) grant to U.T. (P25993).

Data availability

Sequences, the alignment file and the suptree file are available at https://doi.org/10.6084/m9.figshare.9919130.v1.

Supplementary information

Supplementary information available online at http://dev.biologists.org/lookup/doi/10.1242/dev.174623.supplemental

References

Alberts, B. (2007). *Molecular Biology of the Cell*. New York: Garland Science.

Angst, B. D., Marcozzi, C. and Magee, A. I. (2001). The cadherin superfamily: diversity in form and function. *J. Cell Sci.* **114**, 629-641.

Artimo, P., Jonnalagedda, M., Arnold, K., Baratin, D., Csardi, G., de Castro, E., Duvaud, S., Flegel, V., Fortier, A., Gasteiger, E. et al. (2012). ExPASy: SIB bioinformatics resource portal. *Nucleic Acids Res.* **40**, 597-603. doi:10.1093/nar/gks400

Babb, S. G. and Marrs, J. A. (2004). E-cadherin regulates cell movements and tissue formation in early zebrafish embryos. *Dev. Dyn.* **230**, 263-277. doi:10.1002/dvdy.20057

Basilicata, M. F., Frank, M., Solter, D., Brabletz, T. and Stemmler, M. P. (2016). Inappropriate cadherin switching in the mouse epiblast compromises proper signaling between the epiblast and the extraembryonic ectoderm during gastrulation. *Sci. Rep.* **6**, 8263. doi:10.1038/srep26562

Baumgarten, S., Simakov, O., Esherick, L. Y., Liew, Y. J., Lehnert, E. M., Michell, C. T., Li, Y., Hambleton, E. A., Guse, A., Oates, M. E. et al. (2015). The genome of Aiptasia, a sea anemone model for coral symbiosis. *Proc. Natl. Acad. Sci. USA* **112**, 11893-11898. doi:10.1073/pnas.1513318112

Capaldo, C. T. and Macara, I. G. (2007). Depletion of E-cadherin disrupts establishment but not maintenance of cell junctions in Madin-Darby canine kidney epithelial cells. *Mol. Biol. Cell* **18**, 189-200. doi:10.1091/mbc.e06-05-0471

Casper, J., Zweig, A. S., Villarreal, C., Tyner, C., Speir, M. L., Rosenbloom, K. R., Raney, B. J., Lee, C. M., Lee, B. T., Karolchik, D. et al. (2018). The UCSC genome browser database: 2018 update. *Nucleic Acids Res.* **46**, 762-769. doi:10.1093/nar/gkv1275

Chen, J., Sayadian, A.-C., Lowe, N., Lovegrove, H. E. and St Johnston, D. (2018). An alternative mode of epithelial polarity in the Drosophila midgut. *PLoS Biol.* **16**, e3000041. doi:10.1371/journal.pbio.3000041

Clarke, D. N., Miller, P. W., Lowe, C. J., Weis, W. I. and Nelson, W. J. (2016). Characterization of the cadherin-catenin complex of the sea anemone *Nematostella vectensis* and Implications for the evolution of metazoan cell-cell adhesion. *Mol. Biol. Evol.* **33**, 2016-2029. doi:10.1093/molbev/msw084

Clarke, D. N., Lowe, C. J. and James Nelson, W. (2019). The cadherin-catenin complex is necessary for cell adhesion and embryogenesis in Nematostella vectensis. *Dev. Biol.* **447**, 170-181. doi:10.1016/j.ydbio.2019.01.007

Dady, A., Blavet, C. and Duband, J.-L. (2012). Timing and kinetics of E- to N-cadherin switch during neurulation in the avian embryo. *Dev. Dyn.* **241**, 1333-1349. doi:10.1002/dvdy.23813

Detrick, R. J., Dickey, D. and Kintner, C. R. (1990). The effects of N-cadherin misexpression on morphogenesis in Xenopus embryos. *Neuron* **4**, 493-506. doi:10.1016/0896-6273(90)90108-R

Finn, R. D., Clements, J. and Eddy, S. R. (2011). HMMER web server: interactive sequence similarity searching. *Nucleic Acids Res.* **39**, W29-W37. doi:10.1093/nar/gkr367

Francavilla, C., Cattaneo, P., Berezin, V., Bock, E., Ami, D., de Marco, A., Christofori, G. and Cavallaro, U. (2009). The binding of NCAM to FGFR1 induces a specific cellular response mediated by receptor trafficking. *J. Cell. Biol.* **187**, 1101-1116. doi:10.1083/jcb.200903030

Fredman, D., Schwaiger, M., Rentzsch, F. and Technau, U. (2013). *Nematostella vectensis* transcriptome and gene models v2.0. *figshare*. https://doi.org/10.6084/M9.FIGSHARE.807696.

Fritzenwanker, J. H. and Technau, U. (2002). Induction of gametogenesis in the basal cnidarian *Nematostella vectensis* (Anthozoa). *Dev. Genes Evol.* **212**, 99-103. doi:10.1007/s00427-002-0214-7

Fritzenwanker, J. H., Saina, M. and Technau, U. (2004). Analysis of forkhead and snail expression reveals epithelial–mesenchymal transitions during embryonic and larval development of *Nematostella vectensis*. *Dev. Biol.* **275**, 389-402. doi:10.1016/j.ydbio.2004.08.014

Fritzenwanker, J. H., Genikhovich, G., Kraus, Y. and Technau, U. (2007). Early development and axis specification in the sea anemone *Nematostella vectensis*. *Dev. Biol.* **310**, 264-279. doi:10.1016/j.ydbio.2007.07.029

Genikhovich, G. and Technau, U. (2009a). The Starlet sea anemone *Nematostella vectensis*: an anthozoan model organism for studies in comparative genomics and functional evolutionary developmental biology. *Cold Spring Harb. Prot.* **2009**, pdb.emo129. doi:10.1101/pdb.emo129

Genikhovich, G. and Technau, U. (2009b). *In situ* hybridization of Starlet sea anemone (*Nematostella vectensis*) embryos, larvae, and polyps. *Cold Spring Harb. Prot.* **2009**, prot5282. doi:10.1101/pdb.prot5282

Genikhovich, G. and Technau, U. (2009c). Induction of spawning in the starlet sea anemone *Nematostella vectensis*, in vitro fertilization of gametes, and dejellying of zygotes. *Cold Spring Harb. Prot.* **4**, prot5281. doi:10.1101/pdb.prot5281

Giger, F. A. and David, N. B. (2017). Endodermal germ-layer formation through active actin-driven migration triggered by N-cadherin. *Proc. Natl. Acad. Sci. USA* **114**, 10143-10148. doi:10.1073/pnas.1708116114

Gilbert, S. F. (2013). *Developmental Biology*. MA: Sinauer Associates, Inc., Sunderland.

Gumbiner, B. M. (2005). Regulation of cadherin-mediated adhesion in morphogenesis. *Nat. Rev. Mol. Cell Biol.* **6**, 622-634. doi:10.1038/nrm1699

Halbleib, J. M. and Nelson, W. J. (2006). Cadherins in development: cell adhesion, sorting, and tissue morphogenesis. *Genes Dev.* **20**, 3199-3214. doi:10.1101/gad.1486806

Hashimshony, T. (2017). Cnidarians layer up. *Nat. Ecol. Evol.* **1**, 1429-1430. doi:10.1038/s41559-017-0323-3

Hatta, K. and Takeichi, M. (1986). Expression of N-cadherin adhesion molecules associated with early morphogenetic events in chick development. *Nature* **320**, 447-449. doi:10.1038/320447a0

He, S., Del Viso, F., Chen, C.-Y., Ikmi, A., Kroesen, A. E. and Gibson, M. C. (2018). An axial Hox code controls tissue segmentation and body patterning in *Nematostella vectensis*. *Science* **361**, 1377-1380. doi:10.1126/science.aar8384

Holz, O., Apel, D., Steinmetz, P., Lange, E., Hopfenmüller, S., Ohler, K., Sudhop, S. and Hassel, M. (2017). Bud detachment in hydra requires activation of fibroblast growth factor receptor and a Rho-ROCK-myosin II signaling pathway to ensure formation of a basal constriction. *Dev. Dyn.* **246**, 502-516. doi:10.1002/dvdy.24508

Huang, C., Kratzer, M.-C., Wedlich, D. and Kashef, J. (2016). E-cadherin is required for cranial neural crest migration in Xenopus laevis. *Dev. Biol.* **411**, 159-171. doi:10.1016/j.ydbio.2016.02.007

Hulpiau, P. and van Roy, F. (2009). Molecular evolution of the cadherin superfamily. *Int. J. Biochem. Cell Biol.* **41**, 349-369. doi:10.1016/j.biocel.2008.09.027

Hulpiau, P. and van Roy, F. (2011). New insights into the evolution of metazoan cadherins. *Mol. Biol. Evol.* **28**, 647-657. doi:10.1093/molbev/msq233

Iyer, K. V., Piscitello-Gómez, R., Paijmans, J., Jülicher, F. and Eaton, S. (2019). Epithelial viscoelasticity is regulated by mechanosensitive E-cadherin turnover. *Curr. Biol.* **29**, 578-591.e5. doi:10.1016/j.cub.2019.01.021

Kalyaanamoorthy, S., Minh, B. Q., Wong, T. K. F., von Haeseler, A. and Jermiin, L. S. (2017). ModelFinder: fast model selection for accurate phylogenetic estimates. *Nat. Meth.* **14**, 587-589. doi:10.1038/nmeth.4285

Katoh, K. and Standley, D. M. (2013). MAFFT multiple sequence alignment software version 7: improvements in performance and usability. *Mol. Biol. Evol.* **30**, 772-780. doi:10.1093/molbev/mst010

Kersey, P. J., Allen, J. E., Allot, A., Barba, M., Boddu, S., Bolt, B. J., Carvalho-Silva, D., Christensen, M., Davis, P., Grabmueller, C. et al. (2018). Ensembl Genomes 2018: an integrated omics infrastructure for non-vertebrate species. *Nucleic Acids Res.* **46**, D802-D808. doi:10.1093/nar/gkx1011

Kirillova, A., Genikhovich, G., Pukhlyakova, E., Demilly, A., Kraus, Y. and Technau, U. (2018). Germ-layer commitment and axis formation in sea anemone embryonic cell aggregates. *Proc. Natl. Acad. Sci. USA* **115**, 1813-1818. doi:10.1073/pnas.1711516115

Kraus, Y. and Technau, U. (2006). Gastrulation in the sea anemone Nematostella vectensis occurs by invagination and immigration: an ultrastructural study. *Dev. Genes Evol.* **216**, 119-132. doi:10.1007/s00427-005-0038-3

Kraus, Y., Aman, A., Technau, U. and Genikhovich, G. (2016). Pre-bilaterian origin of the blastoporal axial organizer. *Nat. Commun.* **7**, 11694. doi:10.1038/ncomms11694

Kumburegama, S., Wijesena, N., Xu, R. and Wikramanayake, A. H. (2011). Strabismus-mediated primary archenteron invagination is uncoupled from Wnt/b-catenin- dependent endoderm cell fate specification in *Nematostella vectensis* (Anthozoa, Cnidaria): Implications for the evolution of gastrulation. *EvoDevo* **2**, 2. doi:10.1186/2041-9139-2-2

Layden, M. J., Rentzsch, F. and Röttinger, E. (2016). The rise of the starlet sea anemone Nematostella vectensis as a model system to investigate development and regeneration. *Wiley Interdiscip. Rev. Dev. Biol.* **5**, 408-428. doi:10.1002/wdev.222

Leclère, L., Bause, M., Sinigaglia, C., Steger, J. and Rentzsch, F. (2016). Development of the aboral domain in *Nematostella* requires β-catenin and the opposing activities of Six3/6 and Frizzled5/8. *Development* **143**, 1766-1777. doi:10.1242/dev.120931

Leinonen, R., Sugawara, H., Shumway, M. and **International Nucleotide Sequence Database Collaboration**. (2011). The sequence read archive. *Nucleic Acids Res.* **39**, 19-21. doi:10.1093/nar/gkq1019

Letunic, I. and Bork, P. (2018). 20 years of the SMART protein domain annotation resource. *Nucleic Acids Res.* **46**, D493-D496. doi:10.1093/nar/gkx922

Madeira, F., Park, Y. M., Lee, J., Buso, N., Gur, T., Madhusoodanan, N., Basutkar, P., Tivey, A. R. N., Potter, S. C., Finn, R. D. et al. (2019). The EMBL-EBI search and sequence analysis tools APIs in 2019. *Nucleic Acids Res.* **47**, W636-W641. doi:10.1093/nar/gkz268

Magie, C. R., Daly, M. and Martindale, M. Q. (2007). Gastrulation in the cnidarian *Nematostella vectensis* occurs via invagination not ingression. *Dev.Biol.* **305**, 483-497. doi:10.1016/j.ydbio.2007.02.044

Martindale, M. Q. (2004). Investigating the origins of triploblasty: 'mesodermal' gene expression in a diploblastic animal, the sea anemone *Nematostella vectensis* (phylum, Cnidaria; class, Anthozoa). *Development* **131**, 2463-2474. doi:10.1242/dev.01119

Meng, W. and Takeichi, M. (2009). Adherens junction: molecular architecture and regulation. *Cold Spring Harb. Perspec. Biol.* **1**, a002899-a002899. doi:10.1101/cshperspect.a002899

Mitchell, A. L., Attwood, T. K., Babbitt, P. C., Blum, M., Bork, P., Bridge, A., Brown, S. D., Chang, H.-Y., El-Gebali, S., Fraser, M. I. et al. (2019). InterPro in 2019: improving coverage, classification and access to protein sequence annotations. *Nucleic Acids Res.* **47**, D351-D360. doi:10.1093/nar/gky1100

Moya, A., Huisman, L., Ball, E. E., Hayward, D. C., Grasso, L. C., Chua, C. M., Woo, H. N., Gattuso, J.-P., Forêt, S. and Miller, D. J. (2012). Whole transcriptome analysis of the coral Acropora millepora reveals complex responses to CO[?]-driven acidification during the initiation of calcification. *Mol. Ecol.* **21**, 2440-2454. doi:10.1111/j.1365-294X.2012.05554.x

Nakagawa, S. and Takeichi, M. (1998). Neural crest emigration from the neural tube depends on regulated cadherin expression. *Development* **125**, 2963-2971.

Nandadasa, S., Tao, Q., Menon, N. R., Heasman, J. and Wylie, C. (2009). N- and E-cadherins in Xenopus are specifically required in the neural and non-neural ectoderm, respectively, for F-actin assembly and morphogenetic movements. *Development* **136**, 1327-1338. doi:10.1242/dev.031203

Nguyen, L.-T., Schmidt, H. A., von Haeseler, A. and Minh, B. Q. (2015). IQ-TREE: a fast and effective stochastic algorithm for estimating maximum-likelihood phylogenies. *Mol. Biol. Evol.* **32**, 268-274. doi:10.1093/molbev/msu300

Nichols, S. A., Roberts, B. W., Richter, D. J., Fairclough, S. R. and King, N. (2012). Origin of metazoan cadherin diversity and the antiquity of the classical cadherin/β-catenin complex. *Proc. Natl. Acad. Sci. USA* **109**, 13046-13051. doi:10.1073/pnas.1120685109

Nieto, M. A. (2002). The Snail superfamily of zinc-finger transcription factors. *Nat. Rev. Mol. Cell Biol.* **3**, 155-166. doi:10.1038/nrm757

Ninomiya, H., David, R., Damm, E. W., Fagotto, F., Niessen, C. M. and Winklbauer, R. (2012). Cadherin-dependent differential cell adhesion in Xenopus causes cell sorting in vitro but not in the embryo. *J. Cell Sci.* **125**, 1877-1883. doi:10.1242/jcs.095315

Oda, H. and Takeichi, M. (2011). Structural and functional diversity of cadherin at the adherens junction. *J. Cell Biol.* **193**, 1137-1146. doi:10.1083/jcb.201008173

Oda, H., Tsukita, S. and Takeichi, M. (1998). Dynamic behavior of the cadherin-based cell-cell adhesion system during Drosophila gastrulation. *Dev. Biol.* **203**, 435-450. doi:10.1006/dbio.1998.9047

O'Leary, N. A., Wright, M. W., Brister, J. R., Ciufo, S., Haddad, D., McVeigh, R., Rajput, B., Robbertse, B., Smith-White, B., Ako-Adjei, D. et al. (2016). Reference sequence (RefSeq) database at NCBI: current status, taxonomic expansion, and functional annotation. *Nucleic Acids Res.* **44**, D733-D745. doi:10.1093/nar/gkv1189

Pla, P., Moore, R., Morali, O. G., Grille, S., Martinozzi, S., Delmas, V. and Larue, L. (2001). Cadherins in neural crest cell development and transformation. *J. Cell. Physiol.* **189**, 121-132. doi:10.1002/jcp.10008

Pukhlyakova, E., Aman, A. J., Elsayad, K. and Technau, U. (2018). β-Catenin-dependent mechanotransduction dates back to the common ancestor of Cnidaria and Bilateria. *Proc. Natl. Acad. Sci. USA* **115**, 6231-6236. doi:10.1073/pnas.1713682115

Putnam, N. H., Srivastava, M., Hellsten, U., Dirks, B., Chapman, J., Salamov, A., Terry, A., Shapiro, H., Lindquist, E., Kapitonov, V. V. et al. (2007). Sea anemone genome reveals ancestral Eumetazoan Gene Repertoire and Genomic Organization. *Science* **317**, 86-94. doi:10.1126/science.1139158

Rachamim, T., Morgenstern, D., Aharonovich, D., Brekhman, V., Lotan, T. and Sher, D. (2015). The dynamically evolving nematocyst content of an anthozoan, a scyphozoan, and a hydrozoan. *Mol. Biol. Evol.* **32**, 740-753. doi:10.1093/molbev/msu335

Ragkousi, K., Marr, K., McKinney, S., Ellington, L. and Gibson, M. C. (2017). Cell-cycle-coupled oscillations in apical polarity and intercellular contact maintain order in embryonic epithelia. *Curr. Biol.* **27**, 1381-1386. doi:10.1016/j.cub.2017.03.064

Renfer, E., Amon-Hassenzahl, A., Steinmetz, P. R. H. and Technau, U. (2010). A muscle-specific transgenic reporter line of the sea anemone, *Nematostella vectensis*. *Proc. Natl. Acad. Sci. USA* **107**, 104-108. doi:10.1073/pnas.0909148107

Rentzsch, F., Fritzenwanker, J. H., Scholz, C. B. and Technau, U. (2008). FGF signalling controls formation of the apical sensory organ in the cnidarian *Nematostella vectensis*. *Development* **135**, 1761-1769. doi:10.1242/dev.020784

Rogers, C. D., Saxena, A. and Bronner, M. E. (2013). Sip1 mediates an E-cadherin-to-N-cadherin switch during cranial neural crest EMT. *J. Cell Biol.* **203**, 835-847. doi:10.1083/jcb.201305050

Röper, J.-C., Mitrossilis, D., Stirnemann, G., Waharte, F., Brito, I., Fernandez-Sanchez, M.-E., Baaden, M., Salamero, J. and Farge, E. (2018). The major β-catenin/E-cadherin junctional binding site is a primary molecular mechano-transductor of differentiation in vivo. *eLife* **7**, e33381. doi:10.7554/eLife.33381

Salinas-Saavedra, M., Rock, A. Q. and Martindale, M. Q. (2018). Germ layer-specific regulation of cell polarity and adhesion gives insight into the evolution of mesoderm. *eLife* **7**, 1438. doi:10.7554/eLife.36740

Scarpa, E., Szabó, A., Bibonne, A., Theveneau, E., Parsons, M. and Mayor, R. (2015). Cadherin switch during EMT in neural crest cells leads to contact inhibition of locomotion via repolarization of forces. *Dev. Cell* **34**, 421-434. doi:10.1016/j.devcel.2015.06.012

Schäfer, G., Narasimha, M., Vogelsang, E. and Leptin, M. (2014). Cadherin switching during the formation and differentiation of the Drosophila mesoderm - implications for epithelial-to-mesenchymal transitions. *J. Cell Sci.* **127**, 1511-1522. doi:10.1242/jcs.139485

Schindelin, J., Arganda-Carreras, I., Frise, E., Kaynig, V., Longair, M., Pietzsch, T., Preibisch, S., Rueden, C., Saalfeld, S., Schmid, B. et al. (2012). Fiji: an open-source platform for biological-image analysis. *Nat. Meth.* **9**, 676-682. doi:10.1038/nmeth.2019

Schneider, V. A., Graves-Lindsay, T., Howe, K., Bouk, N., Chen, H.-C., Kitts, P. A., Murphy, T. D., Pruitt, K. D., Thibaud-Nissen, F., Albracht, D. et al. (2017). Evaluation of GRCh38 and de novo haploid genome assemblies demonstrates the enduring quality of the reference assembly. *Genome Res.* **27**, 849-864. doi:10.1101/gr.213611.116

Scholz, C. B. and Technau, U. (2003). The ancestral role of Brachyury: expression of NemBra1 in the basal cnidarian *Nematostella vectensis* (Anthozoa). *Dev. Genes Evol.* **212**, 563-570. doi:10.1007/s00427-002-0214-7

Seybold, A., Salvenmoser, W. and Hobmayer, B. (2016). Sequential development of apical-basal and planar polarities in aggregating epitheliomuscular cells of Hydra. *Dev. Biol.* **412**, 148-159. doi:10.1016/j.ydbio.2016.02.022

Shimizu, T., Yabe, T., Muraoka, O., Yonemura, S., Aramaki, S., Hatta, K., Bae, Y.-K., Nojima, H. and Hibi, M. (2005). E-cadherin is required for gastrulation cell movements in zebrafish. *Mech. Dev.* **122**, 747-763. doi:10.1016/j.mod.2005.03.008

Shinzato, C., Shoguchi, E., Kawashima, T., Hamada, M., Hisata, K., Tanaka, M., Fujie, M., Fujiwara, M., Koyanagi, R., Ikuta, T. et al. (2011). Using the Acropora digitifera genome to understand coral responses to environmental change. *Nature* **476**, 320-323. doi:10.1038/nature10249

Shoval, I., Ludwig, A. and Kalcheim, C. (2007). Antagonistic roles of full-length N-cadherin and its soluble BMP cleavage product in neural crest delamination. *Development* **134**, 491-501. doi:10.1242/dev.02742

Steinmetz, P. R. H., Aman, A., Kraus, J. E. M. and Technau, U. (2017). Gut-like ectodermal tissue in a sea anemone challenges germ layer homology. *Nat. Ecol. Evol.* **1**, 1535-1542. doi:10.1038/s41559-017-0285-5

Technau, U. and Steele, R. E. (2011). Evolutionary crossroads in developmental biology: Cnidaria. *Development* **138**, 1447-1458. doi:10.1242/dev.048959

Thurmond, J., Goodman, J. L., Strelets, V. B., Attrill, H., Gramates, L. S., Marygold, S. J., Matthews, B. B., Millburn, G., Antonazzo, G., Trovisco, V. et al. (2019). FlyBase 2.0: the next generation. *Nucleic Acids Res.* **47**, D759-D765. doi:10.1093/nar/gky1003

Tucker, R. P. and Adams, J. C. (2014). Adhesion networks of cnidarians: a postgenomic view. *Int. Rev. Cell Mol. Biol.* **308**, 323-377. doi:10.1016/B978-0-12-800097-7.00008-7

Voolstra, C. R., Li, Y., Liew, Y. J., Baumgarten, S., Zoccola, D., Flot, J.-F., Tambutté, S., Allemand, D. and Aranda, M. (2017). Comparative analysis of the genomes of Stylophora pistillata and Acropora digitifera provides evidence for extensive differences between species of corals. *Sci. Rep.* **7**, 17583-17514. doi:10.1038/s41598-017-17484-x

Williams, E. J., Furness, J., Walsh, F. S. and Doherty, P. (1994). Activation of the Fgf receptor underlies neurite outgrowth stimulated by L1, N-Cam, and N-Cadherin. *Neuron* **13**, 583-594. doi:10.1016/0896-6273(94)90027-2

Winklbauer, R. (2012). Cadherin function during Xenopus gastrulation. In *Adherens Junctions: from Molecular Mechanisms to Tissue Disease (Harris, T.J.C., ed.)*, pp. 301-320. Dordrecht: Springer Netherlands.

Zerbino, D. R., Achuthan, P., Akanni, W., Amode, M. R., Barrell, D., Bhai, J., Billis, K., Cummins, C., Gall, A., Girón, C. G. et al. (2018). Ensembl 2018. *Nucleic Acids Res.* **46**, D754-D761. doi:10.1093/nar/gkx1098

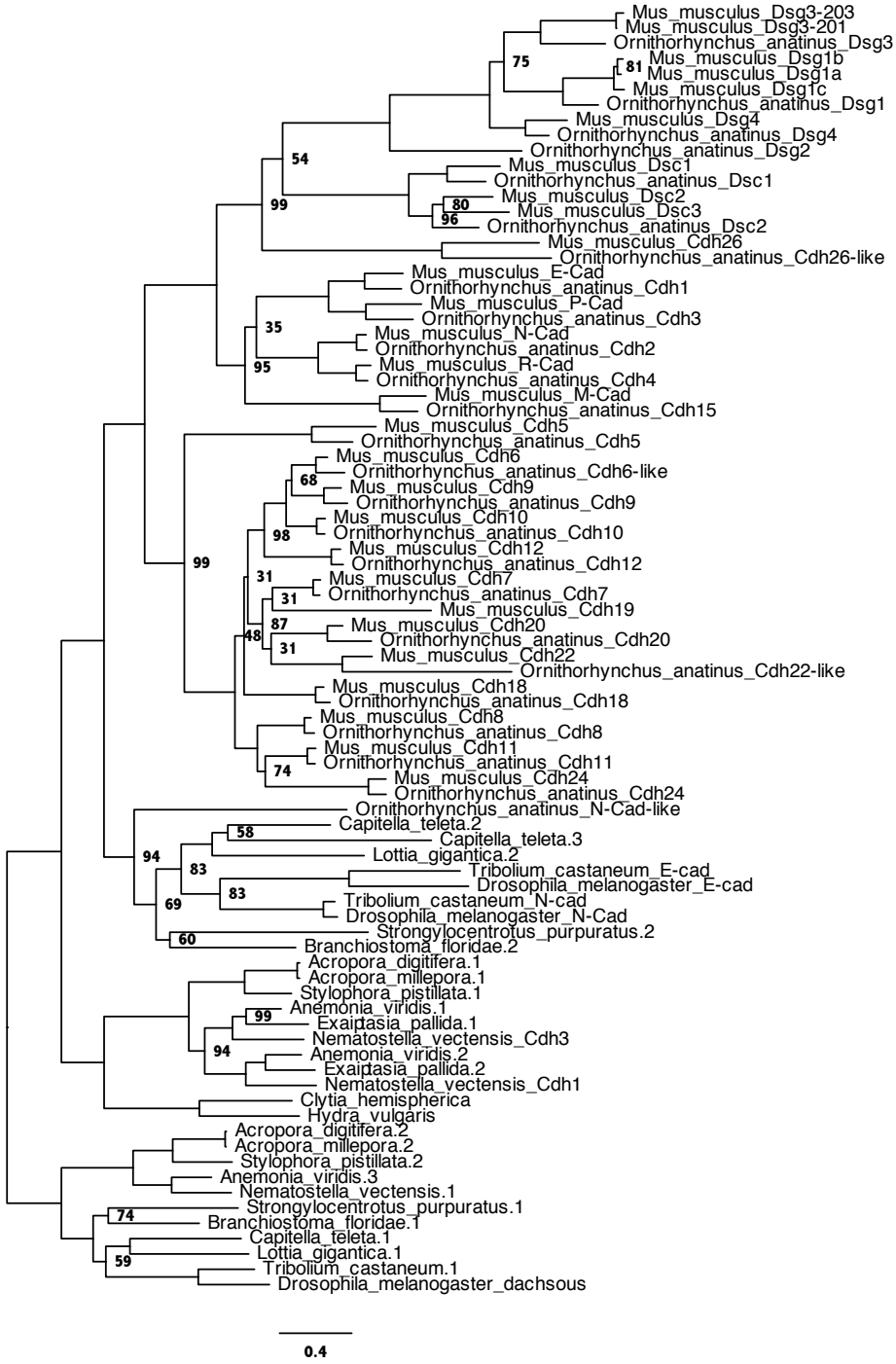

Fig. S1. Phylogenetic analysis of classical cadherins. Extended version of the tree in Fig.1. Dachsous cadherin proteins were used as an outgroup. The phylogenetic tree was constructed with the maximum likelihood method in IQ-tree. The number at the nodes indicates the bootstrap support from the maximum likelihood method.

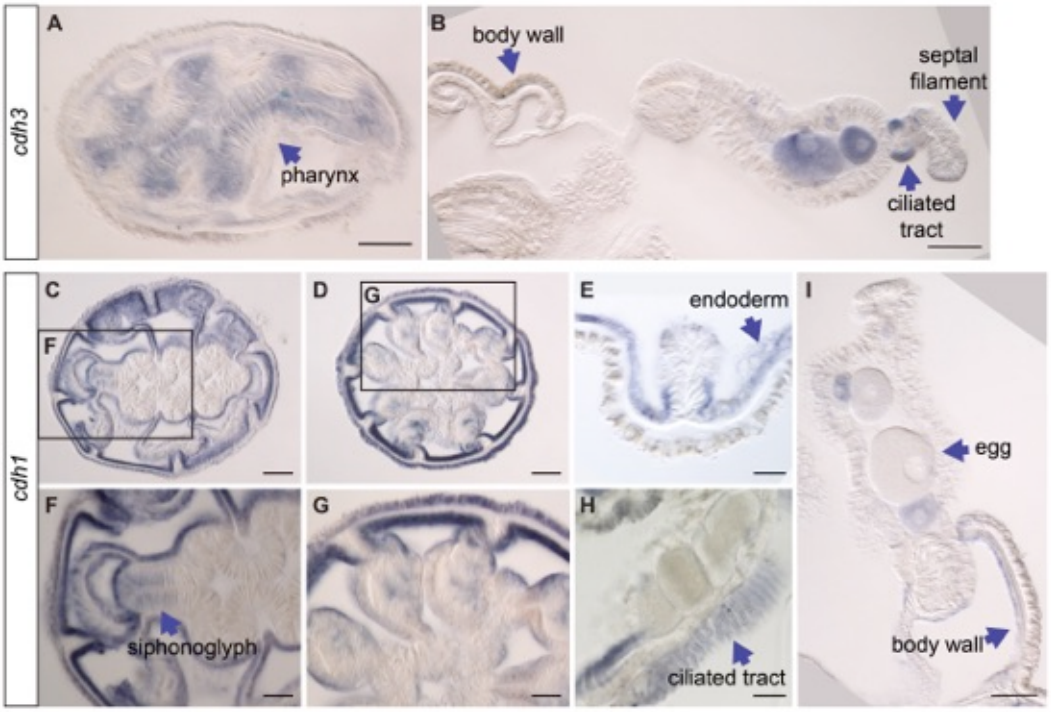

Fig. S2. *cdh1* and *cdh3* expression in adults and juveniles. (A-B) *cdh3* is expressed in the ectoderm of the pharynx, septal filaments and ciliated tract and in the oocytes. (C-I) *cdh1* is expressed in the endoderm, ciliated tract, ciliated lobe of the pharynx – siphonoglyph and small oocytes. Scale bar A-D, I: 100 µm. Scale bar E-H: 50 µm.

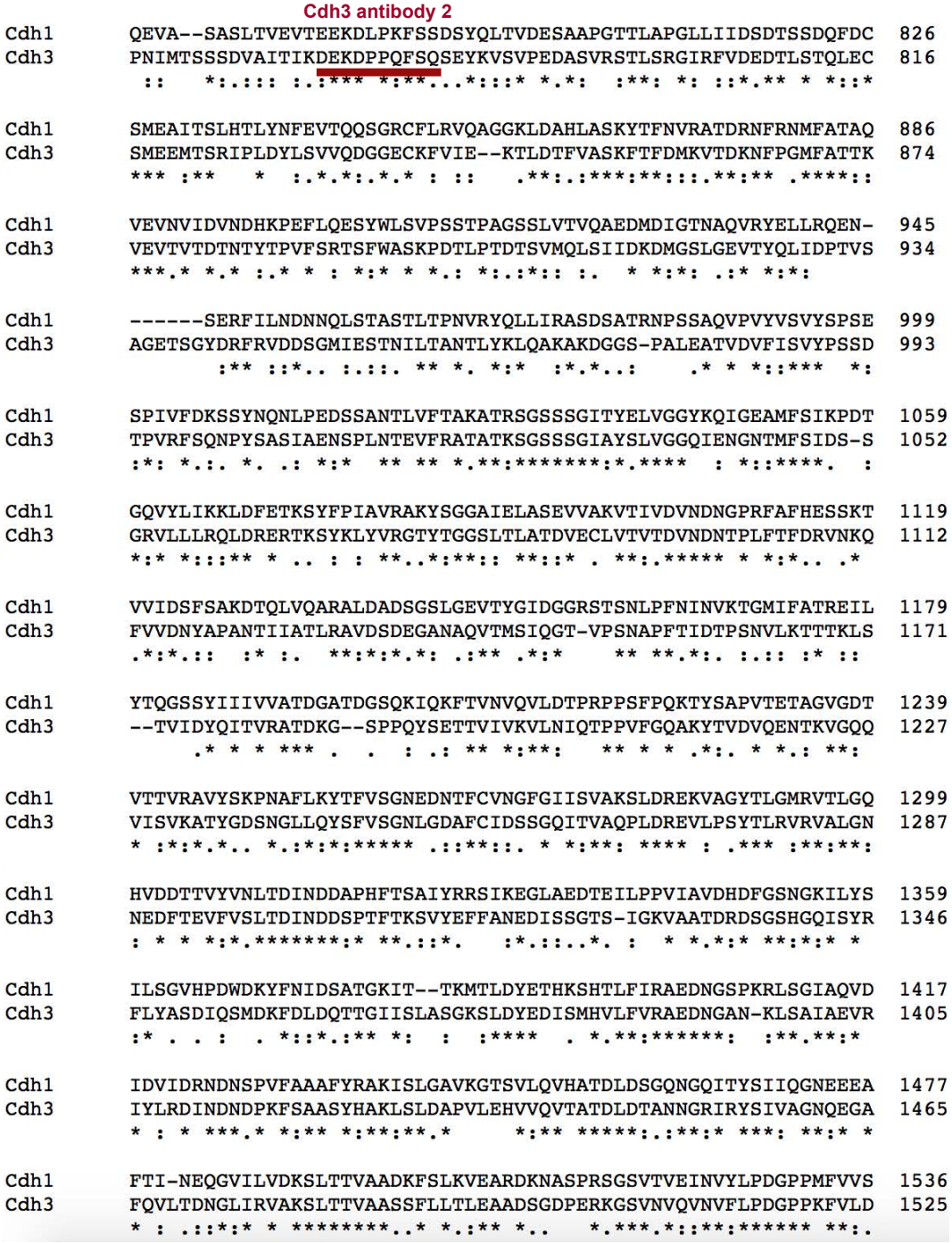

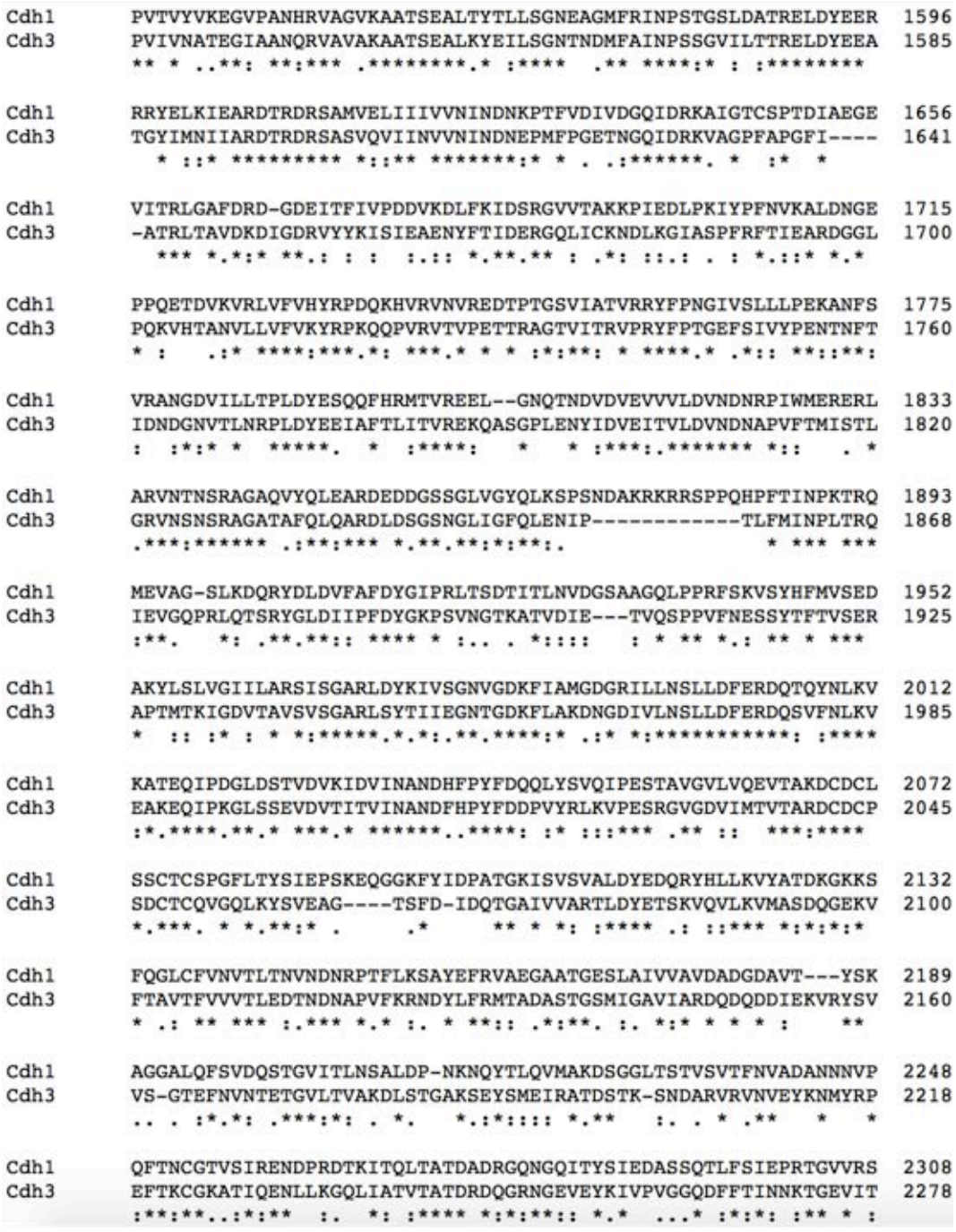

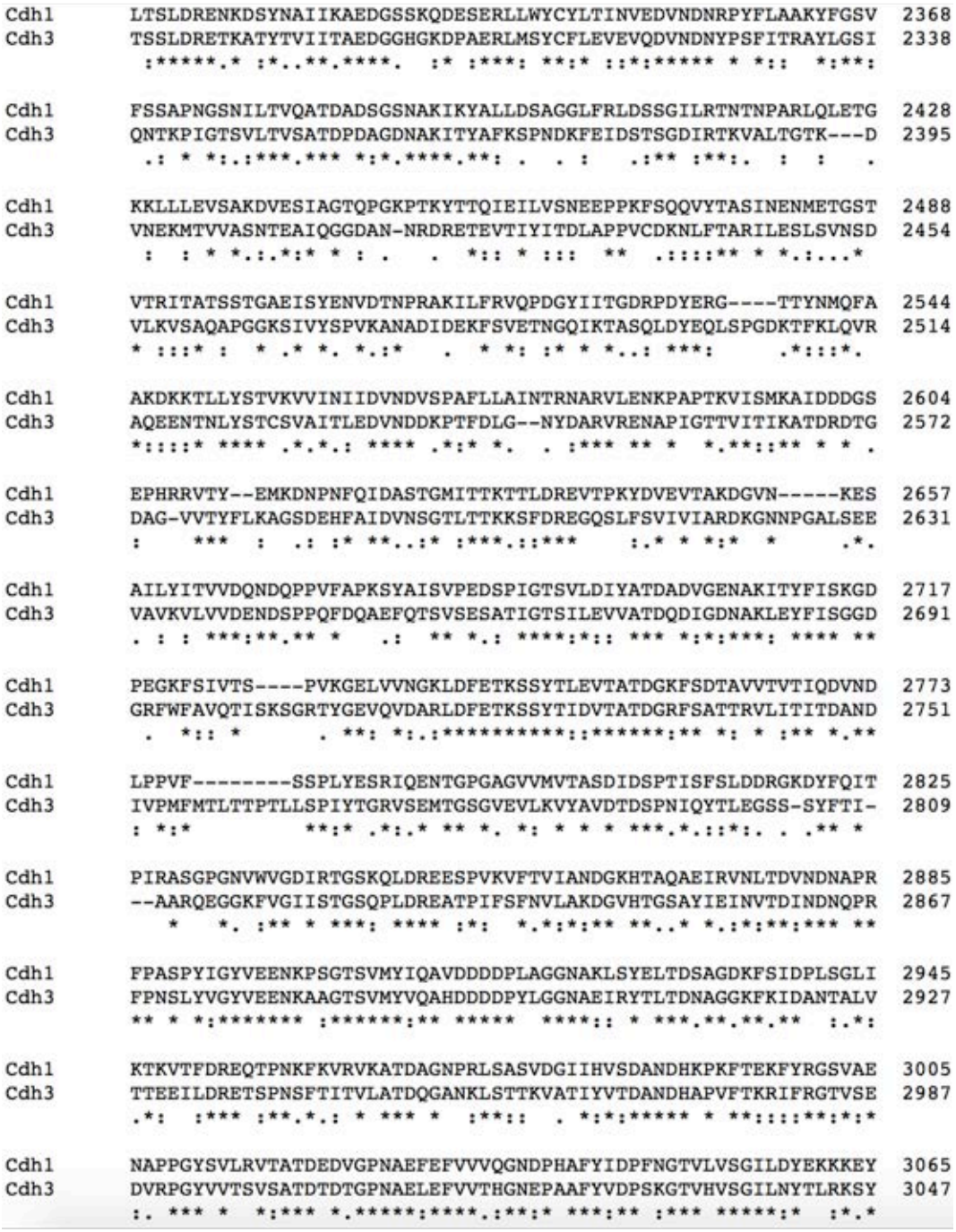

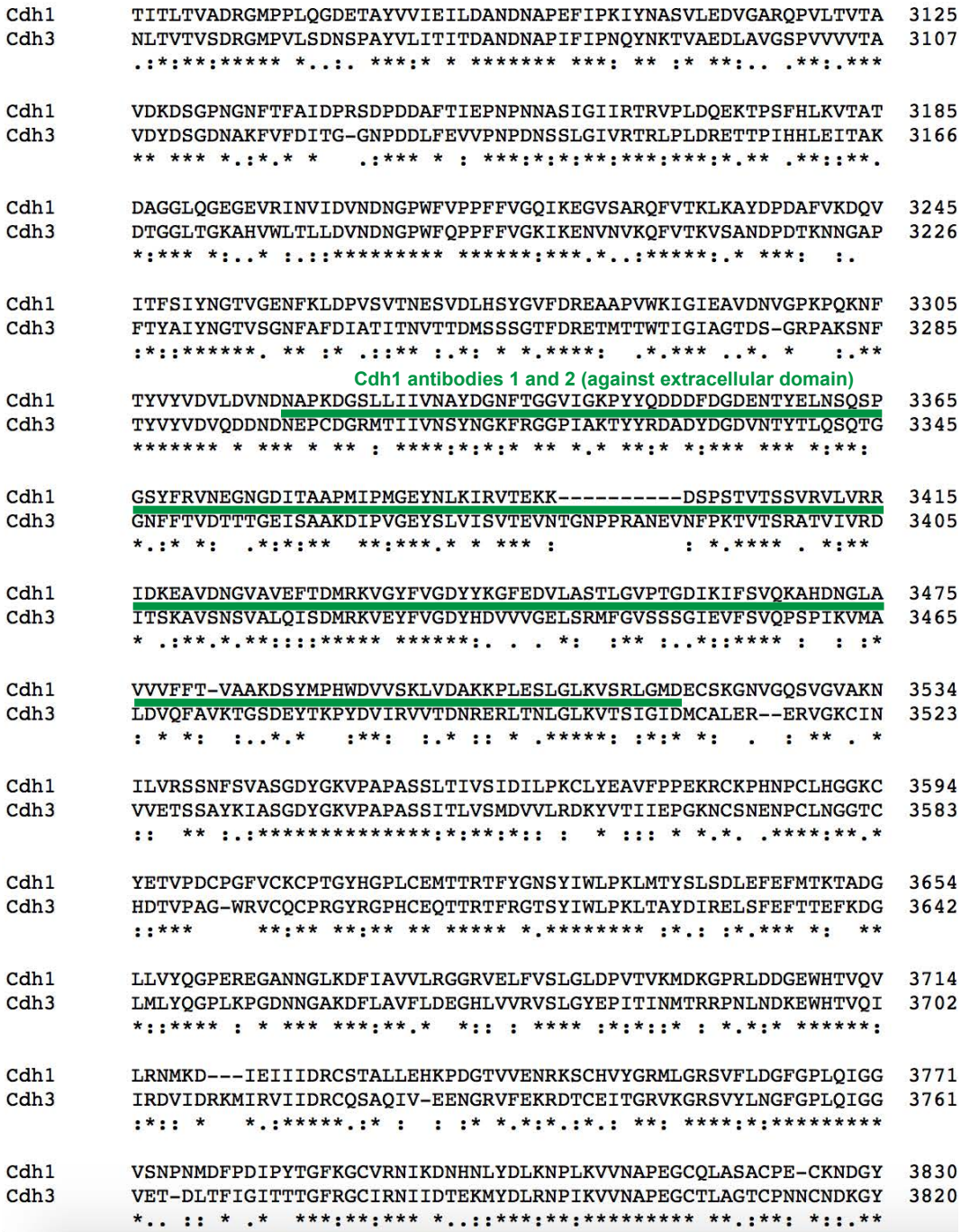


```
Cdh1        TITLTVADRGMPPLQGDETAYVVIEILDANDNAPEFIPKIYNASVLEDVGARQPVLTVTA  3125
Cdh3        NLTVTVSDRGMPVLSDNSPAYVLITITDANDNAPIFIPNQYNKTVAEDLAVGSPVVVVTA  3107
            .:*:**:***** *..:. ***:* * ******* ***: ** :* **:.. .**:.***

Cdh1        VDKDSGPNGNFTFAIDPRSDPDDAFTIEPNPNNASIGIIRTRVPLDQEKTPSFHLKVTAT  3185
Cdh3        VDYDSGDNAKFVFDITG-GNPDDLFEVVPNPDNSSLGIVRTRLPLDRETTPIHHLEITAK  3166
            ** *** *.:*.* *   .:*** * : ***:*:*:**:***:***:*.** .**::**.

Cdh1        DAGGLQGEGEVRINVIDVNDNGPWFVPPFFVGQIKEGVSARQFVTKLKAYDPDAFVKDQV  3245
Cdh3        DTGGLTGKAHVWLTLLDVNDNGPWFQPPFFVGKIKENVNVKQFVTKVSANDPDTKNNGAP  3226
            *:*** *:..* :.::********** ******:***.*..:*****:.* ***:  :.

Cdh1        ITFSIYNGTVGENFKLDPVSVTNESVDLHSYGVFDREAAPVWKIGIEAVDNVGPKPQKNF  3305
Cdh3        FTYAIYNGTVSGNFAFDIATITNVTTDMSSSGTFDRETMTTWTIGIAGTDS-GRPAKSNF  3285
            :*::*******. ** :* .::** :.*: * *.****:  .*.*** ..*. *   :.**

Cdh1        TYVYVDVLDVNDNAPKDGSLLIIVNAYDGNFTGGVIGKPYYQDDDFDGDENTYELNSQSP  3365
Cdh3        TYVYVDVQDDNDNEPCDGRMTIIVNSYNGKFRGGPIAKTYYRDADYDGDVNTYTLQSQTG  3345
            ******* * *** * ** : ****:*:*:* ** *.* **:* *:*** *** *:**:

Cdh1        GSYFRVNEGNGDITAAPMIPMGEYNLKIRVTEKK----------DSPSTVTSSVRVLVRR  3415
Cdh3        GNFFTVDTTTGEISAAKDIPVGEYSLVISVTEVNTGNPPRANEVNFPKTVTSRATVIVRD  3405
            *.:* *:  .*:*:**  **:***.* * *** :          : *.**** . *:**

Cdh1        IDKEAVDNGVAVEFTDMRKVGYFVGDYYKGFEDVLASTLGVPTGDIKIFSVQKAHDNGLA  3475
Cdh3        ITSKAVSNSVALQISDMRKVEYFVGDYHDVVVGELSRMFGVSSSGIEVFSVQPSPIKVMA  3465
            * .:**.*.**::::***** ******:. . . *:  :** :..*::**** :  : :*

Cdh1        VVVFFT-VAAKDSYMPHWDVVSKLVDAKKPLESLGLKVSRLGMDECSKGNVGQSVGVAKN  3534
Cdh3        LDVQFAVKTGSDEYTKPYDVIRVVTDNRERLTNLGLKVTSIGIDMCALER--ERVGKCIN  3523
            : * *:  :..*.*   :**:  :.* :: * .*****: :*:* *:  .  : ** . *

Cdh1        ILVRSSNFSVASGDYGKVPAPASSLTIVSIDILPKCLYEAVFPPEKRCKPHNPCLHGGKC  3594
Cdh3        VVETSSAYKIASGDYGKVPAPASSITLVSMDVVLRDKYVTIIEPGKNCSNENPCLNGGTC  3583
            ::  ** :.:***************:*:**:*:: :  * ::: * *.*. .****:**.*

Cdh1        YETVPDCPGFVCKCPTGYHGPLCEMTTRTFYGNSYIWLPKLMTYSLSDLEFEFMTKTADG  3654
Cdh3        HDTVPAG-WRVCQCPRGYRGPHCEQTTRTFRGTSYIWLPKLTAYDIRELSFEFTTEFKDG  3642
            ::***     **:** **:** ** ***** *.******** :*.: :*.*** *:  **

Cdh1        LLVYQGPEREGANNGLKDFIAVVLRGGRVELFVSLGLDPVTVKMDKGPRLDDGEWHTVQV  3714
Cdh3        LMLYQGPLKPGDNNGAKDFLAVFLDEGHLVVRVSLGYEPITINMTRRPNLNDKEWHTVQI  3702
            *:***** : * *** ***:**.*  *:: : **** :*:*::* : *.*:* ******:

Cdh1        LRNMKD---IEIIIDRCSTALLEHKPDGTVVENRKSCHVYGRMLGRSVFLDGFGPLQIGG  3771
Cdh3        IRDVIDRKMIRVIIDRCQSAQIV-EENGRVFEKRDTCEITGRVKGRSVYLNGFGPLQIGG  3761
            :*:: *   *.:*****.:* :  : :* *.*:*.:*.: **: ****:*:*********

Cdh1        VSNPNMDFPDIPYTGFKGCVRNIKDNHNLYDLKNPLKVVNAPEGCQLASACPE-CKNDGY  3830
Cdh3        VET-DLTFIGITTTGFRGCIRNIIDTEKMYDLRNPIKVVNAPEGCTLAGTCPNNCNDKGY  3820
            *.. :: * .*  ***:**:*** *..::***:**:********* **.:**: *::.**
```

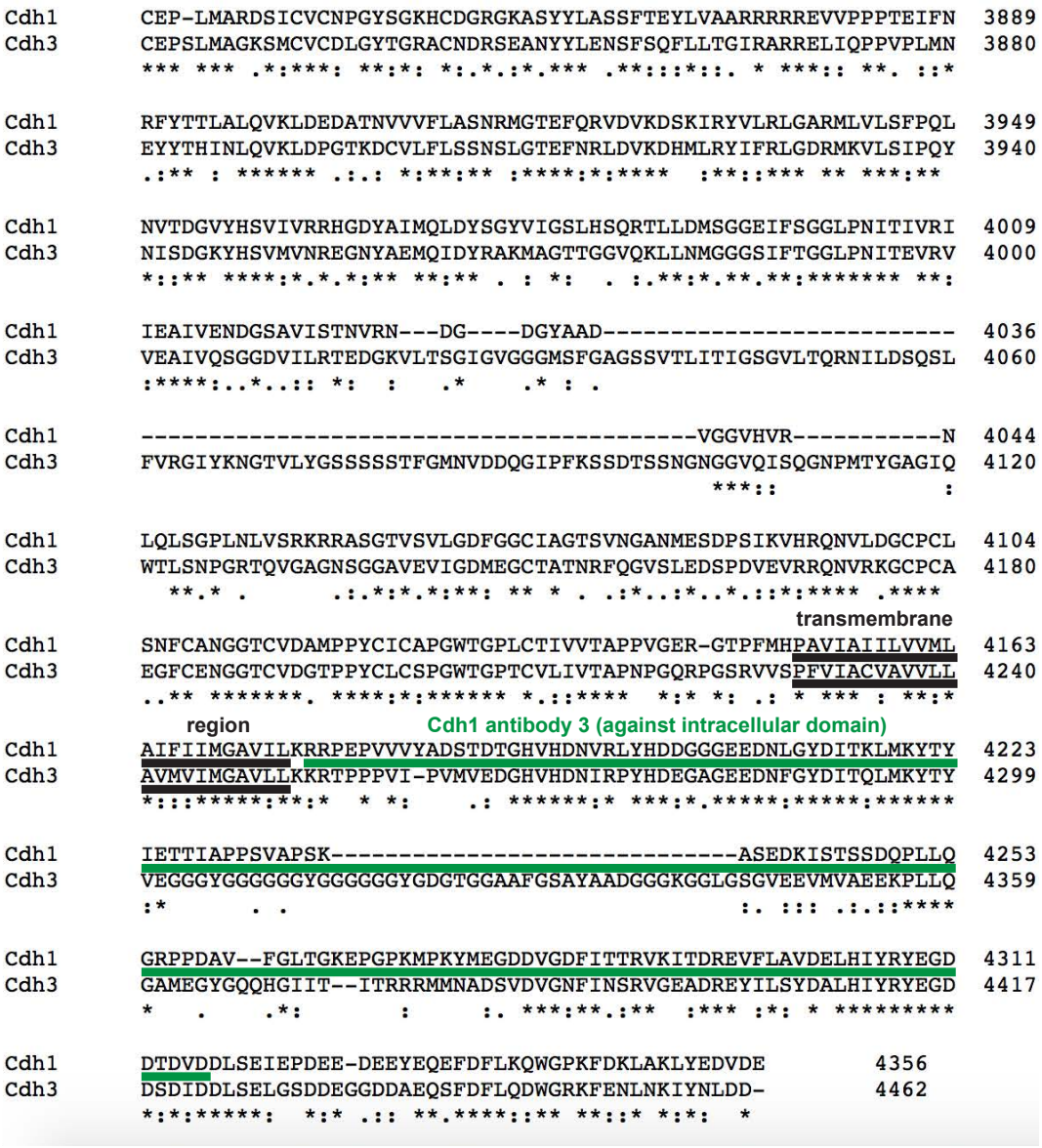

Fig. S3. Protein alignment of the full-length sequences of the Cdh1 and Cdh3. Cdh1 and Cdh3 antibody epitopes and transmembrane protein regions are underlined and recognized with the colors. Transmembrane regions were identified with the SMART protein domain annotation resource. Alignment was performed with the Clustal Omega Multiple Sequence Alignment tool.

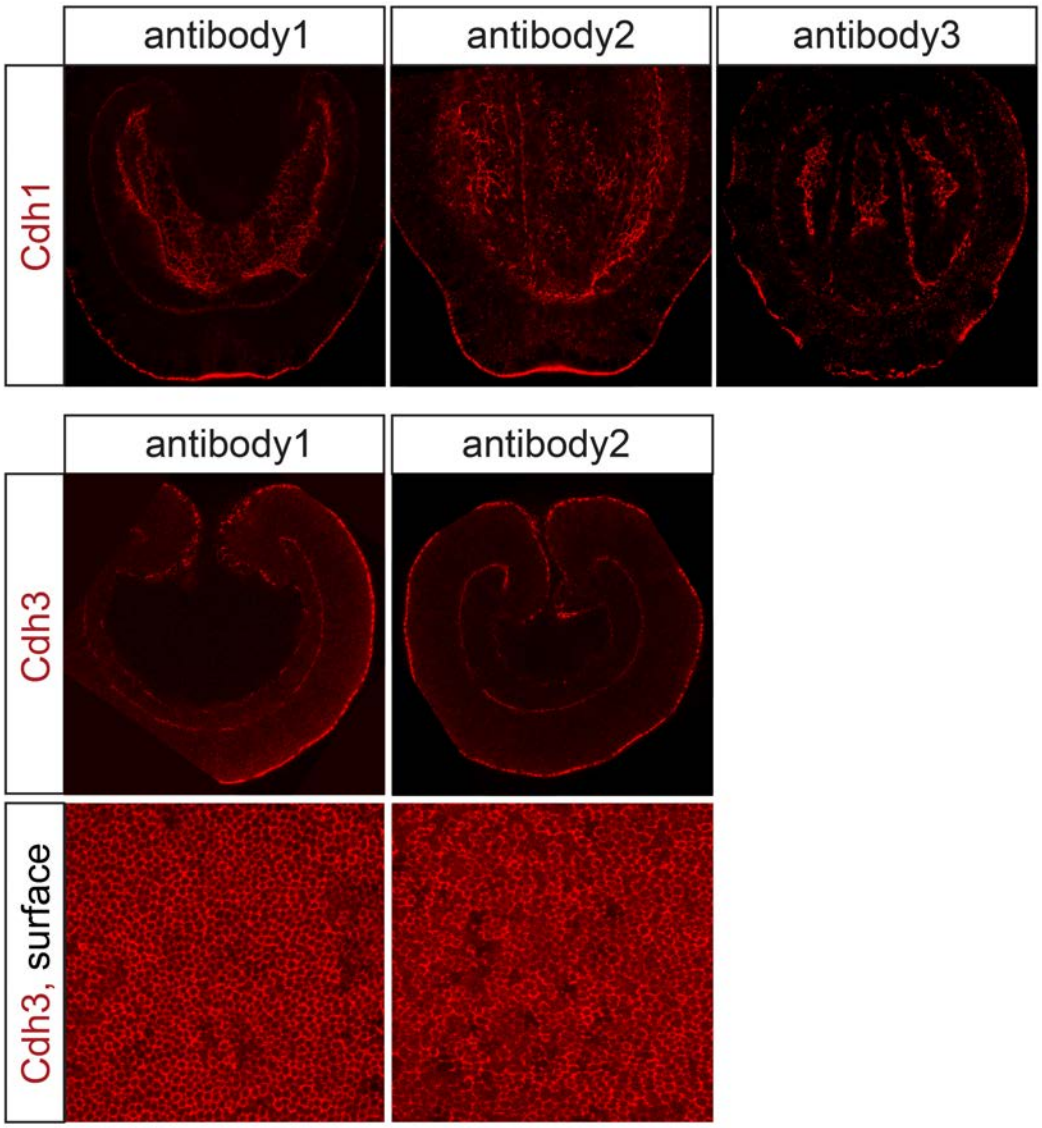

Fig. S4. Custom antibodies generated in different animals against different protein domains result in the same staining pattern. Cdh1 antibody1:domain1 (extracellular) and Cdh1 antibody2:domain1 were raised in rats; Cdh1 antibody3:domain3 (intracellular) was raised in a rabbit. All three custom Cdh1 antibodies show the same staining result. Monoclonal Cdh3 antibody1 and Cdh3 antibody2 were generated against different Cdh3 peptides and result in the same staining pattern.

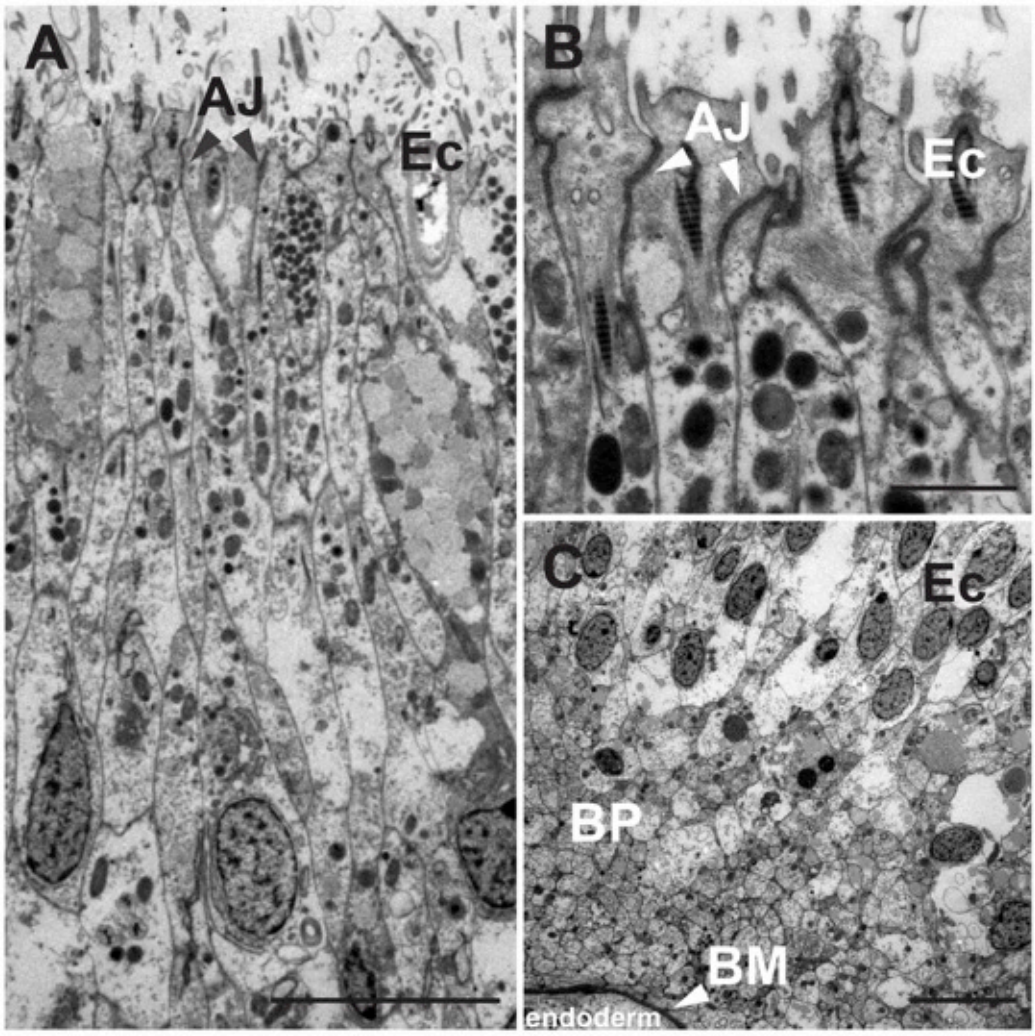

Fig. S5. TEM of the ectoderm of the apical organ. (A,B) Apical side of the ectodermal cells of the apical organ. (C) Basal side of the apical organ ectoderm. AJ apical junctions; Ec ectoderm; BP basal protrusions; BM basal membrane Scale bar A,C: 5 µm. Scale bar B: 1 µm.

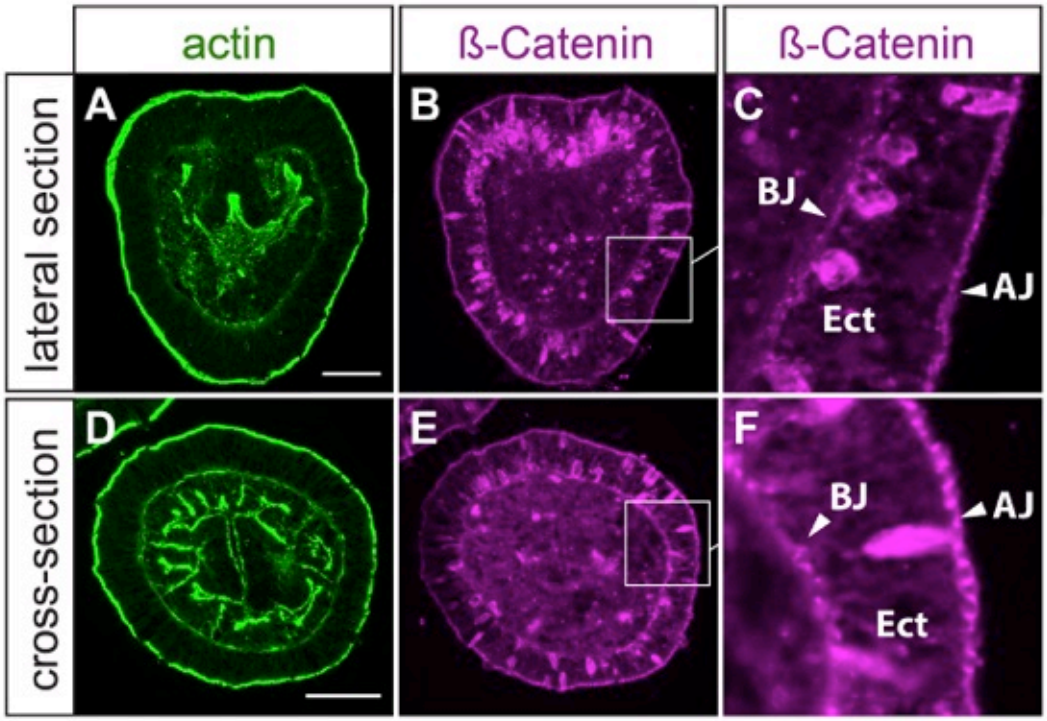

Fig. S6. β-Catenin is localized to the apical and basal adhesion junctions of the body wall ectoderm. β-Catenin antibody and phalloidin staining of vibratome sections of the 4 day old planula to exclude a possible penetration problem of the β-Catenin antibody. Please note that in vibratome sections, the β-Catenin antibody detects the basal junction in the ectoderm, but has a tendency to show unspecific staining in nematocytes and other subcellular structures. Scale bar 50 µm.

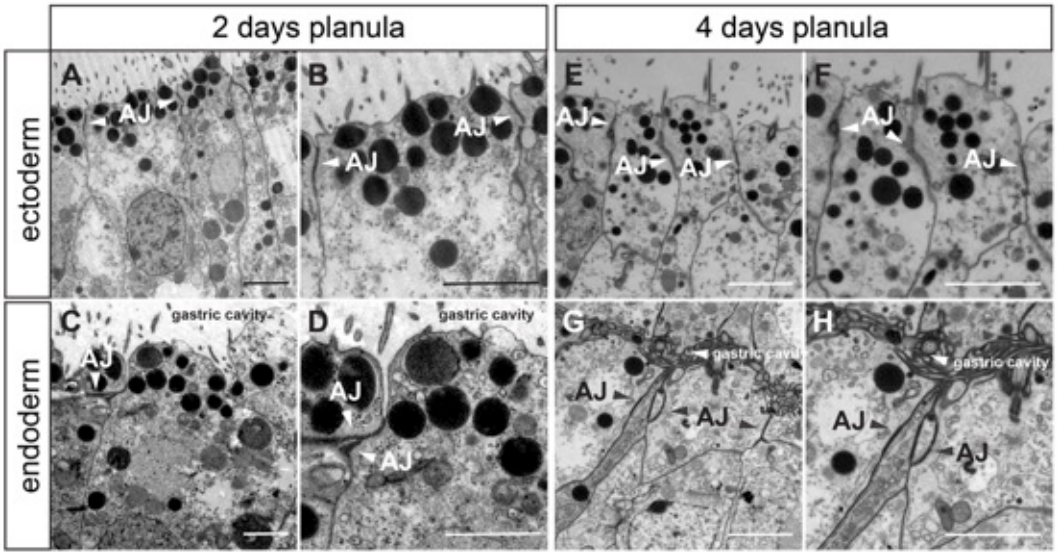

Fig. S7. TEM of the apical adherens junctions of the ectoderm and the endoderm. (A,B) ectoderm, 2 dpf planula; (C,D) endoderm, 2dpf planula; (E,F) ectoderm, 4 dpf planula; (G,H) endoderm, 4 dpf planula. Scale bar 2 µm.

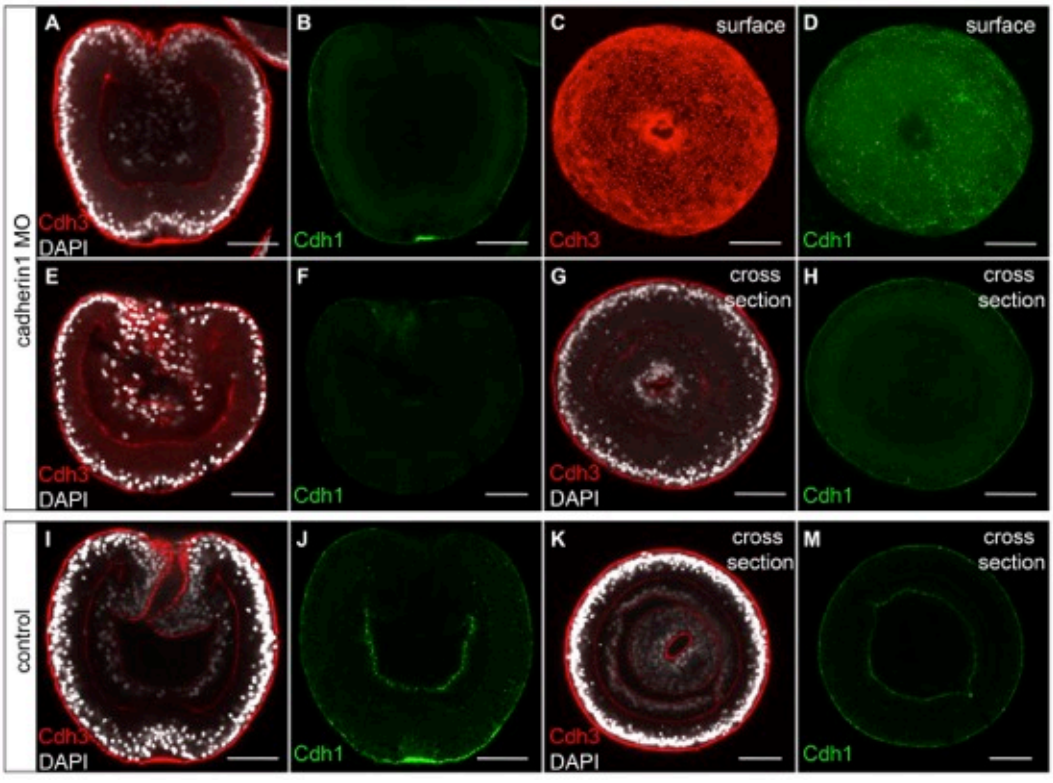

Fig. S8. Cdh1 and Cdh3 expression upon Cdh1 MO knockdown. (A-H) Cdh1 MO injected planula. (I-M) Uninjected control planula. Scale bar 50 µm.

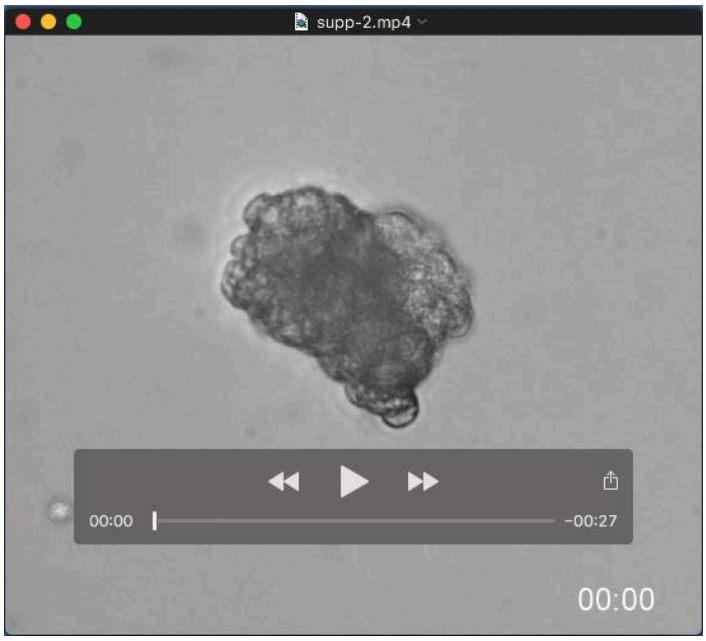

Movie 1 Std MO aggregate development. Time indicates hours and minutes.

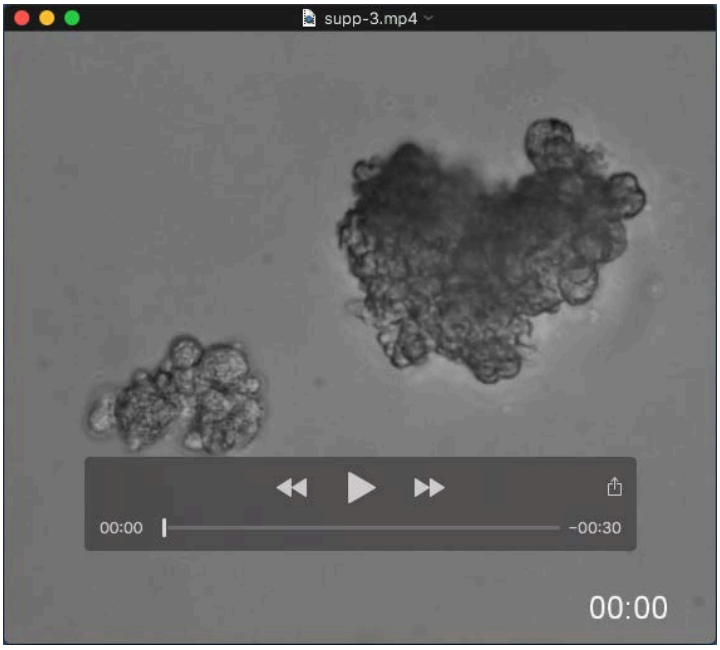

Movie 2 Cdh3 MO aggregate development. Time indicates hours and minutes.

PAPER II: “β-CATENIN-DEPENDENT MECHANOTRANSDUCTION DATES BACK TO THE COMMON ANCESTOR OF CNIDARIA AND BILATERIA”

Authors:
Ekaterina Pukhlyakova, Andrew J. Aman, Kareem Elsayad, and Ulrich Technau

Status:

Published in *PNAS, Proceedings of the National Academy of Sciences of the United States of America*, 2018, vol.115 (24), p. 6231-6236, doi/10.1073/pnas.1713682115

Contributions:

E.P., A.J.A., and U.T. designed research; E.P. and A.J.A. performed research; K.E. contributed new reagents/analytic tools; E.P., A.J.A., K.E., and U.T. analyzed data; and E.P., A.J.A., and U.T. wrote the paper.

β-Catenin–dependent mechanotransduction dates back to the common ancestor of Cnidaria and Bilateria

Ekaterina Pukhlyakova[a], Andrew J. Aman[a,1], Kareem Elsayad[b], and Ulrich Technau[a,2]

[a]Department for Molecular Evolution and Development, Centre of Organismal Systems Biology, University of Vienna, Vienna A-1090, Austria; and [b]Advanced Microscopy Section, Vienna Biocenter Core Facilities GmbH, Vienna A-1030, Austria

Edited by Richard M. Harland, University of California, Berkeley, CA, and approved April 30, 2018 (received for review August 3, 2017)

Although the genetic regulation of cellular differentiation processes is well established, recent studies have revealed the role of mechanotransduction on a variety of biological processes, including regulation of gene expression. However, it remains unclear how universal and widespread mechanotransduction is in embryonic development of animals. Here, we investigate mechanosensitive gene expression during gastrulation of the starlet sea anemone *Nematostella vectensis*, a cnidarian model organism. We show that the blastoporal marker gene *brachyury* is downregulated by blocking myosin II-dependent gastrulation movements. *Brachyury* expression can be restored by applying external mechanical force. Using CRISPR/Cas9 and morpholino antisense technology, we also show that mechanotransduction leading to *brachyury* expression is β-catenin dependent, similar to recent findings in fish and *Drosophila* [Brunet T, et al. (2013) *Nat Commun* 4:1–15]. Finally, we demonstrate that prolonged application of mechanical stress on the embryo leads to ectopic *brachyury* expression. Thus, our data indicate that β-catenin–dependent mechanotransduction is an ancient gene regulatory mechanism, which was present in the common ancestor of cnidarians and bilaterians, at least 600 million years ago.

Nematostella | mechanotransduction | β-catenin | gastrulation | *brachyury*

Embryonic development is governed by a genetic program, which includes numerous feedback loops and ramifications. However, the role of epigenetic cues and physical constraints in influencing development has recently gained support. Mechanical forces can be transformed by cells into biochemical signals in a process called mechanotransduction (1–9). Parameters like cell shape, ability to spread on extracellular matrix, and stiffness of the cell environment can directly govern cell differentiation and proliferation rate (10–15). Recent experimental studies have begun to elucidate roles for mechanotransduction in embryonic development, such as regulation of gene expression, pattern fomation, and organogenesis (16–22). In *Drosophila*, external mechanical stress induced the key mesoderm determinant *twist*, while in zebrafish, mechanical stress induced expression of *brachyury*, which is crucial for mesoderm development in all vertebrates. Notably, in both organisms, this mechanically induced gene expression is dependent on β-catenin (16). However, to date, it is unclear whether these are isolated phenomena or whether this reflects a conserved mechanism. To test whether mechanosensitive gene regulation predates the origin of Bilateria, we chose to study the anthozoan sea anemone *Nematostella vectensis*, a representative of the Cnidaria, the sister group to Bilateria, which emerged ∼600–700 Mya (23, 24). Interestingly, the *Nematostella* homolog of *brachyury* is expressed around the blastopore, and this expression pattern is conserved in most studied embryos, representing diverse bilaterian and nonbilaterian phyla (25–35). As in vertebrates and other deuterostomes, *brachyury* is a direct target of Wnt/β-catenin signaling (36–39). Thus, a blastoporal expression of *brachyury* and its regulation seems to be a widely conserved feature among metazoans (25–35).

Results

The Role of Myosin II During Gastrulation of *N. vectensis*. Gastrulation in *N. vectensis* occurs by invagination and is initiated by the apical constriction of cells at the animal pole, which leads to the formation of the preendodermal plate. Subsequently, the preendodermal plate invaginates into the blastocoel (Movie S1) (40, 41). As actomyosin constriction is involved in apical constriction and cell-shape changes, we examined the necessity of this force-generating mechanism during gastrulation using ML-7, a potent and selective reversible myosin light chain kinase (MLCK) inhibitor. We found that 10 μM ML-7, applied at blastula stage, was sufficient to completely inhibit invagination during gastrulation, although this treatment did not entirely inhibit apical constriction of preendodermal cells (Fig. 1*I*) (42, 43). It is likely that additional, actomyosin-independent mechanisms such as membrane shuttling participate in preendoderm apical constriction (44). To show that the effect of ML-7 is nontoxic and reversible, we washed out the inhibitor after 12 h of treatment, at the time when the control embryos have completed gastrulation. Most of the ML-7 washout embryos (78/100) then gastrulated (Fig. S1) and ultimately develop into polyps. Thus, ML-7 specifically impairs myosin II function required for invagination of the endoderm during *N. vectensis* gastrulation.

Significance

Besides genetic regulation, mechanical forces have been identified as important cues in numerous developmental processes. Mechanical forces can activate biochemical cascades in a process called mechanotransduction. Recent studies in vertebrates and flies elucidated the role of mechanical forces for mesodermal gene expression. However, it remains unclear whether mechanotransduction is a universal regulatory mechanism throughout Metazoa. Here, we show in the sea anemone *Nematostella vectensis* that mechanical pressure can ectopically activate or restore *brachyury* expression. This mechanotransduction is dependent on β-catenin, similar to vertebrates. We propose that a regulatory feedback loop between genetic and mechanical gene activation exists during gastrulation and the β-catenin–dependent mechanotransduction is an ancient regulatory mechanism, which was present in the common ancestor of cnidarians and bilaterians.

Author contributions: E.P., A.J.A., and U.T. designed research; E.P. and A.J.A. performed research; K.E. contributed new reagents/analytic tools; E.P., A.J.A., K.E., and U.T. analyzed data; and E.P., A.J.A., and U.T. wrote the paper.

The authors declare no conflict of interest.

This article is a PNAS Direct Submission.

[1]Present address: Department of Biology, University of Virginia, Charlottesville, VA 22904.

[2]To whom correspondence should be addressed. Email: ulrich.technau@univie.ac.at.

This article contains supporting information online at www.pnas.org/lookup/suppl/doi:10.1073/pnas.1713682115/-/DCSupplemental.

Published online May 21, 2018.

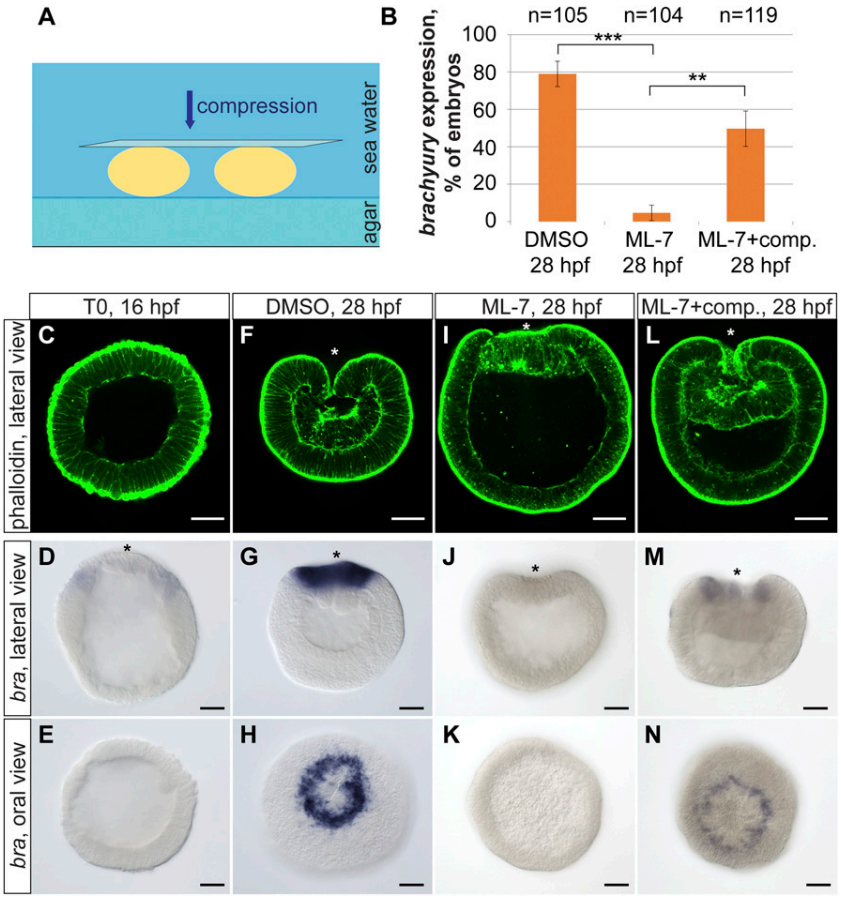

Fig. 1. Mechanically induced *brachyury* expression in the *Nematostella* embryos. (*A*) Scheme of the compression experiment. Embryos are compressed by a coverslip in seawater. (*B*) Quantification of the embryos, expressing *brachyury* upon DMSO control, treatment with ML-7 alone, and treatment with ML-7 combined with mechanical compression. Data from at least three independent experiments are combined and displayed in the graph. Differences between DMSO and ML-7–treated embryos, and between ML-7–treated and ML-7–treated/compressed embryos, are significant, paired two-tailed Student's *t* test (***$P < 0.01$; **$P < 0.02$). (*C–E*) Earliest detectable onset of the ring-like *brachyury* expression in blastulae at 16 hpf marking the presumptive blastopore lip. (*F–H*) *Brachyury* expression in the DMSO-treated control embryos at late gastrula stage (28 hpf). (*I–K*) Gastrulae treated from 16 to 28 hpf with ML-7 show inhibition of invagination of preendodermal plate as well as loss or severe down-regulation of *brachyury* expression. (*L–N*) Mechanical uniaxial global compression can rescue *brachyury* expression in the ML-7–treated embryos. (Scale bar, 50 μm.) Asterisk indicates the oral pole of the embryo.

Blocking Gastrulation Movements Inhibits *Brachyury* Expression, Which Can Be Rescued by Applying External Mechanical Stress. Gastrulation in *Nematostella* is accompanied by the expression of several marker genes. Expression of the T-box gene *brachyury* starts shortly before gastrulation as a broad ring at blastula stage marking the boundary of the preendodermal plate (Fig. 1 *C–E*) (45–48). With the beginning of gastrulation movements, *brachyury* expression intensifies and narrows to a few rows of marginal cells surrounding the blastopore (Fig. 1 *F–H*).

If *brachyury* expression depends on mechanical stress generated by gastrulation movements, we expected *brachyury* expression to be reduced in ML-7–treated embryos. Indeed, in more than 95% of ML-7–treated embryos *brachyury* expression either vanishes completely or is not expressed as a contiguous ring (Fig. 1 *B*, *J*, and *K*). To determine whether loss of *brachyury* expression in ML-7–inhibited embryos is due to the absence of mechanical strains, pregastrulation blastulae were subjected to external pressure for 12 h during ML-7 treatment (Fig. 1*A* and Fig. S2). As controls, spherical blastulae were treated with ML-7 or DMSO without exogenous force. Experimental treatments began in stage-matched blastulae [16 hours postfertilization (hpf)] and were terminated when all of the DMSO-treated control embryos had completed gastrulation (28 hpf). We observed normal *brachyury* expression in a contiguous ring in 50% ($n = 119$) of the ML-7–treated embryos subjected to compression compared with 5% ($n = 104$) in similarly treated embryos with no compression (three independent experiments; $P \leq 0.02$ paired, two-tailed Student's *t* test) (Fig. 1 *B*, *M*, and *N*). These data show that applied mechanical stimulation is sufficient to restore *brachyury* expression in embryos lacking gastrulation strains.

Interestingly, mechanical force applied to the ML-7–treated embryos during gastrulation activated *brachyury* expression only around the blastopore (Fig. 1*N*). Thus, blastoporal cells appear more competent than the rest of the embryo to respond to mechanical forces by altering gene expression, likely because the blastopore cells are a zone of active Wnt/β-catenin signaling and *brachyury* is a direct target of β-catenin (47, 48).

Up-Regulation of *Brachyury* Expression upon External Mechanical Strain Is β-Catenin Dependent. To test whether β-catenin has a role in stress-induced expression of *brachyury*, we used CRISPR/Cas9 technology to mutate the *apc* homolog in *Nematostella* (48–51). Apc is a necessary component of the β-catenin destruction complex and its loss of function is expected to lead to constitutive activation of Wnt/β-catenin signaling (52). Homozygous mutants of *apc* show a discernible phenotype at 3 dpf, as

expected for a negative regulator of Wnt signaling (47, 53). Homozygous *apc* mutants also express *brachyury* ectopically compared with wild-type and heterozygous siblings (Fig. 2 *A–D*). Importantly, this expression was maintained even during ML-7 treatment, which blocks invagination of the preendodermal plate (Fig. 2 *E* and *F*), suggesting that the stabilization of β-catenin is downstream of the mechanotransduction.

As a complementary test, we repeated the ML-7 treatment and application of mechanical strain on embryos where β-catenin expression is knocked down by morpholino (MO) injection (53). *Brachyury* expression was lost in the β-catenin morpholino-injected embryos and could not be rescued by application of external mechanical stress (Fig. 2 *G–K*). Together, these results show that up-regulation of *brachyury* expression upon mechanical stress is β-catenin dependent and that the mechanical stress acts upstream of β-catenin activation.

Prolonged Mechanical Stress Activates Ectopic *Brachyury* Expression. To test whether other areas of the embryo are competent to express *brachyury* in response to mechanical force, we subjected stage-matched spherical blastulae to prolonged compression. We compressed embryos at 15 °C for 26 h until control embryos had completed gastrulation. Incubation at colder temperatures slows down the development and enables the force impact during gastrulation for a longer time. About 40% (74/187) of the compressed embryos had broad, ectopic *brachyury* expression relative to ∼10% (7/68) uncompressed controls (Fig. 3 *A–C*). Interestingly, compression of late gastrulae did not lead to ectopic *brachyury* expression (Fig. 3 *D–F*). Hence, there appears to be a narrow time window in which cells are competent to respond to mechanical forces. This implies that mechanical forces cooperate with the genetic factors to regulate *brachyury* expression during the blastula-to-gastrula transition.

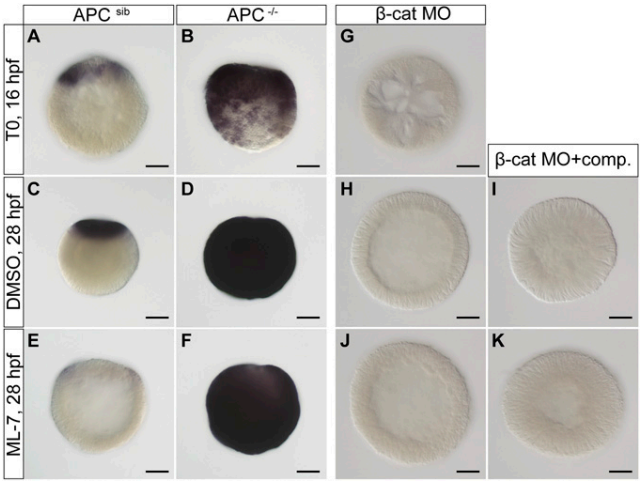

Fig. 2. Up-regulation of *brachyury* expression upon external mechanical strain is β-catenin dependent. (*A–D*) *Brachyury* is ectopically expressed in APC$^{-/-}$ homozygous mutants throughout embryonic development. (*E*) ML-7 leads to down-regulation of *brachyury* in wild-type or heterozyogous embryos. (*F*) ML-7 treatment does not inhibit up-regulation of *brachyury* expression in APC$^{-/-}$ homozygous mutants. (*G* and *H*) β-Catenin morpholino injection leads to the complete inhibition of *brachyury* expression throughout the embryo development in control embryos. (*I* and *K*) Mechanical compression of β-catenin MO-injected embryos combined with DMSO control or ML-7 treatment does not rescue *brachyury* expression. (Scale bar, 50 μm.) APC$^{-/-}$, homozygous mutants; APC^{sib}, siblings, heterozygous mutants, or wild-type embryos.

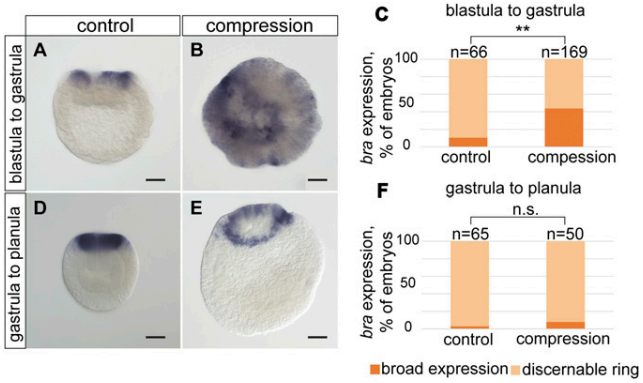

Fig. 3. Prolonged external mechanical stress can cause an overexpression or ectopic *brachyury* expression at blastula and early gastrula stage. (*A*) Control embryo expressing *brachyury* as a ring around the blastopore. (*B*) Overexpression of *brachyury* after long-term embryo compression, applied at blastula stage for 26 h. (*C*) Quantification of the embryos expressing *brachyury* at blastopore or ectopically. (**χ^2 test; $P < 0.01$) (*D*) Strong blastopore expression of *brachyury* in late control gastrula. (*E*) Late gastrula compressed for 26 h. No ectopic *brachyury* expression was detected. (*F*) Quantification of *brachyury* expression after late gastrula compression. Data are pooled from two independent experiments. The difference between control and compressed gastrulae is significant (n.s., nonsignificant; χ^2 test; **$P > 0.05$). (Scale bar, 50 μm.)

Role of Mechanical Strains and Cell-Shape Change During Gastrulation of *N. vectensis*. To monitor the morphogenetic movements and the dynamics of cell-shape changes during gastrulation, we generated a transgenic line expressing the actin-binding protein lifeact-mOrange2 under the control of a recently reported EF1a promoter (54). During gastrulation, presumptive endodermal cells constrict apically, forming a preendodermal plate, which then invaginates into the blastocoel (Movie S1) (40, 41). At the same time, ectodermal cells surrounding the blastopore also undergo extensive morphogenetic changes. The analysis of the time-lapse movies of gastrulating embryos of *Nematostella* revealed that the formation and invagination of the preendodermal plate correlates with extensive elongation of the ectodermal blastopore lip cells, whereas the shape of more aboral cells remains unchanged (Fig. 4*A*, Fig. S4 *A–I*, and Movies S1 and S2). Shortly after, the blastoporal cells constrict on the basal side, thus bending the blastopore lip toward the preendodermal plate and therefore pushing it inside (Fig. 4*D*). Unexpectedly, ML-7 treatment only slightly inhibits apical constriction of the preendodermal cells, and blastoporal cells abutting the preendodermal plate get stretched apically as in the control embryo (Fig. 4 *A–C*). However, sagittal sections of the ML-7–treated gastrulae revealed that the blastoporal marginal cells do not constrict on the basal side (Fig. 4*C*), and hence the blastopore lip does not bend inwards. As a result, the blastopore lip is unable to push in the preendodermal plate during gastrulation. These results suggest that cellular contractility at the basal side of the blastopore lip cells is very important for the morphogenetic movements during gastrulation. We propose that the pushing force of the blastopore lip rather than a pulling force of the apical constriction of the preendodermal cells is a driving force of invagination movement.

Regardless, the fact that blocking actomyosin contraction during gastrulation abolishes expression of several β-catenin target genes (47, 53), such as *brachyury*, *foxA*, *axin*, and *apc*, expressed in the blastopore lip (Fig. S3). Interestingly, ML-7 treatment did not affect *snailA* expressin in the preendodermal plate (Fig. S3 *K* and *L*). These results suggest that the blastopore lip is a sensitive region for β-catenin–dependent mechanotransduction.

To get insights into the mechanical properties of the cells during gastrulation, we used a Brillouin scattering microscope,

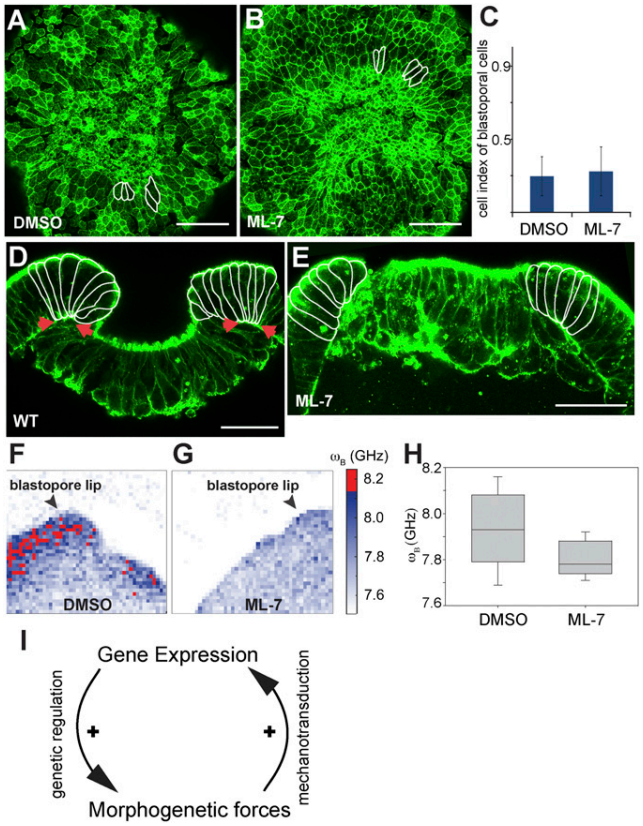

Fig. 4. Effects of ML-7 treatment on blastopore lip cell morphology and stiffness. (*A* and *B*) Oral view of the preendodermal plate and surrounding blastopore lip without (*A*) and with ML-7 (*B*) treatment, phalloidin staining. A few blastopore lip cells are outlined to emphasize the cell shape. (*C*) Differences between cell indexes of blastopore lip cells under DMSO and ML-7 treatment is not significant, paired two-tailed Student's *t* test ($P > 0.1$). (*D* and *E*) Sagittal view of the preendodermal plate and blastopore lip without (*D*) and with ML-7 (*E*) treatment. Blastopore lip cells are outlined. Arrows indicate the basal constriction of the blastopore lip cells in a control embryo, phalloidin staining. (Scale bar, 50 μm.) (*F* and *G*) Representative maps of the Brillouin frequency shift ω_B (proportional to the square root of the longitudinal storage modulus) in the vicinity of the blastopore lip without (*F*) and with (*G*) inhibitor treatment, showing a decrease in stiffness in the treated samples. Regions of high-frequency shift (stiffness) are colored red. Arrowheads mark the blastopore lip region. (*H*) Frequency shift ω_B (which is proportional to the square root of the elastic modulus) in embryos with and without inhibitor. The untreated embryos show an increased frequency shift on average and broader distribution of values relative to the treated ones. (*I*) Proposed positive feedback model of regulating gene expression and cell-shape changes with inherent mechanical stress.

which allows for spatial mapping of the viscoelastic properties of biological materials (55–58). The Brillouin microscope probes the sample pixel per pixel with a single-frequency laser and measures the gigahertz scale (<0.0001-nm wavelength) spectral modification of the scattered light. Spectrally shifted light is the result of inherent collective thermal density fluctuations within the sample, which can be used to calculate the viscoelasticity of the cell.

Our measurements show that the blastopore lip cells appear significantly "stiffer" than the plate cells or cells on the aboral side of the embryo (the elastic modulus in the former is larger than in the latter by on average more than 10%) (Fig. S4 *J* and *K*). Remarkably, cells of the ML-7–treated embryos were significantly softer than cells of the wild-type embryos and blastopore lip cells displayed a similar stiffness as the other parts of the embryo (Fig. 4 *E*–*I*). Our data suggest that contractility and increased longitudinal compressibility (stiffness) of the blastopore lip cells is crucial for the force generation, which drives invagination movements and facilitates mechanosensitive gene expression.

Discussion

Our results show that in *Nematostella*, *brachyury* expression can be induced by β-catenin–dependent mechanotransduction of physical forces. We speculate that during normal development, the gastrulation movements generate the physical forces acting on blastopore lip cells. We propose that mechanical and genetic regulation of gene expression form a feedback loop that robustly enforces *brachyury* expression: early maternal activation of intracellular components of Wnt/β-catenin at the oral pole activate the expression of Wnt ligands in the preendodermal plate at the blastula stage (Fig. 4*I*). Through negative feedback loops, these Wnt genes become expressed as a ring surrounding the preendodermal plate, where they initiate *brachyury* expression at the margin of the blastopore and endoderm in the plate. The contractility of the blastopore lip cells lead to a local higher stiffness. This mechanical stress is then transduced in a β-catenin–dependent manner to enforce *brachyury* expression and other targets of β-catenin in the blastopore lip. Due to the high concentrations of β-catenin at the oral pole, this region is particularly competent to respond to mechanical stress, preventing that undirected physical forces could ectopically activate *brachyury* expression. However, upon prolonged physical stress, *brachyury* can be induced ectopically as well. The contraction of the blastopore lip cells at the basal side then bends the lip inward and pushes the plate into the blastocoel.

Because β-catenin–dependent mechanotransduction and activation of *brachyury* is also found in other Bilateria (16), these findings imply that this mechanism of gene regulation and the feedback between genetic and mechanical gene activation might be an ancient feature of animal development, at least predating the cnidarian–bilaterian split over 600 Mya (23, 24).

Materials and Methods

Animals and Embryo Culturing. Animals were kept in the dark at 18 °C. Spawning and embryo collection were performed as described (59, 60). Work with genetically modified organisms (GMO) of safety level 1 at the Department of Molecular Evolution and Development, University of Vienna, was approved by the Ministery of Economy and Sciences (BMWfW) of Austria.

Live Imaging. Transgenic animals expressing lifeact-mOrange2 under control of the ubiquitous EF1α promoter were generated. Fully transgenic F1 animals were spawned as described (59, 60). Transgenic embryos were embedded in 1% low-melting point agarose (V3841, Promega) and imaged in *Nematostella* medium (NM) with a HCX ApoL40X/0.8W objective using a Leica TCS SP5X confocal microscope. Time stamps were added to the movies using ImageJ software Time Stamper plugin (NIH).

Morpholino Injection. β-Catenin knockdown was performed by zygote injection of previously characterized translation blocking β-cat–MO: 5′ TTCTTCGACTTTAAATCCAACTTCA (53) at a concentration of 500 μM.

Inhibitor Treatment. Prior treatment embryos were kept at 17 °C. For the inhibition of cellular contractility and cellular mechanical tensions within the embryo, ML-7, a selective MLCK inhibitor, was used (Calbiochem, Merk Millipore). All treatments were carried out at 22 °C. At 16 hpf, precisely staged spherical blastulae were selected and treated with 10 μM ML-7/1% DMSO in NM until 28 hpf. Control embryos were treated with 1% DMSO in NM. At least 100 embryos were selected for each treatment, including the experiments with embryo compression. At 28 hpf, embryos were processed for the fixation as described below. To confirm reversibility of ML-7 treatment, at 28 hpf, ML-7–treated embryos were washed 5 × 5 min in NM and left to develop in NM until 42 hpf.

Uniaxial Global Embryo Compression. To restore mechanical strains in ML-7–inhibited embryos, we applied uniaxial global embryo compression to the embryos. For this purpose, we placed exactly 100 embryos on a Petri plate lined with 1.1% low-melting point agarose/10 μM ML-7/NM) in the 10 μM ML-7/1% DMSO/NM solution. Microscopic coverslip size 24 × 50 mm, m = 0.43 g

(Roth, catalog no. 1871) was slowly dragged on top of the embryos without further pressing. In this way, the force compressing the embryos was approximately equivalent to the weight of the coverslip. Since the number of embryos in each experiment was 100, the compressing force was roughly the same in each experiment, which was calculated as: $F = m_{coverslip} \cdot g - Fa$; $Fa = \rho_{water} \cdot g \cdot V_{coverslip}$; $F = 2.61$ mN on 100 embryos. Therefore, ~26 μN was applied to each embryo. Embryos were compressed for 12 h at 22 °C. Three independent experiments were performed. To stimulate ectopic *brachyury* expression, we compressed stage-matched spherical blastulae at 16 hpf and late gastrulae at 28 hpf for 26 h at 16 °C.

Phalloidin Staining. Embryos were fixed in 3.7% formaldehyde/PBS at 4 °C for 1 h. After 7 min acetone shock on ice, embryos were washed five times in PBSTx (PBS with 0.2% Triton X-100) and incubated with Alexa Fluor 488 Phalloidin (Thermo Fisher Scientific) diluted 1:30 in PBSTx at 4 °C, overnight. After the staining, embryos were washed 10 × 10 min in PBSTx, mounted in Vectashield (Vector Laboratories), and imaged with a Leica TCS SP5X confocal microscope.

In Situ Hybridization. In situ hybridizations (ISHs) were conducted as previously described (48, 61). Embryos were imaged and quantified with the Nikon Eclipse 80i compound microscope equipped with DIC optics and Zeiss AxioCam camera. Quantification of the in situ patterns of different treatments within one experiment was done blindly on encoded microscope slides.

Brillouin Scattering Microscopy.

Experimental setup. The setup used for Brillouin scattering microscopy employs a confocal microscope with a high-efficiency cross-dispersion imaging spectrometer described in detail in ref. 58. The only significant difference was the addition of a Lyot stop to suppress high-frequency interference fringes (57) before the spectrum being imaged onto an EM CCD camera. Embryos were embedded in low-melting point agarose as described above and imaged through glass-bottom dishes in a custom sample holder mounted on a 3-axis Piezo stage, which was mounted on a motor stage, and spatial maps of the frequency shift were obtained by translating the sample. In all cases we measured the parallel polarization back-scattering spectra. A transmitted light image could be obtained by illuminating the sample from above via a condenser to image onto a sCMOS camera attached to a side port of the microscope frame.

Imaging. A 1.4 N.A. oil-immersion objective lens (Olympus PLAPON 60XOSC2) was used for excitation/detection. An iris positioned at the entrance port of the microscope was partially closed to reduce the effective N.A. and peak broadening (62). Measurements on 100 nm fluorescent beads yielded a point spread function with a full width at half maximum of 340 nm (690 nm) laterally (axially). In all scans, the laser power at the sample was between 1 and 3 mW and acquisition time per spectrum was between 100 and 300 ms. Depending on the size, a Brillouin map would typically take several to tens of minutes. Wide-field images were taken before and after scans to assure embryos had not moved or changed significantly during the scan.

Data analysis. Calibration measurements were performed between sample measurements on water and ethanol to calibrate the dispersion axis as described in ref. 58. Least-squares fitting of Voigt functions in Matlab (Matlab peakfit.m function: https://terpconnect.umd.edu/~toh/spectrum/InteractivePeakFitter.htm) was used to determine the separation of the peaks along the dispersion axis, which together with the calibration measurements allowed us to deduce the Brillouin frequency shift (ω_B) (56, 58).

Data interpretation. All spatial maps show the Brillouin frequency shift (derived from the mean position of the fitted peaks in the measured spectrum). The frequency shift is related to the longitudinal storage modulus (M') via: $\omega_B = C \cdot n \cdot \lambda^{-1} \sqrt{M'/\rho}$, where n and ρ are the refractive index and mass density of the sample at the measured point, λ is the wavelength of the laser used, and C is a constant that depends on the measurement geometry. It is often observed and can be argued via Lorenz–Lorentz relation that the refractive index squared will scale with the mass density, such that variations in these parameters in a heterogeneous sample will to a good approximation cancel each other out. From this it follows that the longitudinal storage modulus will be proportional to the square of the measured Brillouin frequency shift.

Interpretation of the measured longitudinal storage modulus (M′). M′ is distinct from the Young's Modulus E [as is measured e.g., with atomic force microscopy (AFM)] in that it assumes that laterally the sample size is constrained. It thereby is sensitive to the compressibility of the sample and can be related to E only with knowledge of the Poisson ratio. A large value of M′ would thus mean that if the sample's lateral dimensions are fixed, its longitudinal dimensions (in the direction the sample is probed) would change less when subject to a stress (i.e., it is more "rigid"). It is also worth noting that in Brillouin light scattering, one is measuring the elastic modulus at gigahertz frequencies, compared with the quasistatic regime probed using most perturbation-based techniques. At these frequencies, most materials are at or above their glass transition frequency and thus will appear significantly stiffer. Nevertheless in live cells, an empirical power–law relation between the AFM-measured Young's modulus and the Brillouin-measured longitudinal modulus is often observed (56), suggesting that an increase in the measured Brillouin frequency shift may be assumed to be associated with an increase in the stiffness of cells.

Image Processing. Images were adjusted for levels, brightness, and contrast using FIJI software (63). Focus stacking of ISH images was done using Helicon Focus software (Helicon Soft Ltd). All images were cropped and assembled into the panels using Adobe Illustrator CS6 software.

Cell-Shape Index Measurement. Cell-shape indexes of the blastoporal and aboral cells for the beginning of gastrulation (t0) and for the midgastrulation time point (t1) were calculated as follows: cell index(t) = cell width(t)/cell length(t). Fold change cell index was calculated as cell index(t0)/cell index (t1). $n = 30$, $P \leq 0.01$, paired two-tailed Student's t test. Nondividing cells visible in the middle of the field of view were taken at random for measurements.

ACKNOWLEDGMENTS. We thank Carl-Philipp Heisenberg and Cornelia Schwayer for fruitful discussions, G. Genikhovich for critically reading the first version of the manuscript, E. L. Genikhovich for help in calculating the applied force, and the Advanced Microscopy Facility in Vienna Biocenter Facilities and the Core Facility for Cell Imaging and Ultrastructure Research of the University of Vienna for assistance. This work was funded by Austrian Science Fund Grant P25993 (to U.T.).

1. Wozniak MA, Chen CS (2009) Mechanotransduction in development: A growing role for contractility. *Nat Rev Mol Cell Biol* 10:34–43.
2. Iskratsch T, Wolfenson H, Sheetz MP (2014) Appreciating force and shape—The rise of mechanotransduction in cell biology. *Nat Rev Mol Cell Biol* 15:825–833.
3. Lecuit T, Lenne P-F, Munro E (2011) Force generation, transmission, and integration during cell and tissue morphogenesis. *Annu Rev Cell Dev Biol* 27:157–184.
4. Hoffman BD, Grashoff C, Schwartz MA (2011) Dynamic molecular processes mediate cellular mechanotransduction. *Nature* 475:316–323.
5. Wang N, Tytell JD, Ingber DE (2009) Mechanotransduction at a distance: Mechanically coupling the extracellular matrix with the nucleus. *Nat Rev Mol Cell Biol* 10:75–82.
6. Chen CS (2008) Mechanotransduction–A field pulling together? *J Cell Sci* 121: 3285–3292.
7. Gillespie PG, Walker RG (2001) Molecular basis of mechanosensory transduction. *Nature* 413:194–202.
8. Wang N, Butler JP, Ingber DE (1993) Mechanotransduction across the cell surface and through the cytoskeleton. *Science* 260:1124–1127.
9. Vogel V, Sheetz M (2006) Local force and geometry sensing regulate cell functions. *Nat Rev Mol Cell Biol* 7:265–275.
10. Folkman J, Moscona A (1978) Role of cell shape in growth control. *Nature* 273:345–349.
11. Chen CS, Mrksich M, Huang S, Whitesides GM, Ingber DE (1997) Geometric control of cell life and death. *Science* 276:1425–1428.
12. McBeath R, Pirone DM, Nelson CM, Bhadriraju K, Chen CS (2004) Cell shape, cytoskeletal tension, and RhoA regulate stem cell lineage commitment. *Dev Cell* 6: 483–495.
13. Engler AJ, Sen S, Sweeney HL, Discher DE (2006) Matrix elasticity directs stem cell lineage specification. *Cell* 126:677–689.
14. Nelson CM, et al. (2005) Emergent patterns of growth controlled by multicellular form and mechanics. *Proc Natl Acad Sci USA* 102:11594–11599.
15. Mammoto T, et al. (2011) Mechanochemical control of mesenchymal condensation and embryonic tooth organ formation. *Dev Cell* 21:758–769.
16. Brunet T, et al. (2013) Evolutionary conservation of early mesoderm specification by mechanotransduction in Bilateria. *Nat Commun* 4:2821.
17. Kornikova ES, Korvin-Pavlovskaya EG, Beloussov LV (2009) Relocations of cell convergence sites and formation of pharyngula-like shapes in mechanically relaxed Xenopus embryos. *Dev Genes Evol* 219:1–10.
18. Kornikova ES, Troshina TG, Kremnyov SV, Beloussov LV (2010) Neuro-mesodermal patterns in artificially deformed embryonic explants: A role for mechano-geometry in tissue differentiation. *Dev Dyn* 239:885–896.
19. Beloussov LV, Luchinskaya NN, Ermakov AS, Glagoleva NS (2006) Gastrulation in amphibian embryos, regarded as a succession of biomechanical feedback events. *Int J Dev Biol* 50:113–122.
20. Farge E (2003) Mechanical induction of Twist in the Drosophila foregut/stomodeal primordium. *Curr Biol* 13:1365–1377.
21. Hove JR, et al. (2003) Intracardiac fluid forces are an essential epigenetic factor for embryonic cardiogenesis. *Nature* 421:172–177.
22. Hiramatsu R, et al. (2013) External mechanical cues trigger the establishment of the anterior-posterior axis in early mouse embryos. *Dev Cell* 27:131–144.

23. Park E, et al. (2012) Estimation of divergence times in cnidarian evolution based on mitochondrial protein-coding genes and the fossil record. *Mol Phylogenet Evol* 62: 329–345.
24. Reis dos M, et al. (2015) Uncertainty in the timing of origin of animals and the limits of precision in molecular timescales. *Curr Biol* 25:2939–2950.
25. Technau U (2001) Brachyury, the blastopore and the evolution of the mesoderm. *BioEssays* 23:788–794.
26. Arendt D, Technau U, Wittbrodt J (2001) Evolution of the bilaterian larval foregut. *Nature* 409:81–85.
27. Technau U, Bode HR (1999) HyBra1, a Brachyury homologue, acts during head formation in Hydra. *Development* 126:999–1010.
28. Kispert A, Herrmann BG, Leptin M, Reuter R (1994) Homologs of the mouse Brachyury gene are involved in the specification of posterior terminal structures in Drosophila, Tribolium, and Locusta. *Genes Dev* 8:2137–2150.
29. Spring J, et al. (2002) Conservation of brachyury, Mef2, and snail in the myogenic lineage of jellyfish: A connection to the mesoderm of bilateria. *Dev Biol* 244:372–384.
30. Marcellini S, Technau U, Smith JC, Lemaire P (2003) Evolution of brachyury proteins: Identification of a novel regulatory domain conserved within bilateria. *Dev Biol* 260: 352–361.
31. Lartillot N, Lespinet O, Vervoort M, Adoutte A (2002) Expression pattern of brachyury in the mollusc patella vulgata suggests a conserved role in the establishment of the AP axis in bilateria. *Development* 129:1411–1421.
32. Gross JM, McClay DR (2001) The role of brachyury (T) during gastrulation movements in the sea urchin Lytechinus variegatus. *Dev Biol* 239:132–147.
33. Yamada A, Pang K, Martindale MQ, Tochinai S (2007) Surprisingly complex T-box gene complement in diploblastic metazoans. *Evol Dev* 9:220–230.
34. Technau U, Miller MA, Bridge D, Steele RE (2003) Arrested apoptosis of nurse cells during Hydra oogenesis and embryogenesis. *Dev Biol* 260:191–206.
35. Smith JC, Price BMJ, Green JBA, Weigel D, Herrmann BG (1991) Expression of a Xenopus homolog of brachyury (T) is an immediate-early response to mesoderm induction. *Cell* 67:79–87.
36. Arnold SJ, et al. (2000) Brachyury is a target gene of the Wnt/β-catenin signaling pathway. *Mech Dev* 91:249–258.
37. Turner DA, Rué P, Mackenzie JP, Davies E, Martinez Arias A (2014) Brachyury cooperates with Wnt/β-catenin signalling to elicit primitive-streak-like behaviour in differentiating mouse embryonic stem cells. *BMC Biol* 12:63.
38. Yamaguchi H, Kitagawa Y, Miki K (1999) Brachyury regulatory region active in embryonal carcinoma P19 cells. *Biosci Biotechnol Biochem* 63:608–609.
39. Vonica A, Gumbiner BM (2002) Zygotic Wnt activity is required for brachyury expression in the early Xenopus laevis embryo. *Dev Biol* 250:112–127.
40. Kraus Y, Technau U (2006) Gastrulation in the sea anemone Nematostella vectensis occurs by invagination and immigration: An ultrastructural study. *Dev Genes Evol* 216: 119–132.
41. Magie CR, Daly M, Martindale MQ (2007) Gastrulation in the cnidarian Nematostella vectensis occurs via invagination not ingression. *Dev Biol* 305:483–497.
42. Saitoh M, Ishikawa T, Matsushima S, Naka M, Hidaka H (1987) Selective inhibition of catalytic activity of smooth muscle myosin light chain kinase. *J Biol Chem* 262: 7796–7801.
43. Bain J, McLauchlan H, Elliott M, Cohen P (2003) The specificities of protein kinase inhibitors: An update. *Biochem J* 371:199–204.
44. Lee J-Y, Harland RM (2010) Endocytosis is required for efficient apical constriction during Xenopus gastrulation. *Curr Biol* 20:253–258.
45. Wikramanayake AH, et al. (2003) An ancient role for nuclear beta-catenin in the evolution of axial polarity and germ layer segregation. *Nature* 426:446–450.
46. Scholz CB, Technau U (2003) The ancestral role of brachyury: Expression of NemBra1 in the basal cnidarian Nematostella vectensis (Anthozoa). *Dev Genes Evol* 212:563–570.
47. Röttinger E, Dahlin P, Martindale MQ (2012) A framework for the establishment of a cnidarian gene regulatory network for "endomesoderm" specification: The inputs of ß-catenin/TCF signaling. *PLoS Genet* 8:e1003164.
48. Kraus Y, Aman A, Technau U, Genikhovich G (2016) Pre-bilaterian origin of the blastoporal axial organizer. *Nat Commun* 7:11694.
49. Ikmi A, McKinney SA, Delventhal KM, Gibson MC (2014) TALEN and CRISPR/Cas9-mediated genome editing in the early-branching metazoan Nematostella vectensis. *Nat Commun* 5:5486–5488.
50. Hwang WY, et al. (2013) Efficient genome editing in zebrafish using a CRISPR-Cas system. *Nat Biotechnol* 31:227–229.
51. Wiedenheft B, Sternberg SH, Doudna JA (2012) RNA-guided genetic silencing systems in bacteria and archaea. *Nature* 482:331–338.
52. Stamos JL, Weis WI (2013) The β-catenin destruction complex. *Cold Spring Harb Perspect Biol* 5:a007898.
53. Leclère L, Bause M, Sinigaglia C, Steger J, Rentzsch F (2016) Development of the aboral domain in Nematostella requires β-catenin and the opposing activities of Six3/6 and Frizzled5/8. *Development* 143:1766–1777.
54. Steinmetz PRH, Aman A, Kraus JEM, Technau U (2017) Gut-like ectodermal tissue in a sea anemone challenges germ layer homology. *Nat Ecol Evol* 1:1535–1542.
55. Antonacci G, Braakman S (2016) Biomechanics of subcellular structures by non-invasive Brillouin microscopy. *Sci Rep* 6:37217.
56. Scarcelli G, et al. (2015) Noncontact three-dimensional mapping of intracellular hydromechanical properties by Brillouin microscopy. *Nat Methods* 12:1132–1134.
57. Edrei E, Gather MC, Scarcelli G (2017) Integration of spectral coronagraphy within VIPA-based spectrometers for high extinction Brillouin imaging. *Opt Express* 25: 6895–6903.
58. Elsayad K, et al. (2016) Mapping the subcellular mechanical properties of live cells in tissues with fluorescence emission-Brillouin imaging. *Sci Signal* 9:rs5.
59. Genikhovich G, Technau U (2009) Induction of spawning in the starlet sea anemone Nematostella vectensis, in vitro fertilization of gametes, and dejellying of zygotes. *Cold Spring Harb Protoc* 2009:pdb.prot5281.
60. Fritzenwanker JH, Technau U (2002) Induction of gametogenesis in the basal cnidarian Nematostella vectensis(Anthozoa). *Dev Genes Evol* 212:99–103.
61. Genikhovich G, Technau U (2009) In situ hybridization of starlet sea anemone (Nematostella vectensis) embryos, larvae, and polyps. *Cold Spring Harb Protoc* 2009: pdb.prot5282.
62. Antonacci G, Foreman MR, Paterson C, Toeroek P (2013) Spectral broadening in Brillouin imaging. *Appl Phys Lett* 103:221105.
63. Schindelin J, et al. (2012) Fiji: An open-source platform for biological-image analysis. *Nat Methods* 9:676–682.

Supporting Information

Pukhlyakova et al. 10.1073/pnas.1713682115

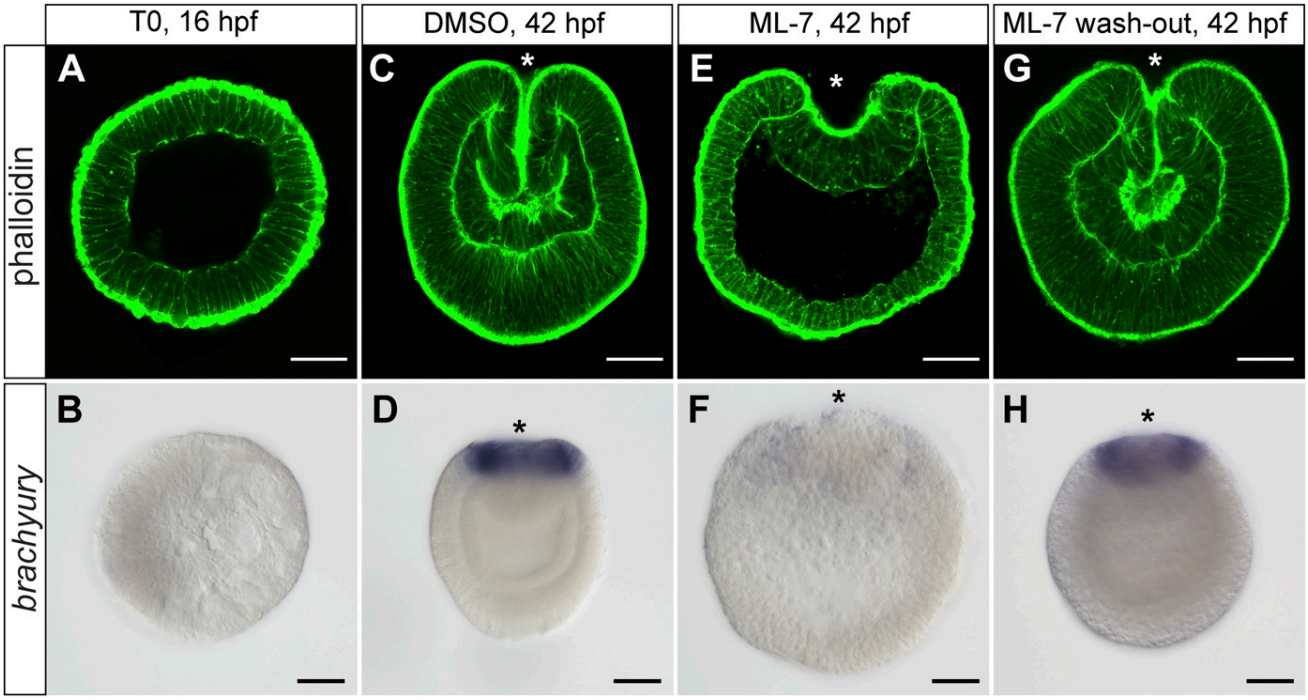

Fig. S1. ML-7 inhibition effects are reversible after washout. (*A* and *B*) Control blastula (16 hpf) at onset of treatment. *Brachyury* expression is not or barely detectable. (*C* and *D*) DMSO control (42 hpf) reflecting endpoint of treatment. *Brachyury* is strongly expressed at blastopore. (*E* and *F*) Embryo treated with ML-7 from 16 hpf until 42 hpf. Gastrulation and *brachyury* expression are inhibited. (*G* and *H*) ML-7 washout. Embryos were treated with ML-7 from 16 hpf until 28 hpf, and after five washes were incubated in sea water until 42 hpf. Gastrulation movements and *brachyury* expression are restored after washout of ML-7. (Scale bar, 50 μm.) Asterisk indicates the oral pole of the embryo.

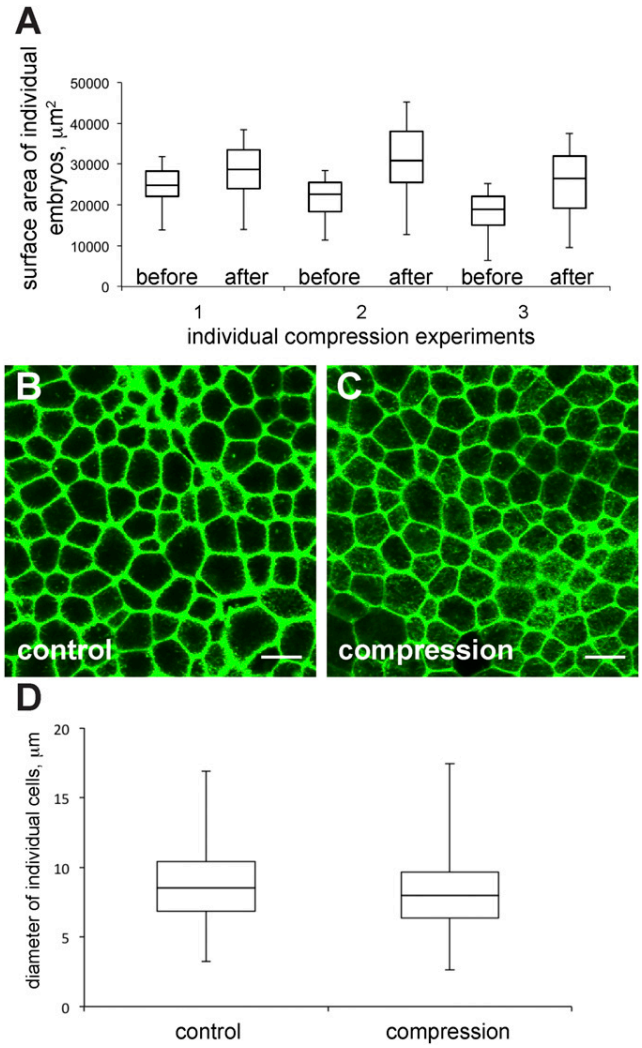

Fig. S2. Global deformation of the embryo and cell-shape analysis after uniaxial compression experiments. (*A*) Measurements of the maximal projection of the embryo surface area before and after compression. In each experiment >100 embryos were compressed. Three independent experiments were performed. Measurements show the variability of the embryo sizes before compression and the deformation effects. (*B* and *C*) Cell-shape analysis before (*B*) and after (*C*) compression. Cells of the plane parallel to the compression plane were analyzed, phalloidin staining. (Scale bar, 10 μm.) (*D*) Quantification of the cell diameters before and after compression. Differences in cell diameters before and after compression are not significant, paired two-tailed Student's *t* test ($P > 0.1$).

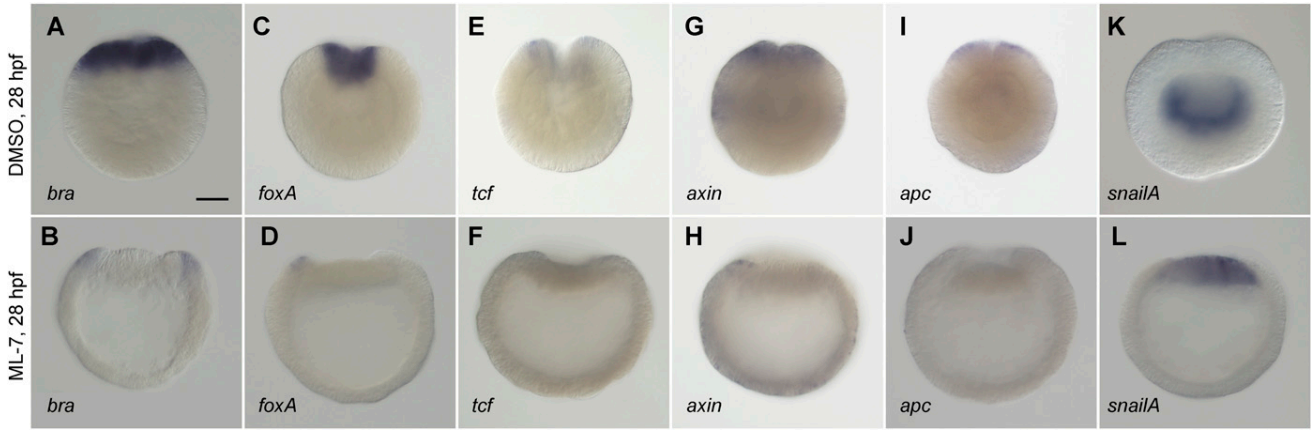

Fig. S3. Putative β-catenin target genes, expressed around the blastopore during gastrulation are down-regulated after ML-7 treatment. (*A* and *B*) *Brachyury* expression in the control and ML-7 treated embryos. (*C* and *D*) *foxA* expression in the control and ML-7 treated embryos. (*E* and *F*) *tcf* expression in the control and ML-7 treated embryos. (*G* and *H*) *axin* expression in the control and ML-7 treated embryos. (*I* and *J*) *apc* expression in the control and ML-7 treated embryos. (*K* and *L*) expression of *snailA*, which is not known to be a target of β-catenin remains unchanged in the control and ML-7 treated embryos. (Scale bar, 50 μm).

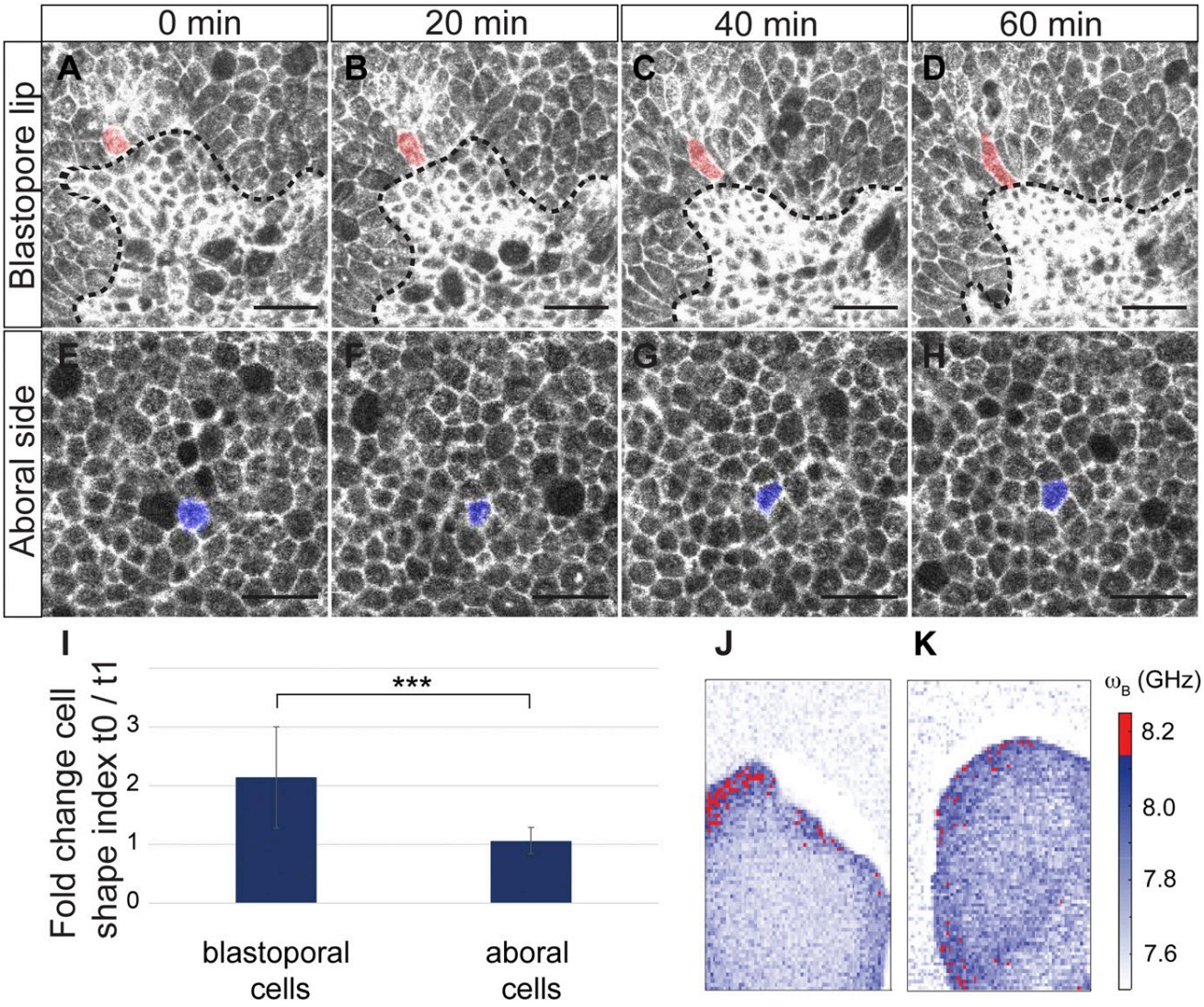

Fig. S4. Cell shape and stiffness change during gastrulation of *N. vectensis.* (*A–D*) During gastrulation, endodermal cells apically constrict, which leads to the stretching of the adjacent blastoporal cells. Such cell morphology change indicates that cells experience directional mechanical tensions. (*E–H*) Morphology of the cell on the aboral side of the embryo does not significantly change during gastrulation. Dashed line defines the preendodermal plate. An example of a blastoporal cell colored in red. An example of an aboral cell colored in blue. (Scale bar, 10 μm.) (*I*) Fold change cell-shape index t0/t1. Increasing of cell-shape index over time indicates cell elongation. (*J* and *K*) Spatial maps of the Brillouin frequency shift ω_B in wild-type embryo during gastrulation in the vicinity of the lip (*J*) and in the aboral side (*K*). A distinct increase in the frequency shift (stiffness) for cells near and at the lip relative to those further away is apparent. Regions of high-frequency shift are colored red for illustrative purposes.

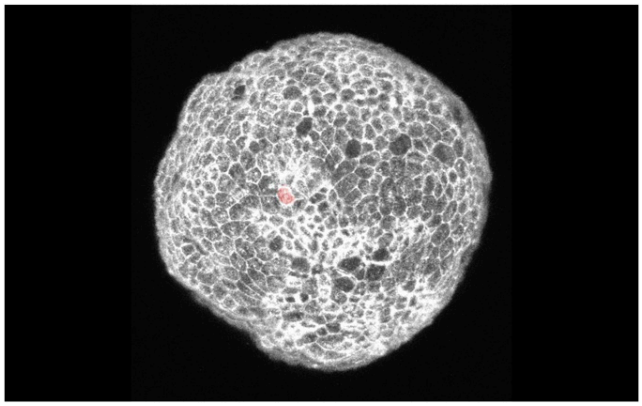

Movie S1. Gastrulation of *N. vectensis*. Oral side view. An example of a blastoporal cell colored in red. Timing is shown in hours:minutes.

Movie S1

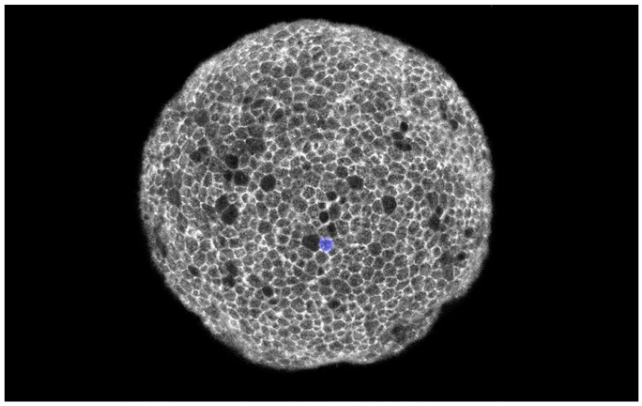

Movie S2. Gastrulation of *N. vectensis*. Aboral side view. An example of an aboral cell colored in blue. Timing is shown in hours:minutes.

Movie S2

PAPER III: “GERM-LAYER COMMITMENT AND AXIS FORMATION IN SEA ANEMONE EMBRYONIC CELL AGGREGATES”

Authors:
Anastasia Kirillova, Grigory Genikhovich, **Ekaterina Pukhlyakova**, Adrien Demilly, Yulia Kraus, and Ulrich Technau

Status:

Published in *PNAS, Proceedings of the National Academy of Sciences of the United States of America*, 2018, vol.115 (8), p. 1813-1818, doi/10.1073/pnas.1711516115

Contributions:

A.K., G.G., Y.K., and U.T. designed research; A.K., G.G., and E.P. performed research; E.P. and A.D. contributed new reagents/analytic tools; A.K. and G.G. analyzed data; and A.K., G.G., Y.K., and U.T. wrote the paper.

Germ-layer commitment and axis formation in sea anemone embryonic cell aggregates

Anastasia Kirillova[a,b,1], Grigory Genikhovich[a,1,2], Ekaterina Pukhlyakova[a], Adrien Demilly[a], Yulia Kraus[b,c,2], and Ulrich Technau[a,2]

[a]Department for Molecular Evolution and Development, Center of Organismal Systems Biology, Faculty of Life Sciences, University of Vienna, A-1090 Vienna, Austria; [b]Department of Evolutionary Biology, Biological Faculty, Moscow State University, 119234 Moscow, Russia; and [c]Koltzov Institute of Developmental Biology, Russian Academy of Sciences, 119334 Moscow, Russia

Edited by Edward M. De Robertis, Howard Hughes Medical Institute and University of California, Los Angeles, CA, and approved January 5, 2018 (received for review June 27, 2017)

Robust morphogenetic events are pivotal for animal embryogenesis. However, comparison of the modes of development of different members of a phylum suggests that the spectrum of developmental trajectories accessible for a species might be far broader than can be concluded from the observation of normal development. Here, by using a combination of microsurgery and transgenic reporter gene expression, we show that, facing a new developmental context, the aggregates of dissociated embryonic cells of the sea anemone *Nematostella vectensis* take an alternative developmental trajectory. The self-organizing aggregates rely on Wnt signals produced by the cells of the original blastopore lip organizer to form body axes but employ morphogenetic events typical for normal development of distantly related cnidarians to re-establish the germ layers. The reaggregated cells show enormous plasticity including the capacity of the ectodermal cells to convert into endoderm. Our results suggest that new developmental trajectories may evolve relatively easily when highly plastic embryonic cells face new constraints.

self-organization | embryonic cell aggregates | body axes | germ layers

Animal embryonic development can be viewed as a robust series of morphogenetic events triggered and controlled by the action of regulatory molecules and physical characteristics of the cells and tissues. These morphogenetic events form a developmental trajectory enabling the formation of a certain body plan. Strikingly, the phylum-specific body plan can be reached by a variety of developmental trajectories. For example, among chordates, radial, holoblastic cleavage of the yolk-poor eggs of the cephalochordate *Branchiostoma* results in the formation of a hollow coeloblastula, which gastrulates by invagination. In contrast, discoidal cleavage of the bird egg results in the formation of a discoblastula lying on top of the yolk and gastrulating via ingression of single cells through the primitive streak (1). Regardless, both developmental trajectories lead to the formation of a typical chordate body plan. Similarly, among different cnidarians, virtually all known modes of gastrulation can be found (2). While invagination is predominant among anthozoans and scyphozoans, hydrozoans gastrulate by unipolar or multipolar ingression, delamination, or epiboly. Nevertheless, after gastrulation, all cnidarians (except a few direct developers) form a typical planula larva. How such differences in development evolved and how they may have contributed to the formation of different body plans remain open questions in biology.

A large body of experimental data indicates that the spectrum of potencies for differentiation and cell behavior in embryonic cells is broader than their prospective fate and actual behavior during normal development (3–7). An extreme case of developmental plasticity is observed in animals capable of developing from a clump of dissociated and reaggregated cells, when the initial body plan is destroyed and then re-established de novo by self-organization (8–11). We reasoned that new developmental trajectories might evolve when cells capable of regulative development respond to new physical constraints, such as the increasing amount of yolk in the abovementioned example. We hypothesized therefore that new developmental trajectories might also be used if embryonic cells face a new context in an experimental situation. To test the extent of the regulative capacity of embryonic cells, we performed dissociation–reaggregation experiments with embryos of the sea anemone *Nematostella vectensis*. In this study, we use a combination of microsurgery and transgenic reporter gene assays to assess the developmental potential of different embryonic cells originating from dissociated *Nematostella* gastrulae and analyze the process of reforming of the body axes and the germ layers.

Results and Discussion

Nematostella is a cnidarian model system amenable to functional studies in embryogenesis. Upon fertilization, the *Nematostella* embryo develops into a hollow blastula, which then gastrulates by invagination, forms a swimming planula larva, and metamorphoses into a primary polyp (12). Recent transplantation experiments have shown that the blastopore lip of the *Nematostella* gastrula has an axis-inducing capacity conveyed by *Wnt1* and *Wnt3*, similar to the blastoporal axial organizer of vertebrates (13, 14). To assess the developmental potential of different embryonic cells, we dissociated *Nematostella* midgastrulae, at the stage when the endoderm just starts to invaginate, into single cells or small clusters of

Significance

Embryonic development of any animal species is a robust series of morphogenetic events tightly controlled by molecular signals. However, the variety of developmental trajectories undertaken by different members of the same phylum suggests that normal development in each particular species might involve only a subset of morphogenetic capacities available to the highly developmentally plastic embryonic cells. Here we show that, faced by a new developmental context, the aggregates of dissociated gastrula cells of the sea anemone *Nematostella vectensis* use an alternative developmental trajectory typical for other, distantly related members of the cnidarian phylum. We conclude that new modes of development may evolve relatively easily due to the versatility and developmental plasticity of embryonic cells.

Author contributions: A.K., G.G., Y.K., and U.T. designed research; A.K., G.G., and E.P. performed research; E.P. and A.D. contributed new reagents/analytic tools; A.K. and G.G. analyzed data; and A.K., G.G., Y.K., and U.T. wrote the paper.

The authors declare no conflict of interest.

This article is a PNAS Direct Submission.

[1]A.K. and G.G. contributed equally to this work.

[2]To whom correspondence may be addressed. Email: grigory.genikhovich@univie.ac.at, yulia_kraus@hydrozoa.org, or ulrich.technau@univie.ac.at.

This article contains supporting information online at www.pnas.org/lookup/suppl/doi:10.1073/pnas.1711516115/-/DCSupplemental.

DEVELOPMENTAL BIOLOGY

two to nine cells [~80 and ~20%, respectively (Fig. S1*A*)] and reaggregated them by centrifugation (Fig. 1*A*). Immediately after centrifugation, the aggregates lacked any sign of axial polarity or germ-layer segregation at both the morphological (Fig. 1 *B* and *C*) and the molecular (Fig. S2 *A*–*T*) level. The completeness of dissociation and the subsequent morphological observations were confirmed by in situ hybridization analysis of the oral markers *Wnt1*, *Wnt3*, *Wnt4*, *Bra*, and *FoxA*, midbody marker *Wnt2*, aboral marker *FGFa1*, endodermal marker *SnailA*, and directive axis markers *BMP2/4* and *Chordin* from 30 min post dissociation (mpd, i.e., immediately after reaggregation) until 6 d post dissociation (dpd) (Fig. S2). Ectodermal and endodermal cell layers began to segregate in several independent regions at 6–12 h post dissociation (hpd) (Fig. 1 *D* and *E*). The ectodermal cell layer formed first, while endoderm remained unepithelialized. By 24 hpd, the germ-layer segregation was complete (Fig. 1 *F* and *G*), and the endodermal marker *snailA* was expressed exclusively in the inner layer of the aggregates (Fig. S2*B*′). At the same stage, we observed the first signs of mouth formation (Fig. 1*H*). Starting from day 2 post dissociation, the aggregates were most similar to planulae: their ectoderm developed cilia, and the aggregates were actively swimming around. Interestingly, larger aggregates looked as if they were built of multiple fused planulae. Mouth and pharynx formation continued over the next 2 d (Fig. 1 *I*–*K*), and by day 6 the hypostomes (oral cones) had developed (Fig. 1*L*). Tentacle formation was complete by day 7–10 (Fig. 1*M*). Depending on the size of the aggregate, one or multiple oral openings formed. To monitor the formation of the oral–aboral axes in aggregates, we performed double in situ hybridization with the oral pole marker *FoxA* and the aboral pole marker *FGFa1* (15) (Fig. 1*N*). Interestingly, the number of *FoxA*-expressing spots exceeded the number of the *FGFa1*-expressing

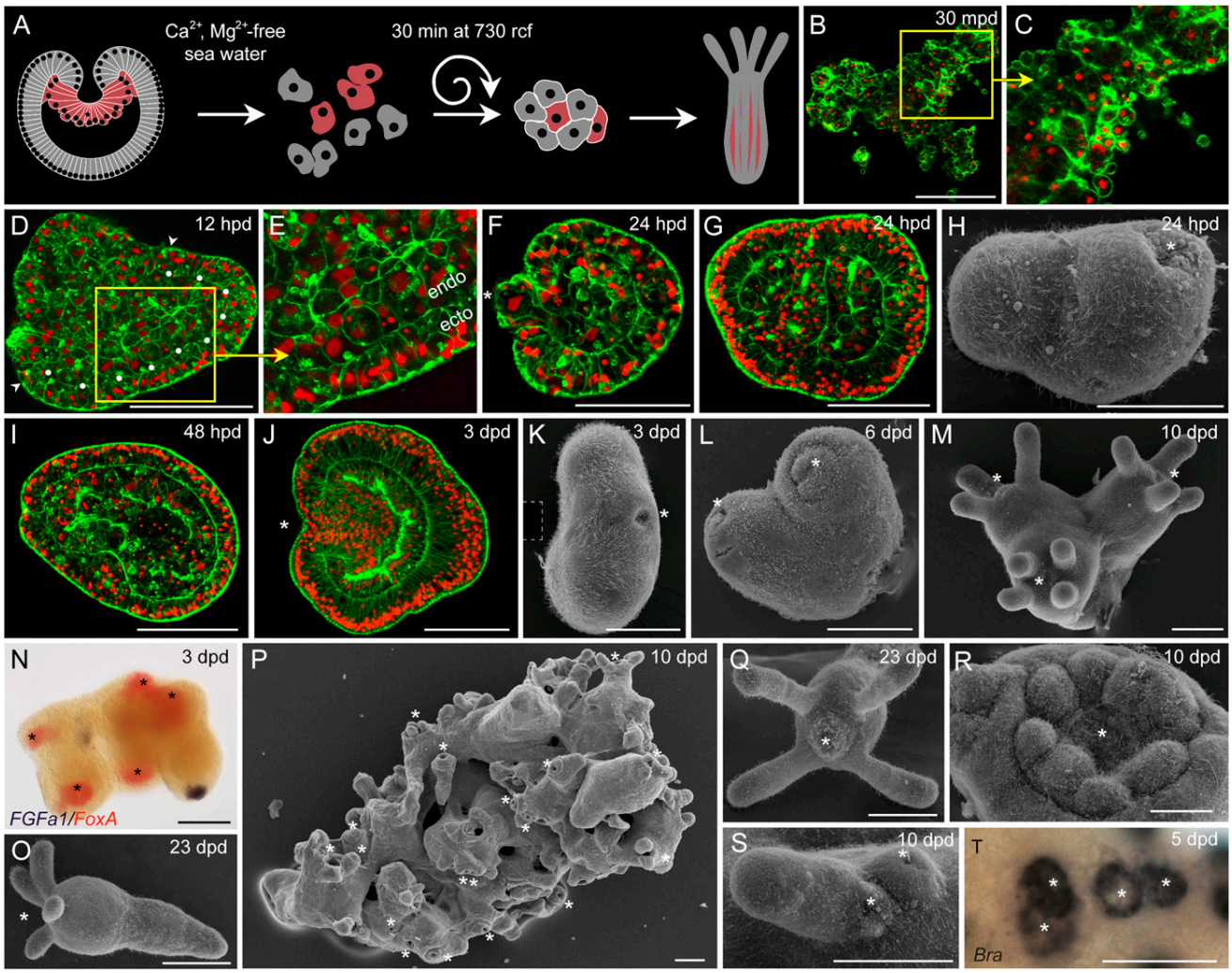

Fig. 1. The course of aggregate development. (*A*) Scheme of the dissociation–reaggregation experiment. (*B*–*M*) Successive stages of aggregate development analyzed by confocal and scanning electron microscopy. Directly after centrifugation, no epithelium is observed (*B* and *C*). Ectoderm epithelialization begins by 12 hpd (*D* and *E*: note a stretch of epithelialized ectoderm along the dotted line between white arrowheads in *D*) and is complete by 24 hpd (*F*: longitudinal optical section; *G*: transverse optical section). First signs of mouth formation become visible (*F* and *H*). Endoderm starts to form an epithelial layer by 48 hpd (*I*) and completes the process by 3 dpd (*J*: note also a well-developed pharynx). Mouth, hypostome, and tentacles form over the next several days (*K*–*M*). Black box (*K*, dashed line) masks the original scale bar. (*N*–*T*) Larger aggregates form multiple heads. (*N*) Double in situ hybridization with the oral marker *FoxA* (red) and aboral marker *FGFa1* (blue) shows that the number of heads/number of aboral poles ratio is 3/1. SEM shows that the number of heads per aggregate and tentacles per head can vary (*O*–*S*). Head structures can form in close proximity to each other, as visualized by SEM at the polyp stage and by in situ hybridization with an oral marker *Brachyury* at an earlier stage (*S* and *T*). (*B*–*G*, *I*, and *J*) Red: nuclei; green: F-actin. Asterisks, mouth; dpd, days post dissociation; ecto, ectoderm; endo, endoderm; hpd, hours post dissociation; mpd, minutes post dissociation. (Scale bars: 100 μm.)

spots by a factor of approximately 3 (mean: 2.98; 95% confidence interval: 2.69–3.27; median: 3.0; $n = 60$). Large aggregates always formed multiple heads with a varying number of tentacles (Fig. 1 *O–S*). Unlike in aggregates of the adult freshwater polyp *Hydra* (16), mouth openings were often located very close to each other (Fig. 1 *S* and *T*), indicating that lateral inhibition is not as prominent as in *Hydra*.

The experiments described above demonstrate that dissociated gastrula tissue of *Nematostella* is capable of re-establishing the normal body plan in the aggregates. Next, we wanted to know whether the self-organizing capacity was restricted to specific parts of the embryo. To this end, we generated aggregates from dissociated oral or aboral halves only. We found that the oral halves were capable of re-establishing the body axes, and eventually they developed into normal polyps (Fig. 2 *A–E*). In contrast, aboral aggregates formed ciliated balls without any sign of axial patterning containing a thin superficial epithelial layer and numerous small unepithelialized cells inside (Fig. 2 *F–J*). Recently, we showed that the capacity to induce ectopic body axes in transplantation experiments, i.e., the axial organizer capacity, is confined to a narrow area of the bend of the blastopore lip of the *Nematostella* gastrula (13). To estimate how many organizer cells are required to initiate axis formation in the aggregates, we determined the approximate amount of cells in the midgastrula at the time of dissociation (median: 6,934; Fig. S1*B*), and the number of cells in the single row of the bend of the blastopore lip (median: 107; Fig. S1*C*). Then we dissociated and reaggregated 100 aboral midgastrula halves together with 2, 5, or 10 oral gastrula halves, respectively, generating 1/50, 1/20, and 1/10 dilutions of oral gastrula halves by aboral gastrula halves. This corresponds to approximately 1/1,550, 1/620, and 1/310 ratios of the organizer cells to aboral half cells (in comparison with the 1/31 ratio when complete gastrulae are dissociated). We observed the formation of ciliated balls without any signs of body axes in all aggregates composed of 1 oral half per 50 aboral halves, 28% head formation in aggregates composed of 1 oral per 20 aboral halves, and 58% head formation in the aggregates composed of 1 oral per 10 aboral halves (Fig. S1*D*).

To find out whether aboral cells retain a memory of their original axial position after dissociation or adopt a new fate according to their new position, we generated a transgenic line ubiquitously expressing a fluorescent lifeact-mOrange2 actin-binding protein driven by an *EF1α* promoter (17–19) (Fig. S3 *A–C*). We then produced mixed aggregates from lifeact-mOrange2–expressing aboral gastrula halves with nontransgenic oral gastrula halves (Fig. 2*K*). We found that fluorescent cells dispersed throughout the entire resulting polyps, including their oral-most regions, indicating that the axial identity was reprogrammed in these originally aboral cells to adopt an oral identity (Figs. 2 *K–N* and 3).

Surprisingly, in this experiment, we detected some fluorescent transgenic cells inside the aggregates (Fig. S4 *A–D*), even though all transgenic lifeact-mOrange2 cells originated from aboral gastrula halves, i.e., prospective ectoderm. We therefore wanted to test more rigorously whether the cells in the aggregate kept their original germ-layer identity. In this respect, two scenarios could be envisaged: (*i*) either the embryonic cells sort out in accordance to their original germ-layer identity as shown in amphibians (20) or (*ii*) they lose the information about their initial germ-layer identity and acquire it de novo in the course of aggregate development. We dissected fluorescent pre-endodermal plates out of the lifeact-mOrange2 embryos using microsurgical techniques (Fig. 2*O*). Then we dissociated these fragments together with the nontransgenic ectodermal cells. We observed that during the first 18 h of aggregate development all fluorescently labeled cells migrated into the inside of the aggregate (Fig. 2 *O–R* and Movie S1). Therefore, we conclude that endodermal cells "remember" their initial fate and are able to sort out to form the inner layer of an aggregate (Fig. 3). Interestingly, the signal necessary for the individual ingression of the endodermal cells does not emanate from the organizer cells of the blastopore lip, since ingression of the endodermal cells also happened in the aggregates made of *EF1a::lifeact-mOrange2* endoderm and aboral ectoderm of the wild-type gastrulae (Fig. 2 *S–V*). Similarly to the aboral half-aggregates (Fig. 2 *G–J*), such aggregates developed into compact balls with an ectodermal layer and a mass of cells inside (Fig. 2 *S–V*). To test whether endodermal cells alone would be able to form aggregates and develop into polyps, we made aggregates out of surgically isolated pre-endodermal plates (Fig. 2*W*). Strikingly, without an ectoderm forming an epithelium on the surface of the aggregate, the endodermal cells became mesenchymal and dispersed. At 3.5 hpd, cells forming filopodia could be observed at the edge of the aggregate. By 12 hpd, the whole aggregate converted to viable, motile mesenchymal cells spread on the surface of the dish, failing to develop and form a polyp (Fig. 2 *W–Z*). Thus, endoderm alone is unable to compensate for the absence of ectoderm.

We then carried out the reciprocal experiment, i.e., forming aggregates consisting of only ectodermal cells. If ectodermal cells are capable of converting into endoderm, we expect them to be located in the inner layer, and—importantly—to start expressing endoderm-specific marker genes. To monitor this conversion, we generated a transgenic line called endoRed, expressing mCherry exclusively in the endoderm under control of the regulatory region of the *SnailA* gene, which encodes an endodermally expressed zinc-finger transcription factor (Fig. S3 *D–F*) (21). By microsurgery, we isolated aboral halves of endoRed offspring gastrulae containing only ectodermal cells. Since aggregates from aboral hemispheres fail to develop into primary polyps (Fig. 2 *F–J*), we dissociated them together with the blastopore lip fragments of the wild-type gastrulae (Fig. 2*A′*). We excluded the possibility of contamination of the aboral halves of the endoRed offspring embryos with the mCherry-expressing cells of the pre-endodermal plate (Fig. 2*B′*; see *SI Materials and Methods* for details) and then followed the development of the aboral endoRed/wild-type blastopore lip aggregates, where not a single fluorescent cell was detected after reaggregation. Thus, any mCherry-expressing cells appearing as the aggregates develop must have originated from aboral ectoderm of the endoRed line. After 1 d, we detected the first cells expressing the endoderm-specific transgene inside the aggregates (Fig. 2*C′*). These cells persisted throughout development, and eventually primary polyps formed with fluorescent patches in the endoderm (Fig. 2 *D′* and *E′*). By comparison, control aggregates made of oral halves of the endoRed gastrulae were fluorescent from the start (Fig. 2 *F′–J′*). Therefore, we conclude that the ectodermal cells of the endoRed embryos were able to contribute to the endoderm of the polyp (Fig. 3). To test whether the presence of wild-type endodermal cells would prevent aboral ectoderm cells from adopting an endodermal fate, we dissociated aboral halves of the endoRed gastrulae together with whole oral halves of wild-type gastrulae including nontransgenic endodermal cells. Notably, we found that the presence of the nontransgenic endoderm did not prevent some aboral ectodermal endoRed cells located inside these aggregates from adopting an endodermal fate (Fig. S4 *E–H*). Interestingly, even in the absence of oral cells, single mCherry-expressing cells were transiently detectable in the aboral ectodermal aggregates, yet this expression faded as the aggregates were arrested in the ciliated ball stage (Fig. S4 *I–L*). This suggests that the internal location might be sufficient to initiate the expression of endodermal marker genes in the aboral ectodermal cells, yet this expression needs to be maintained by signals coming from the blastopore lip cells.

The above result raises the question, which signals emanating from the blastoporal cells could induce and maintain axis and germ-layer formation? Since endodermal cells were capable of sorting out autonomously in the absence of axis-forming signals (Fig. 2 *S–V*), we reasoned that axis formation is central for the development of the aggregates. Therefore, we focused on the role of Wnt/β-catenin signaling and BMP signaling as the signaling

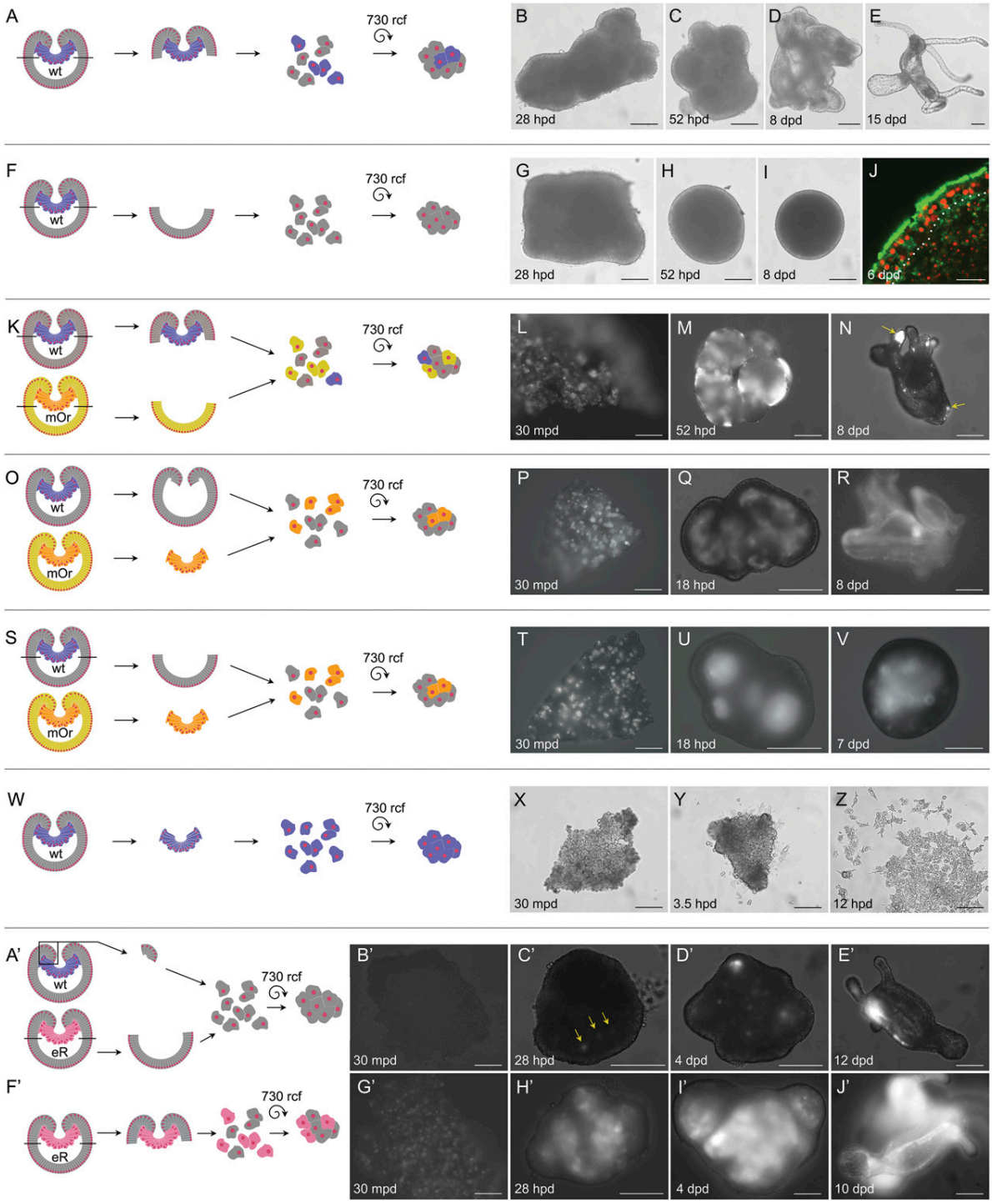

Fig. 2. Differences in capacities of gastrula cells for axis formation and cell-fate specification in the aggregates. (*A*–*E*) Aggregates made of oral halves of gastrulae develop into polyps. (*F*–*J*) Aggregates made of aboral halves of gastrulae develop into ciliated balls. (*J*) Confocal imaging shows that, outside, they have an ectodermal epithelial layer and that their inside is filled with numerous small cells. (*K*–*N*) In aggregates made of oral halves of wild-type gastrulae and aboral halves of gastrulae ubiquitously expressing lifeact-mOrange2, glowing cells are dispersed throughout the aggregate and can be observed both in aboral and oral positions of the polyp (yellow arrows in *N*). (*O*–*R*) In aggregates made of ectoderm of wild-type gastrulae and endoderm of gastrulae ubiquitously expressing lifeact-mOrange2, fluorescent cells migrate into the endoderm. (*S*–*V*) In aggregates made of aboral ectoderm of wild-type gastrulae and endoderm of gastrulae ubiquitously expressing lifeact-mOrange2, fluorescent cells migrate into the endoderm although the organizer cells are missing. (*W*–*Z*) In aggregates made of only endodermal cells, the cells become mesenchymal and migrate out of the aggregate. (*A′*–*E′*) Immediately after centrifugation, mCherry is not expressed in aggregates made of aboral ectoderm of endoRed gastrulae and blastopore lip ectoderm of the wild-type gastrulae (*B′*). Endodermal promoter-driven mCherry expression starts to be detectable in the internal cells of the aggregate from 28 hpd on (yellow arrows in *C′*). Glowing cells are then observed in the endoderm of the forming polyps (*E′*). (*F′*–*J′*) In aggregates made of oral halves of endoRed gastrulae, mCherry is continuously expressed in the endodermal cells. Sample size >30 in every experiment. dpd, days post dissociation; eR, endoRed; hpd, hours post dissociation; mOr, lifeact-mOrange2; mpd, minutes post dissociation; wt, wild type. Black bars on gastrulae denote the position of the cut. (Scale bars: *J*, 15 μm; all others, 100 μm.)

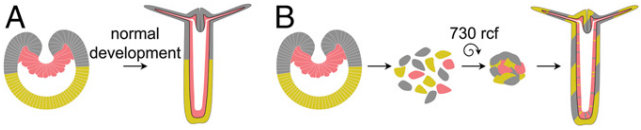

Fig. 3. The summary of the fate of cells during normal development (*A*) and in aggregates (*B*).

molecules of these pathways are expressed at the blastopore and they have previously been shown to have a role in axis formation in *Nematostella* (13, 22–26).

β-catenin knockdown results in the lack of an oral–aboral axis and endoderm formation (22, 23). During normal development, the initial β-catenin signal is most likely based on maternally deposited molecules (13, 27), while the zygotic expression of *Wnt* genes starts to be detectable by in situ hybridization at some point between 6 and 10 hpf (13). Recent transplantation experiments demonstrated that *Wnt1* and *Wnt3* expressed in the blastopore lip are sufficient to convey axial organizer capacity to aboral ectodermal cells of the *Nematostella* gastrula (13). To test whether these two signaling molecules are required for proper axial development and endoderm formation in aggregates, we injected random single blastomeres at the eight-cell stage with plasmids driving the expression of *Wnt1* and *Wnt3* and then made aggregates out of the aboral halves of these injected embryos when they reached the midgastrula stage. Although lacking the pre-endodermal plate cells and the blastopore lip cells, these aggregates developed into primary polyps (Fig. 4 *A–C*). This indicates that *Wnt1* and *Wnt3* are sufficient to rescue proper germ-layer and axis formation and induce self-organization of embryonic aggregates.

BMP signaling plays the central role in establishing and maintaining the second, directive body axis in *Nematostella* (24–26). During normal development, the initial, radially symmetric expression of the central BMP-signaling components *BMP2/4* and *Chordin* starts to be detectable in the blastula around 14 hpf (13) in a β-catenin–dependent manner (Fig. S5*A*). At late gastrula, a BMP-signaling–dependent symmetry break in the expression of *BMP2/4* and *Chordin* occurs, manifesting the establishment of the directive axis (28). Consequently, morpholino knockdown of *BMP2/4* or *Chordin* results in the loss of BMP signaling in the embryo and the lack of the directive axis (24, 25). To assess the role of BMP signaling in self-organizing aggregates, we made aggregates from gastrula-stage embryos injected with the previously tested BMP2/4 morpholino (24). Strikingly, BMP2/4MO aggregates were not only unable to form the directive axes, as we would expect, but also their oral–aboral axes were strongly affected (Fig. 4 *D–F*). Morpholino knockdown of BMP ligands has already been shown to influence the expression of many genes transcribed in restricted domains along the oral–aboral axis (24, 26, 29), suggestive of a possible feedback of the BMP signaling onto the Wnt/β-catenin–signaling system. We set out to test this in more detail in BMP2/4 morphants and morphant aggregates. Although the expression of the inducers of oral development, *Wnt1* and *Wnt3*, was up-regulated in the 24-hpf BMP2/4 morphant gastrula transcriptome (29), *Wnt1*, *Wnt3*, *FoxA*, and *Brachyury* expression domains appeared normal in the BMP2/4 morphants at the 24-hpf gastrula stage. In contrast, the expression of all these genes appeared significantly weaker in 2- and 3-d-old morphant embryos (Fig. S5*B*). Similarly, the expression of *Wnt1*, *Wnt3*, and *Brachyury* was also reduced, and its restriction to the oral poles was severely affected in the BMP2/4MO aggregates (Fig. S6*A*). If BMP signaling is required for the maintenance of the proper expression of *Wnt1* and *Wnt3*, its down-regulation should suppress the inductive capacity of the blastopore lip organizer cells. In line with that, we observed a strong reduction of the axis-inducing capacity of the blastopore lips transplanted from *BMP2/4* and *Chordin* morphant donors to the wild-type recipients (Fig. S5*C*). The presence of the positive feedback of BMP signaling on Wnt/β-catenin signaling also explains our previous observation that, unlike in vertebrates, single-blastomere injection of *Chordin* expression constructs does not lead to the formation of ectopic body axes in *Nematostella*. Paradoxically, analysis of *Frizzled 5/8* expression in BMP2/4 morphants and morphant aggregates suggests that the reduction of the expression of the oral markers *Wnt1*, *Wnt3*, *FoxA*, and *Brachyury* is not accompanied by the expansion of the aboral territory characterized by low levels of β-catenin signaling, but rather by a reduction in *Fz5/8* expression in older morphants and BMP2/4MO aggregates (Figs. S5*B* and S6*B*).

Our experiments showed that aggregates of embryonic cells of the sea anemone *Nematostella* are capable of re-establishing the germ layers and correct axial patterning of the body. Endodermal cells in the aggregates maintained their endodermal identity and were unable to convert into ectoderm, suggesting that this early cell-fate decision is irreversible. Moreover, endodermal cells were able to ingress from the surface of the aggregate autonomously, i.e., in the absence of the oral cells. However, such aggregates remained solid spheres, which suggests that oral signals might still be required for the formation of the defined endodermal layer. Aggregates made exclusively of endodermal cells did not reform polyps but converted into mesenchymal cells. By contrast, ectodermal cells were capable of converting into endoderm and forming normal polyps. Axial patterning in the aggregates relied on Wnt signals from the blastopore lip ectoderm, which has organizer activity (13–15). In contrast, the cells originating from aboral ectoderm acquired new axial identity once dispersed throughout the aggregate. Our results also highlight the importance of BMP signaling in the maintenance of the Wnt-dependent oral–aboral axis in *Nematostella*.

Since the aggregates utilize the same set of developmental regulators as normal embryos, we conclude that these genes are part of a self-organizing gene regulatory network enabling stunning plasticity and ability to respond to a yet-unprecedented developmental context, such as the lack of the cavity in the aggregate, which prevents invagination. To circumvent this constraint, the aggregates of the sea anemone *Nematostella* activate an alternative

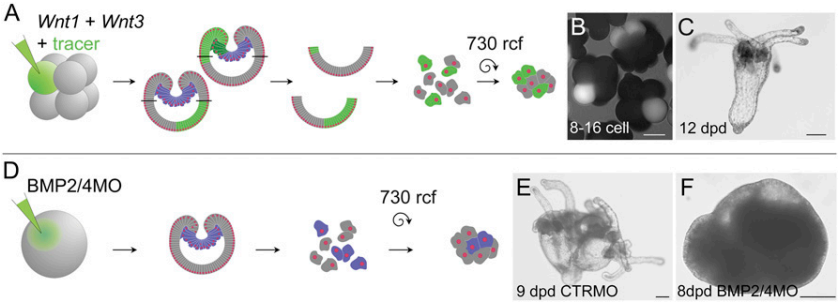

Fig. 4. The role of Wnt/β-catenin and BMP signaling during aggregate development. (*A–C*) Axis formation and endoderm segregation is rescued in 15 of 17 aggregates made from aboral halves of gastrulae, which were coinjected into a single blastomere at the eight-cell stage with plasmids coding for untagged Wnt1 and Wnt3 driven by the *EF1α* promoter and fluorescent tracer (glowing cells in *B*). (*D–F*) *BMP2/4* knockdown results in the lack of morphologically distinct body axes in the aggregates. $n = 32$. (Scale bars: 100 μm.)

developmental trajectory. Instead of invagination, they form germ layers by a combination of delamination of the ectodermal layer; multipolar ingression of the endodermal plate cells, which happened to end up on the surface of the aggregates after centrifugation of the dissociated cells; and cavitation of the mass of cells located inside the aggregates. Curiously, the experimentally modulated development in *Nematostella* aggregates resembles the normal development of other cnidarians, i.e., members of Hydrozoa, which gastrulate usually by ingression of individual cells (30, 31) or delamination (32, 33) (Fig. S7*A*). Unlike gastrulation in most cnidarians and in Bilateria, where it occurs at a certain position in relation to the body axes of an embryo, delamination and ingression in Hydrozoa can be multipolar and not linked to the axial patterning (32–37) (Fig. S7*A*). During morula delamination, when a solid embryo without a blastocoel forms as a result of cleavage, external cells of a morula start to epithelialize and segregate themselves from the inner mass of cells, the future endoderm, which then cavitates and forms an endodermal epithelial layer. In resemblance to the situation during *Nematostella* aggregate development (Fig. S7 *B–E*), the epithelialization of the ectoderm starts in many different regions throughout the morula, and then individual patches of epithelium expand and fuse (32, 33).

Such plasticity is not a unique feature of the embryonic cells of early branching metazoans. In sea urchins and sea stars, dissociated and reaggregated cells of gastrula-stage embryos are just as capable of re-establishing their normal body plans and forming larvae. Interestingly, also in echinoderms, the inner cells of the aggregates form the endodermal layer omitting the invagination step (38–41). However, once the inner cells arrange into an epithelium, and the embryo cavitates, the coelomic pouches form by an enterocoelic process (42), i.e., from evaginations of the gut wall. The comparison of aggregates and normal embryos suggests that alternative developmental trajectories are easily accessible to organisms, unless they have highly derived mosaic development. Moreover, it is likely that this kind of plasticity and the capacity for regulative development were present already at the earliest stages of animal evolution. Since phenotype robustness promotes phenotype evolvability (43), the capacity to change embryonic development without deleterious effects might have facilitated the diversification of the developmental trajectories leading to the formation of animal body plans.

Materials and Methods

Details on the animal culture, transgenic lines, embryo manipulations, microinjections, analyses of dissociation efficiency and determination of the number of the cells in the bend of the blastopore lip, as well as the molecular and histological techniques can be found in the *SI Materials and Methods*.

ACKNOWLEDGMENTS. S. Lysenkov assisted with the statistical analysis; SEM was performed at the Electron Microscopy Laboratory of the Shared Facilities Center of the Moscow State University; and confocal imaging was performed at the Core Facility for Cell Imaging and Ultrastructure Research of the University of Vienna. This work was funded by Austrian Science Foundation Grants P22717 (to U.T.) and P26962 (to G.G.) and by federal project 0108-2018-0003 of the Koltzov Institute of Developmental Biology of the Russian Academy of Sciences (to Y.K.). A.K. was a recipient of a European Molecular Biology Organization short-term fellowship (ASTF 357–2015) and of an Austrian Academic Exchange Service stipend (ICM-2013-03977).

1. Gilbert SF, Raunio AM, eds (1997) *Embryology: Constructing the Organism* (Sinauer Associates, Sunderland, MA), p 538.
2. Tardent P, ed (1978) *Coelenterata, Cnidaria* (Gustav Fischer, Stuttgart).
3. Morgan TH (1895) Half embryos and whole embryos from one of the first two blastomeres. *Anat Anz* 10:623–638.
4. Driesch H (1891) Entwicklungsmechanische Studien I, II [Studies on developmental mechanics I, II]. *Z Wiss Zool* 53:160–184. German.
5. Hörstadius S (1939) The mechanics of sea urchin development. *Biol Rev Camb Philos Soc* 14:132–179.
6. Takahashi K, Yamanaka S (2015) A developmental framework for induced pluripotency. *Development* 142:3274–3285.
7. Green JB, Dominguez I, Davidson LA (2004) Self-organization of vertebrate mesoderm based on simple boundary conditions. *Dev Dyn* 231:576–581.
8. Wilson HV (1907) On some phenomena of coalescence and regeneration in sponges. *J Exp Zool* 5:245–258.
9. Wilson HV (1911) On the behavior of the dissociated cells in hydroids, alcyonaria, and Asterias. *J Exp Zool* 11:281–338.
10. Gierer A, et al. (1972) Regeneration of hydra from reaggregated cells. *Nat New Biol* 239:98–101.
11. Nieuwkoop PD (1992) The formation of the mesoderm in urodelean amphibians VI. The self-organizing capacity of the induced meso-endoderm. *Rouxs Arch Dev Biol* 201:18–29.
12. Genikhovich G, Technau U (2009) The starlet sea anemone *Nematostella vectensis*: An anthozoan model organism for studies in comparative genomics and functional evolutionary developmental biology. *Cold Spring Harb Protoc* 2009:pdb.emo129.
13. Kraus Y, Aman A, Technau U, Genikhovich G (2016) Pre-bilaterian origin of the blastoporal axial organizer. *Nat Commun* 7:11694.
14. Kraus Y, Fritzenwanker JH, Genikhovich G, Technau U (2007) The blastoporal organiser of a sea anemone. *Curr Biol* 17:R874–R876.
15. Fritzenwanker JH, Genikhovich G, Kraus Y, Technau U (2007) Early development and axis specification in the sea anemone Nematostella vectensis. *Dev Biol* 310:264–279.
16. Technau U, et al. (2000) Parameters of self-organization in *Hydra* aggregates. *Proc Natl Acad Sci USA* 97:12127–12131.
17. Riedl J, et al. (2008) Lifeact: A versatile marker to visualize F-actin. *Nat Methods* 5: 605–607.
18. Shaner NC, et al. (2008) Improving the photostability of bright monomeric orange and red fluorescent proteins. *Nat Methods* 5:545–551.
19. Steinmetz PRH, Aman A, Kraus JEM, Technau U (2017) Gut-like ectodermal tissue in a sea anemone challenges germ layer homology. *Nat Ecol Evol* 1:1535–1542.
20. Townes PL, Holtfreter J (1955) Directed movements and selective adhesion of embryonic amphibian cells. *J Exp Zool* 128:53–120.
21. Martindale MQ, Pang K, Finnerty JR (2004) Investigating the origins of triploblasty: 'Mesodermal' gene expression in a diploblastic animal, the sea anemone Nematostella vectensis (phylum, Cnidaria; class, Anthozoa). *Development* 131:2463–2474.
22. Wikramanayake AH, et al. (2003) An ancient role for nuclear beta-catenin in the evolution of axial polarity and germ layer segregation. *Nature* 426:446–450.
23. Leclère L, Bause M, Sinigaglia C, Steger J, Rentzsch F (2016) Development of the aboral domain in Nematostella requires β-catenin and the opposing activities of six3/6 and frizzled5/8. *Development* 143:1766–1777.
24. Saina M, Genikhovich G, Renfer E, Technau U (2009) BMPs and chordin regulate patterning of the directive axis in a sea anemone. *Proc Natl Acad Sci USA* 106:18592–18597.
25. Genikhovich G, et al. (2015) Axis patterning by BMPs: Cnidarian network reveals evolutionary constraints. *Cell Rep* 10:1646–1654.
26. Leclère L, Rentzsch F (2014) RGM regulates BMP-mediated secondary axis formation in the sea anemone Nematostella vectensis. *Cell Rep* 9:1921–1930.
27. Lee PN, Kumburegama S, Marlow HQ, Martindale MQ, Wikramanayake AH (2007) Asymmetric developmental potential along the animal-vegetal axis in the anthozoan cnidarian, Nematostella vectensis, is mediated by dishevelled. *Dev Biol* 310:169–186.
28. Rentzsch F, et al. (2006) Asymmetric expression of the BMP antagonists chordin and gremlin in the sea anemone Nematostella vectensis: Implications for the evolution of axial patterning. *Dev Biol* 296:375–387.
29. Wijesena N, Simmons DK, Martindale MQ (2017) Antagonistic BMP-cWNT signaling in the cnidarian Nematostella vectensis reveals insight into the evolution of mesoderm. *Proc Natl Acad Sci USA* 114:E5608–E5615.
30. Momose T, Schmid V (2006) Animal pole determinants define oral-aboral axis polarity and endodermal cell-fate in hydrozoan jellyfish Podocoryne carnea. *Dev Biol* 292:371–380.
31. Byrum CA (2001) An analysis of hydrozoan gastrulation by unipolar ingression. *Dev Biol* 240:627–640.
32. Kraus YA (2006) Morphomechanical programming of morphogenesis in cnidarian embryos. *Int J Dev Biol* 50:267–275.
33. Kraus Y, et al. (2014) The embryonic development of the cnidarian Hydractinia echinata. *Evol Dev* 16:323–338.
34. Allman GJ (1871) *A Monograph on the Gymnoblastic or Tubularian Hydroids. Vol. I: The Hydroida in General* (Forgotten Books, London), p 154.
35. Schulze FE (1871) *Über den Bau und die Entwicklung von Cordylophora lacustris (Allman)* [*On the anatomy and the development of Cordylophora lacustris (Allman)*] (Wilhelm Engelmann, Leipzig, Germany), p 55. German.
36. Metschnikoff E (1874) Studien über die Entwicklung der Medusen und Siphonophoren. (Studies of the development of jellyfish and siphonophores) *Z Wiss Zool* 24:15–80. German.
37. Harm K (1903) Die Entwicklung von Clava squamata [The development of Clava squamata]. *Z Wiss Zool* 73:115–165. German.
38. Dan-Sohkawa M, Yamanaka H, Watanabe K (1986) Reconstruction of bipinnaria larvae from dissociated embryonic cells of the starfish, Asterina pectinifera. *J Embryol Exp Morphol* 94:47–60.
39. Giudice G (1962) Restitution of whole larvae from disaggregated cells of sea urchin embryos. *Dev Biol* 5:402–411.
40. Yamanaka H, Tanaka-Ohmura Y, Dan-Sohkawa M (1986) What do dissociated embryonic cells of the starfish, Asterina pectinifera, do to reconstruct bipinnaria larvae? *J Embryol Exp Morphol* 94:61–71.
41. Spiegel M, Spiegel ES (1975) The reaggregation of dissociated embryonic sea-urchin cells. *Am Zool* 15:583–606.
42. Tamura M, Dan-Sohkawa M, Kaneko H (1998) Coelomic pouch formation in reconstructing embryos of the starfish Asterina pectinifera. *Dev Growth Differ* 40:567–575.
43. Wagner A (2008) Robustness and evolvability: A paradox resolved. *Proc Biol Sci* 275: 91–100.

Supporting Information

Kirillova et al. 10.1073/pnas.1711516115

SI Materials and Methods

Animal Culture, Dissociation and Transplantation Experiments, and Microinjections. Animals were cultured as previously described (1). Microsurgical isolation of different parts of gastrulae was performed using a Microfeather ophthalmic scalpel under the Nikon SMZ18 dissecting scope. For dissociation experiments, 100 μL of *Nematostella* medium (NM, 16‰ artificial sea water) with gastrula stage embryos was combined with 200 μL of Ca-Mg–free sea water [27 g/L NaCl, 1 g/L Na_2SO_4, 0.8 g/L KCI, 0.18 g/L NaHCO3 in MilliQ water (2)] and dissociated by pipetting through a 200-μL pipette tip. The cell suspension was then transferred into a 2-mL Eppendorf tube, and the tube was filled up to 2 mL with NM and centrifuged at 730 × *g* for 30 min. The pellet was transferred into a Petri dish with NM, cut into small fragments with a scalpel, and allowed to develop at 21 °C. Blastopore lip transplantation experiments were carried out as in ref. 3. Live imaging and microinjection were performed on a Nikon TS100F microscope equipped with a Nikon DS-Qi1Mc camera. In the single blastomere injection experiment (Fig. 4 *A* and *B*), mixtures containing 20 ng/μL *EF1α::Wnt1* and 20 ng/μL *EF1α::Wnt3* together with fluorescent Dextran-Alexa488 were injected into random single blastomeres of the eight-cell-stage embryos as described previously (3). Previously published *BMP2/4* morpholino (GTAAGAAACAGCGTAAGAGAAGCAT), *chordin* morpholino (GTAACAGGTCTCGTATTCTCCGCAT) (4), *β-catenin* morpholino (TTCTTCGACTTTAAATCCAACTTCA) (5), and control morpholino (GATGTGCCTAGGGTACAACAACAAT) (3) were injected at 250-μM concentration.

Analysis of the Dissociation Efficiency. To estimate the efficiency of dissociation, all cells within three nonoverlapping fields of view at 200× magnification were counted on nine independent dissociated samples (27 measurements altogether).

Determination of the Number of Cells in the Gastrula and in the Bend of the Blastopore Lip. To estimate the number of cells in the gastrula at the time of dissociation, midgastrulae were fixed with 3.7% formaldehyde/NM and stained with DAPI. Confocal Z-stacks with a step size of 2 μm were recorded with the Leica SP5X LSM, and the total number of nuclei was determined in six embryos in FIJI (https://imagej.net/Fiji). The number of cells in a single row in the bend of the blastopore lip was determined on 10 phalloidin-Alexa488–stained embryos.

Transgenic Lines. For generation of the *EF1α::Lifeact-mOrange2* transgenic line, Lifeact sequence (6) together with a flexible linker (GDPPVAT) was incorporated into the primer sequence and used for the amplification of the mOrange2 sequence (7): forward primer— ATGGGAGTTGCTGATTTAATTAAAAAATTTGAATCTATTTCTAAAGAAGAAGGAGATCCACCTGTAGCGACTATGGTGAGCAAGGGCGAGG; reverse mOrange2 primer—TTACTTGTACAGCTCGTCCATGC. We then cloned *Lifeact-mOrange2* into the *Nematostella* transgenesis vector downstream from the *EF1α* promoter (8) and injected it into zygotes as described (9). Mosaically transgenic F0 animals were crossed to generate fully transgenic heterozygous F1 animals, which were intercrossed to generate F2. The F2 generation embryos were screened under a Nikon SMZ18 fluorescent dissecting microscope, and strongly glowing gastrulae were used for dissociation experiments.

To generate an endodermally expressed reporter, we combined a 1.6-kb DNA fragment upstream of the translation start site of the endodermally expressed *SnailA* (10, 11) (GenBank accession no. AY651960), the coding part of the first exon, the first intron, and 14 bp of the second exon of *SnailA* with the *mCherry*-coding sequence (7) followed by an SV40 polyadenylation signal and 2 kb of sequence downstream from the *SnailA* translation stop. We noticed that the *SnailA::mCherry* transgene expression was very weak unless the endogenous copy of the *SnailA* gene was mutated, possibly due to SnailA protein being capable of negatively regulating the transcription of the *SnailA* gene (12). We mutated the endogenous copy of *SnailA* by injecting a single guide RNA (500 ng/μL) directed against the GGGTAGTTCTCCCGAGAGAG sequence in the second exon of the *SnailA* gene together with 1.5 μg/μL nls-Cas9 protein (PNA Bio). Homozygous *SnailA* mutant animals with a 4-bp deletion causing a frameshift upstream of the sequence coding for the first zinc finger of the SnailA developed normally into primary polyps, possibly due to compensation from a highly similar paralogue *SnailB* coexpressed with *SnailA* (13). After crossing the mosaic F0, F1 animals carrying the same frameshift mutation [4-bp deletion at scaffold_32:1316373–1316376 (14)] were crossed to generate homozygous mutant F2. Homozygous *SnailA* mutants carrying a SnailA::mCherry transgene (endoRed animals) were crossed, and the resulting gastrulae, 75% of which were mCherry-positive, were used for the dissociation experiments. Before dissociation, all isolated aboral halves of the endoRed progeny gastrulae were tested for the absence of the mCherry-expressing cells under the Nikon TS100F microscope at 100× magnification using the 800-ms exposure on the highly sensitive Nikon DS-Qi1Mc camera. After reaggregation, the aggregates were controlled for the absence of fluorescent cells for the second time using the same procedure as used before dissociation. Only aggregates completely lacking mCherry-positive cells were kept for analysis.

In Situ Hybridization, Antibody and Phalloidin Staining, and SEM. In situ hybridization and phalloidin staining of F-actin were performed as previously described (15, 16). Nuclei were counterstained with TO-PRO-3 (T3605; Life Technologies) or DAPI (D8417; Sigma). For double in situ hybridization, the digoxygenin-labeled and the FITC-labeled RNA probes were added simultaneously and then detected sequentially as in ref. 17. For antibody staining of mOrange2-expressing cells, the aggregates were fixed for 1 h in 4% paraformaldehyde/PTx (1× PBS/0.2% Triton X-100), washed five times for 5 min in PTx, blocked for 2 h in 5% heat-inactivated sheep serum/1% BSA in PTx and stained with mouse anti-mCherry antibody (632543; Clontech) diluted 1:500 in blocking solution overnight at 4 °C. Unbound primary antibody was removed by eight 10-min washes in PTx, and then the embryos were blocked and stained as described above with goat anti-mouse IgG-conjugated with Alexa568 (A-11004; Life Technologies) and washed eight times with PTx and embedded in Vectashield (Vector Labs) for imaging with a Leica SP5X confocal microscope. A *Dynamena* sample was dehydrated in an isopropanol series and embedded in benzyl benzoate/benzyl alcohol and imaged with a Nikon A1 confocal laser-scanning microscope (CLSM). For SEM, the *Nematostella* samples were fixed and treated as in ref. 3 and the *Dynamena* sample as in ref. 18.

1. Genikhovich G, Technau U (2009) Induction of spawning in the starlet sea anemone Nematostella vectensis, in vitro fertilization of gametes, and dejellying of zygotes. *Cold Spring Harb Protoc* 2009:pdb.prot5281.
2. Freeman G (1981) The role of polarity in the development of the hydrozoan planula larva. *Wilehm Roux Arch Dev Biol* 190:168–184.
3. Kraus Y, Aman A, Technau U, Genikhovich G (2016) Pre-bilaterian origin of the blastoporal axial organizer. *Nat Commun* 7:11694.
4. Saina M, Genikhovich G, Renfer E, Technau U (2009) BMPs and chordin regulate patterning of the directive axis in a sea anemone. *Proc Natl Acad Sci USA* 106:18592–18597.
5. Leclère L, Bause M, Sinigaglia C, Steger J, Rentzsch F (2016) Development of the aboral domain in Nematostella requires β-catenin and the opposing activities of six3/6 and frizzled5/8. *Development* 143:1766–1777.
6. Riedl J, et al. (2008) Lifeact: A versatile marker to visualize F-actin. *Nat Methods* 5:605–607.
7. Shaner NC, et al. (2008) Improving the photostability of bright monomeric orange and red fluorescent proteins. *Nat Methods* 5:545–551.
8. Steinmetz PRH, Aman A, Kraus JEM, Technau U (2017) Gut-like ectodermal tissue in a sea anemone challenges germ layer homology. *Nat Ecol Evol* 1:1535–1542.
9. Renfer E, Amon-Hassenzahl A, Steinmetz PR, Technau U (2010) A muscle-specific transgenic reporter line of the sea anemone, Nematostella vectensis. *Proc Natl Acad Sci USA* 107:104–108.
10. Fritzenwanker JH, Genikhovich G, Kraus Y, Technau U (2007) Early development and axis specification in the sea anemone Nematostella vectensis. *Dev Biol* 310:264–279.
11. Martindale MQ, Pang K, Finnerty JR (2004) Investigating the origins of triploblasty: 'Mesodermal' gene expression in a diploblastic animal, the sea anemone Nematostella vectensis (phylum, Cnidaria; class, Anthozoa). *Development* 131:2463–2474.
12. Peiró S, et al. (2006) Snail1 transcriptional repressor binds to its own promoter and controls its expression. *Nucleic Acids Res* 34:2077–2084.
13. Röttinger E, Dahlin P, Martindale MQ (2012) A framework for the establishment of a cnidarian gene regulatory network for "endomesoderm" specification: The inputs of ß-catenin/TCF signaling. *PLoS Genet* 8:e1003164.
14. Putnam NH, et al. (2007) Sea anemone genome reveals ancestral eumetazoan gene repertoire and genomic organization. *Science* 317:86–94.
15. Genikhovich G, Technau U (2009) Anti-acetylated tubulin antibody staining and phalloidin staining in the starlet sea anemone Nematostella vectensis. *Cold Spring Harb Protoc* 2009:pdb.prot5283.
16. Genikhovich G, Technau U (2009) In situ hybridization of starlet sea anemone (Nematostella vectensis) embryos, larvae, and polyps. *Cold Spring Harb Protoc* 2009: pdb.prot5282.
17. Denker E, Manuel M, Leclère L, Le Guyader H, Rabet N (2008) Ordered progression of nematogenesis from stem cells through differentiation stages in the tentacle bulb of Clytia hemisphaerica (Hydrozoa, Cnidaria). *Dev Biol* 315:99–113.
18. Kraus YA (2006) Morphomechanical programming of morphogenesis in cnidarian embryos. *Int J Dev Biol* 50:267–275.

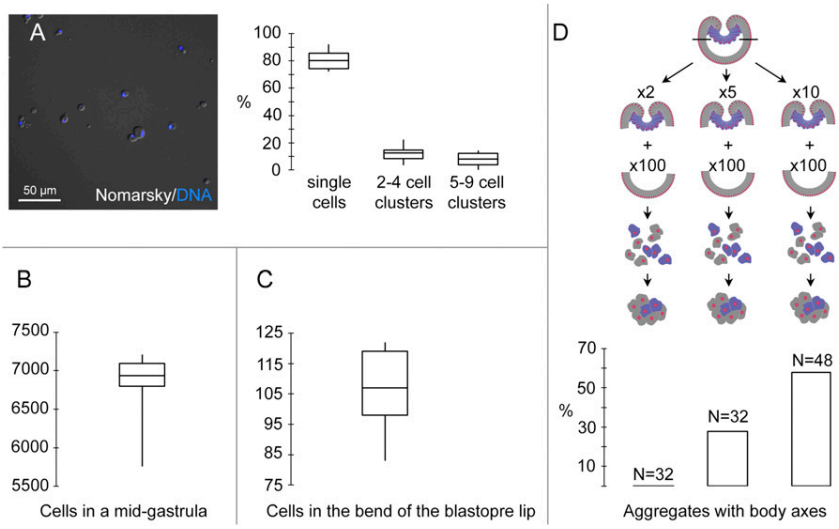

Fig. S1. Efficiency of dissociation of the *Nematostella vectensis* gastrulae and determination of the amount of organizer cells required for induction. (*A*) Dissociation efficiently breaks up the embryos into single cells or small clusters of several cells. A sample image of freshly dissociated *Nematostella* gastrulae stained for 1 min with 5 µg/mL Hoechst 33342 DNA stain and a box plot showing the distribution of single cells and small clusters. Overlay of the Nomarsky contrast and fluorescent image. Clusters containing more than nine cells have not been observed. (*B*) Quantification of the number of cells in a midgastrula at the time of dissociation. (*C*) Quantification of the number of cells in a single circumblastoporal row of cells in the bend of the blastopore lip. (*D*) Efficacy of axis induction in aggregates depending on the ratio of oral gastrula halves to aboral gastrula halves.

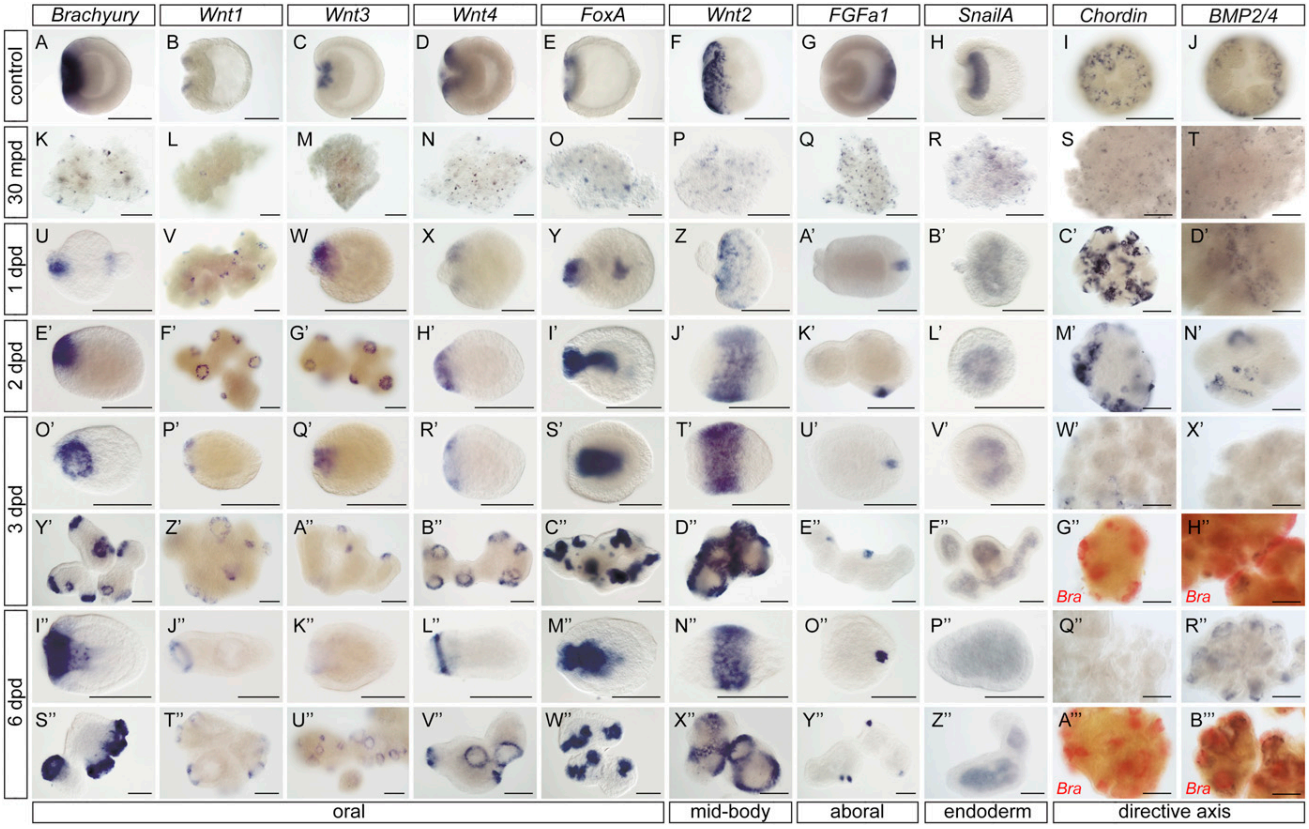

Fig. S2. Marker gene expression during the reestablishment of axial polarity and endoderm formation in aggregates. (*A–J*) Marker gene expression in the control gastrulae at the stage used for dissociation. *Wnt2* is expressed at the oral end in early and midgastrulae; however, its expression shifts into the midbody position later (1). (*K–T*) No signs of axial polarity and endoderm segregation directly after reaggregation. (*U–B'''*) From 1 dpd onward, oral markers *Bra*, *Wnt1*, *Wnt3*, *Wnt4*, and *FoxA* start to be expressed at the forming oral ends, midbody marker *Wnt2* is first expressed orally in a ring and by 2 dpd is displaced into a more aboral position, aboral marker *FGFa1* is expressed at the forming aboral ends, and *SnailA* expression is confined to the segregated endoderm. *Chordin* and *BMP2/4* expression first becomes confined to forming oral ends of the aggregates, and then by 3 dpd *Chordin* expression starts to disappear, while *BMP2/4* expression becomes confined to the forming mesenteries. Large aggregates form multiple oral and multiple aboral domains. dpd, days post dissociation; mpd, minutes post dissociation. (Scale bars: 100 μm.)

1. Kusserow A, et al. (2005) Unexpected complexity of the Wnt gene family in a sea anemone. *Nature* 433:156–160.

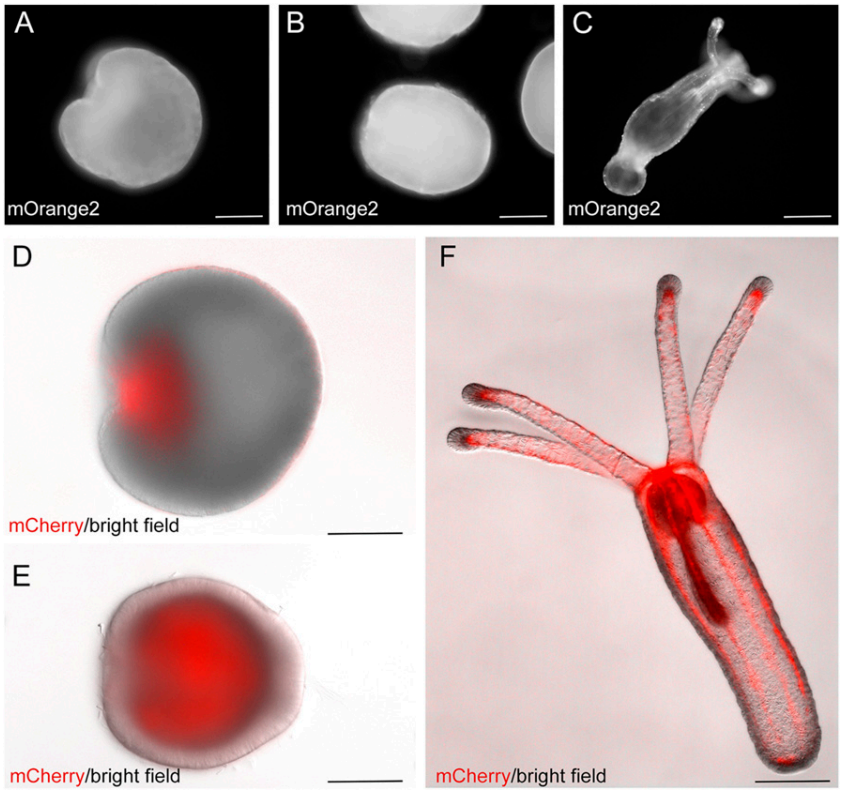

Fig. S3. EF1a::lifeact-mOrange2 and endoRed transgenic lines. (*A*–*C*) Ubiquitous expression of mOrange2 in the gastrula (*A*), planula (*B*), and primary polyp (*C*) of the EF1a::lifeact-mOrange2 line. Epifluorescence images of live specimen. (*D*–*F*) Endodermal expression of mCherry in the gastrula (*A*), planula (*B*), and primary polyp (*C*) of the EF1a::lifeact-mOrange2 line. Merged epifluorescence and bright-field images of live specimen.

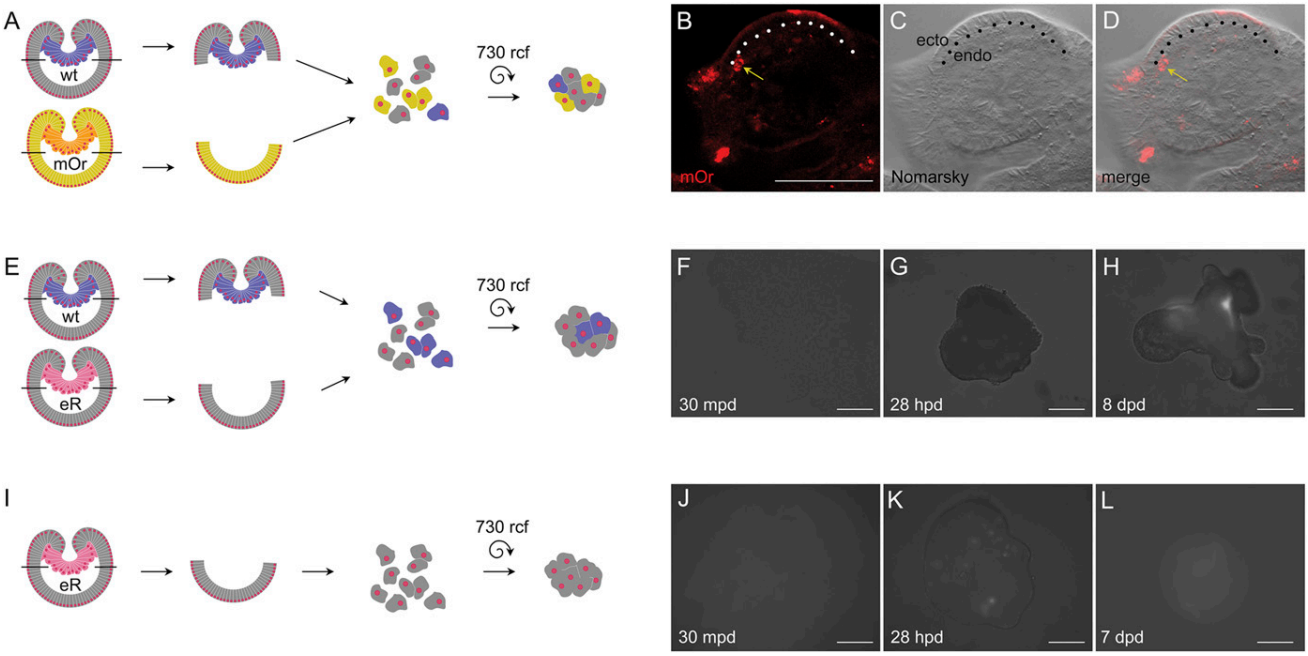

Fig. S4. Fate conversion of the ectodermal cells located inside the aggregate. (*A*–*D*) In aggregates made of oral halves of wild-type gastrulae and aboral halves of gastrulae ubiquitously expressing lifeact-mOrange2, glowing cells can be seen not only in the ectoderm, but also in the endoderm (yellow arrows in *B* and *D*). CLSM image of the embryo stained with an antibody against mOrange2. (*E*–*H*) Cell-fate conversion of the ectodermal cells located inside the aggregate takes place even in the presence of endodermal cells. In aggregates made of oral halves of wild-type gastrulae and aboral ectoderm of endoRed gastrulae, the aggregates are not expressing mCherry (*F*). *SnailA* promoter-driven mCherry expression starts to be detectable in the internal cells of the aggregate from 28 hpd on *G*. Glowing cells are then observed in the endoderm of the forming polyps (*H*). (*I*–*L*) In aggregates made of aboral halves of endoRed gastrulae, mCherry expression is activated in individual internal cells, but it fades as the aggregates are arrested in the ciliated ball stage. (Scale bars: 100 μm.)

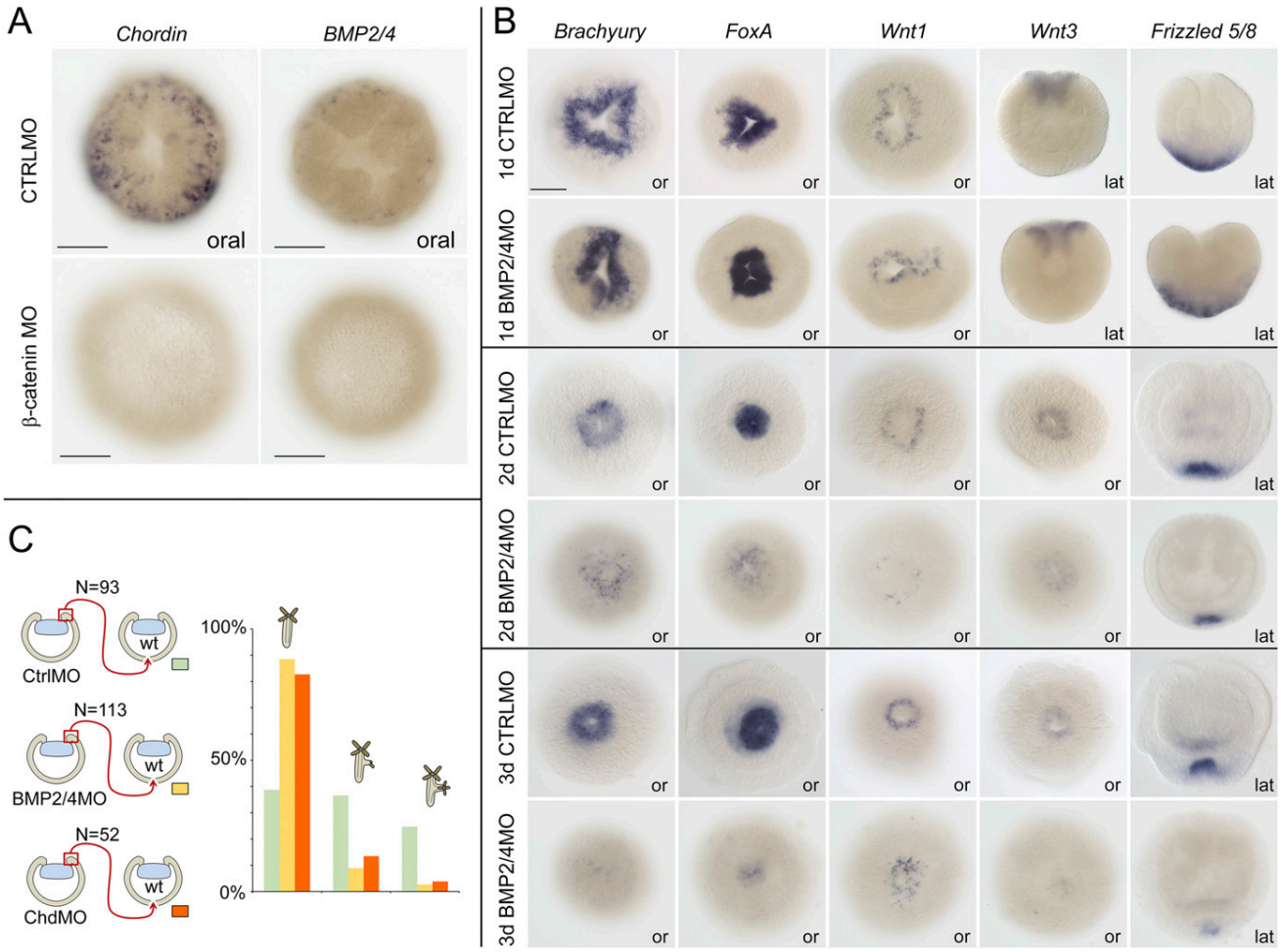

Fig. S5. The role of BMP signaling in oral and aboral development. (*A*) Early radially symmetric expression of *Chordin* and *BMP2/4* is abolished upon *β-catenin* knockdown. (*B*) The expression of the oral markers *Brachyury*, *FoxA*, *Wnt1*, and *Wnt3* and of the aboral marker *Frizzled5/8* is similar in BMP2/4MO and CTRLMO embryos at the gastrula stage. However, the expression of all these gene becomes weaker in 2- and 3-d-old *BMP2/4* morphants, although the location of the expression domain in relation to the oral–aboral body axis remains correct. (*C*) The inductive capacity of the blastopore lips of gastrulae with BMP signaling suppressed by *BMP2/4* or *Chordin* morpholino knockdown is much weaker than in controls. (Scale bars: 100 μm.)

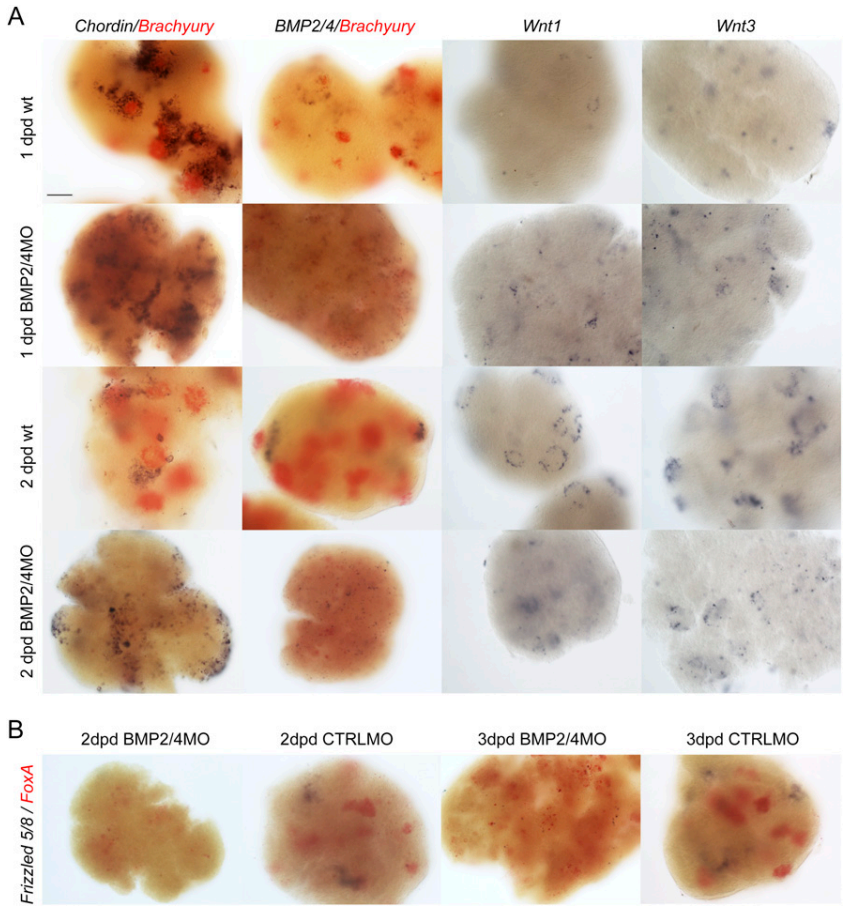

Fig. S6. The role of BMP signaling in aggregates development. (*A*) Oral restriction of *Brachyury*, *Wnt1*, and *Wnt3* in the 1- and 2-dpd BMP2/4MO aggregates is strongly reduced in comparison with uninjected controls. *Chordin* and *BMP2/4* expression is de-regulated as well. (*B*) Oral restriction of *FoxA* and aboral expression of *Frizzled5/8* are suppressed in the *BMP2/4* morphant aggregates in comparison with aggregates made from control morpholino-injected embryos. (Scale bars: 100 μm.)

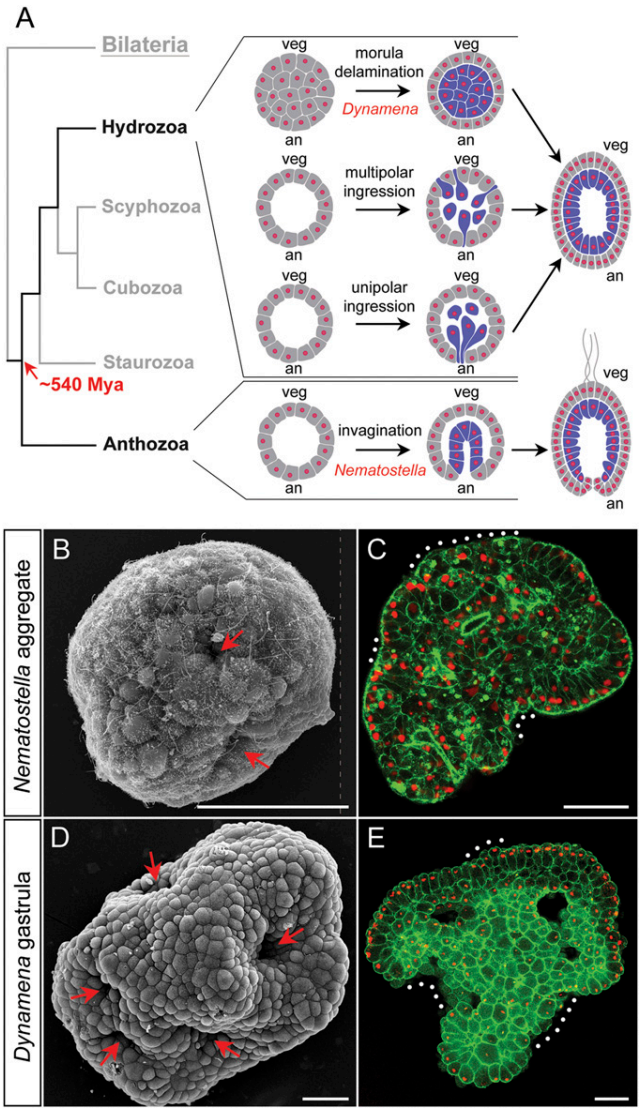

Fig. S7. The alternative developmental trajectory of endoderm segregation in *Nematostella* aggregates resembles the normal development of distantly related hydrozoan cnidarians. (*A*) A subset of modes of hydrozoan and anthozoan gastrulation, all leading to the development of a planula larva. an, animal (future oral) pole; veg, vegetal (future aboral) pole of the cnidarian embryo. Red arrow indicates the last common ancestor of anthozoans and hydrozoans ~540 Mya. (*B* and *C*) The surface (*B*) and a confocal optical section (*C*) of a 6-hpd *Nematostella* aggregate. Grey dashed line represents the edge of the original image. (*D* and *E*) The surface (*D*) and a confocal optical section (*E*) of a gastrulating *Dynamena* embryo (Cnidaria, Hydrozoa).

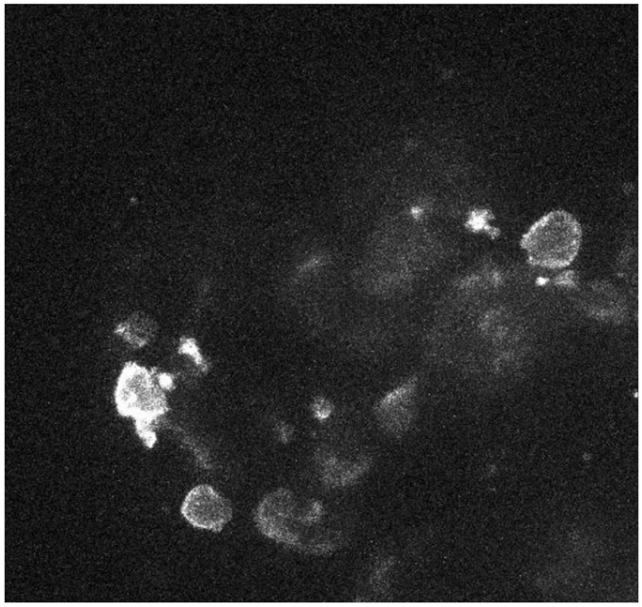

Movie S1. Ingression of fluorescent endodermal cells in the aggregate. Time-lapse recording of the aggregate made of wild-type ectoderm and lifeact-mOrange2–expressing endoderm. Maximum projection of the 110-μm deep Z-stacks taken each 4 min starting at 1 hpd. The first 180 Z-stacks are shown. Most endodermal cells ingress and disappear from the surface of the aggregate by 4.5 hpd.

Movie S1

DISCUSSION

CADHERINS ARE TIGHTLY ASSOCIATED WITH THE EVOLUTION OF EPITHELIA

The evolution of epithelia is intimately connected with the emergence of the multicellularity (Cereijido et al., 2004). The ability of cells to adhere to each other and to form enclosed epithelial layers created a controlled inner milieu of an organism and separated it from the external environment. This would have been the first event, which distinguished an individual animal from a colony. Thus, the epithelium can be viewed as a crucial metazoan innovation. To better understand structure and functions of the first true epithelium, we studied the morphology, function, and molecular characteristics of epithelia in Cnidaria, as basally branching representative phylum belonging to the Eumetazoa, i.e. animals with a true tissue organization.

One of the major characteristic features of epithelia is epithelial polarity, which is closely connected the formation of apical *adherens* cell junctions. The main proteins of the *adherens* junctions, which are responsible for cell adhesion and cell polarity within epithelia and present overall across the Metazoa are cadherins (Hulpiau and van Roy, 2009; Oda and Takeichi, 2011). Although proteins with cadherin domains are present in unicellular choanoflagellates, classical cadherins with intracellular domains binding catenins arose only in metazoans (Nichols et al., 2012). Multiple studies of Bilateria have shown that cadherins are closely connected with the regulation of cell differentiation, cell migration and tissue morphogenesis. *Hydra* and *Nematostella* genomes encode all major proteins known to be involved in the cell junction formation in Bilateria. This means that the common cnidarian–bilaterian ancestor possessed a full genetic inventory for the formation of all types cell junctions in Eumetazoa (Chapman et al., 2010). However, the role of cadherins in non-bilaterians and their evidence for cell adhesion was not shown to date.

Interestingly, classical cadherins show the most noticeable variation in their extracellular region among different metazoan species. For example, cadherins of basal metazoans are substantially larger than those of most bilaterians. Non-bilaterians usually possess huge ancestral classical cadherins, which resemble the extracellular domain composition of FAT, FAT-like, CELSR non-classical cadherins of Bilateria. For example, classical cadherins in mammals possess 4-5 extracellular repeats, while cadherins in cnidarians were predicted to have ~30 extracellular repeats. Thus, mammals have lost the extracellular EGF and LamG and most of the extracellular domains in the course of evolution (Hulpiau and van Roy, 2010) (Figure 4).

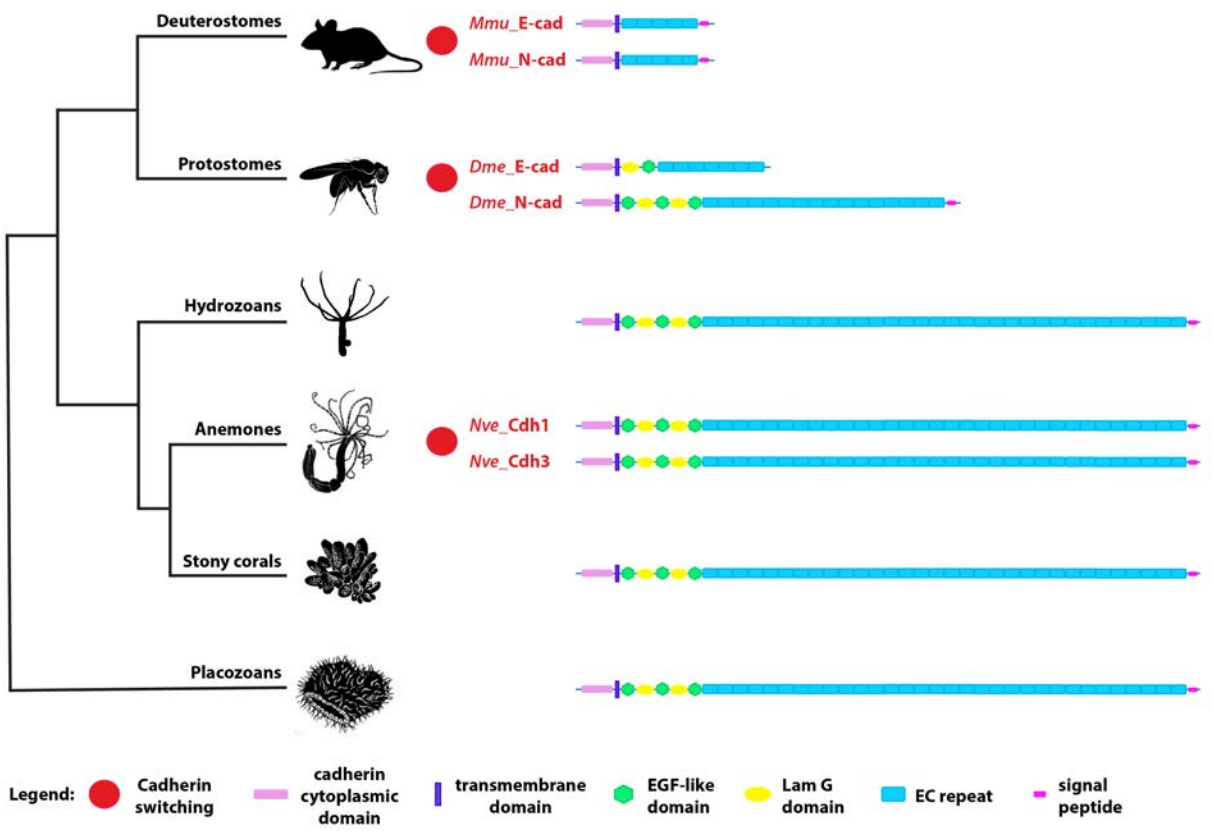

Figure 4. Evolution of a cadherin switching and structure of cadherin proteins across the animal kingdom. Lineage specific cadherin duplications occurred at least three times independently during evolution.

While previous studies have predicted three classical cadherins (*cadherin 1-3*; (Hulpiau and van Roy, 2010)), our analysis showed that cadherin2 is not expressed at any stage and most likely represents a pseudogene. We cloned the other two classical cadherins of *Nematostella vectensis*, *cadherin1* and *cadherin3*, and further investigated their protein domain organization. We showed that classical cnidarian cadherins consist of 30-32 extracellular repeats, several LamG/EGF-like domains proximal to the transmembrane domain and a conserved intracellular domain for binding to the actin cytoskeleton. Cadherin 1 and 3 code for about 4300 amino acids compared to 900 amino acids of classical cadherins in vertebrates. Notably, our phylogenetic analysis of the classical cadherins showed that stony corals and hydrozoans had only a single classical cadherin, which groups basally with two classical cadherins of sea anemones. This suggests that the sea anemones duplicated an ancestral classical cadherin, which led to the two classical cadherins, whereas corals and hydrozoans have retained a single copy.

Cadherin3 is ubiquitously expressed till the beginning of gastrulation. Later on, Cadherin1 started being expressed in the differentiating endoderm and in the aboral ectoderm, while Cadherin3 was down-regulated in the endoderm. However, the role of classical cadherins in cell adhesion and the significance of the different cadherin

expression patterns were unclear.

Our custom-made antibodies showed that classical cadherins are indeed the main components of *adherens* junctions during epithelia and germ layer formation in both embryo and cell aggregate development of *Nematostella* (Kirillova et al., 2018; Pukhlyakova et al., 2019). *Nematostella* development starts with a zygote cleavage, leading to the formation of a single-layered epithelial blastula. Cadherin-positive cell-cell contacts appear after the two first cell divisions. Initially they are distributed along the later side of the blastomeres, and later they localize to the apical and basal sides of the blastomeres, forming the *adherens* junctions between cells (Pukhlyakova et al., 2019). Cadherin3 remains present in the epithelial junctions in all cells of the blastoderm till germ layer segregation. We showed that epithelialization and the dynamics of classical cadherins during germ layer formation in aggregates from gastrula stage embryos are similar to the normal embryo development. Aggregates of dissociated *Nematostella* embryonic cells self-organize in two major steps: the formation of epithelia and a subsequent embryonic patterning. Cadherin3 becomes localized to the cell junctions during the cell aggregate development shortly after re-aggregation, when the first signs of epithelialization becomes apparent. Germ layer formation in *Nematostella* cell aggregates does not occur by invagination, but by a combination of delamination and a multipolar ingression of the endodermal cells, which surprisingly resembles the mechanisms of epithelialization and germ layer formation of the normal development in some hydrozoan Cnidaria (Byrum, 2001; Kraus et al., 2014). Ectodermal cell layer formed first, while the endoderm remained non-epithelialized. Interestingly, endodermal cells alone cannot reform an epithelium and become mesenchymal without ectodermal cell presence. During establishment of the endodermal layer in an aggregate, inner cells started to express Cadherin1, while ectoderm expressed Cadherin1 and Cadherin3 simultaneously. Surprisingly, the timing of epithelialization and germ layer segregation in the cell aggregate is similar to the normal development of an embryo. Aggregates re-establish germ layers and the correct body patterning from the dissociated embryonic cells, showing enormous cell plasticity. Interestingly, self-organizational behavior of embryonic cells is also observed in other systems. For example, dissociated cells of *Hydra* can re-aggregate and form a complete *Hydra* polyp (Technau et al., 2000); and pluripotent stem cell derived three-dimentional organoids can recapitulate kidney, heart and human brain development (Geuens, et al., 2020; Lancaster et al., 2013; Nugraha et al., 2020). We can speculate that, the timing of an embryo and an aggregate epithelialization, and distribution and dynamics of cadherins during germ layer formation are very robust. We observe an amazing developmental plasticity of the Cnidaria, which allows germ layer formation and normal embryo development even under unusual developmental constraints, like the lack of the cavity and mixed position of the cells in a cell aggregate. We show that in a new developmental context, the aggregates of dissociated *Nematostella* embryonic cells take an alternative developmental trajectory, self-organizing into the epithelia and forming the germ layers. We propose that redundancy of the developmental processes ensures

reliable and precise germ layers formation. Cell aggregates employ cell morphogenetic movements typical for normal development of other cnidarians to re-establish the germ layers.

Interestingly, Cadherin3 stays localized at the apical cell junctions even during blastomere cleavage, whereas PAR polarity proteins transiently disappear (Ragkousi et al., 2017; Salinas-Saavedra et al., 2018). Though molecular programs that drive apical-basal polarization are unknown in non-bilaterian animals, our data suggest that cadherins may guide PAR proteins after their temporary loss during cell division and therefore may play a primary role of in establishing of early cell polarity.

Surprisingly, we found that Cadherin3 also localized on the basal-lateral side of the cells. Ultrastructural analysis revealed that the basal cell-cell junctions connect to the actin cytoskeleton and morphologically resemble the *adherens* junctions at the apical side.

Interestingly, hydra epithelial cells are also laterally connected via myoneme-associated junctions at the basal side of the cells (Seybold et al., 2016). Basal junctions have a major contribution in the synchronized contractions of the large myo-epithelial sheets and in the process of bud formation (Holz et al., 2017). Thus, in contrast to most bilaterians, where *adherens* cell junctions are localized only at the apical side of the epithelium, cnidarians have a remarkable and unique epithelial organization, with apical and basal cell-cell junctions. Basal junctions of cnidarian epithelia most likely use a specific molecular mechanism to establish basal polarity and therefore they are of great interest for future research.

Basal cell-cell junctions might be a special innovation of Cnidaria and can play a crucial role in the normal epithelia functioning and morphogenesis. Thus, at blastula stage *Nematostella* embryo undergoes 5-7 pulsations due to synchronous cell divisions as well as basal contractions of blastula cells prior gastrulation start ((Fritzenwanker et al., 2007); time-lapse movies). Since there is no evidence of epithelial ECM support at the early embryo stage, basal junctions might provide an additional support for the stability of the epithelium during embryogenesis.

This non-conventional epithelial organization in Cnidaria could be connected to functions of the ancient epithelia. It has been hypothesized that ancient cell types were less specialized and shared multiple functions. For example, muscle cells in Cnidaria contribute to the epithelium formation and establishing of the barrier with an environment (Arendt, 2008; Jahnel et al., 2014). Basal junctions might additionally stabilize epithelia and provide increased connectivity between cells during acto-myosin contractions and better signal transition between cells in the absence of the defined nervous system. In the course of evolution cells and tissues became more specialized and different functions were distributed among cells. Therefore, the existence of the basal protrusions, linked with the basal cell-cell *adherens* junctions may have lost their crucial significance for the epithelial functionality.

CADHERIN SWITCHING PLAYS AN IMPORTANT ROLE IN EMBRYO MORPHOGENESIS OF *NEMATOSTELLA, DROSOPHILA* AND VERTEBRATES

The increase of body plan complexity during animal evolution is strongly correlated with germ layer segregation and the emergence of the third germ layer - mesoderm. How mesoderm evolved remains one of the most fascinating questions of developmental and evolutionary biology. In Bilateria mesoderm formation usually involves EMT, conjugated with a series of drastic cellular transformations. So, EMT during gastrulation of triploblastic animals includes apical cell constriction, loss of epithelial polarity, activation of the cell migratory mechanisms, ECM digestion and epithelia delamination. A hallmark of EMT is a cadherin switching: down-regulation of E-cadherin and up-regulation of N-cadherin (Lim and Thiery, 2012; Schäfer et al., 2014).

Interestingly, during endoderm formation of the 'diploblastic' *Nematostella*, cells also exhibit some characteristic bilaterian EMT features (Kraus and Technau, 2006; Magie et al., 2007; Shook and Keller, 2003). Gastrulation of *Nematostella* has been described as an invagination with the features of incomplete EMT (Kraus and Technau, 2006; Magie et al., 2007). Studying gastrulation of *Nematostella* gives us an opportunity to tackle the evolutionary origin and potential homology of germ layers, evolution of EMT and its regulation. As gastrulation begins, a group of epithelial cells, called the pre-endodermal plate segregates and undergoes severe morphological and molecular changes. Although pre-endodermal cells retain apical *adherens* junctions and never lose the epithelium completely, invaginating epithelium becomes less columnar; cells apically constrict and become bottle shaped. The nucleus translocates to the basal side; cells lose basal *adherens* junctions, form basal protrusions and filopodia, up-regulate MMP and three laminin chains, composing laminin ECM (Pukhlyakova et al., 2019) (Figure 5). These events imply the activation of the cell migratory program in the pre-endodermal cells similar to the EMT activation mechanism in bilaterians. Intriguingly, gastrulation and germ layer formation in *Nematostella* requires change of cell adhesion alike in Bilateria (Lim and Thiery, 2012; Thiery et al., 2009). We show that formation of the germ layers of *Nematostella* is accompanied by a cadherin switching, which starts with a stepwise down-regulation of Cadherin3. First, Cadherin3 disappears from the basal cell-cell junctions in the pre-endodermal plate. At the beginning of gastrulation we observe the up-regulation of *cadherin1* mRNA and a ubiquitous Cadherin1 protein signal in the nascent endodermal cells. As gastrulation completes and endoderm differentiates, Cadherin1 completely replaces Cadherin3 and forms newly pronounced apical and basal cellular junctions in the inner embryonic cell layer. Thus, Cadherin3 to Cadherin1 protein switching marks endoderm formation during gastrulation. We propose that, the Cadherin3 to Cadherin1 switching in *Nematostella* is analogous to the E-cadherin to N-cadherin switching in vertebrates and insects. As

Cadherin1 and Cadherin3 in *Nematostella* and E-cadherin and N-cadherin in *Drosophila* and vertebrates have different extracellular domain organization and belong to different cadherin subfamily types, they represent cadherin lineage-specific duplications (Hulpiau and van Roy, 2009; Hulpiau and van Roy, 2010).

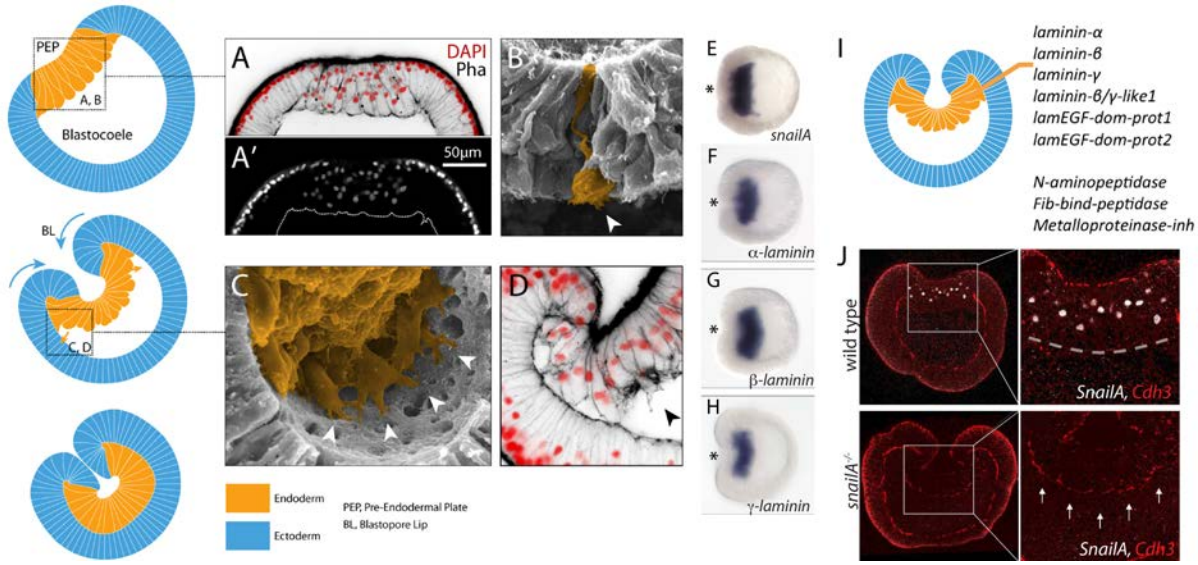

Figure 5. Gastrulation of *Nematostella* occurs by invagination with the features of a partial EMT. A. Pre-endodermal plate formation due to apical constriction of the nascent endodermal cells. **B, C, D.** Invagination of the pre-endodermal plate. Pre-endodermal plate cells become bottle-shaped, form cell protrusions on the basal side (arrowheads). **E.** Expression of the transcription factor *snailA* in the pre-endodermal plate (*in situ* hybridization). **F, G, H.** Expression of the ECM components *α-laminin* (NVE709), *β-laminin* (NVE456) and *γ-laminin* (NVE5664), forming a laminin protein complex (*in situ* hybridization). Asterisk indicates an oral pole of an embryo. **I.** Expression of the ECM components and ECM regulators in the pre-endodermal plate. **J.** Nuclear localization of the SnailA in the pre-endodermal plate. Cadherin3 basal junctions disappear in the pre-endodermal plate cells during gastrulation. Basal junctions retain in the pre-endodermal plate in the *snailA* mutants. After (Technau, 2020) and M. Jovic Master thesis.

Thus, we conclude that a cadherin switching mechanism during EMT evolved convergently in Cnidaria and Bilateria (Figure 4). Since, in contrast to sea anemones, corals and hydrozoa possess only a single copy of classical cadherins, this is another indication of convergent evolution of classical cadherins duplication and a cadherin switching during EMT. However, the role of a single classical cadherin in gastrulation and germ layer formation in corals and hydrozoa remains an open question. It can either suggest that there is no cadherin switching during gastrulation of stony corals and hydrozoa or that non-classical cadherins, like Dachsous, may take part in these processes. A recurrent cadherin switching in evolution implies that the differential cadherin expression is an effective regulatory mechanism, which facilitates tissue morphogenesis and germ layer formation.

EMT in Bilateria and partial EMT in *Nematostella* comprise similar regulatory mechanisms. Loss of the *adherens* junctions increases cell motility and might be one of the crucial steps of EMT. In Bilateria the transcription factor Snail is one of the major regulators of EMT and a direct repressor of e-*cadherin* (Nieto, 2002). Additionally, cadherin molecules in the *adherens* junctions are constantly under turnover through vesicle trafficking. Besides direct repression of *cadherin* transcription, Snail facilitates cadherin endocytosis, stimulating fast cadherin removal from the cell surface (Wu and McClay, 2007). Endocytosis of *adherens* junctions and their subsequent targeting for degradation and recycling can contribute to the more precise temporal control of EMT in Bilateria (Huang et al., 2011; Ivanov et al., 2005).

In *Nematostella snailA* transcription factor is expressed in the pre-endodermal plate during gastrulation. In wild-type embryo basal junctions resolve in the pre-endodermal plate during gastrulation. Knockdown of *snailA* leads to the partial retention of the basal Cadherin3 junctions in the pre-endodermal plate. As a result, endodermal cells remain less motile and more firmly attached to each other, which caused a gastrulation delay (Figure 5). We speculate that the loss of the basal cadherin junctions in *Nematostella* could be controlled indirectly by SnailA transcription factors via endocytosis. We propose that Snail is one of the conserved regulators of cell adhesion during EMT and gastrulation in Bilateria and Cnidaria.

Another possible cell adhesion control mechanism during gastrulation is the distribution of polarity proteins. Interestingly, recent studies have suggested that aPKC/PAR cell polarity proteins (NvaPKC, NvPar-6, NvPar-3, NvPar-1, NvLgl) are degraded in the endoderm during gastrulation (Salinas-Saavedra et al., 2015; Salinas-Saavedra et al., 2018). Ectopic expression of *snails* in the ectoderm destabilizes Par proteins and *adherens* junctions, followed by translocation of β-catenin to the nucleus. This leads to the disruption of epithelia. In turn, CRISPR/Cas9 knock-out of *snail* genes in the F0 generation of embryos led to the retain of apical Par proteins and ß-catenin in the apical cortex of the endodermal cells. Surprisingly, baso-lateral markers NvPar-1 and NvLgl were not visible in the endoderm, suggesting that the loss of these baso-lateral proteins depends on the regulatory factors other than *snails* (Salinas-Saavedra et al., 2018).

Since a aPKC/PAR complex stabilizes β-catenin/cadherin cell adhesion junctions, it was proposed that an endodermal epithelium does not have β-catenin/cadherin cell adhesion system like an ectodermal epithelium (Salinas-Saavedra et al., 2018). However, our results show that cadherin junctions are present in the endoderm, although Cadherin1 replaces Cadhein3 at the cell junctions after a cadherin switching and germ layer specification. Due to different molecular composition *adherens* junctions in different germ layers might have different properties. Indeed, an inner gastrodermal epithelium of juvenile polyps does not have sealing properties as an outer epidermis, suggesting that cell adhesion is differentially regulated in these tissues (Salinas-Saavedra et al., 2018).

Earlier biochemical analysis showed that an intracellular domain of both classical cadherins Cadherin 1 and Cadherin3 forms a complex with α-catenin and β-catenin in *Nematostella.* This demonstrates a deep ancestry of the cadherin-catenin complex as a cell-cell adhesion composite and a signaling module (Clarke et al., 2016). However we and other researchers could not reveal β-catenin in the cell junctions of the endoderm nor in the pharyngeal ectoderm (Pukhlyakova et al., 2019; Salinas-Saavedra et al., 2018). These results show that not all the cell contacts of *Nematostella* epithelium might contain β-catenin and that the *adherens* junctions are qualitatively different in different tissues. Since actin filaments connect to the apical and basal *adherens* junctions, we assume that either another protein could act instead of β-catenin or that β-catenin was not detected at these junctions due to the technical reasons.

Gastrulation is surprisingly tolerant of overall changes in cell adhesion and only when tissue integrity is disrupted, an embryo does not complete gastrulation (Ninomiya et al., 2012) (Winklbauer, 2012). However, the control of the *adherens* junctions is extremely important for the proper cell rearrangements and further cell differentiation during embryo morphogenesis. Differential expression of specific cadherin molecules in Bilateria correlates with the formation of new tissues and organs.
In 1955, Holtfreter and Townes proposed a mechanism that embryonic cells can sort out based on different cell adhesion levels, which leads to the subsequent segregation into germ layers and tissues (Townes and Holtfreter, 1955; Steinberg and Gilbert, 2004; Takeichi, 1995). Later on, a mechanism of differential cortical tension was suggested for the successful cell sorting (Krieg et al., 2008). However the mechanism of germ layer formation in the embryo has never been fully understood. In many species such as chick, mouse, fly and fish N-cadherin starts being expressed at the onset of gastrulation when endodermal cells begin to internalize. It was proposed that in the beginning of gastrulation N-cadherin induce cell motility and active migration from the neighboring cells (Giger and David, 2017; Warga and Kane, 2007). In zebrafish embryo activation of N-cadherin expression triggers active cell migration, and segregation and internalization of endodermal cells without down-regulation of E-cadherin. Cell internalization happened independently of cell adhesion and therefore did not support a key role of differential adhesion for cell sorting, as was proposed previously (Giger and David, 2017). It also correlates with the studies in *Xenopus,* showing that differential adhesion is important for cell sorting *in vitro* but not *in vivo* (Ninomiya et al., 2012). However, differential adhesion could also act redundantly or be involved in the maintenance of germ-layer boundary.

Interestingly, endoderm internalization is independent of E-cadherin down-regulation also in fly and chick embryos, as well as in mammalian epithelial cancer cells (Giger and David, 2017; Hardy et al., 2011; Nieman et al., 1999; Schäfer et al., 2014). In these cases N-cadherin promotes cell movement through different mechanisms independently of cell adhesion: either via activation of FGF signaling, or Rac/Rho systems, which facilitate cell migration, implying that this may be a conserved

mechanism driving germ-layer formation in different species. During gastrulation of the mouse embryo, epiblast cells elongate and apically constrict while entering the primitive streak. Interestingly, nascent mesoderm cells lose E-cadherin, while nascent endoderm cells redistribute it anisotropically on their surface (Viotti et al., 2014). *Snail* mice mutants show a failure of gastrulation EMT (Carver et al., 2001).
Similarly, in *Drosophila* and zebrafish E-cadherin is retained in endodermal cells and required the collective cell migration during gastrulation (Campbell and Casanova, 2015; Montero, 2005).
Besides cell adhesion E-cadherin also mediates cell signaling and stabilizes a feedback loop facilitating Bone Morphogenetic Protein (BMP) expression in the extra-embryonic ectoderm and downstream activity in the epiblast. E-cadherin homophilic binding inhibits Epidermal Growth Factor (EGF) signaling and thus cell growth (Perrais et al., 2007). Interestingly, N-cadherin can substitute E-cadherin for deficient adhesion, but not for signaling, since it cannot form complexes with Receptor Tyrosine Kinases (RTKs) like E-cadherin. Consequently, N-cadherin interacts with FGFR1 receptor affecting FGF and promotes EMT and required for proper mesoderm differentiation (Basilicata et al., 2016; Schäfer et al., 2014). Thus N-cadherin expression plays also an important role mesoderm specification, as well as in neural and somite morphogenesis. Surprisingly, the upstream signals leading to the endoderm differentiation are not conserved between different model organisms. In vertebrates it is Nodal signaling whereas in *Drosophila* Nodal-like does not exist and the endoderm specification happens via Mitogen Activated Protein Kinase Kinase (MAPKK) signaling (Nowotschin et al., 2019).
For example, in *Drosophila* E- and N-cadherin show different effects on differentiation of some mesodermal derivatives due to the different ability of various cadherins to sequester β-catenin – a major Wnt signaling effector (Schäfer et al., 2014).
Nevertheless, modulation of the cell signaling pathways and activation of the cell migratory activity could be a key evolutionary mechanism driving germ-layer formation, which in some species is accompanied by a loss of E-cadherin expression.

In *Nematostella,* overexpression of constructs, encoding transmembrane and intracellular cadherin domains of the sea urchin, could also cause the sequestration of nuclear ß-catenin and block primary invagination and endoderm differentiation (Wikramanayake et al., 2003; Kumburegama et al., 2011). Our knockdown experiments show that knockdown of Cadherin1 or Cadherin3 does not impair gastrulation, probably due to maternal protein deposition. However, classical cadherins are required for maintenance of tissue integrity and proper tissue morphogenesis. Cadherin3 knockdown impedes formation of the cell junctions *de novo*, however it does not affect the earlier established contacts built from the maternal protein. Cadherin1, the only cadherin expressed in the endoderm after gastrulation completion, is crucial for morphogenesis of the endodermal folds – the mesenteries. Cadherin1 is also crucial for the apical organ development. The apical organ forms at the planula stage in the area of aboral ectoderm. Surprisingly,

Cadherin1 is especially strongly expressed in a subpopulation of ectodermal cells, which co-express FGF and give rise to a sensory apical organ. The function of this ectodermal Cadherin1 expression is not totally clear however it can be linked to FGF signaling, which regulates local patterning in the aboral region and apical organ formation (Rentzsch et al., 2008). Interestingly, Cadherin1 knockdown does not disrupt oral patterning, but abolishes FGFa1 expression, which indicates a possible interaction between FGF signaling and Cadherin1. For example, in Bilateria N-cadherin has been shown to interact with FGF receptor, preventing its internalization, and therefore promoting the sustained FGF signaling (Nguyen and Mège, 2016). The interaction of FGF signaling pathway with N-cadherin in Bilateria and Cadherin1 in *Nematostella* might either have evolved several times during evolution or it can be an ancestral mechanism of the cell signaling regulation in sea anemones and Bilateria.

Meanwhile, Cadherin3 is exclusively expressed in the ectoderm with especially strong expression in the oral ectoderm and ectoderm of the pharynx and tentacles. Thus, cadherin expression marks a boundary between ectoderm and endoderm, which is very difficult to discern by morphological criteria. Cadherin3 localization at the cell junctions in the pharynx precisely marked a border between the last ectodermal and the first endodermal cells. In line with studies known for Bilateria (Batlle and Wilkinson, 2012; Halbleib and Nelson, 2006), sea anemones and Bilateria use the same regulatory mechanisms for germ layer formation and tissue morphogenesis, which appeared due to differential expression of independently duplicated classical cadherins. We conclude that differential cadherin expression and its role in tissue boundary formation and tissue differentiation might be a conserved feature shared by Cnidaria and Bilateria.

While the evolutionary origin of mesoderm remains controversial, there are several theories about it. Traditionally, germ layers in Cnidaria were homologized with the endoderm and ectoderm of Bilateria. Later on, the inner layer was called “endomesoderm” due to the identification of a number of mesodermal transcription factors, expressed in the endoderm (Fritzenwanker et al., 2004; Kumburegama et al., 2011; Martindale, 2004; Salinas-Saavedra et al., 2018; Technau and Scholz, 2003). However, recent studies of many endodermal and mesodermal marker genes suggest that the inner layer corresponds to mesoderm, whereas the expression profile of the pharyngeal ectoderm is reminiscent of bilaterian endodermal gut and pancreas, and endodermal functions are performed by the pharyngeal ectoderm itself and its extensions – septal filaments (Hashimshony, 2017; Steinmetz et al., 2017). These studies make a correlation between germ layers of Cnidaria and Bilateria non-trivial and suggest that mesoderm and endoderm might have separated before the bilaterian–cnidarian split. In the light of these findings, it is interesting to note, how the expression territories of different cadherins corresponds to the germ layer description. Our antibody staining analysis shows that there are three areas of the differential cadherin expression in *Nematostella* embryo. Cadherin1 is specific to the inner cell layer; Cadherin3 is solely expressed in the pharyngeal ectoderm and septal

filaments; and in the body wall ectoderm Cadherin1 and Cadherin3 are expressed simultaneously.

MECHANOTRANSDUCTION IS AN ANCIENT GENE REGULATORY MECHANISM

Besides genetic regulation, biomechanical properties of the tissue and mechanical forces generated within the embryo are important regulators of numerous developmental processes. Mechanical forces largely affect cell fates and morphogenesis (Farge, 2003; Ingber, 2006; Orr et al., 2006). Cells can sense their physical environment through mechanotransduction translating mechanical stimuli into biochemical signals. Cells perceive mechanical stress generated by cells themselves, as well as externally applied stress coming from the neighboring cells, ECM or external environment. The main source of mechanical forces generated on the cellular and tissue levels is contractions of the actin-myosin cytoskeleton (Heer and Martin, 2017). The cadherin-catenin adhesion complexes bridge acto-myosin cytoskeleton of neighboring cells and arrange mechanical coupling of the cortices of the adhering cells. Cell adhesion junctions provide the mechanical scaffold for the cortex tension during cell sorting and regulate the mechanical tensions within the embryo driving many morphogenetic processes (Röper et al., 2018; Maitre et al., 2012). It has been proposed that cadherins generate cell adhesion tension and participate in the cortical tension regulation (Maitre and Heisenberg, 2013). Due to mechanotransduction at cadherin junctions cells can sense and respond to physical changes in their environment. There are many feedback loops between cadherin junctions, MyosinII activity and actin cytoskeleton dynamics (Mège and Ishiyama, 2017). For example, MyosinII distribution and therefore cell contractility are dependent on cadherins through Rho and Rac small GTPase (Chan et al., 2017) (Lecuit and Yap, 2015). The levels of N-cadherin influences the levels of cytoskeleton remodeling and myosin activation in *Drosophila* and *Xenopus* tissues (Kumar et al., 2015; Nandadasa et al., 2009). In *Drosophila* it has been shown that N-cadherin affects levels and localization of MyosinII and therefore of cell shape. Authors hypothesized that a balance between differential cell adhesion and differential contractility determines cell sorting, cell rearrangements and cell shape changes during morphogenesis (Chan et al., 2017).

Gastrula regions of *Xenopus* embryo differ in cell adhesion properties (Winklbauer, 2012). Expression of different cadherin molecules changes also biomechanical properties of the tissue. Various expression levels of different cadherins or their combinations in different embryo regions may influence the cortical tension in cells. Cell adhesion tension and cell cortical tension could differ for different adhesion molecules types. Therefore we propose that in *Nematostella* different combinations and concentrations of Cadherin1 and Cadherin3 can change tissue properties and identities in different regions of the developing embryo. For example, in *Nematostella* ectodermal and endodermal epithelia express different amounts of Cadherin1 and

Cadherin3, therefore the molecular composition of the *adherens* junctions varies in different embryonic parts. We hypothesize that the distribution and the molecular composition of the *adherens* junctions can also influence the modulation of the tissue properties in the different embryo territories. Moreover, organized localization of the apical and basal cell *adherens* junctions orchestrates cell behavior and cell shape change. We showed that coordinated apical and basal cell constriction of blastoderm cells guides epithelial invagination during gastrulation and might lead to the heterogenic mechanical properties of different parts of the embryo (Figure 6).

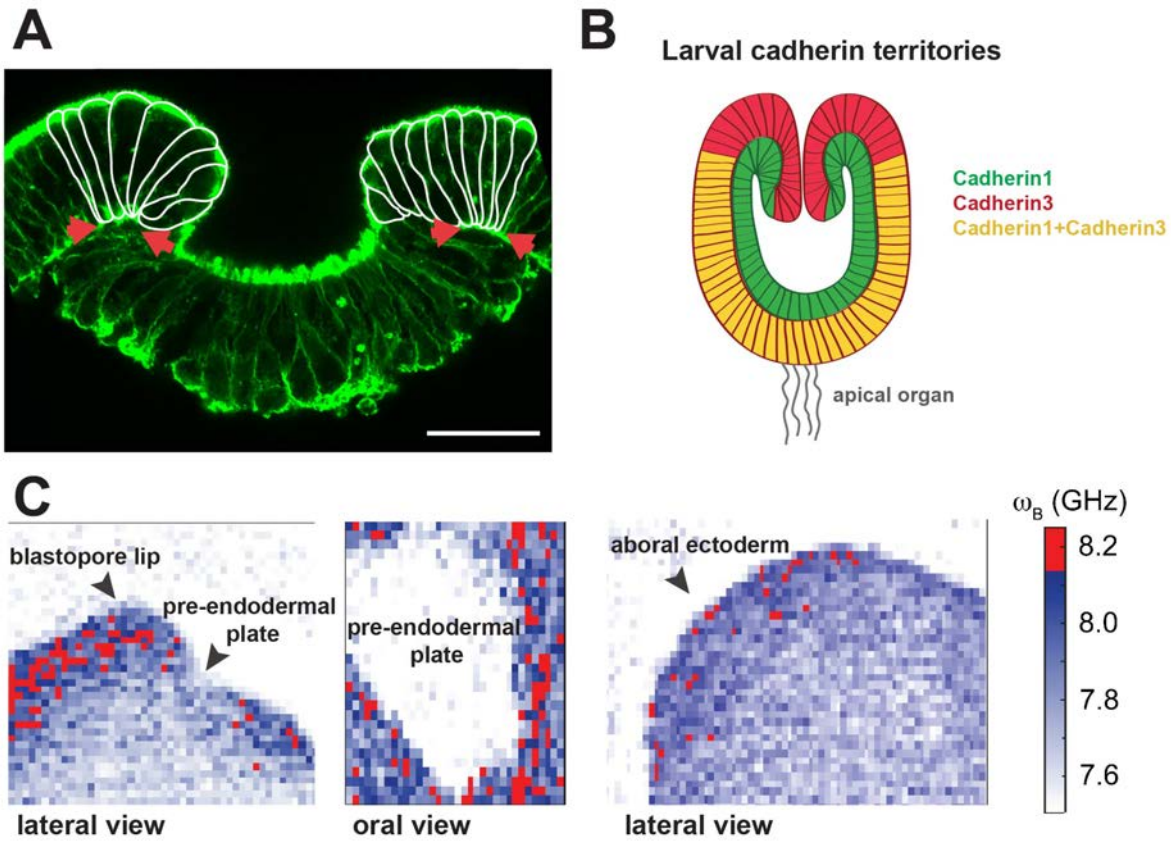

Figure 6. Morphogenetic cell movements during gastrulation create heterogeneity of stiffness in different embryo parts. A. Basal constrictions of the blastoporal cells during *Nematostella* gastrulation (arrows). **B.** Differential expression of cadherins in germ layer of *Nematostella* embryo. **C.** Representative maps of the Brillouin frequency shift ω_B in the blastopore lip, pre-endodermal plate and aboral ectoderm. Frequency shift ω_B is proportional to the square root of the elastic modulus. Regions of high 'stiffness' are colored red. The blastoporal lip shows an increased frequency shift on average relative to the pre-endodermal plate (the lowest 'stiffness') and aboral ectoderm.

We hypothesize that a stiffer blastopore lip might be a necessary parameter for the proper gastrulation movements of *Nematostella*. Our findings show, that a blastopore

lip is significantly stiffer than a pre-endodermal plate and an aboral side of an embryo (Pukhlyakova et al., 2018). We hypothesize that the stiff/soft interface between the blastopore lip and the pre-endodermal plate may generate an epithelium edge reaction similar to the inward bending of on the free edge of the epithelium. Thus, bending of an epithelial sheet due to the difference in mechanical properties and the basal constriction of the blastopore cells creates a pushing force, moving the pre-endodermal plate inwards. Our findings show that the inhibition of the basal constrictions of the blastoporal cells decreases the overall 'stiffness' of the embryo and that the blastopore lip cells showed a similar stiffness as the other embryo parts. Subsequently, this led to the invagination arrest. On the other hand, preserving of the basal cell-cell cadherin junctions in the pre-endodermal plate in the embryos with the down-regulated Snail function slows down but does not block invagination, although the crawling ability of the pre-endodermal plate cells and zippering of the ectoderm and the endoderm is restricted. These findings strongly support that the pushing force of the blastoporal lip rather than the pulling force of the pre-endodermal plate is the driving force of gastrulation of *Nematostella vectensis*. However, a pulling force of the pre-endodermal cells and zippering to the ectoderm are also certainly important for facilitating of invagination.

Cell behavior and mechanical properties of a cell are connected both genetically and mechanically. However, it is extremely difficult to separate their respective influence and to study them independently (Paluch and Heisenberg, 2009). On the one hand the generation of mechanical forces is dictated by molecular signals. On the other hand, there are numerous studies showing that there is a feedback loop between gene expression and cell shape and its physical environment, showing nuclear deformations and change on gene expression upon mechanical strains (Beloussov et al., 2006; Taber, 2007; Maniotis et al., 1997; Wang et al., 2009; Brunet et al., 2013; Hiramatsu et al., 2013; Mammoto et al., 2009). Morphogenetic movements affect gene expression, and, in return, gene expression regulates morphogenetic movements.

Mechanical stimuli can activate biochemical cascades and change gene expression during mechanotransduction. Mechanotransduction has been shown for many species in Bilateria. However, it has been never shown for non-bilaterian animals. We show that mechanotransduction is present in diploblastic sea anemone *Nematostella vectensis* and therefore it appears to be a widespread, if not universal gene regulatory mechanism throughout Metazoa. We show that expression of transcription factor *brachyury* is facilitated by mechanical stress generated by gastrulation movements. Blastoporal cells constrict on the basal side, bending the blastopore lip and generating a pushing force moving the pre-endodermal plate inside. These cellular constrictions affect *brachyury* expression, which intensifies and narrows to a few cell rows around the blastopore. Blocking this basal cellular constrictions by applying of the selective reversible myosin light chain kinase (MLCK) inhibitor impairs *brachyury* expression. Applied external mechanical stimulation is sufficient to rescue *brachyury* expression in embryos without gastrulation strains.

The contractility of the blastopore lip cells leads to a local higher stiffness. Our measurements show that the blastopore lip cells appear significantly “stiffer” than other cells of the embryo or when acto-myosin contractions are inhibited. The mechanical stress of the basal contractions of the blastoporal cells reinforces *brachyury* expression and other targets of β-catenin in a β-catenin–dependent manner. Due to the high concentrations of β-catenin at the oral pole, this region is particularly competent to respond to mechanical stress, preventing that undirected physical forces could ectopically activate *brachyury* expression.

Blocking acto-myosin contractions during gastrulation inhibits expression of other β-catenin target genes in the blastopore lip, but not in the pre-endodermal plate. Moreover, blastoporal cells are competent to respond to mechanical forces in a narrow time window, during blastula-to gastrula transition and gastrulation. This implies that mechanical forces cooperate with the genetic factors to regulate *brachyury* expression in a special and temporal coordinated manner, when morphogenetic cell movements of the blastopore lip are especially active. These results suggest that the blastopore lip is a sensitive area for β-catenin–dependent mechanotransduction, conserved between the sea anemone and Bilateria and that the mechanical forces act upstream of β-catenin signaling. However, it remains unknown what are the exact pathways and mechanisms for mechanotransduction in Cnidaria. Recently, it has been identified that *Nematostella* possesses the components of the YAP/Hippo mechanosensitive signaling pathway – an important regulator of cell proliferation in mammalian epithelia. However, whether this mechanism participates in regulation of gastrulation of *Nematostella* remains an open question for the future investigation (Elbediwy and Thompson, 2018).

In conclusion, we propose that there is a regulatory feedback loop between genetic and mechanical gene activation during gastrulation. This mechanism might be an ancient feature of animal development, and was present in the common ancestor of cnidarians and bilaterians, predating the cnidarian–bilaterian split over 600 Mya.

SCIENTIFIC CONTRIBUTION OF THE PHD PROJECT

Epithelium structure and its cell adhesion junctions are well studied for the bilaterian model organisms (Alberts, 2007). In my PhD thesis I have for the first time in detail described the epithelial organization and cadherin cell junction dynamics during early embryo development of a non-bilaterian sea anemone *Nematostella vectensis*. To this end, I have generated specific antibodies against *Nematostella* classical cadherins: Cadherin1 and Cadherin3, which are now available for the scientific community. These are the first antibodies, which can detect cadherin protein localization in cnidarians. I have found that *Nematostella* epithelium possesses apical and basal cell-cell cadherin junctions. Therefore cnidarian epithelium has a unique

organization, different from the one in bilaterians. I have shown that in spite of the unconventional protein length and domain composition, *Nematostella* cadherins are the major molecules responsible for the cell-cell adhesion and epithelia establishment. I have shown that germ layer formation in *Nematostella* is accompanied by a cadherin switching, similar to the germ layer formation in *Drosophila* and vertebrates. Our data suggest that a cadherin switching evolved convergently several times during evolution. I have described the role of cadherins in a partial EMT during gastrulation and endoderm differentiation. In spite of the previous studies, which suggested that the endodermal epithelium of *Nematostella* lacks normal cell-cell adhesion junctions (Salinas-Saavedra et al., 2018), our findings reveal that during endoderm differentiation Cadherin3 gets replaced for Cadherin1 at the cell junctions. However, endodermal epithelium still forms apical and basal cell-cell adhesion junctions.

During gastrulation and other morphogenetic processes cells change shape and position in coordinated manner, transforming the epithelial sheets. These transformations cause generation of mechanical forces within the tissues. Studies in *Drosophila*, *C.elegans* and vertebrates showed the importance of mechanical forces for the regulation of morphogenesis (Brunet et al., 2013; Cram, 2014; Mammoto et al., 2011; Wozniak and Chen, 2009). Mechanical forces generated by cell can be transformed into biochemical signals in the process, called mechanotransduction. However, there were no evidences for mechanotransduction in non-bilaterian systems. During my PhD thesis I have shown that mechanical pressure can restore or activate β-catenin-dependent *brachyury* expression. We have identified that the coordinated contractility of the cells at the blastopore lip creates the heterogeneity of ‘stiffness’ in different parts of the embryo. This differential ‘stiffness’ can be a necessary condition for the invagination gastrulation movements and for mechanosensitive gene expression, known for Bilateria. Our data suggest that mechanodransduction is a universal ancient regulatory mechanism, present in the morphogenetically active embryo parts, such as blastopore lip during gastrulation. Thus, mechanosensitive gene regulation evolved before cnidarian-bilaterian split at least 600 Mya.

REFERENCES

Aguilar-Cuenca, R., Juanes-García, A. and Vicente-Manzanares, M. (2014). Myosin II in mechanotransduction: master and commander of cell migration, morphogenesis, and cancer. *Cellular and Molecular Life Sciences* **71**, 479–492.

Aigouy, B., Farhadifar, R., Staple, D. B., Sagner, A., Röper, J.-C., Jülicher, F. and Eaton, S. (2010). Cell flow reorients the axis of planar polarity in the wing epithelium of Drosophila. *Cell* **142**, 773–786.

Aladin, D. M. K., Chu, Y. S., Robinson, R. C., Dufour, S., Viasnoff, V., Borghi, N. and Thiery, J. P. (2020). Extracellular domains of E-cadherin determine key mechanical phenotypes of an epithelium through cell- and non-cell-autonomous outside-in signalling. *bioRxiv.*

Alberts, B. (2007). *Molecular Biology of the Cell*. Garland Science.

Alves, C. C., Carneiro, F., Hoefler, H. and Becker, K.-F. (2009). Role of the epithelial-mesenchymal transition regulator Slug in primary human cancers. *Frontiers in Bioscience (Landmark Edition)* **14**, 3041–3050.

Apodaca, G., Gallo, L. I. and Bryant, D. M. (2012). Role of membrane traffic in the generation of epithelial cell asymmetry. *Nature Cell Biology* **14**, 1235–1243.

Arendt, D. (2008). The evolution of cell types in animals: emerging principles from molecular studies. *Nature Reviews Genetics* **9**, 868–882.

Babb, S. G. and Marrs, J. A. (2004). E-cadherin regulates cell movements and tissue formation in early zebrafish embryos. *Developmental Dynamics* **230**, 263–277.

Barrallo-Gimeno, A. and Nieto, M. A. (2005). The Snail genes as inducers of cell movement and survival: implications in development and cancer. *Development* **132**, 3151–3161.

Basilicata, M. F., Frank, M., Solter, D., Brabletz, T. and Stemmler, M. P. (2016). Inappropriate cadherin switching in the mouse epiblast compromises proper signaling between the epiblast and the extraembryonic ectoderm during gastrulation. *Scientific Reports* **6**, 8263.

Batlle, E. and Wilkinson, D. G. (2012). Molecular mechanisms of cell segregation and boundary formation in development and tumorigenesis. *Cold Spring Harbor Perspectives in Biology* **4**, a008227–a008227.

Batlle, E., Sancho, E., Francí, C., Domínguez, D., Monfar, M., Baulida, J. and García De Herreros, A. (2000). The transcription factor snail is a repressor of E-cadherin gene expression in epithelial tumour cells. *Nature Cell Biology* **2**, 84–89.

Baum, B. and Georgiou, M. (2011). Dynamics of adherens junctions in epithelial

establishment, maintenance, and remodeling. *Journal Cell Biology* **192**, 907–917.

Behrens, J. (1999). Cadherins and catenins: role in signal transduction and tumor progression. *Cancer Metastasis Reviews.* **18**, 15–30.

Behrndt, M., Salbreux, G., Campinho, P., Hauschild, R., Oswald, F., Roensch, J., Grill, S. W. and Heisenberg, C.-P. (2012). Forces Driving Epithelial Spreading in Zebrafish Gastrulation. *Science* **338**, 257–260.

Belahbib, H., Renard, E., Santini, S., Jourda, C., Claverie, J.-M., Borchiellini, C. and Le Bivic, A. (2018). New genomic data and analyses challenge the traditional vision of animal epithelium evolution. *BMC Genomics* **19**, 393–15.

Beloussov, L. V. (2016). Morphogenesis can be driven by properly parametrised mechanical feedback. *European Physical Journal* 1–16.

Beloussov, L. V., Luchinskaya, N. N., Ermakov, A. S. and Glagoleva, N. S. (2006). Gastrulation in amphibian embryos, regarded as a succession of biomechanical feedback events. *International Journal Developmental Biology* **50**, 113–122.

Bendel-Stenzel, M. R., Gomperts, M., Anderson, R., Heasman, J. and Wylie, C. (2000). The role of cadherins during primordial germ cell migration and early gonad formation in the mouse. *Mechanisms of Development* **91**, 143–152.

Brunet, T. and King, N. (2017). The Origin of Animal Multicellularity and Cell Differentiation. *Developmental Cell* **43**, 124–140.

Brunet, T., Bouclet, A., Ahmadi, P., Mitrossilis, D. E. M. E. N., Driquez, B., Brunet, A.-C., Henry, L., Serman, F., alle, G. E. L. B. E., nager, C. M. E., et al. (2013). Evolutionary conservation of early mesoderm specification by mechanotransduction in Bilateria. *Nature Communications* **4**, 1–15.

Bryant, D. M., Wylie, F. G. and Stow, J. L. (2005). Regulation of endocytosis, nuclear translocation, and signaling of fibroblast growth factor receptor 1 by E-cadherin. *Molecular Biology of the Cell* **16**, 14–23.

Byrum, C. A. (2001). An analysis of hydrozoan gastrulation by unipolar ingression. *Developmental Biology* **240**, 627–640.

Campbell, H. K., Maiers, J. L. and DeMali, K. A. (2017). Interplay between tight junctions & adherens junctions. *Experimental Cell Research* **358**, 39–44.

Campbell, K. and Casanova, J. (2015). A role for E-cadherin in ensuring cohesive migration of a heterogeneous population of non-epithelial cells. *Nature Communications* **6**, 7998–11.

Canel, M., Serrels, A., Frame, M. C. and Brunton, V. G. (2013). E-cadherin-integrin crosstalk in cancer invasion and metastasis. *Journal of Cell Science* **126**, 393–401.

Cano, A., Perez-Moreno, M., Rodrigo, I., Locascio, A., Blanco, M., Barrio, M.,

Carver, E. A., Jiang, R., Lan, Y., Oram, K. F. and Gridley, T. (2001). The mouse snail gene encodes a key regulator of the epithelial-mesenchymal transition. *Molecular Cell Biology* **21**, 8184–8188.

Cavey, M. and Lecuit, T. (2009). Molecular bases of cell-cell junctions stability and dynamics. *Cold Spring Harbor Perspectives in Biology* **1**, a002998.

Cereijido, M., Contreras, R. G. and Shoshani, L. (2004). Cell adhesion, polarity, and epithelia in the dawn of metazoans. *Physiological Reviews* **84**, 1229–1262.

Chan, E. H., Chavadimane Shivakumar, P., Clément, R., Laugier, E. and Lenne, P.-F. (2017). Patterned cortical tension mediated by N-cadherin controls cell geometric order in the Drosophila eye. *eLife* **6**, 33420.

Chapman, J. A., Kirkness, E. F., Simakov, O., Hampson, S. E., Mitros, T., Weinmaier, T., Rattei, T., Balasubramanian, P. G., Borman, J., Busam, D., et al. (2010). The dynamic genome of Hydra. *Nature* **464**, 592–596.

Chen, C. S. (2008). Mechanotransduction - a field pulling together? *Journal of Cell Science* **121**, 3285–3292.

Ciruna, B. and Rossant, J. (2001). FGF Signaling Regulates Mesoderm Cell Fate Specification and Morphogenetic Movement at the Primitive Streak. *Developmental Cell* **1**, 37–49.

Clarke, D. N., Miller, P. W., Lowe, C. J., Weis, W. I. and Nelson, W. J. (2016). Characterization of the Cadherin-Catenin Complex of the Sea Anemone *Nematostella vectensis* and Implications for the Evolution of Metazoan Cell-Cell Adhesion. *Molecular Biology and Evolution* **33**, 2016–2029.

Clevers, H. (2006). Wnt/beta-catenin signaling in development and disease. *Cell* **127**, 469–480.

Collins, A. G., Cartwright, P., McFadden, C. S. and Schierwater, B. (2005). Phylogenetic context and Basal metazoan model systems. *Integrative and Comparative Biology* **45**, 585–594.

Comijn, J., Berx, G., Vermassen, P., Verschueren, K., van Grunsven, L., Bruyneel, E., Mareel, M., Huylebroeck, D. and van Roy, F. (2001). The two-handed E box binding zinc finger protein SIP1 downregulates E-cadherin and induces invasion. *Molecular Cell* **7**, 1267–1278.

Cowan, C. R. and Hyman, A. A. (2007). Acto-myosin reorganization and PAR polarity in C. elegans. *Development* **134**, 1035–1043.

Cram, E. J. (2014). Mechanotransduction in C. elegans morphogenesis and tissue function. *Progress in Molecular Biology and Translational Science* **126**, 281–316.

Da Silva, S. M. and Vincent, J.-P. (2007). Oriented cell divisions in the extending germ band of Drosophila. *Development* **134**, 3049–3054.

Daniel, J. M. (2007). Dancing in and out of the nucleus: p120(ctn) and the

transcription factor Kaiso. *Biochimica et Biophysica Acta* **1773**, 59–68.

Daniel, J. M. and Reynolds, A. B. (1999). The catenin p120(ctn) interacts with Kaiso, a novel BTB/POZ domain zinc finger transcription factor. *Molecular Cell Biology* **19**, 3614–3623.

Daugherty, R. L., Serebryannyy, L., Yemelyanov, A., Flozak, A. S., Yu, H.-J., Kosak, S. T., deLanerolle, P. and Gottardi, C. J. (2014). α-Catenin is an inhibitor of transcription. *Proceedings of the National Academy of Sciences of the U.S.A.* **111**, 5260–5265.

David, D. J. V., Tishkina, A. and Harris, T. J. C. (2010). The PAR complex regulates pulsed actomyosin contractions during amnioserosa apical constriction in Drosophila. *Development* **137**, 1645–1655.

Delva, E. and Kowalczyk, A. P. (2009). Regulation of cadherin trafficking. *Traffic* **10**, 259–267.

Derycke, L. D. M. and Bracke, M. E. (2004). N-cadherin in the spotlight of cell-cell adhesion, differentiation, embryogenesis, invasion and signalling. *International Journal Developmental Biology* **48**, 463–476.

Duguay, D., Foty, R. A. and Steinberg, M. S. (2003). Cadherin-mediated cell adhesion and tissue segregation: qualitative and quantitative determinants. *Developmental Biology* **253**, 309–323.

Dumstrei, K., Wang, F., Shy, D., Tepass, U. and Hartenstein, V. (2002). Interaction between EGFR signaling and DE-cadherin during nervous system morphogenesis. *Development* **129**, 3983–3994.

Eaton, S. and Simons, K. (1995). Apical, basal, and lateral cues for epithelial polarization. *Cell* **82**, 5–8.

Elbediwy, A. and Thompson, B. J. (2018). Evolution of mechanotransduction via YAP/TAZ in animal epithelia. *Current Opinion in Cell Biology* **51**, 117–123.

Fan, F., Samuel, S., Evans, K. W., Lu, J., Xia, L., Zhou, Y., Sceusi, E., Tozzi, F., Ye, X.-C., Mani, S. A., et al. (2012). Overexpression of snail induces epithelial-mesenchymal transition and a cancer stem cell-like phenotype in human colorectal cancer cells. *Cancer Medicine* **1**, 5–16.

Farge, E. (2003). Mechanical Induction of Twist in the Drosophila Foregut/Stomodeal Primordium. *Current Biology* **13**, 1365–1377.

Fidler, A. L., Darris, C. E., Chetyrkin, S. V., Pedchenko, V. K., Boudko, S. P., Brown, K. L., Gray Jerome, W., Hudson, J. K., Rokas, A. and Hudson, B. G. (2017). Collagen IV and basement membrane at the evolutionary dawn of metazoan tissues. *eLife* **6**, e15040.

Finnerty, J. R. (2004). Origins of Bilateral Symmetry: Hox and Dpp Expression in a Sea Anemone. *Science* **304**, 1335–1337.

Finnerty, J. R. and Martindale, M. Q. (1997). Homeoboxes in Sea Anemones (Cnidaria; Anthozoa): A PCR-Based Survey of *Nematostella vectensis* and *Metridium senile*. *The Biological Bulletin* **193**, 62–76.

Fritz, A. E., Ikmi, A., Seidel, C., Paulson, A. and Gibson, M. C. (2013). Mechanisms of tentacle morphogenesis in the sea anemone *Nematostella vectensis*. *Development* **140**, 2212–2223.

Fritzenwanker, J. H., Genikhovich, G., Kraus, Y. and Technau, U. (2007). Early development and axis specification in the sea anemone *Nematostella vectensis*. *Developmental Biology* **310**, 264–279.

Fritzenwanker, J. H., Saina, M. and Technau, U. (2004). Analysis of forkhead and snail expression reveals epithelial–mesenchymal transitions during embryonic and larval development of *Nematostella vectensis*. *Developmental Biology* **275**, 389–402.

Geuens, T., van Blitterswijk, C.A. & LaPointe, V.L.S. (2020). Overcoming kidney organoid challenges for regenerative medicine. *npj Regenerative Medicine* **5,** 8. https://doi.org/10.1038/s41536-020-0093-4.

Genikhovich, G. and Technau, U. (2009). The Starlet Sea Anemone *Nematostella vectensis*: An Anthozoan Model Organism for Studies in Comparative Genomics and Functional Evolutionary Developmental Biology. *Cold Spring Harbor Protocols* **2009**, pdb.emo129–pdb.emo129.

George-Weinstein, M., Gerhart, J., Blitz, J., Simak, E. and Knudsen, K. A. (1997). N-cadherin promotes the commitment and differentiation of skeletal muscle precursor cells. *Developmental Biology* **185**, 14–24.

Gheldof, A. and Berx, G. (2013). Cadherins and epithelial-to-mesenchymal transition. *Progress in Molecular Biology and Translational Science* **116**, 317–336.

Giger, F. A. and David, N. B. (2017). Endodermal germ-layer formation through active actin-driven migration triggered by N-cadherin. *Proceedings of the National Academy of Sciences* **114**, 10143–10148.

Godt, D. and Tepass, U. (1998). Drosophila oocyte localization is mediated by differential cadherin-based adhesion. *Nature* **395**, 387–391.

Gottardi, C. J., Wong, E. and Gumbiner, B. M. (2001). E-cadherin suppresses cellular transformation by inhibiting beta-catenin signaling in an adhesion-independent manner. *Journal of Cell Biology* **153**, 1049–1060.

Gracia, M., Theis, S., Proag, A., Gay, G., Benassayag, C. and Suzanne, M. (2019). Mechanical impact of epithelial-mesenchymal transition on epithelial morphogenesis in Drosophila. *Nature Communications* **10**, 2951–17.

Gumbiner, B. M. (2000). Regulation of cadherin adhesive activity. *Journal of Cell Biology* **148**, 399–404.

Gumbiner, B. M. (2005). Regulation of cadherin-mediated adhesion in morphogenesis. *Nature Reviews of Molecular and Cell Biology* **6**, 622–634.

Hajra, K. M., Chen, D. Y.-S. and Fearon, E. R. (2002). The SLUG zinc-finger protein represses E-cadherin in breast cancer. *Cancer Research* **62**, 1613–1618.

Halbleib, J. M. and Nelson, W. J. (2006). Cadherins in development: cell adhesion, sorting, and tissue morphogenesis. *Genes & Development* **20**, 3199–3214.

Hardy, K. M., Yatskievych, T. A., Konieczka, J., Bobbs, A. S. and Antin, P. B. (2011). FGF signalling through RAS/MAPK and PI3K pathways regulates cell movement and gene expression in the chicken primitive streak without affecting E-cadherin expression. *BMC Developmental Biology* **11**, 20–17.

Hashimshony, T. (2017). Cnidarians layer up. *Nature Ecology and Evolution* **1**, 1429–1430.

Hatakeyama, J., Wakamatsu, Y., Nagafuchi, A., Kageyama, R., Shigemoto, R. and Shimamura, K. (2014). Cadherin-based adhesions in the apical endfoot are required for active Notch signaling to control neurogenesis in vertebrates. *Development* **141**, 1671–1682.

Hatta, K. and Takeichi, M. (1986). Expression of N-Cadherin Adhesion Molecules Associated with Early Morphogenetic Events in Chick Development. *Nature* **320**, 447–449.

Hazan, R. B., Phillips, G. R., Qiao, R. F., Norton, L. and Aaronson, S. A. (2000). Exogenous expression of N-cadherin in breast cancer cells induces cell migration, invasion, and metastasis. *Journal of Cell Biology* **148**, 779–790.

Heer, N. C. and Martin, A. C. (2017). Tension, contraction and tissue morphogenesis. *Development* **144**, 4249–4260.

Heisenberg, C.-P. and Bellaïche, Y. (2013). Forces in Tissue Morphogenesis and Patterning. *Cell* **153**, 948–962.

Hiramatsu, R., Matsuoka, T., Kimura-Yoshida, C., Han, S.-W., Mochida, K., Adachi, T., Takayama, S. and Matsuo, I. (2013). External mechanical cues trigger the establishment of the anterior-posterior axis in early mouse embryos. *Developmental Cell* **27**, 131–144.

Hirata, H., Tatsumi, H. and Sokabe, M. (2008). Mechanical forces facilitate actin polymerization at focal adhesions in a zyxin-dependent manner. *Journal of Cell Science* **121**, 2795–2804.

Holz, O., Apel, D., Steinmetz, P., Lange, E., Hopfenmüller, S., Ohler, K., Sudhop, S. and Hassel, M. (2017). Bud detachment in hydra requires activation of fibroblast growth factor receptor and a Rho-ROCK-myosin II signaling pathway to ensure formation of a basal constriction. *Developmental Dynamics* **246**, 502–516.

Hong, Y. (2018). aPKC: the Kinase that Phosphorylates Cell Polarity. *F1000Res* **7**, 903.

Howard, J., Grill, S. W. and Bois, J. S. (2011). Turing's next steps: the mechanochemical basis of morphogenesis. *Nature Reviews of Molecular and Cell Biology* **12**, 400–406.

Huang, J., Huang, L., Chen, Y. J., Austin, E., Devor, C. E., Roegiers, F. and Hong, Y. (2011). Differential regulation of adherens junction dynamics during apical-basal polarization. *Journal of Cell Science* **124**, 4001–4013.

Hulpiau, P. and van Roy, F. (2009). Molecular evolution of the cadherin superfamily. *The International Journal of Biochemistry & Cell Biology* **41**, 349–369.

Hulpiau, P. and van Roy, F. (2010). New Insights into the Evolution of Metazoan Cadherins. *Molecular Biology and Evolution* **28**, 647–657.

Ikenouchi, J., Umeda, K., Tsukita, S., Furuse, M. and Tsukita, S. (2007). Requirement of ZO-1 for the formation of belt-like adherens junctions during epithelial cell polarization. *Journal of Cell Biology* **176**, 779–786.

Ingber, D. E. (2006). Mechanical control of tissue morphogenesis during embryological development. *International Journal of Developmental Biology* **50**, 255–266.

Irvine, K. D. and Wieschaus, E. (1994). Cell intercalation during Drosophila germband extension and its regulation by pair-rule segmentation genes. *Development* **120**, 827–841.

Iskratsch, T., Wolfenson, H. and Sheetz, M. P. (2014). Appreciating force and shape — the rise of mechanotransduction in cell biology. *Nature Publishing Group* **15**, 825–833.

Ivanov, A. I., Nusrat, A. and Parkos, C. A. (2005). Endocytosis of the apical junctional complex: mechanisms and possible roles in regulation of epithelial barriers. *Bioessays* **27**, 356–365.

Ivanov, D. B., Philippova, M. P. and Tkachuk, V. A. (2001). Structure and functions of classical cadherins. *Biochemistry Moscow* **66**, 1174–1186.

Jacinto, A., Wood, W., Woolner, S., Hiley, C., Turner, L., Wilson, C., Martinez-Arias, A. and Martin, P. (2002). Dynamic analysis of actin cable function during Drosophila dorsal closure. *Current Biology* **12**, 1245–1250.

Jahnel, S. M., Walzl, M. and Technau, U. (2014). Development and epithelial organisation of muscle cells in the sea anemone *Nematostella vectensis*. *Frontiers in Zoology 2014 11:1* **11**, 44–15.

Kane, D. A., McFarland, K. N. and Warga, R. M. (2005). Mutations in half baked/E-cadherin block cell behaviors that are necessary for teleost epiboly. *Development* **132**, 1105–1116.

Keller, R. E. (1980). The cellular basis of epiboly: an SEM study of deep-cell rearrangement during gastrulation in *Xenopus laevis*. *Journal of Embryology and Experimental Morphology* **60**, 201–234.

Keller, R., Davidson, L. A. and Shook, D. R. (2003). How we are shaped: the biomechanics of gastrulation. *Differentiation* **71**, 171–205.

Kim, D. H., Xing, T., Yang, Z., Dudek, R., Lu, Q. and Chen, Y.-H. (2017). Epithelial Mesenchymal Transition in Embryonic Development, Tissue Repair and Cancer: A Comprehensive Overview. *Journal of Clinical Medicine* **7**, 1.

Kim, N.-G., Koh, E., Chen, X. and Gumbiner, B. M. (2011). E-cadherin mediates contact inhibition of proliferation through Hippo signaling-pathway components. *Proceedings of the National Academy of Sciences of the U.S.A.* **108**, 11930–11935.

Kimberly, E. L. and Hardin, J. (1998). Bottle cells are required for the initiation of primary invagination in the sea urchin embryo. *Developmental Biology* **204**, 235–250.

King, N., Westbrook, M. J., Young, S. L., Kuo, A., Abedin, M., Chapman, J., Fairclough, S., Hellsten, U., Isogai, Y., Letunic, I., et al. (2008). The genome of the choanoflagellate *Monosiga brevicollis* and the origin of metazoans. *Nature* **451**, 783–788.

Kirillova, A., Genikhovich, G., Pukhlyakova, E., Demilly, A., Kraus, Y. and Technau, U. (2018). Germ-layer commitment and axis formation in sea anemone embryonic cell aggregates. *Proceedings of the National Academy of Sciences of the U.S.A.* **115**, 1813–1818.

Klezovitch, O. and Vasioukhin, V. (2015). Cadherin signaling: keeping cells in touch. *F1000Res* **4**, 550.

Knust, E. and Bossinger, O. (2002). Composition and formation of intercellular junctions in epithelial cells. *Science* **298**, 1955–1959.

Kraus, Y. A. and Markov, A. V. (2016). The gastrulation in Cnidaria: A key to understanding phylogeny or the chaos of secondary modifications? *Zhurnal Obshchei Biologii* **77**, 83–105.

Kraus, Y. and Technau, U. (2006). Gastrulation in the sea anemone *Nematostella vectensis* occurs by invagination and immigration: an ultrastructural study. *Developmental Genes and Evolution* **216**, 119–132.

Kraus, Y., Flici, H., Hensel, K., Plickert, G., Leitz, T. and Frank, U. (2014). The embryonic development of the cnidarian *Hydractinia echinata*. *Evolution & Development* **16**, 323–338.

Krieg, M., Arboleda-Estudillo, Y., Puech, P. H., Käfer, J., Graner, F., Müller, D. J. and Heisenberg, C. P. (2008). Tensile forces govern germ-layer organization in zebrafish. *Nature Cell Biology* **10**, 429–436.

Kubow, K. E., Vukmirovic, R., Zhe, L., Klotzsch, E., Smith, M. L., Gourdon, D., Luna, S. and Vogel, V. (2015). Mechanical forces regulate the interactions of fibronectin and collagen I in extracellular matrix. *Nature Communications* **6**, 8026–11.

Kumar, A., Gupta, T., Berzsenyi, S. and Giangrande, A. (2015). N-cadherin negatively regulates collective *Drosophila* glial migration through actin cytoskeleton remodeling. *Journal of Cell Science* **128**, 900–912.

Kumburegama, S., Wijesena, N., Xu, R. and Wikramanayake, A. H. (2011). Strabismus-mediated primary archenteron invagination is uncoupled from Wnt/b-catenin- dependent endoderm cell fate specification in *Nematostella vectensis* (Anthozoa, Cnidaria): Implications for the evolution of gastrulation. *EvoDevo* **2**, 2.

Kunwar, P. S., Sano, H., Renault, A. D., Barbosa, V., Fuse, N. and Lehmann, R. (2008). Tre1 GPCR initiates germ cell transepithelial migration by regulating Drosophila melanogaster E-cadherin. *Journal of Cell Biology* **183**, 157–168.

Kusserow, A., Pang, K., Sturm, C., Hrouda, M., Lentfer, J., Schmidt, H. A., Technau, U., Haeseler, von, A., Hobmayer, B., Martindale, M. Q., et al. (2005). Unexpected complexity of the Wnt gene family in a sea anemone. *Nature* **433**, 156–160.

Lancaster, M. A., Renner, M., Martin, C.-A., Wenzel, D., Bicknell, L. S., Hurles, M. E., Homfray, T., Penninger, J. M., Jackson, A. P. and Knoblich, J. A. (2013). Cerebral organoids model human brain development and microcephaly. *Nature* **501**, 373–379.

Laundon, D., Larson, B. T., McDonald, K., King, N. and Burkhardt, P. (2019). The architecture of cell differentiation in choanoflagellates and sponge choanocytes. *PLoS Biol* **17**, e3000226.

Lecuit, T. and Lenne, P.-F. (2007). Cell surface mechanics and the control of cell shape, tissue patterns and morphogenesis. *Nature Reviews Molecular Cell Biology* **8**, 633–644.

Lecuit, T. and Yap, A. S. (2015). E-cadherin junctions as active mechanical integrators in tissue dynamics. *Nature Cell Biology* **17**, 533–539.

Lecuit, T., Lenne, P.-F. and Munro, E. (2011). Force generation, transmission, and integration during cell and tissue morphogenesis. *Annual Reviews of Cell Developmental Biology* **27**, 157–184.

Lee, J. Y. (2003). Mechanisms of cell positioning during *C. elegans* gastrulation. *Development* **130**, 307–320.

Lee, J.-Y. (2011). Uncorking gastrulation: the morphogenetic movement of bottle cells. *WIREs Developmental Biology* **1**, 286–293.

Lee, P. N., Kumburegama, S., Marlow, H. Q., Martindale, M. Q. and Wikramanayake, A. H. (2007). Asymmetric developmental potential along the animal–vegetal axis in the anthozoan cnidarian, *Nematostella vectensis*, is mediated by Dishevelled. *Developmental Biology* **310**, 169–186.

Leptin, M., Casal, J., Grunewald, B. and Reuter, R. (1992). Mechanisms of early Drosophila mesoderm formation. *Development. Supplement.* 23–31.

Levayer, R., Pelissier-Monier, A. and Lecuit, T. (2011). Spatial regulation of Dia and Myosin-II by RhoGEF2 controls initiation of E-cadherin endocytosis during epithelial morphogenesis. *Nature Cell Biology* **13**, 529–540.

Leys, S. P. and Riesgo, A. (2012). Epithelia, an evolutionary novelty of metazoans. *Journal of Experimental Zoology* **318**, 438–447.

Lim, J. and Thiery, J. P. (2012). Epithelial-mesenchymal transitions: insights from development. *Development* **139**, 3471–3486.

Loh, C.-Y., Chai, J. Y., Tang, T. F., Wong, W. F., Sethi, G., Shanmugam, M. K., Chong, P. P. and Looi, C. Y. (2019). The E-Cadherin and N-Cadherin Switch in Epithelial-to-Mesenchymal Transition: Signaling, Therapeutic Implications, and Challenges. *Cells* **8**, 1118.

Magie, C. R., Daly, M. and Martindale, M. Q. (2007). Gastrulation in the cnidarian *Nematostella vectensis* occurs via invagination not ingression. *Developmental Biology* **305**, 483–497.

Maitre, J. L., Berthoumieux, H., Krens, S. F. G., Salbreux, G., Julicher, F., Paluch, E. and Heisenberg, C. P. (2012). Adhesion Functions in Cell Sorting by Mechanically Coupling the Cortices of Adhering Cells. *Science* **338**, 253–256.

Maitre, J.-L. and Heisenberg, C.-P. (2013). Three functions of cadherins in cell adhesion. *Current Biology* **23**, 626–633.

Mammoto, A., Connor, K. M., Mammoto, T., Yung, C. W., Huh, D., Aderman, C. M., Mostoslavsky, G., Smith, L. E. H. and Ingber, D. E. (2009). A mechanosensitive transcriptional mechanism that controls angiogenesis. *Nature* **457**, 1103–1108.

Mammoto, T., Mammoto, A., Torisawa, Y.-S., Tat, T., Gibbs, A., Derda, R., Mannix, R., de Bruijn, M., Yung, C. W., Huh, D., et al. (2011). Mechanochemical control of mesenchymal condensation and embryonic tooth organ formation. *Developmental Cell* **21**, 758–769.

Maniotis, A. J., Chen, C. S. and Ingber, D. E. (1997). Demonstration of mechanical connections between integrins, cytoskeletal filaments, and nucleoplasm that stabilize nuclear structure. *Proceedings of the National Academy of Sciences of the U.S.A.* **94**, 849–854.

Marques, A. C. and Collins, A. G. (2004). **Cladistic analysis of Medusozoa and cnidarian evolution.** *Invertebrate Biology* **123**, 23–42.

Martindale, M. Q. (2004). Investigating the origins of triploblasty: `mesodermal' gene expression in a diploblastic animal, the sea anemone *Nematostella vectensis* (phylum, Cnidaria; class, Anthozoa). *Development* **131**, 2463–2474.

Matus, D. Q., Thomsen, G. H. and Martindale, M. Q. (2007). FGF signaling in gastrulation and neural development in *Nematostella vectensis*, an anthozoan cnidarian. *Development Genes and Evolution* **217**, 137–148.

Mellman, I. and Nelson, W. J. (2008). Coordinated protein sorting, targeting and distribution in polarized cells. *Nature Publishing Group* **9**, 833–845.

Mège, R. M. and Ishiyama, N. (2017). Integration of Cadherin Adhesion and Cytoskeleton at Adherens Junctions. *Cold Spring Harbor Perspectives in Biology* **9**, a028738.

Montero, J. A. (2005). Shield formation at the onset of zebrafish gastrulation. *Development* **132**, 1187–1198.

Moran, Y., Fredman, D., Praher, D., Li, X. Z., Wee, L. M., Rentzsch, F., Zamore, P. D., Technau, U. and Seitz, H. (2014). Cnidarian microRNAs frequently regulate targets by cleavage. *Genome Research* **24**, 651–663.

Munro, E., Nance, J. and Priess, J. R. (2004). Cortical flows powered by asymmetrical contraction transport PAR proteins to establish and maintain anterior-posterior polarity in the early *C.elegans* embryo. *Developmental Cell* **7**, 413–424.

Nandadasa, S., Tao, Q., Menon, N. R., Heasman, J. and Wylie, C. (2009). N- and E-cadherins in *Xenopus* are specifically required in the neural and non-neural ectoderm, respectively, for F-actin assembly and morphogenetic movements. *Development* **136**, 1327–1338.

Nelson, W. J. (2004). Convergence of Wnt, -Catenin, and Cadherin Pathways. *Science* **303**, 1483–1487.

Nguyen, T. and Mège, R. M. (2016). N-Cadherin and Fibroblast Growth Factor Receptors crosstalk in the control of developmental and cancer cell migrations. *European Journal of Cell Biology* **95**, 415–426.

Nichols, S. A., Roberts, B. W., Richter, D. J., Fairclough, S. R. and King, N. (2012). Origin of metazoan cadherin diversity and the antiquity of the classical cadherin/β-catenin complex. *Proceedings of the National Academy of Sciences of the U.S.A.* **109**, 13046–13051.

Nieman, M. T., Prudoff, R. S., Johnson, K. R. and Wheelock, M. J. (1999). N-cadherin promotes motility in human breast cancer cells regardless of their E-cadherin expression. *Journal of Cell Biology* **147**, 631–644.

Niessen, C. M., Leckband, D. and Yap, A. S. (2011). Tissue organization by cadherin adhesion molecules: dynamic molecular and cellular mechanisms of morphogenetic regulation. *Physiological Reviews* **91**, 691–731.

Nieto, M. A. (2002). The Snail superfamily of zinc-finger transcription factors. *Nature Reviews Molecular Cell Biology* **3**, 155–166.

Nieto, M. A., Huang, R. Y.-J., Jackson, R. A. and Thiery, J. P. (2016). EMT: 2016. *Cell* **166**, 21–45.

Ninomiya, H., David, R., Damm, E. W., Fagotto, F., Niessen, C. M. and Winklbauer, R. (2012). Cadherin-dependent differential cell adhesion in *Xenopus*

causes cell sorting *in vitro* but not in the embryo. *Journal of Cell Science* **125**, 1877–1883.

Nose, A., Nagafuchi, A. and Takeichi, M. (1988). Expressed recombinant cadherins mediate cell sorting in model systems. *Cell* **54**, 993–1001.

Nowotschin, S., Hadjantonakis, A.-K. and Campbell, K. (2019). The endoderm: a divergent cell lineage with many commonalities. *Development* **146**, dev150920.

Nugraha, B., Buono, M.F., von Boehmer, L., Hoerstrup, S.P., Emmert, M.Y. (2019). Human Cardiac Organoids for Disease Modeling. Clinical Pharmacology and Therapeutics. **105**, 1, 79-85.

Oda, H. and Takeichi, M. (2011). Structural and functional diversity of cadherin at the adherens junction. *Journal of Cell Biology* **193**, 1137–1146.

Oda, H., Tsukita, S. and Takeichi, M. (1998). Dynamic behavior of the cadherin-based cell-cell adhesion system during Drosophila gastrulation. *Developmental Biology* **203**, 435–450.

Orr, A. W., Helmke, B. P., Blackman, B. R. and Schwartz, M. A. (2006). Mechanisms of mechanotransduction. *Developmental Cell* **10**, 11–20.

Orsulic, S. and Kemler, R. (2000). Expression of Eph receptors and ephrins is differentially regulated by E-cadherin. *Journal of Cell Science* **113 (Pt 10)**, 1793–1802.

Ozawa, M., Ringwald, M. and Kemler, R. (1990). Uvomorulin-catenin complex formation is regulated by a specific domain in the cytoplasmic region of the cell adhesion molecule. *Proceedings of the National Academy of Sciences of the U.S.A.* **87**, 4246–4250.

Palmer, L. G. (2017). Epithelial transport in The Journal of General Physiology. *Journal of General Physiology* **149**, 897–909.

Paluch, E. and Heisenberg, C.-P. (2009). Biology and Physics of Cell Shape Changes Review in Development. *Current Biology* **19**, R790–R799.

Peinado, H., Portillo, F. and Cano, A. (2004). Transcriptional regulation of cadherins during development and carcinogenesis. *International Journal of Developmental Biology* **48**, 365–375.

Perez-Moreno, M. and Fuchs, E. (2006). Catenins: keeping cells from getting their signals crossed. *Developmental Cell* **11**, 601–612.

Perrais, M., Chen, X., Perez-Moreno, M. and Gumbiner, B. M. (2007). E-cadherin homophilic ligation inhibits cell growth and epidermal growth factor receptor signaling independently of other cell interactions. *Molecular Biology of the Cell* **18**, 2013–2025.

Piccolo, S. (2013). Developmental biology: Mechanics in the embryo. *Nature* **504**, 223–225.

Portillo, F. and Nieto, A. (2000). The transcription factor Snail controls epithelial–mesenchymal transitions by repressing E-cadherin expression. *Nature Cell Biology* **2**, 76–83.

Powell, D. W. (1981). Barrier function of epithelia. *American Journal of Physiology* **241**, G275–88.

Pukhlyakova, E. A., Kirillova, A. O., Kraus, Y. A., Zimmermann, B. and Technau, U. (2019). A cadherin switch marks germ layer formation in the diploblastic sea anemone *Nematostella vectensis. Development* **146**, dev174623.

Pukhlyakova, E., Aman, A. J., Elsayad, K. and Technau, U. (2018). β-Catenin-dependent mechanotransduction dates back to the common ancestor of Cnidaria and Bilateria. *Proceedings of the National Academy of Sciences of the. U.S.A.* **115**, 6231–6236.

Putnam, N. H., Srivastava, M., Hellsten, U., Dirks, B., Chapman, J., Salamov, A., Terry, A., Shapiro, H., Lindquist, E., Kapitonov, V. V., et al. (2007). Sea Anemone Genome Reveals Ancestral Eumetazoan Gene Repertoire and Genomic Organization. *Science* **317**, 86–94.

Qian, X., Karpova, T., Sheppard, A. M., McNally, J. and Lowy, D. R. (2004). E-cadherin-mediated adhesion inhibits ligand-dependent activation of diverse receptor tyrosine kinases. *EMBO Journal.* **23**, 1739–1748.

Ragkousi, K., Marr, K., McKinney, S., Ellington, L. and Gibson, M. C. (2017). Cell-Cycle-Coupled Oscillations in Apical Polarity and Intercellular Contact Maintain Order in Embryonic Epithelia. *Current Biology* **27**, 1381–1386.

Rehfeld, A., Nylander, M. and Karnov, K. (2017). Glandular Epithelium and Glands. In *Compendium of Histology* (ed. Cham, pp. 101–120.

Rentzsch, F., Anton, R., Saina, M., Hammerschmidt, M., Holstein, T. W. and Technau, U. (2006). Asymmetric expression of the BMP antagonists chordin and gremlin in the sea anemone *Nematostella vectensis*: Implications for the evolution of axial patterning. *Developmental Biology* **296**, 375–387.

Rentzsch, F., Fritzenwanker, J. H., Scholz, C. B. and Technau, U. (2008). FGF signalling controls formation of the apical sensory organ in the cnidarian *Nematostella vectensis*. *Development* **135**, 1761–1769.

Reynolds, A. B. and Roczniak-Ferguson, A. (2004). Emerging roles for p120-catenin in cell adhesion and cancer. *Oncogene* **23**, 7947–7956.

Riga, A., Castiglioni, V. G. and Boxem, M. (2020). New insights into apical-basal polarization in epithelia. *Current Opinion in Cell Biology* **62**, 1–8.

Ringrose, J. H., van den Toorn, H. W. P., Eitel, M., Post, H., Neerincx, P., Schierwater, B., Altelaar, A. F. M. and Heck, A. J. R. (2013). Deep proteome profiling of *Trichoplax adhaerens* reveals remarkable features at the origin of metazoan multicellularity. *Nature Communications* **4**, 1408–7.

Rodriguez-Boulan, E. and Macara, I. G. (2014). Organization and execution of the epithelial polarity programme. *Nature Publishing Group* **15**, 225–242.

Roignot, J., Peng, X. and Mostov, K. (2013). Polarity in mammalian epithelial morphogenesis. *Cold Spring Harbor Perspectives in Biology* **5**, a013789–a013789.

Romano, L. A. and Runyan, R. B. (2000). Slug is an essential target of TGFbeta2 signaling in the developing chicken heart. *Developmental Biology* **223**, 91–102.

Royer, C. and Lu, X. (2011). Epithelial cell polarity: a major gatekeeper against cancer? *Cell Death Differentiation.* **18**, 1470–1477.

Röper, J.-C., Mitrossilis, D., Stirnemann, G., Waharte, F., Brito, I., Fernandez-Sanchez, M.-E., Baaden, M., Salamero, J. and Farge, E. (2018). The major β-catenin/E-cadherin junctional binding site is a primary molecular mechano-transductor of differentiation in vivo. *eLife* **7**, 773.

Saina, M., Genikhovich, G., Renfer, E. and Technau, U. (2009). BMPs and Chordin regulate patterning of the directive axis in a sea anemone. *Proceedings of the National Academy of Sciences of the U.S.A.* **106**, 18592–18597.

Salinas-Saavedra, M., Rock, A. Q. and Martindale, M. Q. (2018). Germ layer-specific regulation of cell polarity and adhesion gives insight into the evolution of mesoderm. *eLife* **7**, 1438.

Salinas-Saavedra, M., Stephenson, T. Q., Dunn, C. W. and Martindale, M. Q. (2015). Par system components are asymmetrically localized in ectodermal epithelia, but not during early development in the sea anemone *Nematostella vectensis*. *EvoDevo* **6**, 20–20.

Sasaki, N., Sasamura, T., Ishikawa, H. O., Kanai, M., Ueda, R., Saigo, K. and Matsuno, K. (2007). Polarized exocytosis and transcytosis of Notch during its apical localization in Drosophila epithelial cells. *Genes Cells* **12**, 89–103.

Sauka-Spengler, T. and Bronner-Fraser, M. (2008). A gene regulatory network orchestrates neural crest formation. *Nature Publishing Group* **9**, 557–568.

Sawyer, J. M., Harrell, J. R., Shemer, G., Sullivan-Brown, J., Roh-Johnson, M. and Goldstein, B. (2010). Apical constriction: A cell shape change that can drive morphogenesis. *Developmental Biology* **341**, 5–19.

Schäfer, G., Narasimha, M., Vogelsang, E. and Leptin, M. (2014). Cadherin switching during the formation and differentiation of the Drosophila mesoderm - implications for epithelial-to-mesenchymal transitions. *Journal of Cell Science* **127**, 1511–1522.

Schlegelmilch, K., Mohseni, M., Kirak, O., Pruszak, J., Rodriguez, J. R., Zhou, D., Kreger, B. T., Vasioukhin, V., Avruch, J., Brummelkamp, T. R., et al. (2011). Yap1 acts downstream of α-catenin to control epidermal proliferation. **144**, 782–795.

Schwaiger, M., Schönauer, A., Rendeiro, A. F., Pribitzer, C., Schauer, A., Gilles, A. F., Schinko, J. B., Renfer, E., Fredman, D. and Technau, U. (2014). Evolutionary conservation of the eumetazoan gene regulatory landscape. *Genome Research* **24**, 639–650.

Sefton, M., Sánchez, S. and Nieto, M. A. (1998). Conserved and divergent roles for members of the Snail family of transcription factors in the chick and mouse embryo. *Development* **125**, 3111–3121.

Sekiguchi, R. and Yamada, K. M. (2018). Basement Membranes in Development and Disease. *Current Topics in Developmental Biology* **130**, 143–191.

Seybold, A., Salvenmoser, W. and Hobmayer, B. (2016). Sequential development of apical-basal and planar polarities in aggregating epitheliomuscular cells of *Hydra. Developmental Biology* **412**, 148–159.

Shewan, A. M., Maddugoda, M., Kraemer, A., Stehbens, S. J., Verma, S., Kovacs, E. M. and Yap, A. S. (2005). Myosin 2 is a key Rho kinase target necessary for the local concentration of E-cadherin at cell-cell contacts. *Molecular Biology of the Cell* **16**, 4531–4542.

Shook, D. and Keller, R. (2003). Mechanisms, mechanics and function of epithelial–mesenchymal transitions in early development. *Mechanisms of Development* **120**, 1351–1383.

Simske, J. S. and Hardin, J. (2001). Getting into shape: epidermal morphogenesis in Caenorhabditis elegans embryos. *Bioessays* **23**, 12–23.

Skoglund, P., Rolo, A., Chen, X., Gumbiner, B. M. and Keller, R. (2008). Convergence and extension at gastrulation require a myosin IIB-dependent cortical actin network. *Development* **135**, 2435–2444.

Spassky, N. and Meunier, A. (2017). The development and functions of multiciliated epithelia. *Nature Publishing Group* **18**, 423–436.

St Johnston, D. and Ahringer, J. (2010). Cell polarity in eggs and epithelia: parallels and diversity. *Cell* **141**, 757–774.

Steinberg, M. S. (1970). Does differential adhesion govern self-assembly processes in histogenesis? Equilibrium configurations and the emergence of a hierarchy among populations of embryonic cells. *J. Exp. Zool.* **173**, 395–433.

Steinberg, M. S. and Gilbert, S. F. (2004). *Townes and Holtfreter (1955): directed movements and selective adhesion of embryonic amphibian cells.* Wiley-Blackwell.

Steinberg, M. S. and Takeichi, M. (1994). Experimental specification of cell sorting, tissue spreading, and specific spatial patterning by quantitative differences in cadherin expression. *Proceedings of the National Academy of Sciences of the U.S.A.* **91**, 206–209.

Steinmetz, P. R. H., Aman, A., Kraus, J. E. M. and Technau, U. (2017). Gut-like

ectodermal tissue in a sea anemone challenges germ layer homology. *Nature Ecology and Evolution* **1**, 1535–1542.

Stepniak, E., Radice, G. L. and Vasioukhin, V. (2009). Adhesive and signaling functions of cadherins and catenins in vertebrate development. *Cold Spring Harbor Perspectives in Biology* **1**, a002949.

Stockinger, A., Eger, A., Wolf, J., Beug, H. and Foisner, R. (2001). E-cadherin regulates cell growth by modulating proliferation-dependent beta-catenin transcriptional activity. *Journal of Cell Biology* **154**, 1185–1196.

Suyama, K., Shapiro, I., Guttman, M. and Hazan, R. B. (2002). A signaling pathway leading to metastasis is controlled by N-cadherin and the FGF receptor. *Cancer Cell* **2**, 301–314.

Taber, L. A. (2007). Theoretical study of Beloussov's hyper-restoration hypothesis for mechanical regulation of morphogenesis. *Biomechanics and Modeling in Mechanobiology* **7**, 427–441.

Takeichi, M. (1988). The cadherins: cell-cell adhesion molecules controlling animal morphogenesis. *Development* **102**, 639–655.

Takeichi, M. (1995). Morphogenetic roles of classic cadherins. *Current Opinion in Cell Biology* **7**, 619–627.

Tanentzapf, G., Smith, C., McGlade, J. and Tepass, U. (2000). Apical, lateral, and basal polarization cues contribute to the development of the follicular epithelium during Drosophila oogenesis. *Journal of Cell Biology* **151**, 891–904.

Tanos, B. and Rodriguez-Boulan, E. (2008). The epithelial polarity program: machineries involved and their hijacking by cancer. *Oncogene* **27**, 6939–6957.

Technau, U. (2020). Gastrulation and germ layer formation in the sea anemone *Nematostella vectensis* and other cnidarians. *Mechanisms of Development* **163**, 103628.

Technau, U. and Scholz, C. B. (2003). Origin and evolution of endoderm and mesoderm. *International Journal of Developmental Biology* **47**, 531–539.

Technau, U., Cramer von Laue, C., Rentzsch, F., Luft, S., Hobmayer, B., Bode, H. R. and Holstein, T. W. (2000). Parameters of self-organization in Hydra aggregates. *Proceedings of the National Academy of Sciences of the U.S.A.* **97**, 12127–12131.

Tepass, U., Tanentzapf, G., Ward, R. and Fehon, R. (2001). Epithelial cell polarity and cell junctions in Drosophila. *Annual Reviews in Genetics.* **35**, 747–784.

Tepass, U., Truong, K., Godt, D., Ikura, M. and Peifer, M. (2000). Cadherins in embryonic and neural morphogenesis. *Nature Reviews in Molecular and Cell Biology* **1**, 91–100.

Thiery, J. P., Acloque, H., Huang, R. Y. J. and Nieto, M. A. (2009). Epithelial-

mesenchymal transitions in development and disease. *Cell* **139**, 871–890.

Tian, X., Liu, Z., Niu, B., Zhang, J., Tan, T. K., Lee, S. R., Zhao, Y., Harris, D. C. H. and Zheng, G. (2011). E-cadherin/β-catenin complex and the epithelial barrier. *Journal of Biomedicine and Biotechnology* **2011**, 567305–6.

Townes, P. L. and Holtfreter, J. (1955). Directed Movements and Selective Adhesion of Embryonic Amphibian Cells. *Journal of Experimental Zoology* **128**, 53–120.

Turksen, K. (2017). Building barriers. *Tissue Barriers* **5**, e1400866.

Tyler, S. (2003). Epithelium--the primary building block for metazoan complexity. *Integrative and Comparative Biology* **43**, 55–63.

Vaezi, A., Bauer, C., Vasioukhin, V. and Fuchs, E. (2002). Actin cable dynamics and Rho/Rock orchestrate a polarized cytoskeletal architecture in the early steps of assembling a stratified epithelium. *Developmental Cell* **3**, 367–381.

van Roy, F. (2014). Beyond E-cadherin: roles of other cadherin superfamily members in cancer. *Nature Reviews Cancer* **14**, 121–134.

Vasioukhin, V., Bauer, C., Yin, M. and Fuchs, E. (2000). Directed actin polymerization is the driving force for epithelial cell-cell adhesion. *Cell* **100**, 209–219.

Veltmaat, J. M., Orelio, C. C., Ward-Van Oostwaard, D., Van Rooijen, M. A., Mummery, C. L. and Defize, L. H. (2000). Snail is an immediate early target gene of parathyroid hormone related peptide signaling in parietal endoderm formation. *International Journal of Developmental Biology* **44**, 297–307.

Viotti, M., Nowotschin, S. and Hadjantonakis, A.-K. (2014). SOX17 links gut endoderm morphogenesis and germ layer segregation. *Nature Cell Biology* **16**, 1146–1156.

Wacker, S., Grimm, K., Joos, T. and Winklbauer, R. (2000). Development and control of tissue separation at gastrulation in *Xenopus*. *Developmental Biology* **224**, 428–439.

Waddington, C. H. (2014). *The Strategy of the Genes*. Routledge.

Wang, N., Tytell, J. D. and Ingber, D. E. (2009). Mechanotransduction at a distance: mechanically coupling the extracellular matrix with the nucleus. *Nature Publishing Group* **10**, 75–82.

Warga, R. M. and Kane, D. A. (2007). A role for N-cadherin in mesodermal morphogenesis during gastrulation. *Developmental Biology* **310**, 211–225.

Webb, D. J., Donais, K., Whitmore, L. A., Thomas, S. M., Turner, C. E., Parsons, J. T. and Horwitz, A. F. (2004). FAK-Src signalling through paxillin, ERK and MLCK regulates adhesion disassembly. *Nature Cell Biology* **6**, 154–161.

Wei, Y. and Mikawa, T. (2000). Formation of the avian primitive streak from spatially restricted blastoderm: evidence for polarized cell division in the elongating streak. *Development* **127**, 87–96.

Weng, M. and Wieschaus, E. (2016). Myosin-dependent remodeling of adherens junctions protects junctions from Snail-dependent disassembly. *Journal of Cell Biology* **212**, 219–229.

Weng, M. and Wieschaus, E. (2017). Polarity protein Par3/Bazooka follows myosin-dependent junction repositioning. *Developmental Biology* **422**, 125–134.

Wertz, P. W. and Squier, C. A. (1991). Cellular and molecular basis of barrier function in oral epithelium. *Critical Reviews in Therapeutic Drug Carrier Systems* **8**, 237–269.

Wheelock, M. J., Shintani, Y., Maeda, M., Fukumoto, Y. and Johnson, K. R. (2008). Cadherin switching. *Journal of Cell Science* **121**, 727–735.

Wikramanayake, A. H., Hong, M., Lee, P. N., Pang, K., Byrum, C. A., Bince, J. M., Xu, R. and Martindale, M. Q. (2003). An ancient role for nuclear β-catenin in the evolution of axial polarity and germ layer segregation. *Nature* **426**, 446–450.

Williams, E. J., Furness, J., Walsh, F. S. and Doherty, P. (1994). Activation of the FGF Receptor Underlies Neurite Outgrowth Stimulated by L1, N-Cam, and N-Cadherin. *Neuron* **13**, 583–594.

Williams, E. J., Williams, G., Howell, F. V., Skaper, S. D., Walsh, F. S. and Doherty, P. (2001). Identification of an N-cadherin motif that can interact with the fibroblast growth factor receptor and is required for axonal growth. *Journal of Biological Chemistry* **276**, 43879–43886.

Winklbauer, R. (2012). Cadherin Function During *Xenopus* Gastrulation. In *Adherens Junctions: from Molecular Mechanisms to Tissue Development and Disease* (ed. Harris, T., pp. 301–320. Dordrecht: Springer Netherlands.

Wolpert, L. (1992). Gastrulation and the evolution of development. *Development. Supplement.* 7–13.

Wozniak, M. A. and Chen, C. S. (2009). Mechanotransduction in development: a growing role for contractility. *Nature Reviews Molecular Cell Biology* **10**, 34–43.

Wu, S. Y. and McClay, D. R. (2007). The Snail repressor is required for PMC ingression in the sea urchin embryo. *Development* **134**, 1061–1070.

Yagi, T. and Takeichi, M. (2000). Cadherin superfamily genes: functions, genomic organization, and neurologic diversity. *Genes & Development* **14**, 1169–1180.

Yamada, S. and Nelson, W. J. (2007). Localized zones of Rho and Rac activities drive initiation and expansion of epithelial cell-cell adhesion. *Journal Cell Biology* **178**, 517–527.

Yamanaka, T., Horikoshi, Y., Suzuki, A., Sugiyama, Y., Kitamura, K., Maniwa, R.,

Nagai, Y., Yamashita, A., Hirose, T., Ishikawa, H., et al. (2001). PAR-6 regulates aPKC activity in a novel way and mediates cell-cell contact-induced formation of the epithelial junctional complex. *Genes Cells* **6**, 721–731.

Yang, J. and Weinberg, R. A. (2008). Epithelial-Mesenchymal Transition: At the Crossroads of Development and Tumor Metastasis. *Developmental Cell* **14**, 818–829.

Yap, A. S., Niessen, C. M. and Gumbiner, B. M. (1998). The juxtamembrane region of the cadherin cytoplasmic tail supports lateral clustering, adhesive strengthening, and interaction with p120ctn. *Journal Cell Biology* **141**, 779–789.

Yeaman, C., Grindstaff, K. K. and Nelson, W. J. (1999). New perspectives on mechanisms involved in generating epithelial cell polarity. *Physiological Reviews* **79**, 73–98.

Young, P. E., Pesacreta, T. C. and Kiehart, D. P. (1991). Dynamic changes in the distribution of cytoplasmic myosin during *Drosophila* embryogenesis. *Development* **111**, 1–14.

Yuksel, H. and Turkeli, A. (2017). Airway epithelial barrier dysfunction in the pathogenesis and prognosis of respiratory tract diseases in childhood and adulthood. *Tissue Barriers* **5**, e1367458.

Zallen, J. A. (2007). Planar polarity and tissue morphogenesis. *Cell* **129**, 1051–1063.

Zhong, Y., Brieher, W. M. and Gumbiner, B. M. (1999). Analysis of C-cadherin regulation during tissue morphogenesis with an activating antibody. *Journal Cell Biology* **144**, 351–359.